Università degli Studi di Ferrara

DOCTORAL COURSE IN
"CHEMICAL SCIENCES"

CYCLE XXXII

DIRECTOR Prof. Cavazzini Alberto

Investigation of Mass Transfer Phenomena and Thermodynamic Properties of new Generation Porous Particles for High-Efficient Separations in Liquid Chromatography Through Experimental and Theoretical Approaches

Scientific/Disciplinary Sector (SDS) CHIM/01

Candidate
Felletti Simona

Supervisor
Prof. Cavazzini Alberto

Co-Supervisor
Dr. Catani Martina

Years 2016/2019

List of papers

This thesis is based on not yet published results obtained during my Ph.D. studies and on the following submitted or published papers. Reprints are appended at the end of the thesis.

(I) **Recent advancements and future directions of superficially porous chiral stationary phases for ultrafast high-performance enantioseparations**, M. Catani, O. H. Ismail, F. Gasparrini, M. Antonelli, L. Pasti, N. Marchetti, S. Felletti, A. Cavazzini, *Analyst*, 142, **2017**, 555-566. Reprinted with permission from the The Royal Society of Chemistry.

(II) **Future perspectives in high efficient and ultrafast chiral liquid chromatography through zwitterionic teicoplanin-based 2-μm superficially porous particles**, O. H. Ismail, M. Antonelli, A. Ciogli, C. Villani, A. Cavazzini, M. Catani, S. Felletti, D. S. Bell, F. Gasparrini, *J. Chromatogr. A*, 1520, **2017**, 91-102. Reprinted with permission from Elsevier.

(III) **New frontiers and cutting edge applications in ultra high performance liquid chromatography through latest generation superficially porous particles**, M. Catani, S. Felletti, O. H. Ismail, F. Gasparrini, L. Pasti, N. Marchetti, V. Costa, A. Cavazzini, **2017**, *Anal. Bioanal. Chem.*, DOI 10.1007/s00216-017-0842-4. Reprinted with permission from Springer.

(IV) **The Way to Ultrafast, High-Throughput Enantioseparations of Bioactive Compounds in Liquid and Supercritical Fluid Chromatography**, O. H. Ismail, S. Felletti, C. De Luca, L. Pasti, N. Marchetti, V. Costa, F. Gasparrini, A. Cavazzini, M. Catani, *Molecules*, **2018**, 23, 2709; doi:10.3390/molecules23102709

(V) **On the effect of chiral selector loading and mobile phase composition on adsorption properties of latest generation fully- and superficially-porous Whelk-O1 particles for high-efficient ultrafast enantioseparations**, S. Felletti, C. De Luca, O. H. Ismail, L. Pasti, V. Costa, F. Gasparrini, A. Cavazzini, M. Catani, *J Chromatogr A*. 1579 **2018** 41–48. Reprinted with permission from Elsevier.

(VI) **Recent Achievements and Future Challenges in Supercritical Fluid Chromatography for the Enantioselective Separation of Chiral Pharmaceuticals**, Felletti, S., Ismail, O.H., De Luca, C. Costa V., Gasparrini F, Pasti L, Marchetti N, Cavazzini A., Catani M, *Chromatographia*, **2019**, 82, 65-75. Reprinted with permission from Springer.

(VII) **Modeling the nonlinear behavior of a bioactive peptide in reversed-phase gradient elution chromatography**, C. De Luca, S. Felletti, M. Macis, W. Cabri, G. Lievore, T. Chenet, L. Pasti, M, Morbidelli, A. Cavazzini, M. Catani, A. Ricci, **2019**, *J. Chromatogr. A*, https://doi.org/10.1016/j.chroma.2019.460789. Reprinted with permission from Elsevier.

(VIII) **Exploring stationary-phase diffusion and adsorption-desorption kinetics in Whelk-O1 and zwitterionic-teicoplanin chiral stationary phases**, S. Felletti, C. De Luca, G. Lievore, L. Pasti, T. Chenet, O. H. Ismail, G. Mazzoccanti, F. Gasparrini, A. Cavazzini, M. Catani, **2019** (in preparation)

(IX) **Pore size effect on zwitterionic teicoplanin based chiral stationary phases: kinetic and thermodynamic investigation**, O. H. Ismail, M. Catani, S. Felletti, M. Ye, A. Cavazzini, F. Gasparrini, **2019** (in preparation)

(X) **New Whelk-O1 Pirkle-type chiral stationary phases for ultra-high performance ultra-fast enantioseparations**, M. Catani, O. H. Ismail, S. Felletti, F. Gasparrini, L. Pasti, V. Costa, A. Cavazzini, *American Pharmaceutical Review*, 20, 4, May-June **2017**

Contents

CHAPTER 1

Introduction

Chromatography was originally developed by the Russian botanist Tswett in 1903 to extract plant pigments from vegetal mixtures [1]. However, only the late 60s saw the birth of a new kind of technique: the so-called High Performance Liquid Chromatography (HPLC). It consists of a liquid mobile phase carrying analytes percolating through a packed bed made of silica-based porous particles. The separation is the result of different degrees of interaction between analytes and stationary phase. In the last 40 years, thanks to the continuous progress regarding both instruments, able to perform analysis at higher flow rates and pressures, and the use of particles with reduced diameter, chromatography has experienced a rapid development becoming one of the most used separation method. This new technique, which makes use of pressures up to 1500 bar and high efficient columns, is called Ultra-High Performance Liquid Chromatography (UHPLC).

Another powerful technique, very similar to HPLC in terms of instrument and software, is the so-called Supercritical Fluid Chromatography (SFC). The main difference between SFC and LC is the use of high-pressurized carbon dioxide (CO_2) mixed with other solvents (usually methanol, ethanol, isopropanol) as mobile phase. CO_2 is used in its supercritical state, obtained when temperature and pressure are near or above the critical point (for CO_2: T_c = 31°C and P_c = 74 bar). A supercritical fluid has different characteristics: it has intermediate density and diffusivity between gas and liquid, and supercritical CO_2 shows a viscosity comparable to a gas and 10 times lower than a liquid. For these reasons, SFC has numerous advantages over LC (either normal phase and reversed phase) [2–5], for example faster and more efficient analysis thanks to lower viscosity and higher diffusion coefficients (higher mass transfer), more rapid equilibration, lower operating cost and solvent consumption [6–9].

Nowadays, LC and SFC cover different fields of application, including biological and chemical samples (drugs, pesticides, additives, proteins, etc.). The need of developing more and more efficient and fast separation methods has led, in the last years, to the preparation of particles with smaller and smaller diameter. As a matter

of fact, sub-2 μm fully porous particles (FPPs) and the so-called second generation of superficially porous particles (SPPs) are widely commercialized and routinely employed (Fig. 1.1).

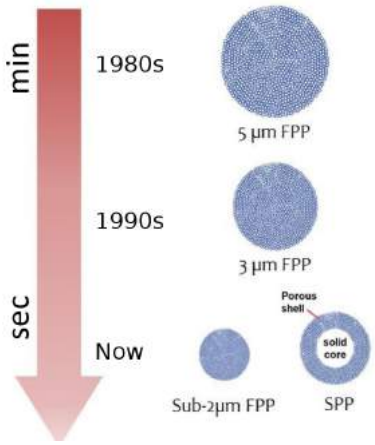

Figure 1.1: Evolution of particles used as stationary phase over the years.

The main advantages of SP particles with a solid core are the reduction of the longitudinal diffusion due to the minor accessible volume, an improvement of solid-liquid mass transfer by shortening the diffusion path length across the particle and finally a reduced eddy diffusion.
From a theoretical point of view, one of the main challenge is to understand all the thermodynamic and kinetic factors that affect a chromatographic separation, from the column performance to the retention behaviour of analytes. It is clear that there are a lot of possibilities concerning the choice of the correct type of stationary (SP or FP particles and their physico-chemical and geometric characteristics) and mobile phases (reverse or normal phase, polar organic mode, supercritical fluid chromatography, hydrophilic interaction, etc.) both having a deep impact on the separation performance.
The aim of my PhD program has been the evaluation of kinetic and thermodynamic factors affecting chromatographic separation in the field of both chiral and achiral chromatography, through the combination of effective theoretical and experimental approaches. To this end, different types of stationary phases and different elution modes have been studied and compared.

1.1 Stationary phases for ultrafast separations

On the one hand, in the field of achiral separations, numerous progresses have been made in the last 40 years [10], leading to the introduction in the market of sub-2 μm fully porous particles and the second-generation of superficially porous particles [11, 12]. It is well known that the reduction of the particle diameter leads to an improvement in terms of chromatographic performance, since the efficiency of a column (evaluated through H, the height equivalent to a theoretical plate) is inversely proportional to the particle diameter, d_p.

On the other hand, chiral LC have experienced its advancement only in recent years, with the transition from 3-5 μm FPPs to sub-2μm FPPs and 2 μm SPPs, mainly due to difficulties in the functionalization of small particles, agglomeration issues during the synthesis process and a lack of fundamental studies related to the mass transfer phenomena occurring in chiral chromatography [13–16].

Gasparrini and coworkers were the first to report on sub-2 μm FPPs functionalized with teicoplanin chiral selector in 2010, obtaining second-time scale and very efficient separations [17]. One year later, Lindner and coworkers presented the first example of 2.7 μm SPPs for ion chromatography for the separation of different derivatized amino acids [18]. In 2012 Chankvetadze et al. compared the efficiencies of polysaccharide-based CSPs prepared on both FP and SP particles [19]. However, the most complete study on the performance comparison between chiral SPPs and FPPs has been performed by Armstrong and coworkers some years later [20, 21]. In these works, different chiral selectors (such as macrocyclic antibiotics and cyclodextrins) and different modes of chromatography (RP, NP, HILIC) have been used, leading to the conclusion that SP particles outperformed FP ones in terms of both performance and speed of analysis.

Nevertheless, literature lacks works aimed at explaining the complex mass transfer phenomena occurring in chiral chromatography, where the contribution of the adsorption-desorption kinetics cannot be neglected. The importance of these more detailed studies lies in the possibility to fully understand enantioseparation process and to enhance the kinetic and thermodynamic performances of fully- or superficially-porous particles.

CHAPTER 2

Models of Chromatography

Equilibrium or kinetic theories could be used for modeling chromatographic processes [22]. On the one hand, equilibrium theories are employed in the so-called **ideal chromatography**, when mobile and stationary phases are constantly at equilibrium, since the rate of mass transfer kinetics is assumed to be infinite and axial dispersion negligible (column efficiency is infinite). In *linear, ideal chromatography* injection and band profiles correspond, the only difference states in a delay (time or volume) which depends on the retention factor and the mobile phase velocity. *Nonlinear, ideal chromatography* can provide information on the only influence of equilibrium thermodynamics on overloaded (or high-concentration) band profiles, independently from mass transfer kinetics and axial dispersion.
On the other hand, **nonideal chromatography** describes a more realistic case through kinetic theories, where the column has a finite efficiency and non-equilibrium effects take place due to slow mass transfer or adsorption processes. Several models are available and will be discussed in Chapter 3
However, during a chromatographic process both mass transfer phenomena and equilibrium thermodynamics could change depending on experimental conditions [23]. By assuming that no reaction take place between the components of the chromatographic system, it follows that the only constant parameter is the mass of the injected samples. For this reason, a differential mass balance equation (MBE) for each single component of the system could be written. This equation describes the accumulation of each component in a slice of column of thickness ∂z in a ∂t time interval (Fig. 2.1). In order to correctly solve the system of partial differential

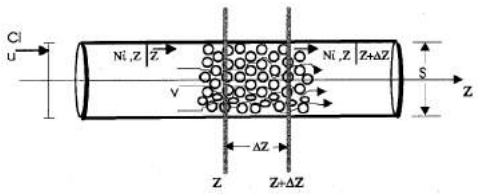

Figure 2.1: Differential mass balance in a column slice. [23]

equations, a set of initial and boundary conditions and the relationship between the concentrations of the analytes in the mobile and stationary phases must be defined.

2.1 The ideal model

The ideal model of chromatography assumes that the equilibrium between the two phases, mobile and stationary, is instantaneous and that there are no sources of band broadening of kinetic origin, since the efficiency of the chromatographic column is infinite [22–26]. Under these assumptions the differential mass balance equation for a single component is:

$$\frac{\partial C}{\partial t} + F\frac{\partial q}{\partial t} + u\frac{\partial C}{\partial z} = 0 \tag{2.1}$$

where C and q are the concentrations of the analyte in the mobile and stationary phases, respectively. $F = ((1 - \epsilon_t)/\epsilon_t)$ is the phase ratio and $\epsilon_t = V_0/V_{col}$ the total porosity of the column (with V_0 and V_{col} the thermodynamic void volume and the column volume, respectively).

Through the use of the theory of characteristics, it is possible to study the migration and the change of a band profile during a chromatographic experiment. Eq. 2.1 can be rewritten as:

$$\frac{\partial C}{\partial t} + \frac{u}{1 + F\frac{dq}{dC}}\frac{\partial C}{\partial z} = 0 \tag{2.2}$$

This equation shows that the migration velocity of a given concentration zone, u_z, is associated to the mobile phase concentration, C, and to the local curvature of the isotherm (Fig. 2.2):

$$u_z = \frac{u}{1 + F\frac{dq}{dC}} \tag{2.3}$$

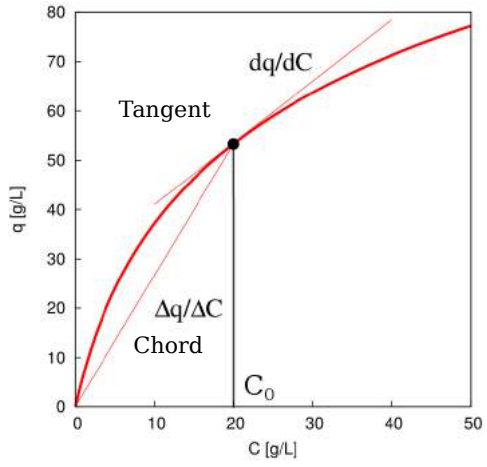

Figure 2.2: Graphical explanation of migration velocity associated with a concentration (isotherm tangent) and velocity of molecules at C_0 (chord).

As a consequence, the velocity u_z associated with a concentration is constant. On the contrary, molecules contained in a volume of solution at concentration C migrate at the velocity U_s, given by the slope of the isotherm chord, $\Delta q/\Delta C$ (Fig. 2.2), of the concentration shock generated on the front of the band:

$$U_s = \frac{u}{1 + F\frac{\Delta q}{\Delta C}} \tag{2.4}$$

2.2 The equilibrium-dispersive model

The Equilibrium Dispersive (ED) model assumes that mobile and stationary phases are always in equilibrium and the contributions to band broadening (axial dispersion and mass transfer kinetics) are lumped into an apparent axial dispersion term, D_a, calculated under linear conditions [23]. A single component system can be described by one single partial differential equation, the mass balance equation:

$$\frac{\partial C}{\partial t} + F\frac{\partial q}{\partial t} + u\frac{\partial C}{\partial z} = D_a\frac{\partial^2 C}{\partial z^2} \tag{2.5}$$

and by two other equations:

$$q = f(C) \quad \text{and} \quad D_a = \frac{uL}{2N} \tag{2.6}$$

with q the isotherm equation, L the column length and N the the number of theoretical plates.

2.3 The Lumped Kinetic Model

In the lumped kinetic model all nonequilibrium effects related to band broadening are described by a simple first-order kinetic equation:

$$\frac{\partial q}{\partial t} = k_I c - k_{II} q \tag{2.7}$$

with k_I and k_{II} rate constants. This model can be applied to different cases depending on the rate limiting step of the process (adsorption-desorption or mass-transfer kinetics). Concerning linear chromatography, one has:

$$\frac{\partial q}{\partial t} = k'_m\Big(c - \frac{q}{a}\Big) \tag{2.8}$$

with $a = q/c^*$ the Henry's constant, c^* is the mobile phase concentration in equilibrium with the stationary phase concentration q and k'_m the apparent mass-transfer coefficient.

The solution of this model (Eq. 2.5 and 2.8) under linear conditions can be derived in the Laplace domain [22, 27]. The study of the moments of the concentration profile resulting from a pulse injection leads to the plate height equation [28]:

$$H = \frac{2D_a}{u} + \frac{2u}{k'_m F}\Big(\frac{k}{1+k}\Big)^2 \tag{2.9}$$

where $k = aF$ is the retention factor. van Deemter et al. assumed that the D_a coefficient is made of two contributions: the molecular diffusivity (with D_m the molecular diffusion coefficient) and eddy dispersion.

$$D_a = \gamma D_m + \lambda d_p u \tag{2.10}$$

with d_p the particle diameter, γ and λ constants.
The combination of Eq. 2.11 and 2.10 leads to the well known van Deemter equation:

$$H = A + \frac{B}{u} + Cu \tag{2.11}$$

Eq. 2.11 states that H is the sum of the independent transport and kinetics phenomena.

2.4 The General Rate Model

The general rate model takes into account all the contributions of transport and kinetic phenomena to the band broadening. Indeed, it considers two different mass balance equations for the analyte: one related to the mobile phase percolating between the interstitial volume of packed particles and one for the stagnant mobile phase inside the pores. Moreover, diffusion is supposed to take place between the flowing stream of mobile phase and the stagnant mobile phase, while adsorption-desorption kinetics between the stagnant mobile phase and the surface of the adsorbent.
The mass balance equation in the bulk mobile phase in the interstitial volume of particles is written:

$$\frac{\partial C}{\partial t} + u_h \frac{\partial C}{\partial z} + F\frac{\partial \bar{q}}{\partial t} = D_L \frac{\partial^2 C}{\partial z^2} \tag{2.12}$$

with r_p the particle radius, D_L the axial dispersion coefficient expressed as the sum of the molecular and the eddy diffusion coefficients, $\partial\bar{q}/\partial t = 3/(r_p M_F)$ is the rate of adsorption averaged over the particle, where M_F is the mass flux of the analyte from the bulk mobile phase to the external surface of the stationary phase and r_p the particle diameter.

The diffusion of the solute inside the pores of the stationary phase particles is described through the following partial differential equation:

$$\epsilon_p \frac{\partial C_p}{\partial t} + (1+\epsilon_p)\frac{\partial C_s}{\partial t} = D_p\left(\frac{\partial^2 C_p}{\partial r^2} + \frac{2}{r}\frac{\partial C_p}{\partial r}\right) \tag{2.13}$$

where ϵ_p is the particle porosity, D_p the analyte diffusion coefficient inside the pores, C_p and C_s the concentration of the analyte inside the pores and adsorbed on the stationary phase, respectively.
The analytical solution of the general rate model under linear conditions can be derived in the Laplace domain after some simplifications and the moments of this analytical solution can easily be derived in the time domain. From the moments, the plate height equation can be obtained. The HETP is defined as follows [22]:

$$H = \frac{L}{N} = \frac{\sigma^2}{t_R^2} = \frac{\bar{\mu}_2}{\mu_1^2}L \tag{2.14}$$

where $\sigma^2 = \bar{\mu}_2$ is the second moment and μ_1 the first moment.
If the injection pulse has a negligible width, one can obtain:

$$H = \frac{2D_L}{u} + 2\left(\frac{k_1}{1+k_1}\right)^2\left[\frac{ud_p^2}{60FD_p} + \frac{ud_p}{6Fk_f} + \left(\frac{k_p}{1+k_p}\right)^2\frac{u}{Fk_{ads}}\right] \tag{2.15}$$

with k_f the rate coefficient and k_{ads} the adsorption rate constant. k_1 and k_p are defined as follows:

$$k_1 = F\Big[\epsilon_p + (1-\epsilon_p)K_a\Big] \quad \text{and} \quad k_p = \frac{1-\epsilon_p}{\epsilon_p}K_a \tag{2.16}$$

with K_a the adsorption equilibrium constant. Also in this case, after some manipulations, Eq. 2.15 is found to be equivalent to Eq. 2.11.

CHAPTER 3

Equilibrium Isotherms

The knowledge of the equilibrium adsorption isotherm of the component(s) is pivotal for the integration of the differential mass balance equations reported in Chapter 2, independently from the model of chromatography used. Adsorption isotherms correlate the concentration of each analyte in the mobile, C, and in the stationary phase, q, at equilibrium and at constant temperature and pressure. All the possible interactions between the solutes and the two phases, mobile and stationary, have an influence on the adsorption isotherm. For this reason, these functions provide information on thermodynamic properties able to describe band profiles and chromatographic separations in nonlinear conditions.
There are a lot of different adsorption models available in literature, able to correctly fit experimental profiles, accounting for the heterogeneity of the adsorbent surface and all the possible interactions between adsorbate-adsorbent and adsorbate-adsorbate.

3.1 Ideal Adsorption on Homogeneous Surfaces

This first type of isotherms assumes a localized adsorption on a homogeneous surface with no significant adsorbate–adsorbate interactions.

3.1.1 Linear isotherm

The linear isotherm is useful for analyical applications where small concentrations and small amounts of analyte are commonly employed. It considers the concentrations in the mobile, C, and in the stationary, q, phases directly proportional:

$$q = a\,C \tag{3.1}$$

where the slope, $a = k/F$, is related to the retention factor of the analyte, k.
The only drawback is that this isotherm is not able to accurately describe nonlinear or preparative chromatography, where the competition of adsorbed molecules cannot be neglected.

3.1.2 Langmuir isotherm

The Langmuir isotherm is the simplest and one of the most frequently used model to describe adsorption in liquid chromatography. It assumes that the adsorption process is monolayer with no adsorbate-adsorbate interactions and that the surface is made by only one type of adsorption site, leading to a homogeneous adsorption. The Langmuir isotherm is defined as:

$$q = \frac{q_s b C}{1 + bC} \tag{3.2}$$

with q_s the saturation capacity and b the adsorption or binding constant. It is worth noting that if $C \to 0$, Eq. 3.2 reduces to a linear isotherm $q = q_s b\, C$, with $q_s b = a$, the Henry's constant.
This model can also be applied to chiral separations following the assumption that only enantioselective interactions are significant, *i.e.* nonselective interactions are considered to have a negligible contribution to retention of enantiomers. It follows that average energies and constants of adsorption can be defined for each enantiomer (denoted hereafter i= 1,2), leading to the definition of the competitive Langmuir model:

$$q_i = \frac{q_s b_i C_i}{1 + b_1 C_1 + b_2 C_2} \tag{3.3}$$

3.2 Ideal Adsorption on Heterogeneous Surfaces

This type of isotherms assumes a localized adsorption on a heterogeneous surface with no significant adsorbate–adsorbate interactions.

3.2.1 Bilangmuir isotherm

The bilangmuir adsorption model considers two different types of homogeneous sites on the adsorbent surface, *i.e.* covered with two different kinds of chemical groups. As a consequence, the isotherm equation is derived from the addition of the two independent contributions of the two sites (1 and 2) [23, 29]:

$$q = \frac{a_1 C}{1 + b_1 C} + \frac{a_2 C}{1 + b_2 C} \tag{3.4}$$

In case of chiral separations, the two types of sites are considered selective (responsible for enantioselective interactions), sel, and nonselective (where both enantiomers behave identically), $nsel$ [30–33]. The competitive bilangmuir isotherm is then written as:

$$q_i = \frac{q_{sel} b_{i,sel} C_i}{1 + b_{1,sel} C_1 + b_{2,sel} C_2} + \frac{q_{nsel} b_{nsel} C_i}{1 + b_{nsel}(C_1 + C_2)} \tag{3.5}$$

3.2.2 Tóth isotherm

This type of isotherm assumes a unimodal adsorption energy distribution on a heterogeneous surface of adsorption, whose width is related to the parameter ν ($0 < \nu < 1$). For a single component system one has [23, 34]:

$$q = \frac{q_s b C}{\left[1 + (bC)^{\nu}\right]^{1/\nu}} \tag{3.6}$$

If $\nu \to 1$ Eq. 3.6 reduces to the Langmuir one (Eq. 3.2).
Also in this case, it is possible to correctly describe enantiomeric separations though a competitive Tóth isotherm model:

$$q_i = \frac{q_s b_i C_i}{\left[1 + (\sum_{i=1}^{N} b_i C_i)^{\nu}\right]^{1/\nu}} \tag{3.7}$$

It is worth noting that the heterogeneity parameter, ν, is the same for both enantiomers.

3.3 Nonideal Adsorption on a Homogeneous Surface

This class of isotherms account for homogeneous surfaces on which the adsorbed molecules interact, *i.e.* adsorption could be multilayer.

3.3.1 Moreau isotherm

The Moreau isotherm describes the adsorption on a homogeneous surface with a defined monolayer saturation capacity, q_s, with adsorbate–adsorbate interactions [35]:

$$q = q_s \frac{bC + Ib^2C^2}{1 + 2bC + Ib^2C^2} \tag{3.8}$$

with I the adsorbate–adsorbate interaction parameters, also defined as:

$$I = exp\Big(\frac{\epsilon_{AA}}{RT}\Big) \tag{3.9}$$

where ϵ_{AA} is the interaction energy between two adsorbed molecules A, R is the universal gas constant and T is the absolute temperature.

3.3.2 BET isotherm

The extended liquid–solid BET isotherm assumes that the adsorption process can take place onto the bare silica surface or onto an already adsorbed layer of analyte, with b_s and b_l equilibrium constants [23, 36, 37]. The equation is:

$$q = \frac{q_s b_s C}{(1 - b_l C)(1 - b_l C + b_s C)} \tag{3.10}$$

If $b_l\, C \ll 1$ the former equation coincides with Eq. 3.2, that is the classical convex upward Langmuir isotherm. Conversely, when the interaction energy between two adsorbate molecules increases, the system is described by a convex downward type isotherm.

3.4 Surface Excess and Excess Isotherms

Excess isotherm describes the adsorption behaviour of mobile phase components (commonly a binary mixture of solvents) on the surface of the adsorbent; for this reason its knowledge is pivotal for the deep understanding of the chromatographic processes and separations. Mobile phase components, due to their characteristics, could be selectively adsorbed or adsorbed in different amounts on the surface of the adsorbent particles, having a deep influence on the retention behaviour of the analytes. Excess adsorption isotherms can provide clues on differences of the adsorption of solvents, able to describe packing properties, such as polar properties (amount of free residual silanols), hydrophobic properties (coverage density) and homogeneity of bonded ligands [38, 39].
For the calculation of excess isotherm the so-called minor disturbance method has been used (also referred to as 'peak on a plateau' method [23]). It consists in generating small perturbations, made by an injection of an excess of one of the mobile phase components over the other, when a steady-state equilibrium between mobile and stationary phase has been reached. These perturbations are able to generate peaks that move through the column with a linear velocity defined as [40]:

$$u_{\phi A} = \frac{F_v L}{V_0 + S\big[(d\Gamma_A)/(d\phi_A)\big]} \tag{3.11}$$

where ϕ_A is the volume fraction of component A in the bulk mixture, F_v the volumetric flow rate, V_0 the thermodynamic void volume, S the total surface area of the adsorbent in the column and Γ_A is the surface excess of component A. The retention volume of the disturbance peak can therefore be written as:

$$V_{R,A}(\phi) = \frac{F_v L}{u_{\phi_A}} = V_0 + S\frac{d\Gamma_A}{d\phi_A} \tag{3.12}$$

The integration of the Eq. 3.14 leads to the definition of the excess adsorption expression:

$$\Gamma_A = \frac{1}{S}\int_0^1 \big(V_{R,A}(\phi) - V_0\big)d\phi_A \tag{3.13}$$

where V_0 is calculated by:

$$V_0 = \int_0^1 V_{R,A}(\phi)\, d\phi \tag{3.14}$$

In order to have the complete dependence of the excess amount (or the retention times of the perturbation) of one of the two compounds over the entire concentration range, it is necessary to repeat the experiment with different mobile phase compositions, covering the range from one pure component to the other.
It is possible to rewrite the surface excess by using volumes and volume fraction concentration, as indicated by many authors [40–42]:

$$\Gamma_A = V_A^a - V^a\phi_A \tag{3.15}$$

with V_A^a the volume of component A adsorbed and V^a the volume of the adsorbed phase.
By extrapolating the slope of the excess isotherm on the decreasing branch in its linear region [41], it is possible to estimate the total amount of component A adsorbed on the adsorbent surface. The equation of the tangent is given by:

$$V_A^a \equiv \Gamma_A + V^a\phi_A \equiv b + ax \tag{3.16}$$

with a and b the slope of the inflection tangent and the y-intercept.

3.5 Large-Scale Purification of Large Biomolecules

The principles of nonlinear chromatography and the study of adsorption isotherms can be applied to large-scale purifications of large biomolecules in order to gain indispensable information able to describe and predict band profiles and separations under overloaded chromatographic conditions. It is well known that therapeutic peptides and proteins are to be purified from their related impurities in order to reach the desired degree of purity required for pharmaceutical scopes and that the development of purification processes must be fast and not product consuming to possibly limit total manufacturing costs. To this end, process modeling for the description of analyte elution, based on thermodynamic studies, could be a useful tool for the design and optimization of experimental process parameters.

3.5.1 Overloaded gradient elution chromatography

In gradient elution, the fraction of the organic modifier, ϕ (and by consequence the eluotropic strength of the mobile phase) is progressively increased during a chromatographic run. Gradient elution chromatography is usually used for the separation of complex mixtures in which the retention factors of the analytes have a strong dependence on the percentage of modifier in the mobile phase, such as proteins and peptides. In this case, the equilibrium isotherm is not constant during the separation, *i.e.* the velocity associated with a concentration in the ideal model depends on time and location, contrary to isocratic separations. To account for these changes, it is assumed that the isotherm parameters are a function of ϕ, independently from the gradient. In order to model gradient elution when a linear gradient [43] is used, it is worth introducing the linear solvent strength (LSS) model [44–47] for reversed-phase HPLC, which describes the variation of retention factor, k, with ϕ [48]:

$$\ln k(\phi) = \ln k_0 - S\phi \tag{3.17}$$

with k_0 the retention factor (extrapolated) at $\phi = 0$ and S a characteristic coefficient of the system solute-mobile phase composition. Taking into account the simple Langmuir isotherm (Eq. 3.2) the relationship between isotherm parameters (namely a and b) and ϕ can be easily obtained, knowing that $k = aF = q_s bF$:

$$a(\phi) = a_0\, e^{(-S\phi)} \tag{3.18}$$

where $a_0\,(= k_0/F)$ is the Henry's constant at $\phi = 0$. In the hypothesis that q_s remains unchanged in the range of variation of ϕ [23,49,50] , b and ϕ are correlated by the same relation as in Eq. 3.18:

$$b(\phi) = b_0\, e^{(-S\phi)} \tag{3.19}$$

where b_0 is the adsorption constant at $\phi = 0$. Through the combinations of the Lanmguir equation (Eq. 3.2) and Eq. 3.19, the isotherm describing the adsorption process under a linear gradient can be defined:

$$q(\phi) = \frac{q_s\, b_0\, e^{(-S\phi)} C}{1 + b_0\, e^{(-S\phi)} C} \tag{3.20}$$

3.5.2 Affinity Chromatography for Protein Purification

The purification of biomolecules is a very challenging process due to the presence of a very complex mixture of other cell culture components [51]. Concerning non-mAb proteins, a new downstream scheme has to be developed for each molecule. Affinity chromatography is one of the most powerful technique used to perform recombinant protein capture and purification. It is based on the use of affinity tags which provide a specific and reversible interaction between the protein of interest (POI) and a ligand covalently bonded on the solid support [52]. Proteases are often used for the removal of the tag from the POI, which makes the method expensive and with low specificity, and as a consequence not suitable for large-scale purifications [53]. In order to undergo these problems, to simplify the purification process and to achieve high protein yield and purity, a "universal" downstream template, based on split-intein affinity chromatography, has been used.
Inteins are self-splicing elements able to excise themselves from a host-intein precursor protein through a process known as "protein splicing". Due to their cleaving ability, the stationary phase resin is functionalized with a N-intein affinity tag, while the C-terminal intein is fused to the POI as a tag. The capture of the POI from the crude lysate occurs due to the high affinity between these two tags. A pH-shift triggers the intein-mediated C-terminal cleavage reaction, causing the release of the POI, as reported in Fig. 3.1. After the elution, a regeneration step is required in order to get rid of the C-intein tag.

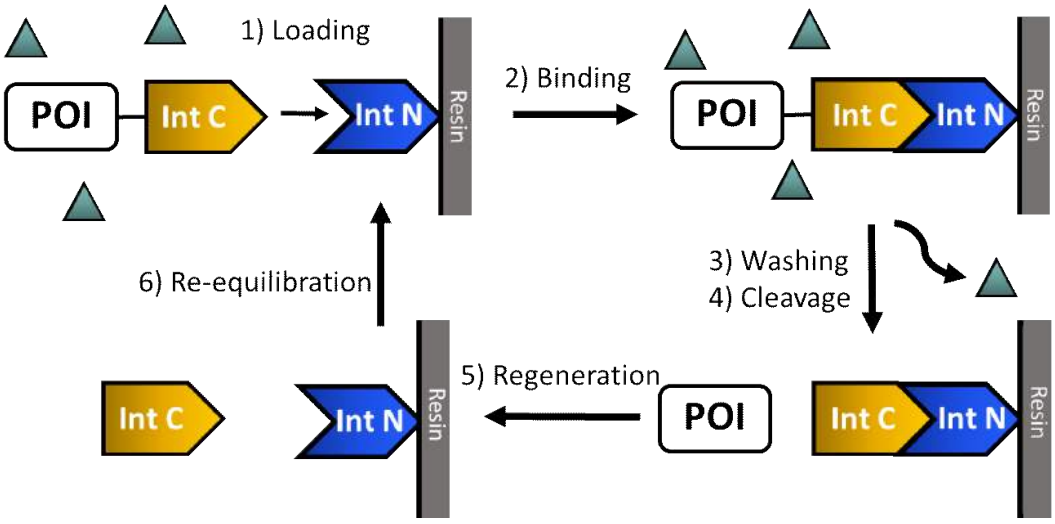

Figure 3.1: Intein resin purification and regeneration cycle. Triangles: other cell components.

This chromatographic process is modeled through the lumped kinetic model:

$$\frac{\partial q}{\partial t} = k'_m(q* - q) \tag{3.21}$$

with q the solid phase concentration of the protein, $q*$ the equilibrium solid phase concentration of the protein and k'_m the mass transfer coefficient. For the determination of k'_m the following expression, that approximates the effect of hindered mass transfer due to pore blockage and other effects, is used [54]:

$$k'_m = k_m^{max}\left[S_1 + (1 - S1)\Big(1 - \frac{q}{q_s}\Big)\right] \tag{3.22}$$

with k_m^{max} the maximum mass transfer coefficient when there is no protein adsorption, S_1 describes the maximum hindrance, S_2 indicates the non-linearity of the increase in hindrance and q_s the saturation capacity of the resin. All the above mentioned parameters are obtained from the breakthrough curves fittings at different flow rates and concentrations.

A modified Lanmguir isotherm is used for the description of the adsorption of the protein:

$$H = H_{ref}\left(\frac{pH}{pH_{ref}}\right)^N \qquad q* = \frac{Hc}{1 + Hc/q_s} \tag{3.23}$$

where H is the Henry's coefficient, H_{ref} is is the Henry's coefficient measured at the reference pH value, pH_{ref}, and N is the change of the Henry's coefficient with the pH. H_{ref} and q_s are directly derived from breakthrough curves fittings [55].

CHAPTER 4

Mass transfer kinetics in liquid chromatography

In this chapter the fundamental theoretical basis of mass transfer kinetics in liquid chromatography are presented.
The detailed study of the different sources of band broadening of kinetic origin (diffusion, eddy dispersion, mass transfer resistance, finite rate of adsorption/desorption process) is possible only under linear conditions, since in this case the influence of thermodynamic equilibria on band profiles becomes negligible [23].
The well known van Deemter equation correlates the high equivalent to a theoretical plate, H (or its adimensional form $h = H/d_p$ with d_p the particle diameter) to the interstitial velocity, u_e (or ν in reduced coordinates), and permits the evaluation of the efficiency of a chromatographic column [56]. It is defined as:

$$h = a(\nu) + \frac{b}{\nu} + c_s\nu + c_{ads}\nu + h_{heat} \tag{4.1}$$

where $a(\nu)$ is the eddy dispersion, b the longitudinal diffusion, c_s the solid-liquid mass transfer resistance across the stationary phase and c_{ads} accounts for slow adsorption–desorption kinetics (in achiral RP-LC this term is usually negligible) and finally h_{heat} is an additional source of band broadening due to the friction between the eluent at high flow rate and particles.
The interstitial velocity is defined as:

$$\nu = \frac{F_v d_p}{\pi r^2 \epsilon_e D_m} \tag{4.2}$$

being r the column radius, ϵ_e the external porosity and D_m the bulk molecular diffusion coefficient.
The independent evaluation of the single factors contributing to band broadening is made possible through the coupling of proper models of diffusion in porous media and experimental measurements [56–63].

4.1 Longitudinal diffusion

The longitudinal diffusion term (b term of Eq. 4.1) can be easily estimated through peak parking (PP) experiments [64–66] since it is the only contribution to band broadening in absence of flow, due to the relaxation of axial concentration gradient through the porous particles and the interstitial volume. PP consists in different steps: i) small injection of analyte at a defined flow rate; ii) the flow is switched off when the analyte reaches roughly the middle of the column; iii) the band is free to diffuse for a defined parking time, t_p; iv) the flow is resumed at the previous flow rate. From PP, the effective diffusion coefficient, D_{eff}, can be calculated by plotting the variance of the chromatographic peak, σ_x^2 , to the parking time, t_p:

$$D_{eff} = \frac{1}{2}\frac{\Delta\sigma_x^2}{\Delta t_p} \tag{4.3}$$

The longitudinal diffusion term can therefore be calculated:

$$b = 2(1+k_1)\frac{D_{eff}}{D_m} = 2\big(1+k_1\big)\gamma_{eff} \tag{4.4}$$

where D_m is the molecular diffusion coefficient of the analyte in the mobile phase mixture, γ_{eff} is the dimesionless effective diffusion coefficient and k_1 ($= (t_R - t_e)/t_e$) is the so-called zone retention factor, being t_R the retention time and t_e the time spent by the molecule in the interstitial volume.

4.1.1 Models of diffusion in porous media

D_{eff} accounts for all the contributions to diffusion of the analyte in the composite material made of the porous zone impregnated by the eluent (D_p) and the bulk mobile phase (D_m). For the interpretation of D_{eff} different models are available in literature: the simple time-averaged diffusion model elaborated by Knox [65] and the more realistic Effective Medium Theory (EMT) models of Maxwell and Torquato [67–70].

Time-averaged or parallel model

The time-averaged diffusion model, also referred to as parallel model, was elaborated by Knox in 1983 [65]. It assumes that the mass fluxes in the particles and in the external eluent are additive:

$$D_{eff} = \frac{\gamma_e D_m + \frac{1-\epsilon_e}{\epsilon_e}\big(1-\rho^3\big)D_p}{1+k_1} \tag{4.5}$$

with γ_e the obstructive geometrical factor and $\rho = r_{core}/r_p$ is the ratio between the radius of the core and that of the whole particle (ρ = 0 for fully porous particles and 1 for non-porous ones). This model, despite the simple description of the distribution of the sample in the different phases, provides approximate yet acceptable values for D_{eff}.

Effective Medium Theory

Effective medium theories (EMT) are able to correctly describe the micro-structure of particles leading to a much more accurate representations of D_{eff}.
Maxwell Model: The Maxwell model is the most basic and simple variant among all the EMT models [60]. It considers:

$$b = 2\big(1 + k_1\big)\gamma_{eff} = \frac{2}{\epsilon_e} \cdot \frac{1 + 2\beta(1 - \epsilon_e)}{1 - \beta(1 - \epsilon_e)} \tag{4.6}$$

with β the polarizability constant:

$$\beta = \frac{\alpha_{part} - 1}{\alpha_{part} + 2} \tag{4.7}$$

and α_{part} is the relative particle permeability defined as the ratio of the permeability of the particle zone (including diffusion in the stagnant mobile phase and surface diffusion), D_{part}, over that of the interstitial zone, D_m:

$$\alpha_{part} = \frac{\epsilon_e k_1}{1 - \epsilon_e} \cdot \frac{D_{part}}{D_m} \tag{4.8}$$

Torquato Model: The Torquato model is an extension of the Maxwell model and provides a more accurate description of the effective properties of a composite material since it takes into account the random distribution of porous (being both fully porous and core-shell) particles inside the column [60, 71, 72].

$$D_{eff} = \frac{1}{\epsilon_e(1 + k_1)} \left[\frac{1 + 2(1 - \epsilon_e)\beta - 2\epsilon_e\xi_2\beta^2}{1 - (1 - \epsilon_e)\beta - 2\epsilon_e\xi_2\beta^2} \right] D_m \tag{4.9}$$

with

$$\beta = \frac{\frac{1-\rho^3}{1+\rho^3/2}\Omega - 1}{\frac{1-\rho^3}{1+\rho^3/2}\Omega + 2} \tag{4.10}$$

ξ_2 is equal to 0.3277 if core-shell particles are in physical contact [71].

4.2 Solid-liquid mass transfer resistance

The c_s term of Eq. 4.1 describes the solid-liquid mass transfer resistance due to the diffusion across the porous particle. This term can be calculated theoretically by the

Laplace transform of the general rate model of chromatography [72–74]:

$$c_s = \frac{1}{30} \cdot \frac{\epsilon_e}{1-\epsilon_e} \left(\frac{k_1}{1+k_1} \right)^2 \left[\frac{1+2\rho+3\rho^2-\rho^3-5\rho^4}{(1+\rho+\rho^2)^2} \right] \cdot \frac{D_m}{D_p} \tag{4.11}$$

4.3 Adsorption-desorption kinetics

The c_{ads} term of Eq. 4.1 accounts for the finite rate of adsorption and desorption of analyte molecules between the adsorbed layer and the pores filled of eluent. In case of small molecular weight compounds this term has a negligible effect on h, due to the very high adsorption rate constant, k_a [72, 74]. On the other hand, concerning proteins and the most retained enantiomer in case of chiral analytes, the adsorption-desorption process could have a significant impact on the efficiency of the separation. The c_{ads} term is derived according to the Laplace transform of the general rate model of chromatography [23, 75–77]:

$$c_{ads} = 2 \cdot \frac{\epsilon_e}{1-\epsilon_e} \cdot \frac{1}{1-\epsilon_p} \cdot \frac{1}{1-\rho^3} \left(\frac{k_1}{1+k_1} \right)^2 \left(\frac{k_p}{1+k_p} \right)^2 \frac{D_m}{k_{ads} d_p^2} \tag{4.12}$$

with $k_p = (1-\epsilon_p)K_a/\epsilon_p$ (where K_a is the adsorption equilibrium constant) and k_{ads} the kinetic adsorption constant.

4.4 Eddy dispersion

The eddy dispersion term (a term of Eq. 4.1) is due to the irregularities in the stream path in the through-pores of the packed beds. Three classes of flow heterogeneities can be defined, as reported by Giddings [78]: trans-channel eddy dispersion, short-range inter-channel eddy dispersion and trans-column eddy dispersion. However, a mathematical expression describing the correct and complete structure of the packed beds has not been found yet. As a consequence, $a(\nu)$ can be experimentally estimated by subtracting to h the values of b and c [72].
On the one hand, concerning achiral systems (where $c_{ads} = 0$), one has:

$$a(\nu) = h - \frac{b}{\nu} - c_s \nu \tag{4.13}$$

On the other hand, in chiral systems (where $c_{ads} \neq 0$), an independent evaluation of $a(\nu)$ and c_{ads} cannot be obtained, since the following equation is derived:

$$a(\nu) + c_{ads}\nu = h - \frac{b}{\nu} - c_s \nu \tag{4.14}$$

CHAPTER 5

Results and Discussion

In the following chapter the results obtained during my Ph.D. studies are reported. For further details, the reader is referred to reprints of the full papers appended at the end of the thesis.
In the discussion, some sensitive data have been intentionally omitted.

5.1 Mass transfer kinetics in new generation porous particles for ultrafast high-efficient separations

5.1.1 Kinetic comparison of C_{18} columns prepared on SPPs and FPPs

Kinetic performance and mass transfer kinetics of three C_{18} 100×3 mm columns packed with 1.9 μm FPPs Titan^{TM} particles, 2.0 μm SPPs Ascentis particles and 1.7 μm FPPs BEH particles, respectively, have been investigated with mobile phase made of ACN/water 60:40 v/v. Titan particles are characterized by a narrow particle size distribution (nPSD) with a relative standard deviation (RSD) smaller than 10%, almost comparable to that of SPPs (roughly 5%), contrary to the normal trend for fully porous particles, with a RSD larger than 15%. Nevertheless, the gain in efficiency and performance of a nPSD is still under debate [72].
van Deemter curves have been measured for three analytes (nitrobenzene, toluene and butylbenzene) on the three columns and the single contributions to band broadening have been independently evaluated through peak parking (PP) method and Effective Medium Theory (EMT). As an example, in Fig. 5.1 van Deemter curves measured on the three columns for nitrobenzene are reported. 1.9 μm FPPs column displays excellent kinetic performances, comparable to 2.0 μm SPPs column in terms of number of plates per meter ($N/m \sim$ 300 000) at the minimum of the van Deemter curve, minimum plate height ($h_{min} \sim 1.6$) and optimal velocity ($\nu_{opt} > 6$) for the three compounds. The longitudinal diffusion term, b, was found to be

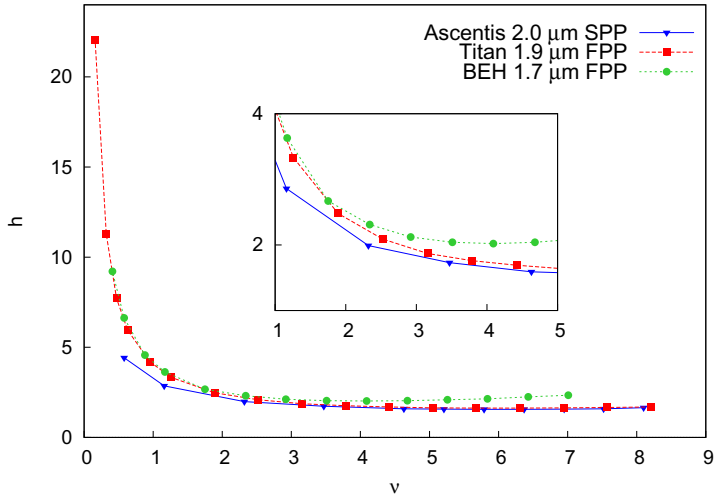

Figure 5.1: Overlapped reduced van Deemter curves measured on Ascentis, Titan and BEH columns for nitrobenzene. MP = ACN/water 60:40 v/v.

very similar on the two FPPs columns and 40% lower on the SPPs column, due to the presence of the solid core. This explains the lower van Deemter curve measured for SPPs column at small interstitial velocities if compared to its FPPs counterparts. On the other hand, solid-liquid mass transfer coefficients, c_s, are very close for the three columns, with a maximum difference of 20% between SPPs and 1.9 μm FPPs. Eddy dispersion term contributions ($a(\nu)$) for the three columns are reported in Fig. 5.2. As can be evinced, on the one hand, for the 1.7 μm FPPs column the effect of

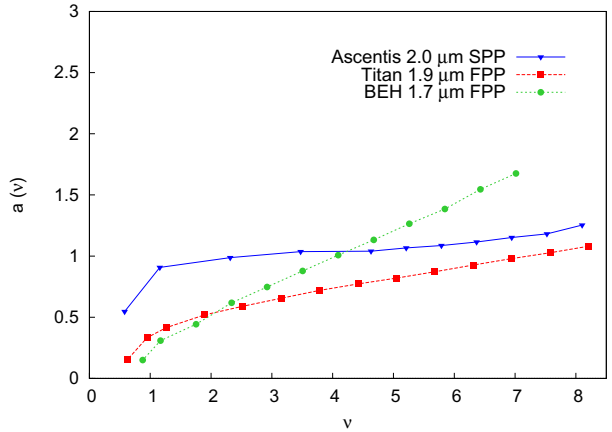

Figure 5.2: Eddy dispersion, $a(\nu)$, contributions for nitrobenzene on the three columns.

frictional heating is particularly evident from the rapid growth of the plot when $\nu >$ 2.5. On the other hand, $a(\nu)$ values measured on the 1.9 μm FPPs column are lower if compared to SPPs column, indicating that the narrow particle size distribution is responsible for reduced flow inhomogeneities in the packed bed, contributing to make the overall efficiency comparable to that measured on SPPs column.

5.1.2 Kinetic comparison of CSPs prepared on SPPs and FPPs (Papers I, II, III, IV, VIII, IX and X)

Chromatographic behavior and performance of columns designed for ultrafast high performance enantioseparations and packed with both sub 2-μm and sub 3-μm fully porous particles and the second generation of core-shell particles have been investigated under different chromatographic conditions and with different analytes.
CSPs have been prepared with different chiral selectors, as reported in Fig. 5.3, including macrocyclic glycopeptides, polysaccharides, Pirkle-type ones, cyclofructans and ion-exchangers, to name but a few.
Whelk-O1 Pirkle type (or brush-type) chiral selector was the first to be investigated (Fig. 5.3 b). The synthesis of this type of selector is particularly easy (even with sub-2μm particles), since both particle aggregation and clogging are absent [79]. Furthermore, Whelk-O1 selector offers a wide range of applications since it can be used in normal phase (NP), polar organic mode (POM), reversed phase (RP) and supercritical fluid chromatography (SFC) conditions. Moreover, it is stable at high pressure and temperature, leading to a high selectivity over a broad range of chiral compounds and mass transfer kinetics are supposed to be fast. All these reasons lead to the use of Whelk-O1 selector for ultrafast enantioseparations.
The study was conducted on 2.5 μm and 1.8 μm FPPs and 2.6 μm SPPs functionalized with Whelk-O1 chiral selector with the same preparation protocol. Nevertheless, SPPs column showed a larger surface density of chiral selector (20%) if compared to its FPPs counterparts. Kinetic and thermodynamic properties of these three columns have been investigated in normal phase conditions using *trans*-stilbene oxide (TSO) enantiomers as probe compounds. In Fig. 5.4 chromatograms showing the separation of TSO enantiomers at the minimum of the van Deemter curve on the three columns are reported. On the one hand, from these plots it is evinced that the two FPPs have the same k and α values, while SPPs column exhibits smaller retention and larger selectivity, probably due to the higher surface density of chiral selector. On the other hand, the efficiencies registered on the three columns are comparable with those usually reported for RPLC ($N/m > 200\,000$) (**X**).
Thanks to the advances in particle functionalization and production, the use of short columns (1 cm long) and very high flow rates (5-8 mL/min) it is possible to resolve enantiomeric separation in less than 1 second (Figure 5.5) (**III**).

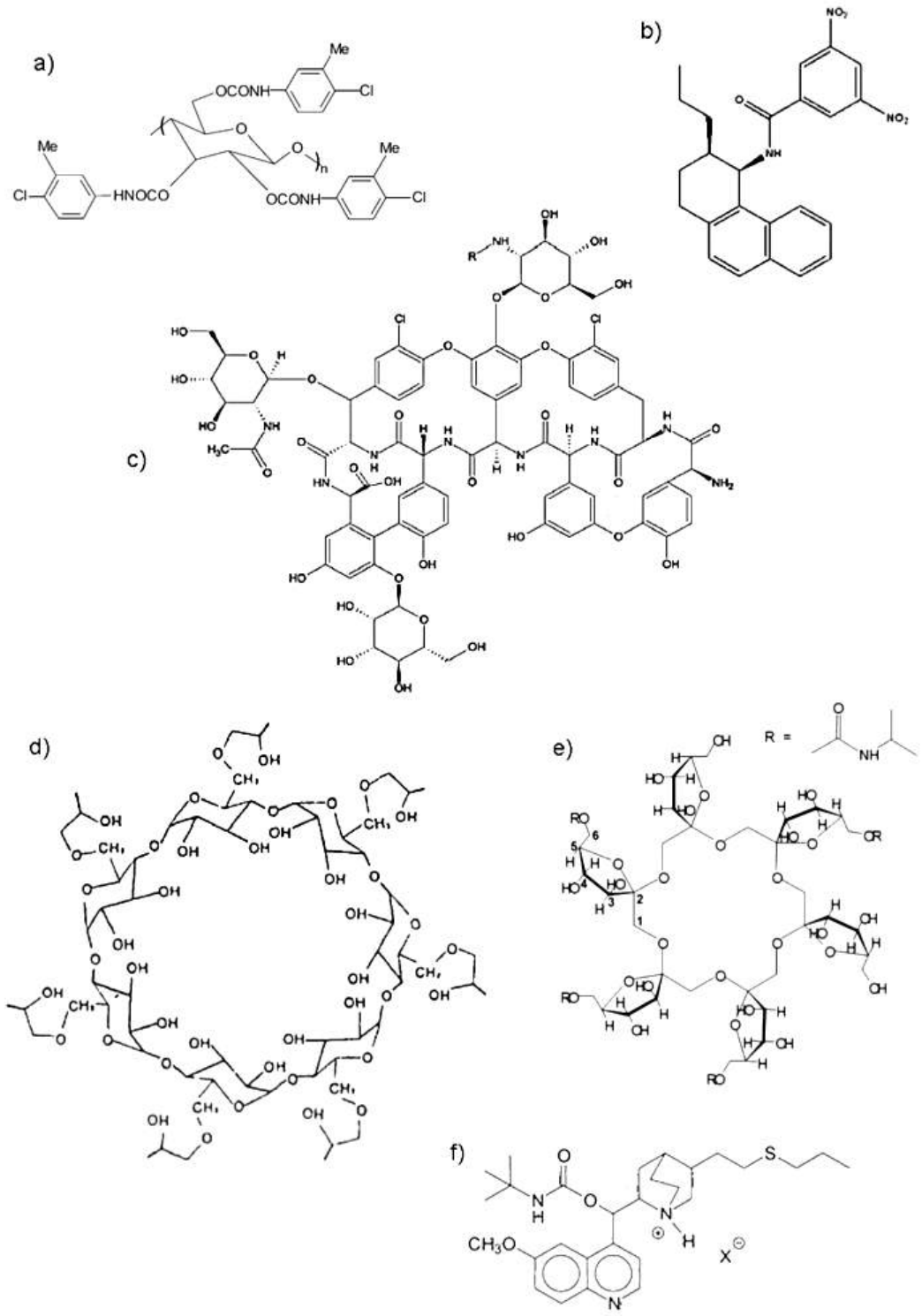

Figure 5.3: Chemical structures of chiral selectors employed for the preparation of CSPs. (a) Cellulose tris(4-chloro-3-methyl-phenylcarbamate); (b) Whelk-O1; (c) teicoplanin; (d) cyclodextrin; (e) cyclofructan functionalized with the isopropyl carbamate group (CF6-P); (f) quinine carbamate derivative. Reproduced from **I** with permission from The Royal Society of Chemistry.

Kinetic performance of a new CSP, prepared by covalently bonding a teicoplanin selector (Fig. 5.3 c) on 2.0 μm SPPs, has been compared with other two analogous CSPs based, respectively, on 2.7 μm SPPs and 1.9 μm FPPs in HILIC conditions (eluent: ACN/H_2O 85:15 + 20 mM ammonium formate). All CSPs were synthe-

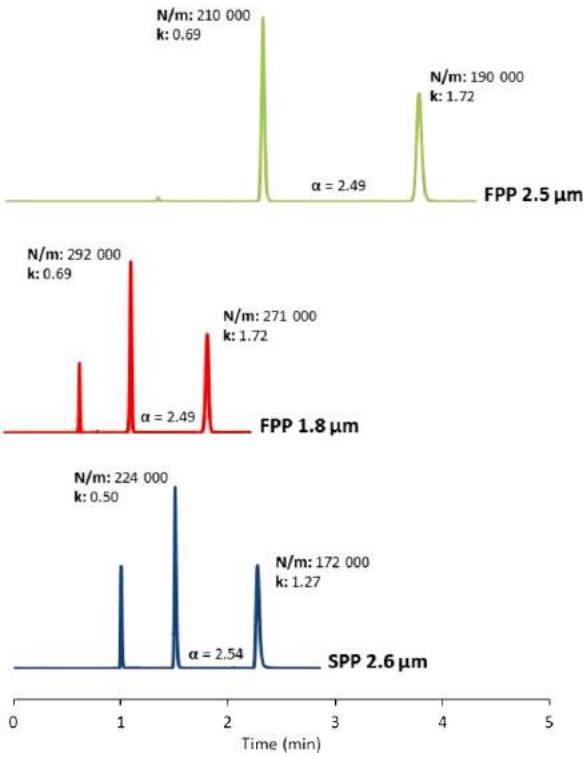

Figure 5.4: Separation of TSO enantiomers on the three columns at the flow rate corresponding to the minimum of the van Deemter curve (from top to bottom, respectively, 1.2, 1.8 and 1.5 mL/min). CCl_4 was used as dead volume marker. Retention factor (k), selectivity (α) and efficiency (N/m) are reported. (**X**)

sized according to the same proprietary bonding protocol immobilizing teicoplanin selector onto the three types of silica particles, leading to its zwitterionic version (**II**). Also in this case, a larger surface density of chiral selector has been found for SPPs, suggesting a larger accessibility of the external layers of this type of particles with respect to FPPs.

The comparison of van Deemter curves shows that the CSP prepared on 2.0 μm SPPs exhibited excellent performance (300 000 N/m), very close to that obtained in RP achiral chromatography, outperforming the other two CSPs prepared on 2.7 μm SPPs and 1.9 μm FPPs (Fig. 5.6). Moreover, this column is characterized by a very flat C-branch of the van Deemter curve, indicating an extremely fast mass transfer and by consequence the possibility to be operated at high flow rates without remarkable loss of efficiency. These CSPs can be used for the separation of different

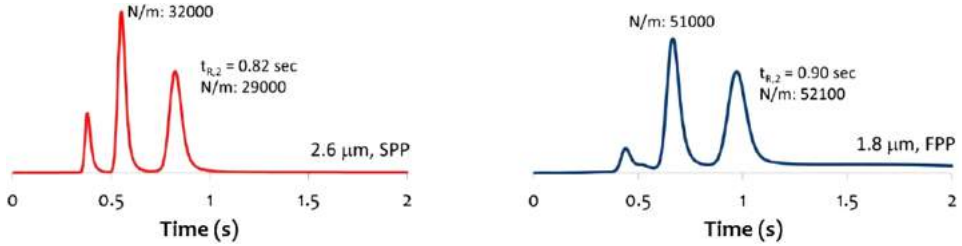

Figure 5.5: Ultrafast enantioseparations of TSO enantiomers on 10×3.0 mm columns packed with 2.6 μm SPPs (left) and 1.8 μm FPPs (right) Whelk-O1 CSPs. Reprinted from **III** with permission.

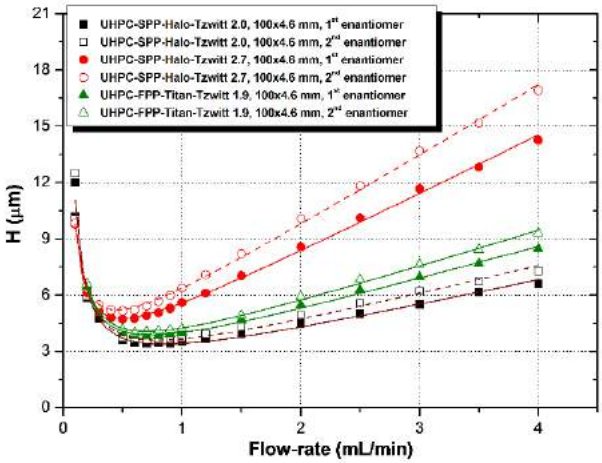

Figure 5.6: van Deemter plots of 1^{st} (solid lines) and 2^{nd} (dashed lines) eluted enantiomers of 2-(4-chloro-phenoxy)-propionic acid on the three 100×4.6 mm columns. Eluent: ACN/H_2O 85:15 + 20 mM $HCOONH_4$, T: 35°C. (**II**)

classes of compounds. As an example, the chromatograms of four chiral samples on the three columns are reported in Fig. 5.7. The 2.0 μm SPPs column, independently from the analyte, showed the highest resolution and the best efficiency values for the first eluted enantiomer and efficiency comparable to the 1.9 μm FPPs column for the second eluted enantiomer.

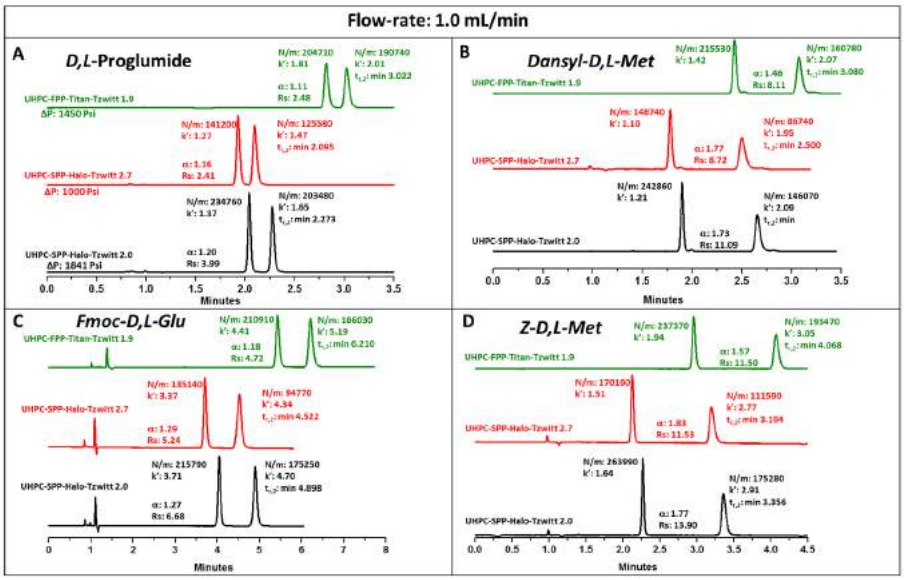

Figure 5.7: Separations of the racemic analytes on the three columns at flow-rate: 1.0 mL/min. (A) D,L-Proglumide, (B) Dansyl-D,L-Methionine, (C) Fmoc-D,L-Glutamine, (D) Z-D,L-Methionine. Eluent: ACN/H_2O 85:15 + 20 mM $HCOONH_4$, T: 35°C. (**II**)

In order to evaluate the impact of high porosity silica on the performance of these zwitterionic teicoplanin-based CSPs, three columns have been in-house packed with SP particles with different geometrical characteristics: 2.0 μm - 90Å, 2.7 μm - 90Å and 2.7 μm - 160Å (**IX**). In Fig. 5.8 and 5.9 van Deemter plots measured

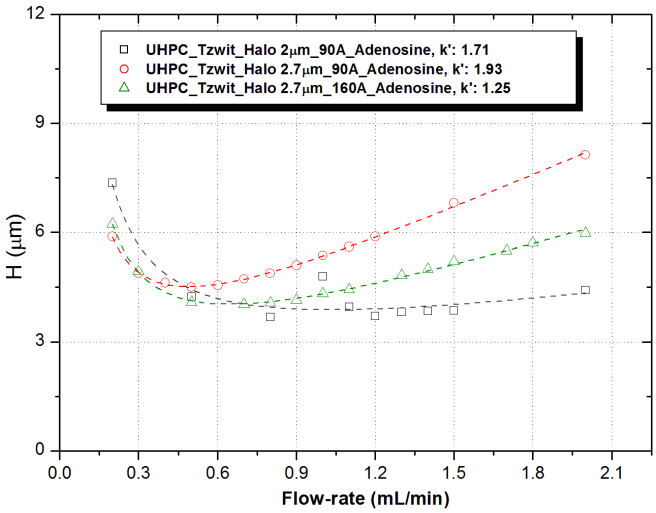

Figure 5.8: Comparison between van Deemter curves measured for Adenosine on the three columns. MP = ACN/H_2O 85/15 + 15 mM $HCOONH_4$, T = 35 °C. (**IX**)

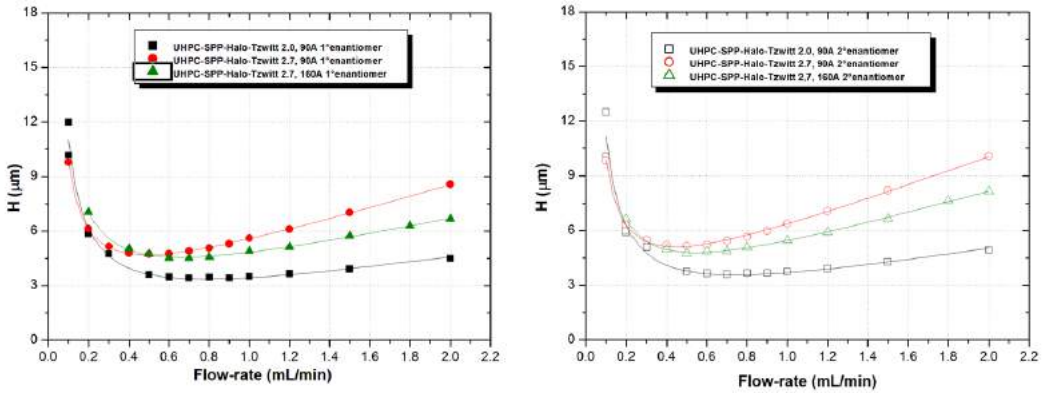

Figure 5.9: Comparison between van Deemter curves measured for 2-(4-Chloro-phenoxy)-propionic acid on the three columns. 1^{st} eluted enantiomer: left, 2^{nd} eluted enantiomer: right. MP = ACN/H_2O 85/15 + 15 mM $HCOONH_4$, T = 35 °C. (**IX**)

on the three columns for Adenosine and 2-(4-Chloro-phenoxy)-propionic acid, respectively, are reported. As can be evinced, 2.0 μm - 90Å column shows the best kinetic performance (with roughly $N/m \sim 300\,000$) with a very flat C-branch. A comparison between the two columns packed with 2.7 μm particles has shown the deep impact of the pore size on the chromatographic performance: surprisingly, the worst results were obtained with 2.7 μm - 90Å column ($N/m \sim 200\,000$) compared to 2.7 μm - 160Å ($N/m \sim 240\,000$). It was observed that the wider the pores the flatter the C-branch of the van Deemter plot to parity of particle diameters, probably due to the smaller surface area (m^2/g) available for adsorption.

To further assess the potential of these CSPs, two additional 20×4.6 mm columns were in house packed with these teicoplanin-based phases. In Fig. 5.10 the separation of a mixture of haloxyfop and ketorolac is reported at flow rates as high as 8.0 mL/min. As can be evinces, the baseline separation of the two couples of enantiomers on both columns is achieved in 8 s with very high efficiencies. The

combination of high efficiency and high enantioselectivity leads to maintain excellent resolution values.

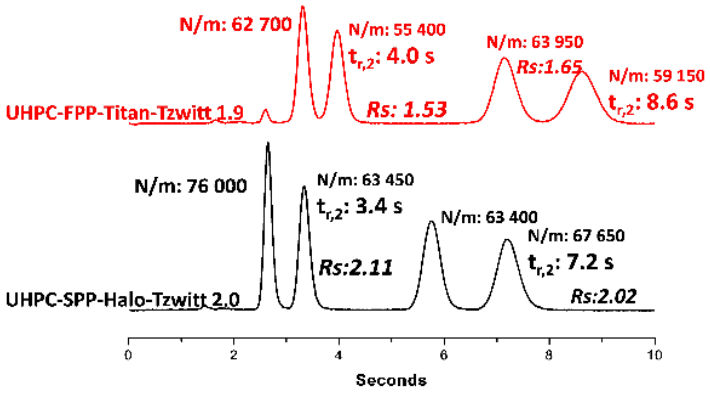

Figure 5.10: Ultrafast enantioseparation of a racemic mixture containing Haloxyfop (firstly eluted pair of peaks) and Ketorolac (secondly eluted pair of peaks) on the 1.9 μm FPPs (top) and on the 2.0 μm SPPs (bottom) columns. (**II**)

In order to give a more complete explanation of mass transfer phenomena and to possibly correlate chemico-physical properties of porous particles to kinetic values, a detailed study of van Deemter curves and of all the sources of band broadening on Whelk-O1 2.5 μm FPPs and 2.6 μm SPPs CSPs and zwitterionic-teicoplanin 1.9 μm FPPs and 2.0 μm SPPs CSPs has been performed **(VIII)**.

Fig. 5.11 reports the overlapped reduced van Deemter curves of the first and second eluted enantiomer on each column under study. Through the combination of stop-flow and dynamic measurements the independent estimation of the sources of band broadening (b, c_s and c_{ads}) is possible (see Chapter 4).

Table 5.1: Reduced longitudinal diffusion coefficient (b), reduced solid-liquid mass transfer resistance coefficient (c_s), reduced adsorption-desorption coefficient (c_{ads}) measured on Whelk-O1 and Teicoplanin-based CSPs.

Column	b		c_s		c_{ads}
	1^{st}	2^{nd}	1^{st}	2^{nd}	2^{nd}
2.5 μm FPPs Whelk-O1	2.4	2.4	0.026	0.037	0.029
2.6 μm SPPs Whelk-O1	2.0	2.0	0.013	0.022	0.080
1.9 μm FPPs Teico	2.0	2.0	0.060	0.064	0.115
2.0 μm SPPs Teico	1.7	1.7	0.039	0.045	0.207

In Table 5.1 all these calculated parameters are shown. As can be evinced, the first and second eluted enantiomers on the same column are characterized by the same b term. Through the application of the parallel model of diffusion it was found that the adsorption of enantiomers on these CSPs is localized. In agreement with the geometric characteristics of core-shell particles that account for a reduced intra-particle space available for diffusion, the c_s term is smaller on SPPs than on FPPs.

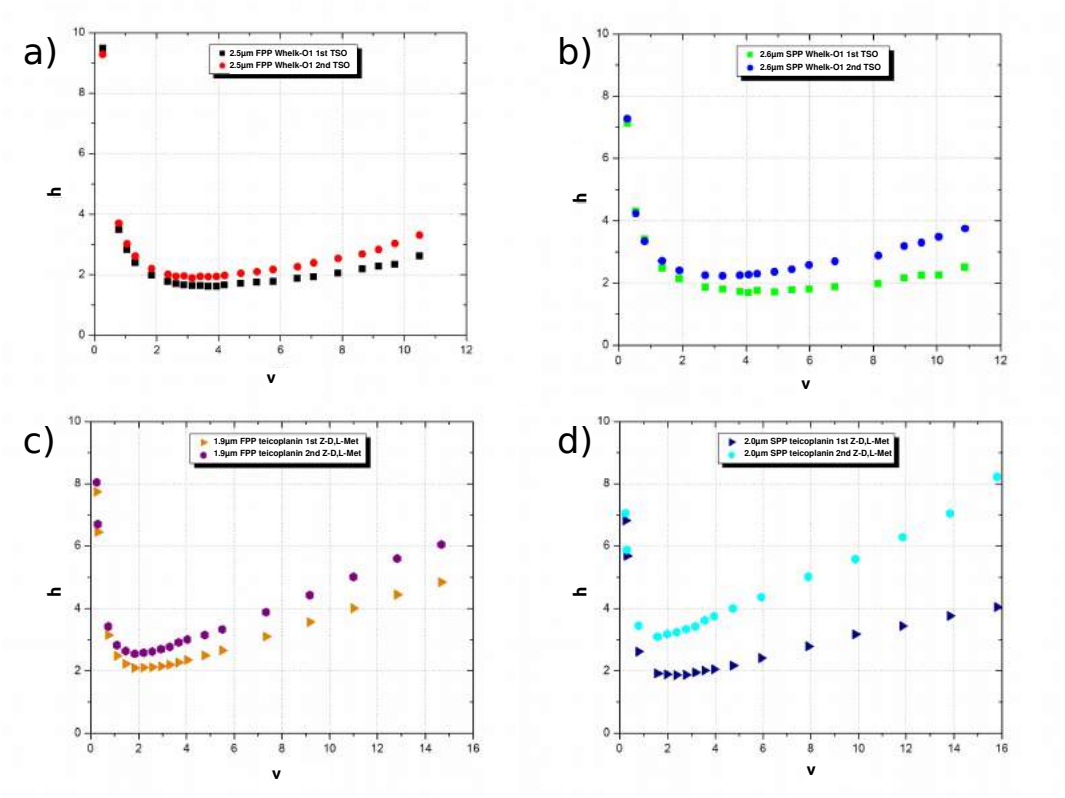

Figure 5.11: Reduced van Deemter curves of: a) first and second eluted TSO enantiomers on the Whelk-O1 2.5 μm FPPs b) first and second eluted TSO enantiomers on the Whelk-O1 2.6 μm SPPs c) first and second eluted Z-D,L-Met enantiomers on the Teicoplanin-based 1.9 μm FPPs d) first and second eluted Z-D,L-Met enantiomers on the Teicoplanin-based 2.0 μm SPPs. (**VIII**)

Moreover, the impact of adsorption-desorption kinetics on the performance of the four columns has been evaluated through a semi-empirical approach based on the comparison with achiral species for which the $c_{ads} \rightarrow 0$. This study has shown that adsorption-desorption kinetics is directly linked to the surface density of chiral selector, indeed SPPs are characterized by a larger surface density and a slower adsorption-desorption kinetics.

Concerning polysaccharide-bases CSPs, a set of three columns with dimensions 100×2 mm packed with 3 μm FPPs functionalized with different amount of cellulose tris(4-chloro-3-methylphenylcarbamate) (Fig. 5.3 a) as chiral selector, namely 0.5%, 1% and 2% (w/w), was studied and compared. Retention behavior of two test compounds (2-(benzylsulfinyl)benzamide, BSBA, and 2-(3-bromobenzylsulfinyl)N-methyl-benzamide, MBBSBA) is shown in Fig. 5.12 with pure ACN as mobile phase. As can be evinced, retention is deeply influenced by both the structure of the analyte and the content of selector loaded: indeed higher retention values are the result of minor number of substituents on the compound and a higher amount of chiral selector on the SP. As an example, Fig. 5.13 shows the reduced van Deemter curves measured on the 1% column for the two couples of enantiomers. Also in this case, the structure of the analyte plays a pivotal role in the shape of the van Deemter curve especially for the second eluted enantiomer. Concerning the "non-

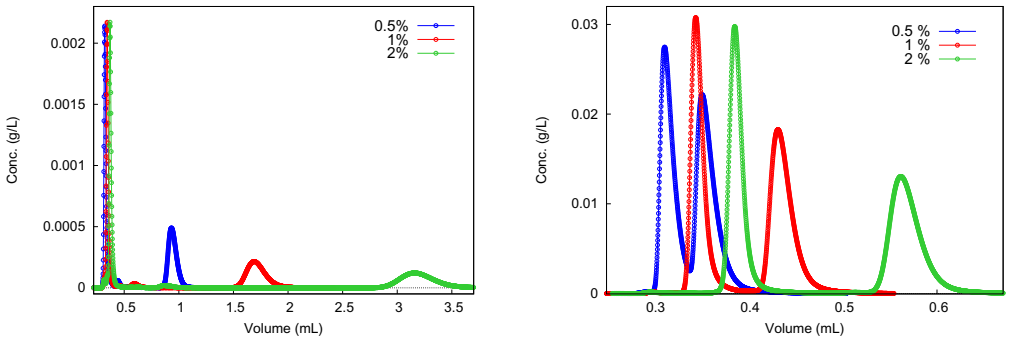

(a) (b)

Figure 5.12: Dependence of retention on the amount of polysaccharide-based chiral selector for: **a**) BSBA enantiomers and **b**) MBBSBA enantiomers. Mobile phase: 100% ACN. Injection volume: 7 μL, injected concentration: 1 g/L.

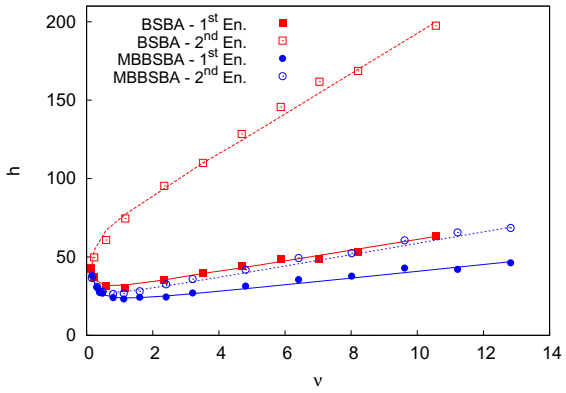

Figure 5.13: Comparison between van Deemter curves measured for BSBA (red) and MBBSBA (blue) enantiomers on 1% column. MP = 100% ACN.

substituted" BSBA enantiomers (red), an unusual convex van Deemter curve is observed for the most retained enantiomer, independently from the amount of selector. It has been demonstrated that this strange behavior is due to both a large eddy dispersion and a very small contribution of diffusion inside the porous particle ($D_{part} \rightarrow 0$), verified with PP experiments and the application of the Maxwell expression for effective diffusion (b-term for the 2^{nd} enantiomer is smaller if compared to the 1^{st} enantiomer and the c_S-term for the 2^{nd} enantiomer $\rightarrow \infty$). This indicates that the second enantiomer is more likely to diffuse into the mobile phase rather than inside the porous particle, due to the presence of very strong H-bonding type interactions with the non-substituted amino group able to hinder the diffusion process and leading to the very high retention seen in Fig. 5.12 **a**. On the other hand, the N-methylation of the amino moiety of MBBSBA enantiomers leads to an increase in retention of the first eluted enantiomer and a decrease in enantioselectivity due to the minor number of possible H-bonding type interactions with the stationary phase. In this case, diffusion coefficients of the two enantiomers are very close to each other, bringing to similar b- and c_S-terms.

5.1.3 Supercritical Fluid Chromatography for Enantioselective Separation (Papers IV and VI)

In the last years in the field of high speed enantioseparations, SFC has been largely used thanks to its versatility, its green character, the introduction of latest generation SFC equipments and the improvement in particle technology. Moreover, due to the low viscosity of CO_2, SFC allows to run faster separations than in LC without remarkable loss of efficiency and with reduced backpressure. Fig. 5.14 reports some examples of ultrafast enantioseparations obtained in SFC conditions. However, the excessively large extra-column band broadening of current SFC instruments usually represents a limitation of the chromatographic performance especially when using new generation CSPs. In order to overcome this problem, some authors modified commercial SFC instruments by replacing standard tubing and flow cell being able to obtain extra-column variance values similar to those measured for HPLC instruments [80–82]. One of the most used class of CSPs is based on immobi-

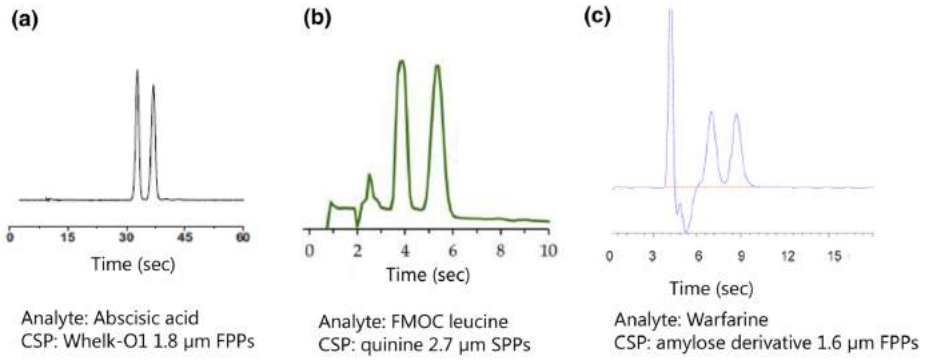

Figure 5.14: Ultrafast enantioseparations in SFC. a) Abscisic acid enantiomers. Column: 50×4.6 mm, Whelk-O1 1.8 μm FPPs. Flow rate: 3.5 mL/min. Instrument: Waters Acquity UPC^2 [83]. b) FMOC leucine enantiomers. Column: 30×4.6, quinine-based 2.7 μm SPPs. Flow rate: 20 mL/min. Instrument: Jasco SFC-2000-7 [84]. c) Warfarin enantiomers. Column: 50×3 mm, amylose-based 1.6 μm FPPs. Flow rate: 3.75 mL/min. Instrument: low-dispersion-modified Agilent 1260 Infinity SFC [81]. Reprinted by permission from **VI**.

lized polysaccharide derivatives. These chiral selectors offer large applicability and high loadability, for these reasons they are commonly employed for both analytical purposes and high-throughput screening analysis. In Fig. 5.15 an example of multiple injections in a single experimental run (MISER) chromatographic technique is presented on a 10×4.0 mm Chiralpak AD-3 column packed with 3 μm FPPs. The separation of Tröger's base enantiomers in a 96-well microplate of samples has been performed in 33 min.

Chiral SFC has also been applied for quantitative analysis of APIs and their metabolites, as the second dimension in highly selective multidimensional chromatography approaches (2D LC-SFC). An other application of polysaccharide-based CSPs is for the separation of chiral compounds with biological activity such as pesticides,

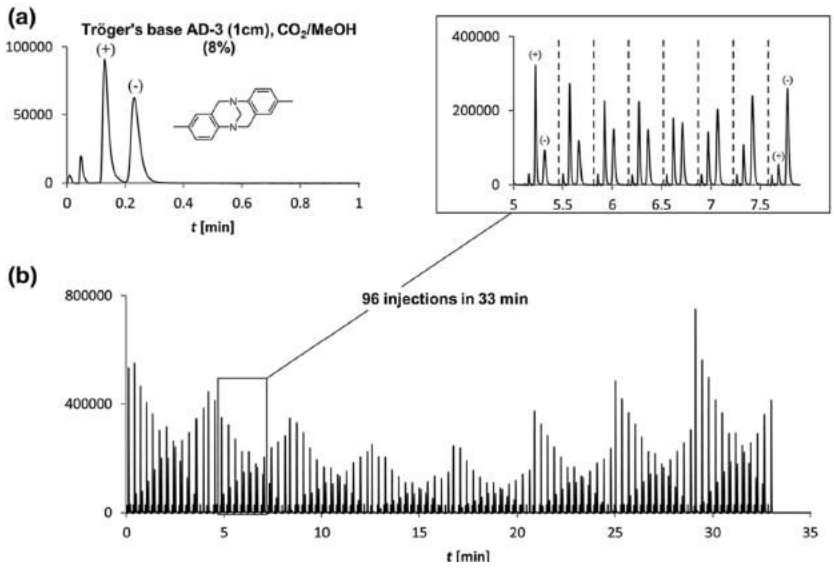

Figure 5.15: a) Separation of Tröger's base enantiomers (concentrations between 0.4 and 1 mg/mL) on a Chiralpak AD-3 column packed with 3 μm FPPs functionalized with an amylose derivative. b) Injection of a 96-well plate with MISER approach on the same column [85]. Reproduced with permission from **VI**.

fungicides in foods and herbicides, to name but a few.

Pirkle-type chiral selectors exist in both the enantiomeric versions, allowing for both the separation of a broad range of compounds and most surprisingly for the determination of the enantiomeric excess of samples for therapeutic use, by using columns functionalized with the same chiral selector but with opposite configuration. Through this approach, named "Inverted Chirality Columns Approach" (ICCA), it is possible to reverse the elution order of enantiomers, leading to their correct identification. One example is reported in Fig. 5.16 where two complemen-

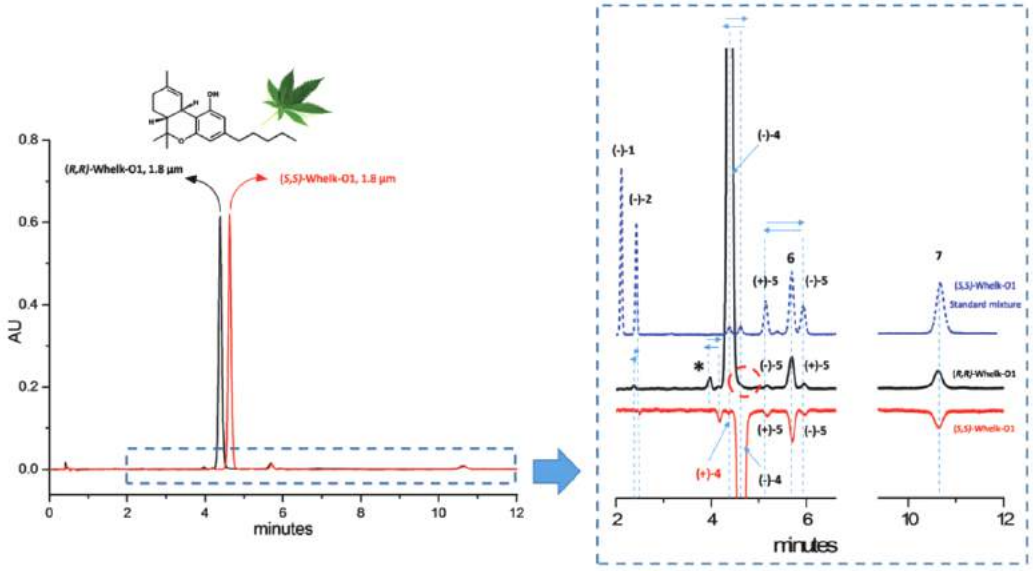

Figure 5.16: ICCA protocol applyed to a Bedrocan® ethanol extract. A zoom of the chromatogram between 2 and 6 min is shown in the inset together with the separation of a standard mixture of six-component cannabinoids (dotted chromatogram). The asterisk denotes a chiral unknown impurity [86]. Reproduced with permission from **VI**.

tary sub-2 μm FPPs functionalized with (S,S)- and (R,R)-Whelk-O1 chiral selectors have been employed in SFC conditions (CO_2/MeOH, 98:2 %v/v) for the determination of the enantiomeric excess of (-)-Δ^9-THC in medicinal marijuana(Bedrocan®).

5.1.4 Closing Remarks

Kinetic and thermodynamic performances, with special emphasis on mass transfer kinetics, of new and very efficient particle formats, such as sub-3 μm and sub-2 μm FPPs and sub-3 μm SPPs, with different functionalization, have been analysed and compared. More in detail, the independent estimation of different sources of band broadening has been performed on both achiral and chiral stationary phases through the coupling of experimental and theoretical measurements. The major advantages of SPPs compared to their FP counterparts lie in smaller longitudinal diffusion and mass transfer resistance for both achiral and chiral separations. Concerning chiral columns, SPPs are characterized by higher enantioselectivity and enantioresolution, but slower adsorption-desorption kinetics, due to the larger density of chiral selector, which negatively impact on the c-brach of the van Deemter plot. Moreover, it has been demonstrated that C_{18} sub-2 μm FPPs with a narrow particle size distribution (nPSD) show performance comparable to SPPs at high flow rates. These results indicate that SPPs do not always outperform FPPs, especially for ultrafast applications. Taking into account 3.0 μm polysaccharide-based FPPs, through the application of effective theory describing diffusion in porous media, it has been demonstrated the deep influence of the analyte on both retention and unusual convex van Deemter plots observed.

The introduction in the market of these advanced materials has represented the major innovation in the field of high-throughput ultrafast enantioseparations. Nevertheless, the transition from traditional HPLC and SFC to UHPLC and UHPSFC requires the production of equipments able to provide very large back pressures with minimal extra-column volumes through innovative designs for detectors, injectors, column fittings, etc.

Even if considerable progress has been made in the field of chiral separations, deeper studies on the effect of particle characteristics (particle type, surface bonding density, etc.) on the adsorption-desorption kinetics and, consequently, on column efficiency and speed of analysis are needed.

5.2 Thermodynamic properties of porous particles for high-efficient separations through nonlinear chromatography (Paper V and VII)

5.2.1 Effect of chiral selector loading and mobile phase composition on CSPs

Adsorption isotherms have been investigated on a variety of MP compositions and on different CSPs (Teicoplanin, Whelk-O1 and Polysaccharide) in order to shed light on some unanswered questions, such as whether the chiral selector content has an effect on enantiorecognition, if the chiral recognition process is independent from particle formats, how it is influenced by experimental variables, etc.
Whelk-O1 CSPs have been prepared respectively on 1.8 μm and 2.5 μm FPPs and 2.6 μm SPPs and adsorption isotherms of TSO enantiomers (concentrations from 3 to 50 g/L) were measured through IM at five different compositions of mobile phase components (hexane/ethanol): 90/10, 92/8, 95/5, 97/3 and 100/0% (v/v) (**V**).
The behavior of (overloaded) Z-D,L-Methionine enantiomers (concentrations: 3, 6, 12 and 25 g/L) was studied through IM on the 2.0 μm SPPs and 1.9 μm FPPs Teicoplanin-based CSPs in HILIC conditions at three different mobile phase compositions: 83:17, 85:15 and 87:13 % v/v ACN/H_2O + 20 mM $HCOONH_4$.
Finally, adsorption isotherms of a chiral sulfoxide have been investigated on three 100×2 mm columns packed with 3 μm FPPs functionalized with 0.5%, 1% and 2% (w/w) of a cellulose tris(4-chloro-3-methylphenylcarbamate) chiral selector in polar organic mode (POM) using pure ACN and pure MeOH as mobile phases.
On the one hand, results of IM show that a competitive Bilangmuir adsorption model in almost all the cases is able to accurately fit experimental data. In Fig. 5.17, some examples of the comparison between experimental and simulated peaks obtained with the above-mentioned isotherm are reported for: **a**) Whelk-O1 1.8 μm FPPs at 90:10, 92:8, 95:5 and 97:3 % (v/v) of HEX/EtOH; **b**) Teicoplanin-based 1.9 μm FPPs at ACN/H_2O 85:15 + 20 mM $HCOONH_4$; **c**) Polysaccharide-based 3 μm FPPs at 100% ACN.
On the other hand, concerning Whelk-O1 CSPs, the Tóth isotherm was employed with mobile phase made of pure hexane, since when ethanol is absent, the polar groups present on the surface are uncovered and free to interact with analytes, making the surface more heterogeneous (Fig. 5.18 left). Conversely, for Polysaccharide-based CSPs with 100% methanol as mobile phase the simple single Langmuir isotherm has been used (Fig. 5.18 right). This indicates the deep influence of the mobile phase components on the surface chemistry of the chiral selector and by consequence on the interaction between analyte and selector.

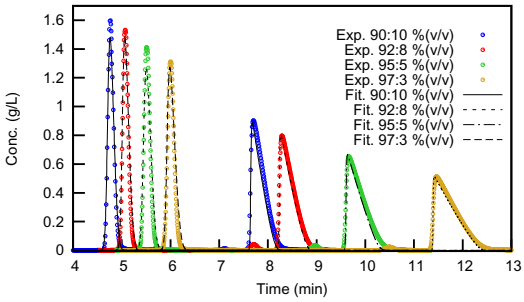

(a)

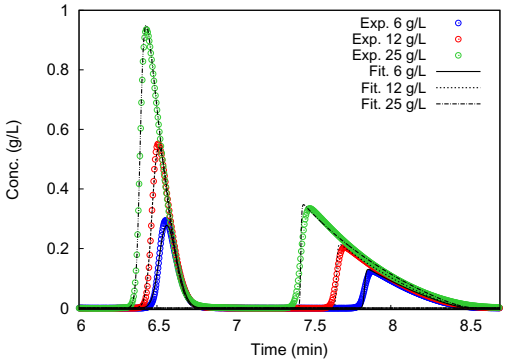

(b)

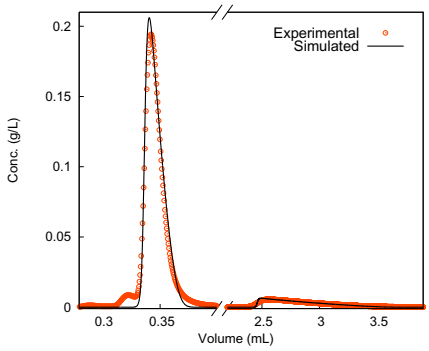

(c)

Figure 5.17: Experimental (colored circles) and calculated (full lines) overloaded profiles measured through IM with a Bilangmuir isotherm. **a**) TSO enantiomers on Whelk-O1 1.8 μm FPPs at different MP compositions, injected concentration = 40 g/L, (**V**); **b**) Z-D,L-Methionine enantiomers on Teicoplanin-based 1.9 μm FPPs at 85:15 % v/v ACN/H_2O + 20 mM $HCOONH_4$, concentrations = 6 g/L, 12 g/L and 25 g/L; **c**) 2-(benzyl-sulfinyl)benzamide enantiomers on Polysaccharide-based 3 μm FPPs at 100% ACN, concentration = 1 g/L.

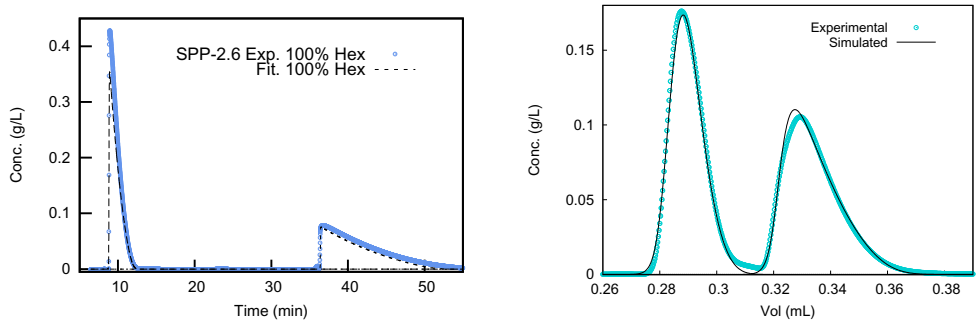

(a) (b)

Figure 5.18: Experimental (colored circles) and calculated (full lines) overloaded profiles measured through IM with: Tóth isotherm model for TSO enantiomers on Whelk-O1 2.6 μm SPPs at 100% Hex, injected concentration = 40 g/L (**a**), (**V**) ; Langmuir isotherm model for 2-(benzyl-sulfinyl)benzamide enantiomers on Polysaccharide-based 3.0 μm FPPs (1% of chiral selector) at 100% MeOH, injected concentration = 1 g/L (**b**).

Table 5.2: Bilangmuir isotherm parameters calculated through IM at different percentage of strong MP modifier on Whelk-O1 CSPs. (**V**)

MP (% EtOH)	Column	Selective Site			Nonselective Site	
		q_{sel} (g/L)	$b_{1,sel}$ (L/g)	$b_{2,sel}$ (L/g)	q_{nsel} (g/L)	b_{nsel} (L/g)
10	FPP-1.8	42	0.010	0.063	100	0.012
	FPP-2.5	42	0.011	0.071	96	0.013
	SPP-2.6	22	0.022	0.095	50	0.015
8	FPP-1.8	38	0.011	0.071	101	0.012
	FPP-2.5	41	0.013	0.082	102	0.013
	SPP-2.6	22	0.025	0.105	39	0.019
5	FPP-1.8	40	0.011	0.090	104	0.015
	FPP-2.5	36	0.011	0.111	105	0.017
	SPP-2.6	22	0.024	0.128	50	0.020
3	FPP-1.8	33	0.012	0.142	106	0.018
	FPP-2.5	30	0.013	0.170	108	0.020
	SPP-2.6	15	0.025	0.212	49	0.027

In Tables 5.2 and 5.3 the Bilangmuir and Tóth isotherm parameters as a function of the percentage of ethanol (from 10 to 3% and 0%, v/v) for the three Whelk-O1 columns are listed, respectively. As can be evinced, in both cases, the two FPPs columns show very similar values of both binding constants (b) and saturation capacities (q), indicating that the preparation of these CSPs with fully porous particles is a very reproducible and robust process. Conversely, the SPPs column exhibits larger binding constants when compared to FPPs, suggesting a deep influence of the surface density of chiral selector. Indeed, a high amount of selector loaded may be responsible for higher interaction energy between analyte and selective sites, but at the same time, it could bring to the formation of aggregates between two or more chiral selectors behaving as nonselective sites.

Table 5.3: Tóth isotherm parameters calculated through IM with a MP made of pure hexane on Whelk-O1 CSPs. (**V**)

Column	q_s (g/L)	b_1 (L/g)	b_2 (L/g)	ν
FPP-1.8	94	0.110	0.589	0.71
FPP-2.5	96	0.128	0.697	0.71
SPP-2.6	30	0.289	1.425	0.81

In order to study the effect of the strong MP modifier amount on binding constant and saturation capacity, the excess isotherms for the three Whelk-O1 columns have been calculated. Excess isotherms for HEX/EtOH mixtures are reported in Fig. 5.19. From these plots, one can observe that the composition of the stationary phase can be considered constant only when % EtOH $>$ 10-15% (*i.e.* when all polar sites have been saturated by EtOH). Conversely, when $0 \leq \%\,\text{EtOH} < 15$, the composition of the stationary phase changes with ethanol content. Since our measurements have been performed in this first region of the isotherm, from Table 5.2, some interesting results can be obtained. On the one hand, higher ethanol content leads to an opposite trend in the behavior of saturation capacities: q_{sel} increases while q_{nsel} decreases. On the other hand, binding constants for the first eluted enantiomer ($b_{1,sel}$) are essentially constant, while an increase of ethanol provokes a decrease of binding constants for the second eluted enantiomer ($b_{2,sel}$) and for nonselective sites (b_{nsel}). The overall effect is a decrease in retention with increasing ethanol content in MP, due to the combination of both selective and nonselective contributions (see Fig. 5.17 a).

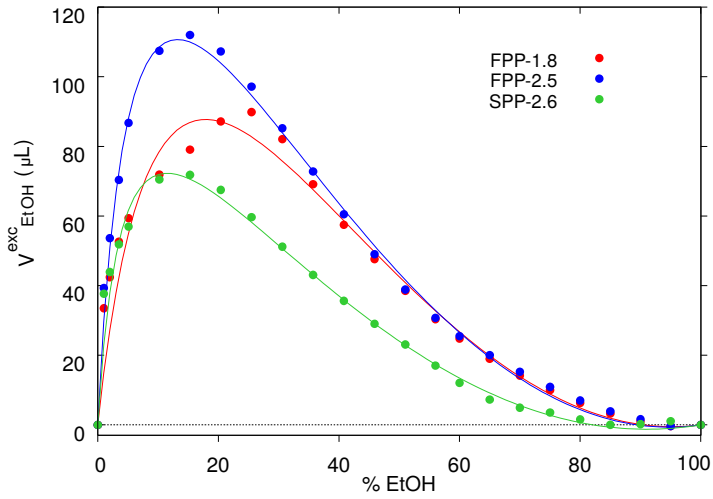

Figure 5.19: Excess adsorption isotherms on the three Whelk-O1 columns, expressed as excess volume of EtOH adsorbed on the stationary phase (V^{exc}_{EtOH}) as a function of % (v/v) of EtOH in MP. Experimental (full circles), fitted curves (full lines). (**V**)

Table 5.4: Bilangmuir isotherm parameters calculated through IM at different percentage of MP components on Teicoplanin-based CPSs.

MP (% ACN/H_2O)	Column	Selective Site			Nonselective Site	
		q^s_{sel} (g/L)	$b_{1,sel}$ (L/g)	$b_{2,sel}$ (L/g)	q^s_{nsel} (g/L)	b_{nsel} (L/g)
83:17	FPP-1.9	0.9	0.03	1.49	76.2	0.03
	SPP-2.0	0.6	0.05	1.55	41.9	0.05
85:15	FPP-1.9	1.0	0.04	1.32	124.6	0.02
	SPP-2.0	0.7	0.05	1.23	78.0	0.03
87:13	FPP-1.9	1.1	0.05	1.25	131.5	0.02
	SPP-2.0	0.8	0.06	1.09	109.0	0.02

Concerning Teicoplanin-based CSPs, Table 5.4 reports the results of IM simulations. From these data it is evinced that a higher amount of water leads to a decrease of the saturation capacities and an increase of binding constants. This can be easily explained by taking into account the chromatographic mode used: HILIC. In this particular case a film of water is adsorbed on the stationary phase, whose thickness directly depends on the amount of water in the MP, leading to a reduction of the availability of polar sites to adsorption, hindering hydrogen bonding type interactions and possibly enhancing enantioselective interactions ($b_{2,sel}$ increases with water content). Moreover, also in this case, it was found that SP particles were characterized by larger selective and nonselective binding and smaller saturation capacities if compared to FPPs.

Data related to effect of the chiral selector loading (namely 0.5, 1 and 2%) are reported in Tables 5.5 and 5.6 for Polysaccharide-based CSPs with pure ACN and pure MeOH as mobile phases, respectively. As can be evinced from Table 5.5, in 100% ACN, increasing the percentage of selector brings to an increase in both selective and nonselective saturation capacities. The increase in q_{nsel} is believed to be due to parts of the chiral selector structure acting as nonselective site. The dramatic decrease in b_{nsel} with the increase of the percentage of selector can be due to the different accessibility of the residual silanols present on the surface of the particles. Small amount of chiral selector coated onto silica (0.5%) can enhance the accessibility of the residue silanols, bringing to high binding constant due to nonselective secondary chemical adsorption. Moving to higher selector loadings leads to a shielding of the residue silanols. As a consequence, binding constants decrease as the interaction between enantiomers and silanols is hindered. Moreover, ACN as mobile phase provokes very large binding constant (and retention factors) for the second enantiomer in the selective site, $b_{2,sel}$, independently from the amount of chiral selector loading, suggesting the great enantiodiscrimination capacity of these CSPs with 100% ACN as MP. Conversely, moving to 100% MeOH as MP leads to a deep change in retention and adsorption. Indeed, methanol, as protic solvent, is

Table 5.5: Bilangmuir isotherm parameters calculated through Inverse Method at different percentage of chiral selector loading for BSBA with 100% ACN as mobile phase

Column	Selective Site		Nonselective Site		
	q_{sel} (g/L)	$b_{1,sel}$ (L/g)	$b_{2,sel}$ (L/g)	q_{nsel} (g/L)	b_{nsel} (L/g)
PHEC 0.5%	0.8	0.2	34.1	0.2	3.2
PHEC 1%	1.6	0.4	33.7	0.4	1.7
PHEC 2%	3.0	0.7	33.3	0.8	0.3

Table 5.6: Langmuir isotherm parameters calculated through Inverse Method at different percentage of chiral selector loading for 2^{nd} enantiomer of BSBA with 100% MeOH as mobile phase

Column	q_s (g/L)	b (L/g)
PHEC 0.5%	0.3	3.4
PHEC 1%	0.8	2.4
PHEC 2%	1.5	2.7

able to interfere with analyte-chiral selector H-bonding and to interact with all adsorption centers, be they polar or non-polar, "hindering" the adsorption of analyte molecules, by masking polar adsorption sites. As a consequence, the adsorption isotherm becomes a simple Langmuir one since the first enantiomer is completely not retained.

5.2.2 Modeling of overloaded profiles under gradient elution chromatography (Paper VII)

The adsorption behavior of octreotide and glucagone, therapeutic peptides, has been studied and modeled under gradient elution RP-LC (ACN/H_2O mixtures + Trifluoroacetic acid, TFA) on a 150×4.6 mm column packed with 5 μm C_{18} FPPs and a 100×4.6 mm column packed with 10 μm C_8 FPPs, respectively. In the first step of this work, the volume fraction of the organic modifier in MP, ϕ, at which the target peptide elutes has been estimated through a simple gradient run (Fig. 5.20). Secondly, adsorption isotherms have been calculated in isocratic conditions through IM in a defined broader range of ϕ in order to evaluate the influence of the organic modifier concentration on the retention, and on isotherm parameters.

In Fig. 5.21 **a** and 5.22 **a** examples of the application of IM are reported for isocratic elutions at ϕ = 0.24 for different concentrations of octreotide and ϕ varying from 0.30 to 0.32 for glucagone, respectively. The very good agreement between experimental and simulated data was obtained with a Langmuir adsorption model for all the organic modifier concentrations studied (see Table 5.7 for details).

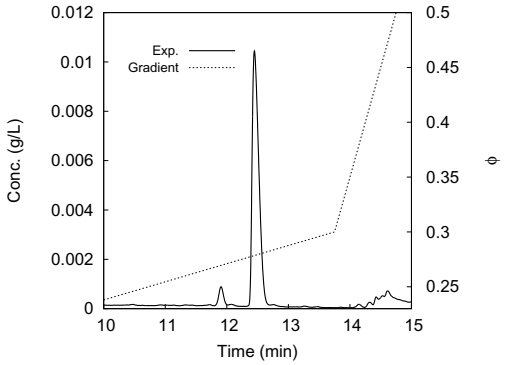

Figure 5.20: Experimental gradient elution profile of the crude octreotide peptide. Injected concentration: 0.2 g/L; injected volume: 5 μL. (**VII**)

Once the dependence of b on ϕ has been obtained through an exponential fitting, following Eq. 3.20 it is possible to perform the simulation of gradient elution experiments, as reported in Fig. 5.21 **b** and 5.22 **b** for octreotide and glucagone, respectively.

Table 5.7: Adsorption isotherm parameters obtained through IM with a Langmuir model at different mobile phase compositions obtained for octreotide. (**VII**)

ϕ	b (L/g)	q_s (g/L)
0.23	8.14	0.72
0.24	5.69	0.74
0.25	4.65	0.66
0.28	1.86	0.63

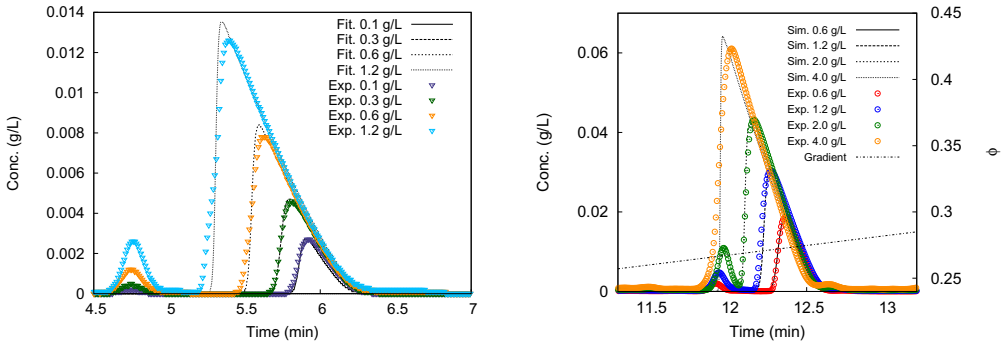

(a) (b)

Figure 5.21: Comparison between experimental (colored points) and simulated (lines) peaks obtained with IM (Langmuir isotherm) for four concentrations of the crude octreotide: a) isocratic conditions (ϕ = 0.24); b) gradient conditions. Injected volume = 5 μL. (**VII**)

The same experiments have been carried out with a different ion pairing agent (ammonium acetate) for glucagone peptide, for the sake of comparison and to possibly verify the effect of ion pairing agents on the thermodynamics of adsorption. Interestingly it has been found that the simple Langmuir isotherm model does not account for the optimal fitting of experimental profiles, obtained instead with a Moreau isotherm which accounts for adsorbate–adsorbate interactions (Fig. 5.23).

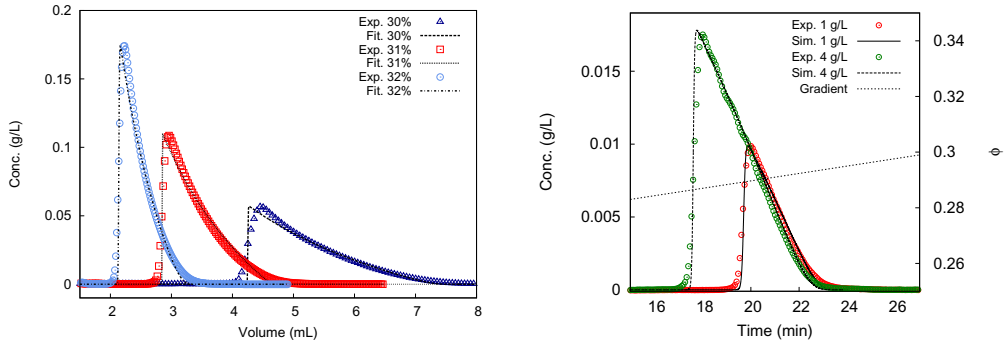

(a) (b)

Figure 5.22: Comparison between experimental (colored points) and simulated (lines) peaks obtained with IM (Langmuir isotherm) for glucagone: a) isocratic conditions (ϕ = 0.30 - 0.32), injected concentration = 4 g/L; b) gradient conditions. Injected volume = 20 μL, injected concentrations = 1 and 4 g/L.

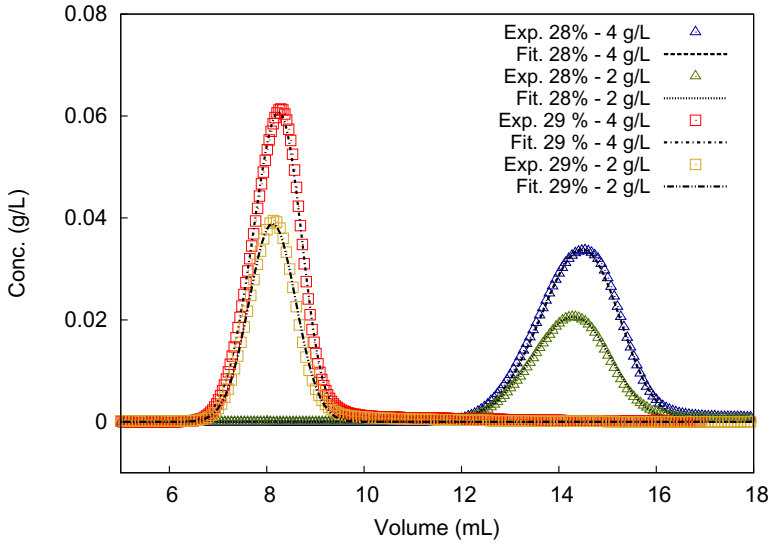

Figure 5.23: Comparison between experimental (colored points) and simulated (lines) peaks obtained with IM (Moreau isotherm) for glucagone measured at ϕ = 0.28, with triangles and ϕ = 0.29, with squares.

5.2.3 Split-intein Mediated Affinity Chromatography

A short column (40×5 mm), packed with an affinity resin functionalized with a N-intein affinity tag, was tested and characterized. The porosity of the resin was measured by inverse size exclusion chromatography (iSEC) with elution of different dextran standards (from 1000 to 2000000 g/mol), obtaining a total porosity (ϵ_t) of 0.93, particle porosity (ϵ_p) of 0.85 and an external porosity (ϵ_e) of 0.52.

The breakthrough curves (BTC) of the protein of interest (POI) have been obtained through high volume injections on the resin at different concentrations (0.3, 0.6, 1.0 g/L) and different flow rates (0.2, 0.5, 1 mL/min). The saturation capacity of the resin, the maximum mass transfer coefficient, the parameters of the correlation, the Henry's coefficient measured at the reference pH value are fitted from the BTC by using a mathematical model (see Section 3.5.2). An example is reported in Fig.

5.24.

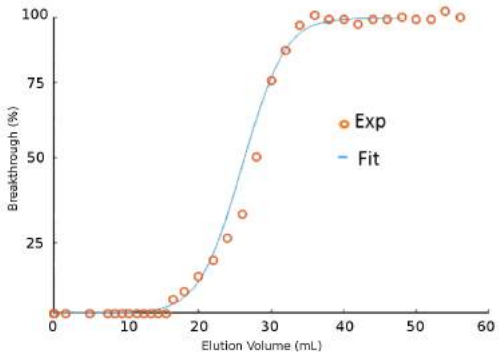

Figure 5.24: Fitting of breakthrough curve of the POI measured at 280 nm, flow rate = 0.5 mL/min, feed concentration = 0.6 g/L.

Afterwards, the effect of the flow rate on the cleavage capacity of the resin was performed with injection of the crude lysate directly into the intein column (Fig. 5.25). As can be evinced, no significant effect was observed. The presence of uncleaved

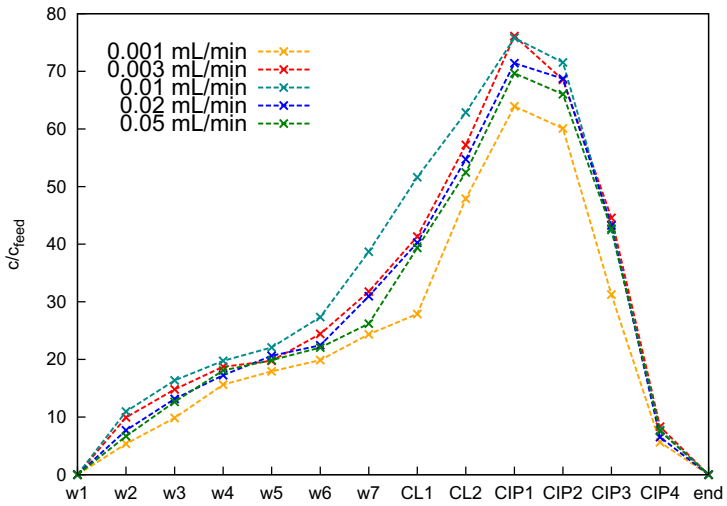

Figure 5.25: Effect of the flow rate on cleavage step. "w" indicates washing step, "CL" states for cleavage and "CIP" is for cleaning in place step. Numbers indicate the fraction analysed.

POI in the wash, cleavage and CIP steps led to the investigation of the effect of the length of the washing step. It was found that the binding of the POI to the resin was remarkably influenced by the washing step. Indeed, a short wash led to the elution of the POI in the CIP step, otherwise, a long wash led to the untimely elution during the same step.

Note: purification protocol, protein, resin type and final data have been deliberately omitted.

5.2.4 Closing Remarks

On the one hand, the investigation of adsorption behavior of target compounds is a fundamental tool for the thermodynamic characterisation of stationary phases, being either chiral or achiral. These measurements could help to correlate chemico-physical properties (specific loading of chiral selector, particle type and geometry, surface area, etc.) of porous particles to thermodynamic quantities affecting retention and the enantiorecognition process (binding constants, saturation capacities, etc.). These information are of fundamental importance especially when moving to ultrafast enantioseparations. Indeed, they can be the key point to explain and understand the kinetic behavior of particles, knowing that, for example, larger binding constant causes longer adsorption-desorption times, which negatively impacts on the c-term of the van Deemter equation.

Moreover this approach can be applied to predict the adsorption behavior of products of pharmaceutical interest, which permits to investigate the feasibility of purification process through preparative chromatography and to provide information that may help to optimize large-scale purifications.

On the other hand, some preliminary results related to the selective purification of a target protein through split-intein mediated affinity chromatography have been reported. Also in this case, information obtained through the study of thermodynamic properties of the resin used (such as the saturation capacity) are of fundamental importance for a possible scale up of the purification process.

Bibliography

[1] M. S. Tswett, "Tr. protok. varshav. obshch. estestvoistpyt," *Otd. Biol.*, vol. 14, 1905.

[2] C. Brunelli, Y. Zhao, M. H. Brown, and P. Sandra, "Pharmaceutical analysis by supercritical fluid chromatography: Optimization of the mobile phase composition on a 2-ethylpyridine column," *J. Sep. Sci.*, vol. 31, pp. 1299–1306, 2008.

[3] C. Brunelli, Y. Zhao, M. H. Brown, and P. Sandra, "Development of a supercritical fluid chromatography high-resolution separation method suitable for pharmaceuticals using cyanopropyl silica," *J. Chromatogr. A*, vol. 1185, pp. 263–272, 2008.

[4] A. G.-G. Perrenoud, J. Boccard, J.-L. Veuthey, and D. Guillarme, "Analysis of basic compounds by supercritical fluid chromatography: Attempts to improve peak shape and maintain mass spectrometry compatibility," *J. Chromatogr. A*, vol. 1262, pp. 205–213, 2012.

[5] M. de la Puente, P. L. Soto-Yarritu, and J. Burnett, "Supercritical fluid chromatography in research laboratories: design, development and implementation of an efficient generic screening for exploiting this technique in the achiral environment," *J. Chromatogr. A*, vol. 1218, pp. 8551–8560, 2011.

[6] L. T. Taylor, "Supercritical fluid chromatography," *Anal. Chem.*, vol. 82, pp. 4925–4935, 2010.

[7] E. Lesellier, "Retention mechanisms in super/subcritical fluid chromatography on packed columns," *J. Chromatogr. A*, vol. 1216, pp. 1881–1890, 2009.

[8] T. A. Berger, "Feasibility of screening large aqueous samples for thermally unstable pesticides using high efficiency packed column supercritical fluid chromatography with multiple detectors," *Chromatographia*, vol. 41, pp. 471–484, 1995.

[9] A. G.-G. Perrenoud, J.-L. Veuthey, and D. Guillarme, "Comparison of ultra-high performance supercritical fluid chromatography and ultra-high perfor-

mance liquid chromatography for the analysis of pharmaceutical compounds," *J. Chromatogr. A*, vol. 1266, pp. 158–167, 2012.

[10] U. D. Neue, *HPLC Columns: Theory, Technology and Practice*. Wiley-VCH, 1997.

[11] J. J. Kirkland, J. J. DeStefano, and T. J. Langlois, "Fused-core particles for hplc columns," *Am. Lab*, vol. February, no. 39, pp. 18–21, 2007.

[12] J. J. DeStefano, S. A. Schuster, J. M. Lawhorn, and J. J. Kirkland, "Performance characteristics of new superficially porous particles," *J. Chromatogr. A*, vol. 1258, pp. 76–83, 2012.

[13] O. H. Ismail, M. Catani, L. Pasti, A. Cavazzini, A. Ciogli, C. Villani, D. Kotoni, F. Gasparrini, and D. S. Bell, "Experimental evidence of the kinetic performance achievable with columns packed with the new 1.9 μm fully porous particles Titan c_{18}," *J. Chromatogr. A*, vol. 1454, pp. 86–92, 2016.

[14] M. Catani, O. H. Ismail, F. Gasparrini, M. Antonelli, L. Pasti, N. Marchetti, S. Felletti, and A. Cavazzini, "Recent advancements and future directions of superficially porous chiral stationary phases for ultrafast high-performance enantioseparations," *Analyst*, vol. 142, pp. 555–566, 2017.

[15] A. Cavazzini, L. Pasti, A. Massi, N. Marchetti, and F. Dondi, "Recent applications in chiral high performance liquid chromatography: A review," *Anal. Chim. Acta*, vol. 706, pp. 205–222, 2011.

[16] M. Catani, S. Felletti, O. H. Ismail, F. Gasparrini, L. Pasti, N. Marchetti, C. D. Luca, V. Costa, and A. Cavazzini, "New frontiers and cutting edge applications in ultra high performance liquid chromatography through latest generation superficially porous particles with particular emphasis to the field of chiral separations," *Anal. Bioanal. Chem.*, vol. 410, pp. 2457–2465, 2018.

[17] G. Cancelliere, A. Ciogli, I. D'Acquarica, F. Gasparrini, J. Kocergin, D. Misiti, M. Pierini, H. Ritchie, P. Simone, and C. Villani, "Transition from enantioselective high performance to ultra-high performance liquid chromatography: A case study of a brush-type chiral stationary phase based on sub-5-micron to sub-2-micron silica particles," *J. Chromatogr. A*, vol. 1217, pp. 990–999, 2010.

[18] R. J. Reischl, L. Hartmanova, M. Carrozzo, M. Huszar, P. Frühauf, and W. Lindner, "Chemoselective and enantioselective analysis of proteinogenic amino acids utilizing n-derivatization and 1-d enantioselective anion-exchange chromatography in combination with tandem mass spectrometric detection," *J. Chromatogr. A*, vol. 1218, pp. 8379–8387, 2011.

[19] K. Lomsadze, G. Jibuti, T. Farkas, and B. Chankvetadze, "Comparative high-performance liquid chromatography enantioseparations on polysaccharide based stationary phases prepared by coating totally porous and core-shell silica particles," *J. Chromatogr. A*, vol. 1234, pp. 50–55, 2012.

[20] D. C. Patel, Z. S. Breitbach, M. F. Wahab, C. L. Barhate, and D. W. Armstrong, "Gone in seconds: praxis, performance and peculiarities of ultrafast chiral liquid chromatography with superficially porous particles," *Anal. Chem.*, vol. 87, pp. 9137–9148, 2015.

[21] D. A. Spudeit, M. D. Dolzan, Z. S. Breitbach, W. E. Barber, G. A. Micke, and D. W. Armstrong, "Superficially porous particles vs. fully porous particles for bonded high performance liquid chromatographic chiral stationary phases: Isopropyl cyclofructan 6," *J. Chromatogr. A*, vol. 1363, pp. 89–95, 2014.

[22] A. Cavazzini and A. Felinger, *Liquid Chromatography: Fundamentals and Instrumentation*. Elsevier: Volume1, Chapter 2, 2017.

[23] G. Guiochon, A. Felinger, D. G. Shirazi, and A. M. Katti, *Fundamentals of Preparative and Nonlinear Chromatography*. Second Edition: Academic Press, Elsevier, 2006.

[24] E. Wicke, "Empirische und theoretische untersuchungen der sorptionsgeschwindigkeit von gasen an porösen stoffen ii.," *Kolloid Z*, vol. 86, pp. 295–313, 1939.

[25] J. N. Wilson, "A theory of chromatography," *J. Am. Chem. Soc.*, vol. 62, pp. 1583–1591, 1940.

[26] D. DeVault, "A theory of chromatography," *J. Amer. Chem. Soc.*, vol. 65, pp. 532–540, 1943.

[27] A. Felinger and G. Guiochon, "Comparison of the kinetic models of linear chromatography," vol. 60, p. S175, 2004.

[28] G. G. Götmar G, Fornstedt T, "Peak tailing and mass transfer kinetics in linear chromatography. dependence on the column length and the linear velocity of the mobile phase.," *J. Chromatogr. A*, vol. 831, p. 17, 1999.

[29] J. D. Andrade, *Surface and Interfacial Aspects of Biomedical Polymers*. New York, NY, Vol. 2, 35: Plenum Press, j. d. andrade (ed.) ed., 1985.

[30] A. Felinger, D. M. Zhou, and G. Guiochon, "Determination of the single component and competitive adsorption isotherms of the 1-indanol enantiomers by the inverse method," *J. Chromatogr. A*, vol. 1005, pp. 35–49, 2003.

[31] A. Cavazzini, M. Remelli, and F. Dondi *J. Microcol. Sep.*, vol. 9, pp. 295–302, 1997.

[32] P. Jandera, V. Bačkovská, and A. Felinger, "Analysis of the band profiles of the enantiomers of phenylglycine in liquid chromatography on bonded teicoplanin columns using the stochastic theory of chromatography," *J. Chromatogr. A*, vol. 919, pp. 67–77, 2001.

[33] D. Zhou, K. Kaczmarski, A. Cavazzini, X. Liu, and G. Guiochon, "Modeling of the separation of two enantiomers using a microbore column," *J. Chromatogr. A*, vol. 1020, pp. 199–217, 2003.

[34] J. Tóth *Acta Chim. Acad. Sci. Hung.*, vol. 69, p. 311, 1971.

[35] M. Moreau, P. Valentin, C. Vidal-Madjar, B. C. Lin, and G. Guiochon, "Adsorption isotherm model for multicomponent adsorbate-adsorbate interactions," *J. Colloid Interface Sci.*, vol. 141, pp. 127–136, 1991.

[36] F. Gritti, W. Piątkowski, and G. Guiochon, "Comparison of the adsorption equilibrium of a few low-molecular mass compounds on a monolithic and a packed column in reversed-phase liquid chromatography," *J. Chromatogr. A*, pp. 81–107, 2002.

[37] F. Gritti and G. Guiochon, "New thermodynamically consistent competitive adsorption isotherm in rplc," *J. Coll. Interf. Sci.*, vol. 264, pp. 43–59, 2003.

[38] B. Buszewski, S. Bocian, and A. Felinger, "Excess isotherms as a new way for characterization of the columns for reversed-phase liquid chromatography," *J. Chromatogr. A*, vol. 1191, pp. 72–77, 2008.

[39] B. Buszewski, M. Jaroniec, and R. K. Gilpin, "Influence of eluent composition on retention and selectivity of alkylamide phases under reversed-phase conditions," *J. Chromatogr. A*, vol. 668, pp. 293–299, 1994.

[40] P. Vajda, A. Felinger, and G. Guiochon, "Evaluation of surface excess isotherms in liquid chromatography," *J. Chromatogr. A*, vol. 1291, pp. 41–47, 2013.

[41] G. Schay, "Adsorption of solutions of nonelectrolytes," in *Surface and Colloid Science* (E. M. (Ed.), ed.), pp. 155–212, 1969.

[42] J. J. Kipling and E. H. M. Wright, "Adsorption from binary systems of limited concentration range: application of some fundamental concepts," *J. Chem. Soc.*, vol. 855, 1962.

[43] M. A. Stadalius, M. A. Quarry, T. H. Mourey, and L. R. Snyder, "Conventional chromatographic theory versus "critical" solution behavior in the separation of large molecules by gradient elution," *J. Chromatogr.*, vol. 358, pp. 17–37, 1986.

[44] L. R. Snyder and M. A. Stadalius, *High-Performance Liquid Chromatography: Advances and Perspectives*, vol. 4. Academic Press, New York, 1986.

[45] L. R. Snyder and J. J. Kirkland, *Introduction to Modern Liquid Chromatography*. Wiley-Interscience, 1979.

[46] P. Jandera and J. Churáček, *Gradient elution in column liquid chromatography: theory and practice*, vol. 31 of *Journal of Chromatography Library*. Elsevier, 1985.

[47] N. Marchetti, F. Dondi, A. Felinger, R. Guerrini, S, and A. Cavazzini, "Modeling of overloaded gradient elution of nociceptin/orphanin fq in reversed-phase liquid chromatography," *J. Chromatogr. A*, vol. 1079, pp. 162–172, 2005.

[48] L. R. Snyder, *High-performance liquid chromatography. Advances and perspectives*, vol. 1. New York: Academic Press, 1980.

[49] A. Felinger and G. Guiochon *J. Chromatogr. A*, vol. 796, pp. 59–74, 1998.

[50] A. Felinger and G. Guiochon *Biotechnol. Prog.*, vol. 12, pp. 638–644, 1996.

[51] M. Angarita, T. Müller-Späth, D. Baur, R. Lievrouw, G. Lissens, and M. Morbidelli, "Twin-column capturesmb: a novel cyclic process for protein a affinity chromatography," *J. Chromatogr. A*, vol. 1389, pp. 85–95, 2015.

[52] D. Pfister, L. Nicoud, and M. Morbidelli, *Continuous Biopharmaceutical Processes*. Cambridge University Press, 2018.

[53] D. Guan and Z. Chen, "Affinity purification of proteins in tag-free form: Split intein-mediated ultrarapid purification (sirp)," *Methods Mol. Biol.*, vol. 1495, pp. 1–12, 2017.

[54] C. K. S. Ng, H. Osuna-Sanchez, E. Valéryc, E. Sørensen, and D. G.Bracewell, "Design of high productivity antibody capture by protein a chromatography using an integrated experimental and modeling approach," *J. Chromatogr. B*, vol. 899, pp. 116–126, 2012.

[55] D. Baur, M. Angarita, T. Müller-Späth, and M. Morbidelli, "Optimal model-based design of the twin-column captureSMB process improves capacity utilization and productivity in protein a affinity capture.," *Biotechnol J.*, vol. 11, pp. 135–145, 2016.

[56] F. Gritti and G. Guiochon *J. Chromatogr. A*, vol. 1221, pp. 2–40, 2012.

[57] G. Desmet, K. Broeckhoven, J. De Smet, S. Deridder, G. V. Baron, and P. Gzil, "Errors involved in the existing B-term expressions for the longitudinal diffusion in fully porous chromatographic media. Part I: Computational data in ordered pillar arrays and effective medium theory," *J. Chromatogr. A*, vol. 1188, pp. 171–188, 2008.

[58] F. Gritti and G. Guiochon, "Theoretical and experimental impact of the bed aspect ratio on the axial dispersion coefficient of columns packed with 2.5μm particles," *J. Chromatogr. A*, vol. 1262, pp. 107–121, 2012.

[59] G. Desmet, "Comparison techniques for hplc column performance," *LC GC Eur.*, vol. 21, pp. 310–317, 2008.

[60] G. Desmet and S. Deridder, "Effective medium theory expressions for the effective diffusion in chromatographic beds filled with porous, non-porous and porous-shell particles and cylinders. Part I: Theory," *J. Chromatogr. A*, vol. 1218, pp. 32–45, 2011.

[61] S. Deridder, M. Catani, A. Cavazzini, and G. Desmet, "A theorethical study on the advantage of core-shell particles with radially-oriented mesopores," *J. Chromatogr. A*, vol. 1456, pp. 137–144, 2016.

[62] S. Bruns, T. Müllner, M. Kollmann, J. Schachtner, A. Höltzel, and U. Tallarek, "Confocal laser scanning microscopy method for quantitative characterization of silica monolith morphology," *Anal. Chem.*, vol. 82, pp. 6569–6575, 2010.

[63] S. Bruns and U. Tallarek, "Physical reconstruction of packed beds and their morphological analysis: Core-shell packings as an example," *J. Chromatogr. A*, vol. 1218, pp. 1849–1860, 2011.

[64] J. H. Knox and L. McLaren, "New gas chromatographic method for measuring gaseous diffusion coefficients and obstructive factors," *Anal. Chem.*, vol. 36, pp. 1477–1482, 1964.

[65] J. H. Knox and H. P. Scott, "B and C terms in the van Deemter equation for liquid chromatography," *J. Chromatogr.*, vol. 282, pp. 297–313, 1983.

[66] K. Miyabe, Y. Matsumoto, and G. Guiochon, "Peak parking-moment analysis. A strategy for the study of the mass-transfer kinetics in the stationary phase," *Anal. Chem.*, vol. 79, pp. 1970–1982, 2007.

[67] J. C. Giddings, *Dynamics of Chromatography*. New York, NY: Marcel Dekker, 1960.

[68] R. W. Stout, J. J. DeStefano, and L. R. Snyder, "High-performance liquid chromatographic column efficiency as a function of particle composition and geometry and capacity factor," *J. Chromatogr.*, vol. 282, pp. 263–286, 1983.

[69] F. Gritti and G. Guiochon, "General HETP equation for the study of mass-transfer mechanisms in RPLC," *Anal. Chem.*, vol. 78, pp. 5392–5347, 2006.

[70] H. T. Davis, "The effective medium theory of diffusion in composite media," *J. Am. Ceram. Soc.*, vol. 60, pp. 499–501, 1977.

[71] S. Torquato, "Effective electrical conductivity of two-phase disordered composite media," *J. Appl. Phys*, vol. 58, pp. 3790–3797, 1985.

[72] F. Gritti and G. Guiochon, "Mass transfer kinetics, band broadening and column efficiency," *J. Chromatogr. A*, vol. 1221, pp. 2–40, 2012.

[73] K. Kaczmarski and G. Guiochon, "Modeling of the mass-transfer kinetics in chromatographic columns packed with shell and pellicular particles," *Anal. Chem.*, vol. 79, pp. 4648–4656, 2007.

[74] K. Kaczmarski, "On the optimization of the solid core radius of superficially porous particles for finite adsorption rate," *J. Chromatogr. A*, vol. 1218, pp. 951–958, 2011.

[75] K. Kaczmarski, A. Cavazzini, P. Szabelski, D. Zhou, X. Liu, and G. Guiochon, "Application of the general rate model and the generalized Maxwell-Stefan equation to the study of the mass transfer kinetics of a pair of enantiomers," *J. Chromatogr. A*, vol. 962, pp. 57–67, 2002.

[76] K. Miyabe, "Moment equations for chromatography using superficially porous spherical particles," *Anal. Sci.*, vol. 27, pp. 1007–1017, 2011.

[77] F. Gritti and G. Guiochon, "Possible resolution gain in enantioseparations afforded by core-shell particle technology," *J. Chromatogr. A*, vol. 1348, pp. 87–96, 2014.

[78] J. C. Giddings, *Dynamics of Chromatography*. New York: Marcel Dekker, 1965.

[79] O. H. Ismail, L. Pasti, A. Ciogli, C. Villani, J. Kocergin, S. Anderson, F. Gasparrini, A. Cavazzini, and M. Catani, "Pirkle-type chiral stationary phase on core–shell and fully porousparticles: Are superficially porous particles always the better choice toward ultrafast high-performance enantioseparations?," *J. Chromatogr. A*, vol. 1466, pp. 96–104, 2016.

[80] T. A. Berger, "Kinetic performance of a 50 mm long 1.8 μm chiral column in supercritical fluid chromatography.," *J. Chromatogr. A*, vol. 1459, pp. 136–144, 2016.

[81] T. A. Berger, "Preliminary kinetic evaluation of an immobilized polysaccharide sub-2 μm column using a low dispersion supercritical fluid chromatograph.," *J. Chromatogr. A*, vol. 1510, pp. 82–88, 2017.

[82] O. H. Ismail, G. L. Losacco, G. Mazzoccanti, A. Ciogli, C. Villani, M. Catani, L. Pasti, S. Anderson, A. Cavazzini, and F. Gasparrini, "Unmatched kinetic performance in enantioselective supercritical fluid chromatography by combining latest generation whelk-o1 chiral stationary phases with a low-dispersion in-house modified equipment.," *Anal. Chem.*, vol. 90, pp. 10828–10836, 2018.

[83] L. Sciascera, O. Ismail, A. Ciogli, D. Kotoni, A. Cavazzini, L. Botta, T. Szczerba, J. Kocergin, C. Villani, and F. Gasparrini, "Expanding the potential of chiral chromatography for high-throughput screening of large compound libraries by means of sub-2 μm Whelk-O1 stationary phase in supercritical fluid conditions," *J. Chromatogr. A*, pp. 160–168, 2015.

[84] D. C. Patel, Z. S. Breitbach, J. Yu, K. A. Nguyen, and D. W. Armstrong, "Quinine bonded to superficially porous particles for high-efficiency and ultrafast liquid and supercritical fluid chromatography," *Anal. Chim. Acta*, vol. 963, pp. 164–174, 2017.

[85] K. Kawatzki, M. Biba, E. L. Regalado, and C. J. Welch, "Miser chiral supercritical fluid chromatography for high throughput analysis of enantiopurity," *J. Chromatogr. A*, vol. 1429, pp. 374–379, 2016.

[86] G. Mazzoccanti, O. H. Ismail, I. D'Acquarica, C. M. Villani, C. M. Wilcox, A. Cavazzini, and F. Gasparrini, "Cannabis through the looking glass: chemo- and enantio-selective separation of phytocannabinoids by enantioselective ultra high performance supercritical fluid chromatography.," *Chem Commun*, vol. 53, pp. 12262–12265, 2017.

Paper I

Analyst

CRITICAL REVIEW

View Article Online
View Journal | View Issue

Cite this: *Analyst*, 2017, **142**, 555

Recent advancements and future directions of superficially porous chiral stationary phases for ultrafast high-performance enantioseparations

Martina Catani,[a] Omar H. Ismail,[b] Francesco Gasparrini,[b] Michela Antonelli,[b] Luisa Pasti,[a] Nicola Marchetti,[a] Simona Felletti[a] and Alberto Cavazzini*[a]

Received 24th November 2016,
Accepted 20th December 2016

DOI: 10.1039/c6an02530g

rsc.li/analyst

This review focuses on the use of superficially porous particles (SPPs) as chiral stationary phases for ultra-high performance liquid enantioseparations. In contrast to what happened in achiral separations where core–shell particles invaded the market, the introduction of SPPs in chiral liquid chromatography (LC) has been relatively recent. This is due in part to the technical difficulties in the preparation of these phases, and in part to scarce understanding of mass transfer phenomena in chiral chromatography. As a matter of fact, nowadays, the development of superficially porous CSPs is still in its infancy. This paper covers the most recent advancements in the field of core–shell technology applied to chiral separations. We review the kinds of chiral selectors that have been used for the preparation of these phases, by discussing the advantages of chiral SPPs over their fully-porous counterparts for high efficient high throughput enantioseparations. Notwithstanding the apparently obvious advantages in terms of the mass transfer of chiral SPPs, some critical aspects that could impact their development are presented.

1. Introduction

In 2006 Kirkland introduced the so-called second generation superficially porous particles (SPPs),[1,2] also referred to as core–shell, solid–core, Fused-Core™ or pellicular particles. Prepared by a proprietary nanoparticle technology, these 2.7 μm C_{18}

[a]*Dept. of Chemistry and Pharmaceutical Sciences, University of Ferrara, via L. Borsari 46, 44121 Ferrara, Italy. E-mail: cvz@unife.it; Fax: +39 0532 240709; Tel: +39 0532 455331*
[b]*Department of Drug Chemistry and Technology, "Sapienza" Università di Roma, P.le A. Moro 5, 00185 Roma, Italy*

Martina Catani

Martina Catani was born in 1989. She received a master's degree in Chemistry in 2013 from the University of Ferrara. Since 2014 she has been a PhD student at the same university under the supervision of Prof. Alberto Cavazzini. Her research activity focuses around the investigation of the thermodynamics and the kinetics of separations in liquid chromatography with different kinds of stationary phases, including C_{18}, perfluorinated and chiral ones. During her PhD program, she spent periods of study in the groups of Prof. Gert Desmet (Brussels) and Prof. Attila Felinger (Pécs).

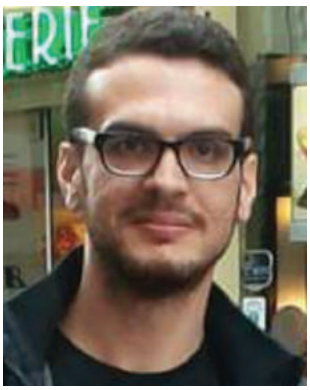

Omar H. Ismail

Omar H. Ismail was born in 1989. He has a master's degree in Medicinal Chemistry from the Sapienza University of Rome, and, currently, is a PhD student in Pharmaceutical Sciences at the same university. His scientific studies are focused on the theoretical evaluation of the new generation of sub-2 μm C_{18} columns in RP-ultra-high performance chromatography (RP-UHPLC). In addition, his research includes the development of sub-2 μm chiral stationary phases, using Pirkle/brush-type selectors, starting from the optimization of the synthetic strategies to the kinetic/thermodynamic evaluation of the columns packed with those CSPs. He is the co-author of 10 publications in peer-reviewed international scientific journals.

spherical particles were made of a 1.7 μm solid core surrounded by a 0.5 μm porous shell. The advantage of a porous zone occupying roughly three-quarters of the total volume of the particle is that it allows for a higher loading than the first generation core–shell particles developed in the late 1960s, which were made of a 50 μm solid core surrounded by a porous layer of only 1–2 μm.[3,4] Second generation core–shell particles have represented a breakthrough innovation into the market of chromatographic columns, providing efficiencies very similar to those of columns packed with 1.7 μm spherical fully porous particles but at a significantly lower back-pressure.[5–8] Since their introduction, a very large number of core–shell particles have been commercialized by different manufacturers with specific processes of preparation, surface chemistries and functionalization.[9–13]

The employment of SPPs in chiral liquid chromatography (LC) is more recent.[14–16] To the best of our knowledge, the first report about the use of chiral SPPs in LC is by Lindner's group in 2011.[17] They reported about the enantioseparation of amide type amino acid derivatives on a cinchona alkaloid-based anion exchanger CSP prepared on 2.7 μm fused-core particles. In this study, however, not much emphasis was given to the novelty of the CSP, nor to the advantages of the core–shell technology for efficient chiral separations.

Chankvetadze and his group[18] were the first to investigate the characteristics of a pellicular CSP from a fundamental viewpoint. They used a polysaccharide-based CSP obtained by coating 2.6 μm pellicular particles. Following these authors, the principal advantages in using chiral SPPs compared to (chiral) fully porous particles (FPPs) lie in a higher enantioselectivity at a comparable content of the chiral selector, a limited dependence of the plate height on the mobile phase flow rate and a larger enantioresolution per analysis time.[18,19]

The most comprehensive work aimed at evaluating the performance of chiral SPPs for high-efficiency and high-throughput enantioseparations has been done by Armstrong and coworkers.[20–23] They have studied a wide variety of bonded brush-type CSPs prepared on 2.7 μm SPPs, including cyclofructan-6 based, β-cyclodextrin and macrocyclic antibiotics (among which are, in particular, teicoplanin, teicoplanin aglycone and vancomycin).[20] The emerging concept from these studies is that chiral SPPs outperform, in terms of kinetic performance, their FPP counterparts practically in all modes of chromatography, *i.e.*, reversed-phase (RP), normal phase (NP), polar organic and HILIC.[20–24] Thanks to the employment of very short columns (5 cm) packed with chiral SPPs operated at high flow rates, Armstrong and colleagues have very recently obtained striking results in the field of ultra-fast chiral chromatography. By carefully reducing the extra-column volume of the equipment used in their measurements, they have indeed performed the sub-second separation of several enantiomers on various stationary phases (quinine- and teicoplanin-based) and under a variety of chromatographic modes.[25,26]

Looking at these extraordinary results, it would seem difficult to think about different approaches to achieve ultra-fast chiral separations *via* LC. However, at the same time as Armstrong's group, Ismail *et al.*[27] published the first example of a sub-second enantioseparation performed on chiral FPPs. In particular, they report about the separation of *trans*-stilbene oxide enantiomers on a 10 × 3.0 mm column packed with 1.8 μm Pirkle-type Whelk-O1 FPPs in 0.9 seconds (retention factor of the more retained enantiomer is about 1.7). Furthermore, in this study, some of the above-mentioned advantages theoretically provided by SPPs over FPPs towards ultrafast chiral chromatography have been challenged. Essentially, on the one hand, these authors point out about

Francesco Gasparrini

Francesco Gasparrini, born in 1945, earned a Laurea in Chemistry in 1969 (University of Camerino). He has been a Professor of Organic Chemistry since 1986 at the Sapienza University of Rome; he was the Co-Chairman of the 2nd ISCD (1991) and of the 16th ISCD (2005). Awards: from the Italian Chemical Society (2001, "Structure Determination and Molecular Interactions" and 2011, award in the memory of Prof. Piero Pino); from the Analytical Chemistry Division of the Italian Chemical Society (2013, Arnaldo Liberti medal). He is the author of ca. *210 peer-reviewed papers and 15 patents (3 new CSPs are commercially available: DACH-DNB by Regis, USA; Chirobiotig-TAG and P-CAP by Sigma Aldrich, USA).*

Luisa Pasti

Luisa Pasti was born in 1964, and she has a master's degree in Chemistry and a PhD in Chemical Sciences from the University of Ferrara. She was a research fellow at the Vrije Universiteit Brussel, in the group of Prof. Désiré L. Massart from 1996 to 1998. She was employed in the Enichem Research Center. In 2007 she became an Assistant Professor at the University of Ferrara, until 2014 when she became an Associate Professor of Analytical Chemistry. Her research is concerned with both the theoretical and experimental development of chromatography and chromatography-like techniques. Practical applications of this research include the characterization of microporous and mesoporous materials.

the difficulty of achieving highly efficient packed beds by a slurry packing of polar SPPs (such as the chiral ones). On the other hand, they mention the importance of a deeper investigation of if and how the kinetics of adsorption–desorption depends on the surface density of chiral ligands. Not only could this be very important to understand how the resolution, selectivity and loading of chiral ligands are connected, but it is also fundamental to compare the performance of chiral SPPs and FPPs of similar particle sizes. The chemical functionalization of these particles (even if performed under identical experimental conditions) has been indeed shown to lead to different results in terms of the surface density of the chiral selector.[21,24,27] Following these authors, the assumption that chiral SPPs are the only support suitable to prepare chiral columns for ultrafast enantioseparations is therefore possibly premature.

The scope of this review is to provide an overview of the most important achievements in the field of fast and ultrafast chiral separations permitted by the use of core–shell technology. In doing so, the different CSPs that have been prepared in a pellicular format have been described; the fundamentals of mass transfer in chiral chromatography have been discussed; a critical comparison of the pros and cons of chiral SPPs and FPPs for ultrafast enantioseparations has been proposed by focussing on some critical aspects that, in our opinion, need to be further investigated for the successful implementation of core–shell technology in chiral separations.

2. Mass transfer in chiral chromatography

In this section, the fundamentals of mass transfer in chiral chromatography are shortly summarized. The equation from which this discussion starts from is the well-known van Deemter equation,[28] which correlates the height equivalent to a theoretical plate, H (or its adimensional form, $h = H/d_p$, where d_p is the particle diameter) to the mobile phase velocity. Since there is no flow inside the mesoporous silica employed in LC, the right velocity to refer to is the interstitial velocity, u_e, *i.e.* the velocity of the mobile phase moving between particles:[29]

$$u_e = \frac{F_v}{\pi r_c^2 \varepsilon_e} \quad (1)$$

or, in reduced coordinates:

$$\nu = \frac{u_e d_p}{D_m}. \quad (2)$$

In eqn. (1) and (2), F_v is the flow rate, r_c the inner column radius, D_m the bulk molecular diffusion coefficient and ε_e the external column porosity, defined as:

$$\varepsilon_e = \frac{V_e}{V_{col}} \quad (3)$$

with V_{col} and V_e, respectively, the geometric and the external volume of the column. V_e can be determined, *e.g.*, through inverse size exclusion chromatography (ISEC) or pore blocking.[28,30–32] Under the hypothesis that the different mass transfer phenomena are independent of each other, the van Deemter equation, in reduced coordinates, is written as:

$$h = a(\nu) + \frac{b}{\nu} + c_s\nu + c_{ads}\nu + h_{heat} \quad (4)$$

where $a(\nu)$ is the eddy dispersion, b represents the longitudinal diffusion term, c_s is the mass transfer resistance across the stationary phase and c_{ads} is a term accounting for slow adsorption–desorption kinetics. This term is usually omitted in achiral RP LC, owing to the very fast adsorption–desorption process under these conditions (unless the separation of very

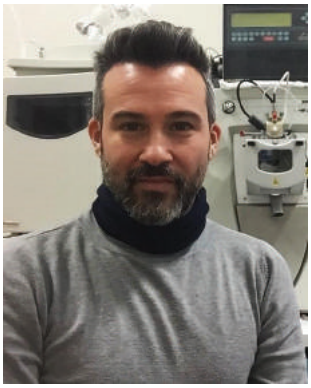

Nicola Marchetti

Nicola Marchetti was born in 1976. He has a master's degree in Chemistry and received his PhD in Chemical Sciences from the University of Ferrara in 2005. He was a post-doctoral research fellow at the University of Tennessee (Knoxville, TN, USA) from 2006 to 2008, in the group of Prof. Georges Guiochon. Then he returned to Italy and was appointed as a fixed-term Assistant Professor at the University of Ferrara from 2010. Now, he is a senior temporary Assistant Professor and his research activities focus on LC-MS and sample extraction, particularly the qualitative–quantitative analytical characterization of complex matrices of environmental, biological and food origin.

Alberto Cavazzini

Alberto Cavazzini (1970) has a master's degree in Chemistry and received his PhD in Chemical Sciences from the University of Ferrara in 2000. He was a research fellow at the University of Tennessee (Knoxville, TN, USA) and Oak Ridge National Laboratories (Oak Ridge, TN, USA) from 2000 to 2002, in the group of Prof. Georges Guiochon. In 2002 he returned to Italy after accepting an Assistant Professor position at the University of Ferrara, which he held until 2014 when he became a Professor of Analytical Chemistry. His research activities focus on separation science, particularly on liquid chromatography and chromatographic-like techniques.

large molecules, such as proteins, is considered). In chiral LC, on the other hand, the adsorption–desorption kinetics can be significantly slow also for low molecular-weight compounds and, particularly, for the second eluted enantiomer.[33] The term h_{heat} in eqn (4) accounts for the frictional heating due to the stream of the mobile phase against the bed under significant pressure. This contribution must be considered with columns packed with very fine particles, irrespective of whether they are chiral or achiral.[20,23,31,34]

The study of mass transfer in porous media has tremendously advanced in the last few years. Nowadays an accurate and independent evaluation of the individual factors contributing to peak broadening in LC is possible.[28,35–39] Conversely, the approach based on the nonlinear fitting of the experimental h data collected at different flow rates – traditionally employed for the estimation of van Deemter's equation coefficients – is to be avoided leading to parameters that are not physically meaningful.[40]

The longitudinal (or axial) diffusion term describes the band broadening due to the relaxation of the axial concentration gradient through the porous particles and the interstitial volume, in the absence of a flow. Since this is the only contribution to the band broadening when the flow is switched off, it is the best estimated through peak parking experiments. These consist of: (1) taking at a constant, arbitrary linear velocity as a sample zone somewhere in the middle of the chromatographic column; (2) suddenly stopping the flow; (3) leaving the band free to diffuse during a certain parking time, t_p; (4) resuming the flow rate to move the band out of the column. The variance (in length units) of the eluted peak, σ_x^2, is measured ($\sigma_x^2 = L^2/N$, where L is the column length and N the number of theoretical plates) and the procedure is repeated (keeping the flow rate constant) for different parking times. The slope of the σ_x^2 *vs.* t_p plot gives an estimate of the D_{eff}, being:[34,41]

$$D_{eff} = \frac{1}{2}\frac{\Delta\sigma_x^2}{\Delta t_p}. \quad (5)$$

Through D_{eff}, the longitudinal diffusion term can be calculated. In reduced coordinates, it is:

$$b = 2(1 + k_1)\frac{D_{eff}}{D_m} = 2(1 + k_1)\gamma_{eff} \quad (6)$$

where γ_{eff} ($= D_{eff}/D_m$) is the dimensionless effective diffusion coefficient and k_1 is the zone retention factor, defined as:

$$k_1 = \frac{t_R - t_e}{t_e} \quad (7)$$

t_R being the retention time and t_e is the time spent by a species molecule in the interstitial volume. By invoking the ergodic hypothesis,[42–44] it is straightforward to show that:

$$k_1 \equiv \frac{n_{part}}{n_e} = \frac{1 - \varepsilon_e}{\varepsilon_e}\left[\varepsilon_p + (1 - \varepsilon_p)K_a\right](1 - \rho^3) \quad (8)$$

where n_{part} and n_e represent the number of molecules in the particle volume and in the interstitial volume, respectively,

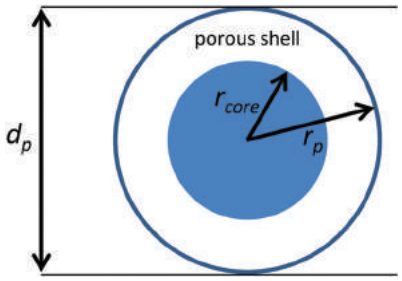

Fig. 1 Structure of a core–shell particle. d_p: particle diameter; r_p: particle radius; r_{core}: inaccessible core radius.

K_a is the distribution coefficient (equilibrium constant) of the sample between the porous zone and the eluent (see Fig. 1), $\rho = r_{core}/r_p$ is the ratio between the radius of the core and that of the whole particle (ρ is thus 0 for fully porous particles and 1 for non-porous ones) and ε_p is the particle porosity, *i.e.* the fraction of the particle volume that is occupied by pores:

$$\varepsilon_p = \frac{V_{pores}}{V_{part}} \quad (9)$$

V_{pores} and V_{part} being the pore and the particle volume, respectively. For core–shell particles, ε_p can be calculated as:[45]

$$\varepsilon_p = \frac{\varepsilon_t - \varepsilon_e}{(1 - \varepsilon_e)(1 - \rho^3)} \quad (10)$$

where ε_{tot} ($= V_0/V_{col}$, being V_0 the void volume) is the total column porosity.[46]

Finally, k_1 is connected to the more often employed phase retention factor, $k(= \frac{t_R - t_0}{t_0}$, t_0 being the void time), *via*:

$$k_1 = \frac{(1 + k)\varepsilon_{tot}}{\varepsilon_e} - 1. \quad (11)$$

Eqn (11) directly originates from the fact that the migration velocity of a retained component, u_R, can be referred to as either the migration velocity of an unretained compound, u_0, or as the interstitial velocity, *i.e.*:[47]

$$u_R = \frac{u_0}{1 + k} = \frac{u_e}{1 + k_1}. \quad (12)$$

The c_s term appearing in eqn (4) describes the solid–liquid mass transfer resistance due to the diffusion across the particle. Since there is an absence of flow inside the particles, this term is velocity-independent, which makes it easier to establish a theoretically-sound expression for this contribution. Following Kaczmarski,[48] for superficially porous spherical particles, this term can be written as:

$$c_s = \frac{1}{30}\frac{\varepsilon_e}{1 - \varepsilon_e}\left[\frac{k_1}{1 + k_1}\right]^2 \frac{1 + 2\rho + 3\rho^2 - \rho^3 - 5\rho^4}{(1 + \rho + \rho^2)^2} \frac{D_m}{D_{pz}\left(\varepsilon_p + (1 - \varepsilon_p)K_a\right)} \quad (13)$$

where D_{pz} is the diffusion coefficient in the porous zone, which can be estimated from D_{eff}, once a model of diffusion

through the porous medium has been defined.[28,35,36] For instance, in the simplest case of the so-called parallel or time-averaged model proposed by Knox (where all mass fluxes inside and outside the particle are considered additives),[49] D_{pz} is simply given by:

$$D_{pz} = \frac{(1 + k_1)D_{eff} - \gamma_e D_m}{k_1} \quad (14)$$

γ_e being the so-called obstructive geometrical factor. For a randomly packed column of impermeable spheres with a porosity of about 0.4, γ_e is approximatively 0.65 (ref. 50) (otherwise γ_e can be experimentally estimated through pore blocking[30]).

The expression of the term associated with a slow adsorption–desorption kinetics obtained by the Laplace transformation of the general rate model of chromatography,[45,51] is written in the case of superficially porous particles:[48,52,53]

$$c_{ads} = 2\frac{\varepsilon_e}{1-\varepsilon_e}\frac{1}{1-\varepsilon_p}\frac{1}{1-\rho^3}\left(\frac{k_1}{1+k_1}\right)^2\left(\frac{k_p}{1+k_p}\right)^2\frac{D_m}{k_{ads}{d_p}^2} \quad (15)$$

where k_p is:

$$k_p = \frac{1-\varepsilon_p}{\varepsilon_p}K_a \quad (16)$$

and k_{ads} is the kinetic adsorption constant. eqn (15) reveals that the calculation of c_{ads} requires the independent estimation of k_{ads} that – as will be discussed in the following – makes the estimation of this term *via* LC nontrivial.

The eddy dispersion term, $a(\nu)$ in eqn (4), is caused by the erratic flow profile in the through-pores of the packed bed. It includes *trans*-channel eddy dispersion, short-range inter-channel eddy dispersion, and *trans*-column eddy dispersion. Despite the fundamental work of Giddings that culminated in the well-known coupling theory,[42] there is still considerable debate in the literature regarding the values of the geometrical parameters needed to describe the complex structures of packed beds. Much work in this direction has been done by Tallarek and coworkers, who proposed a sophisticated approach based on the morphological reconstruction of the stationary phase structure and the calculation of the transport properties in the reconstructed materials.[38,39,54] In achiral systems, where the contribution of c_{ads} is negligible, the experimental estimation of $a(\nu)$ can be achieved by subtracting, from accurately measured h values (eqn (4)), both the longitudinal diffusion and the mass transfer terms (estimated, respectively, by eqn (6) and (13)).[28] In chiral systems, in contrast, this approach cannot be pursued since c_{ads} cannot be neglected. By ignoring frictional heating, indeed, the subtraction of b and c_s terms from h values, leads to

$$a(\nu) + c_{ads}\nu = h - \frac{b}{\nu} - c_s\nu \quad (17)$$

showing that an independent evaluation of the $a(\nu)$ and c_{ads} terms is not possible with this approach. Either $a(\nu)$ or c_{ads} must be estimated by different routes. As it was mentioned before, $a(\nu)$ can be quantified by the theoretical estimation of *trans*-channel, short-range, inter-channel and *trans*-column eddy dispersions.[33] Otherwise, $a(\nu)$ could be measured by employing achiral compounds eluted on the chiral column under investigation. Both approaches have some limitations. In the former case, the theoretical estimation of single terms of eddy dispersion, and thus $a(\nu)$, is difficult to assess. In the second case, one assumes that the eddy dispersion for achiral compounds is the same as for chiral ones, which could not be even in the case when they have similar retention factors.[55]

On the other hand, the determination of c_{ads} could be made by the microscopic model of chromatography, such as the so-called stochastic theory of chromatography.[42–44] This model focuses on the behavior of a single molecule during its chromatographic migration through the column. This erratic process is described as the sum of a random number of (random) events corresponding to visits in the stationary phase and movements in the mobile phase between two successive adsorptions. Accordingly, the time spent by a molecule inside the column is the sum of the times spent by the molecule in the stationary phase and those elapsed in the mobile phase between two successive adsorptions.[44,56–60] From the analysis of the peak shape, the stochastic model allows for the estimation of both the average adsorption time, τ_s, and the flying time, as well as of the number of adsorption–desorption steps. Thus, from the average adsorption time, the estimation of k_{ads} is possible, as follows:[42]

$$k_{ads} = \frac{1}{\tau_s}. \quad (18)$$

The difficulty of accurately measuring the adsorption–desorption kinetics has definitely slowed down the developments of high-efficiency, high-throughput enantioseparations, independent of whether core–shell or fully porous particles are employed.

3. Advantages and drawbacks of core–shell and fully-porous chiral particles for ultrafast high-efficiency enantioseparations

It is well known that core–shell particles offer some important advantages to speed up mass transfer compared to FPPs. The contributions to band broadening coming from both longitudinal diffusion (b-term of the van Deemter equation) and solid–liquid mass transfer resistance (c_s-term of the van Deemter equation) are indeed reduced by the presence of the inaccessible core. But, possibly, an even more important advantage of SPPs is that packed beds made of these particles are claimed to be more efficient than those packed with FPPs, even if admittedly this has been so far demonstrated only for hydrophobic C_{18} SPPs. It turned out that indeed columns packed with C_{18} SPPs are extremely efficient owing to their very low eddy dispersion.[32,34,61] Granted that the explanation of

this remains to a large extent unknown, the most accepted hypothesis is that the roughness of the C_{18} core–shell particles limits particle slipping after the release of the high pressure employed for the preparation of the packed bed by slurry-packing. This should basically reduce the bed heterogeneity in the radial direction and thus $a(\nu)$.[9,11]

The design and preparation of chiral SPPs has reflected the aim of exploiting the above mentioned advantages also in the field of chiral separations *via* LC. Recently, the proof-of-concept demonstration of ultrafast chiral separations on chiral SPPs was presented by Armstrong's group. In a series of publications, Armstrong and coworkers described several examples of subsecond enantioseparations performed on core–shell based CSPs.[20–23]

For all these reasons, core–shell CSPs have been considered the best candidate for the transition from traditional chiral-high performance LC (HPLC) to fast or ultrafast chiral ultra-high performance LC (UHPLC).

In spite of these very promising results, some of the authors of this review[27] have recently pointed out that to draw a definitive conclusion on whether SPPs are the only (or, possibly, the best) option towards the realization of high-efficiency, high-throughput CSPs, a deeper investigation of some aspects is necessary. In their study, Ismail *et al.*[27] compared the kinetic behavior of Whelk-O1 CSPs prepared on 2.6 μm core–shell particles and on both 2.5 and 1.8 μm FPPs. Two critical issues were identified. The first is about the experimental difficulty in the preparation, through high-pressure slurry packing, of efficient packed beds made of polar SPPs (in their case chiral Whelk-O1 SPPs). The second is the lack of information regarding the kinetics of adsorption–desorption on CSPs and, in particular, if and how the surface density of a chiral selector may affect it.

The difficulty to efficiently pack a chromatographic bed impinges on the kinetic performance of the column, basically through the *a*-term of the van Deemter equation. Following Ismail *et al.*, the slurry packing of polar SPPs is more difficult than that of C_{18} ones.[28,31,32] However, it is complicated to understand which are the critical factors determining the quality of the packing of chiral core–shell particles. Not only is the preparation of stable slurry suspensions of polar core–shell particles something that can create problems, but also the fine control of the experimental conditions of packing appears difficult to optimize, not to say, to standardize. Quite unpredictable results were obtained by changing some experimental conditions that are commonly varied to improve the quality of packing. For instance, it was observed that the kinetic performance (estimated through the minimum of the van Deemter curves) of chiral core–shell columns, otherwise packed under identical experimental conditions, changed dramatically by changing the time of compression of the bed.[27] However, this did not follow a clearly decipherable pattern. For instance, it was not possible to find any correlation between the compression time and column efficiency. On the other hand, these issues were not observed during the preparation of columns packed with fully porous chiral particles. These findings suggest that much work has still to be done to improve the packing of polar SPPs to get the maximum benefit in terms of column efficiency.

The second consideration by Ismail *et al.*[27] concerns the adsorption–desorption kinetics and, mainly, if and how it depends on the surface density of the chiral selector. While in achiral chromatography the kinetics of adsorption–desorption is practically never an issue (unless the separation of very large molecules is considered), in chiral chromatography even low molecular-weight molecules can exhibit slow adsorption–desorption. This can be particularly evident for the more retained enantiomer, which is often characterized by a strongly tailed peak.[18] However, there are no systematic studies in the literature aimed at investigating these features, while more attention has been paid to the dependence of thermodynamics (*e.g.*, the enantioselectivity) on the amount of the chiral selector bound to the surface.[18,19]

This is, however, particularly important as several research groups have independently reported about the experimental difficulty to obtain the same surface coverage (μmol m^{-2}) of the chiral selector on superficially and fully porous particles, even if the functionalization of both kinds of particles was carried out under identical experimental conditions.[21,24,27] Incidentally, these conditions are such that the amount of the chiral selector is always in a large excess with respect to the estimated number of reactive surface silanols. For instance, Ismail *et al.*[27] found that the functionalization of base SPPs leads to a significantly larger surface coverage of the chiral selector (roughly +20%) than that of native fully porous silica particles. They suggested that this could be due to different reasons, including a larger accessibility of the external layers of particles (with respect to the inner ones) or a different surface chemistry of base silica FPPs and SPPs. Both Spudeit *et al.*[21] and Patel *et al.*[20] reported very similar findings. On the other hand, Dolzan *et al.*[24] found the opposite behavior, the surface coverage of chiral selectors being larger on fully- than on superficially-porous particles. Obviously, since the specific surface area (m^2 g^{-1}) of FPPs is larger than that of SPPs, the total amount of the chiral selector bound per gram of base silica is always greater on FPPs than on SPPs. In light of these aspects, it is fundamental to know how the adsorption–desorption kinetics is affected by the surface density of the chiral selector. If the adsorption–desorption kinetics depended on the surface density of chiral selectors, this last one would possibly become one of the most important parameters to be considered during the preparation of high efficiency CSPs for ultrafast separations.

One last aspect that is worth discussing in this paragraph is regarding the effect of frictional heating. This is generated by the stream of the mobile phase against the packed bed of the column through which it percolates under a significant pressure gradient.[62–64] It can happen in RP as well as in NP, even though in the latter mode it is less evident due to a smaller back pressure under these conditions.[20] The heat produced locally is dissipated in both the radial and longitudinal directions of the column. This generates longitudinal and

radial temperature gradients, whose amplitude depends on the degree of thermal insulation of the column (either adiabatic or isothermal).[65–67] It is evident that, in this respect, chiral core–shell particles offer, at least theoretically, a significant advantage over fully porous ones exactly as it happens in achiral chromatography.

4. Chiral selectors prepared on SPPs

In this section, the classes of chiral selectors that have been prepared on superficially porous particles are briefly reviewed. Their structures are schematically represented in Fig. 2. Simultaneously, some of the applications for which they have been employed are described.

4.1 Polysaccharide-based CSPs

The first report about polysaccharide-based CSPs made on SPPs is that by Lomsadze *et al.* in 2012.[18] 2.6 μm SPPs were coated with cellulose tris(4-chloro-3-methylphenylcarbamate). These particles were used to prepare a packed column (250 × 4.6 mm, *L* × ID), whose chromatographic behavior was compared to that of the other two columns, namely, (i) a home-made 250 × 4.6 mm column packed with 3 μm FPPs functionalized in house with the same chiral selector and (ii) a commercial 250 × 4.6 mm Lux Cellulose-4 (from Phenomenex), also packed with 3 μm FPPs coated with cellulose tris(4-chloro-3-methylphenylcarbamate). The difference between the last two columns (apart from the packing) is the loading of the chiral selector that was almost four times larger on the commercial phase than on the home-made one. The authors concluded that the SPP column outperformed the FPP ones in terms of the plate number, resolution per unit time and optimal flow rate range. On the other hand, they observed that the commercial FPP column showed the highest selectivity, by virtue of a larger amount (in the paper by Lomsadze *et al.*,[18] this is the total amount per gram of base silica and not the surface density) of the chiral selector. Thus, this observation contrasts with that by Ismail *et al.*[27] who found a larger selectivity on the core–shell CSP with respect to the fully porous counterpart, in spite of a significantly smaller total amount of the chiral selector on the SPPs. The authors also mentioned about the difficulty of preparing polysaccharide-based CSPs on small silica particles due to the formation of numerous particle aggregates. The same CSPs were used by Fanali and co-workers to pack capillary columns for capillary chromatography and electrochromatography.[68,69] The authors encountered several difficulties to adequately operate these capillaries most likely owing to their inefficient packing.

In a recent paper,[19] Chankvetadze's group prepared two other polysaccharide-based CSPs on SPPs, by respectively coating cellulose tris(3,5-dimethylphenylcarbamate) on 2.8 μm particles and amylose tris(3,5-dimethylphenylcarbamate) on 3.6 μm particles. This study was aimed at demonstrating the potential of polysaccharide-based SPP CSPs to perform fast chiral separations. Indeed some interesting examples of enantioseparations performed in less than half a minute were reported by Chankvetadze's group (see Fig. 3), even though admittedly there is not enough information to evaluate the real kinetic performance of these CSPs.

4.2 Pirkle-type CSPs

By using a layer-by-layer self-assembly approach, Wu *et al.* synthetized SPPs with *trans*-(1*R*,2*R*)-diaminocyclohexane (DACH). These particles were tested as CSPs for LC towards the separation of several couples of enantiomers including binaphthol, bromo-substituted binaphthol and biphenantrol.[70] In a very basic approach (apparently based on the comparison of only two chromatograms, in addition to being recorded under different experimental conditions), these authors compared the performance of this column with that of a column packed with DACH-functionalized periodic mesoporous silica, by concluding that the SPP version of the CSP allows for a better performance and shorter analysis times than the FPP one.

The Whelk-O1 chiral selector was used by Ismail *et al.*[27] to functionalize 2.6 μm SPPs. The performance of a column packed with these particles was compared, under NP conditions, to that of the other two columns packed with 2.5 μm and 1.8 μm FPPs. Contrary to the initial expectations, the performance of the column packed with SPPs was worse than that of the column packed with 1.8 μm FPPs and quasi-comparable to that of the column packed with 2.5 μm FPPs. As it was widely discussed in previous paragraphs, this was presumably due to the combined effect of a slower adsorption–desorption kinetics and a greater contribution of eddy dispersion on the Whelk-O1 SPPs than on the FPPs. A series of chromatograms showing the ultrafast enantioseparation of *trans*-stilbene oxide enantiomers on two columns (10 × 4.6 mm and 10 × 3.0 mm, *L* × ID) packed with 2.6 μm SPP and 1.8 μm FPP Whelk-O1 particles are reported in Fig. 4. See the figure caption for details.

4.3 Macrocyclic antibiotic CSPs

Macrocyclic antibiotics including teicoplanin, teicoplanin aglycone (TAG) and vancomycin were employed by Armstrong and co-workers to prepare 2.7 μm core–shell CSPs.[20] Columns of different geometrical characteristics (either 10 or 5 mm long with a 4.6 mm I.D.) were slurry packed with these CSPs. The ultrafast separation (<30 s) of a wide range of amino acids was performed with teicoplanin and TAG CSPs.

The performance of a 10 × 4.6 mm vancomycin SPP column was compared to that of the commercial Chirobiotic V column of the same dimensions by Barhate and colleagues.[22] The former column exhibited better peak shapes, greater performance and a higher resolution for the separation of fluorinated and desfluorinated pharmaceuticals.

Finally, macrocyclic antibiotic SPP-based columns were employed for the sub-minute[20] and sub-second[25] screening of achiral and chiral compounds in various chromatographic modes. Some remarkable examples of sub-second enantioseparations are reported in Fig. 5. See the figure caption for more details.

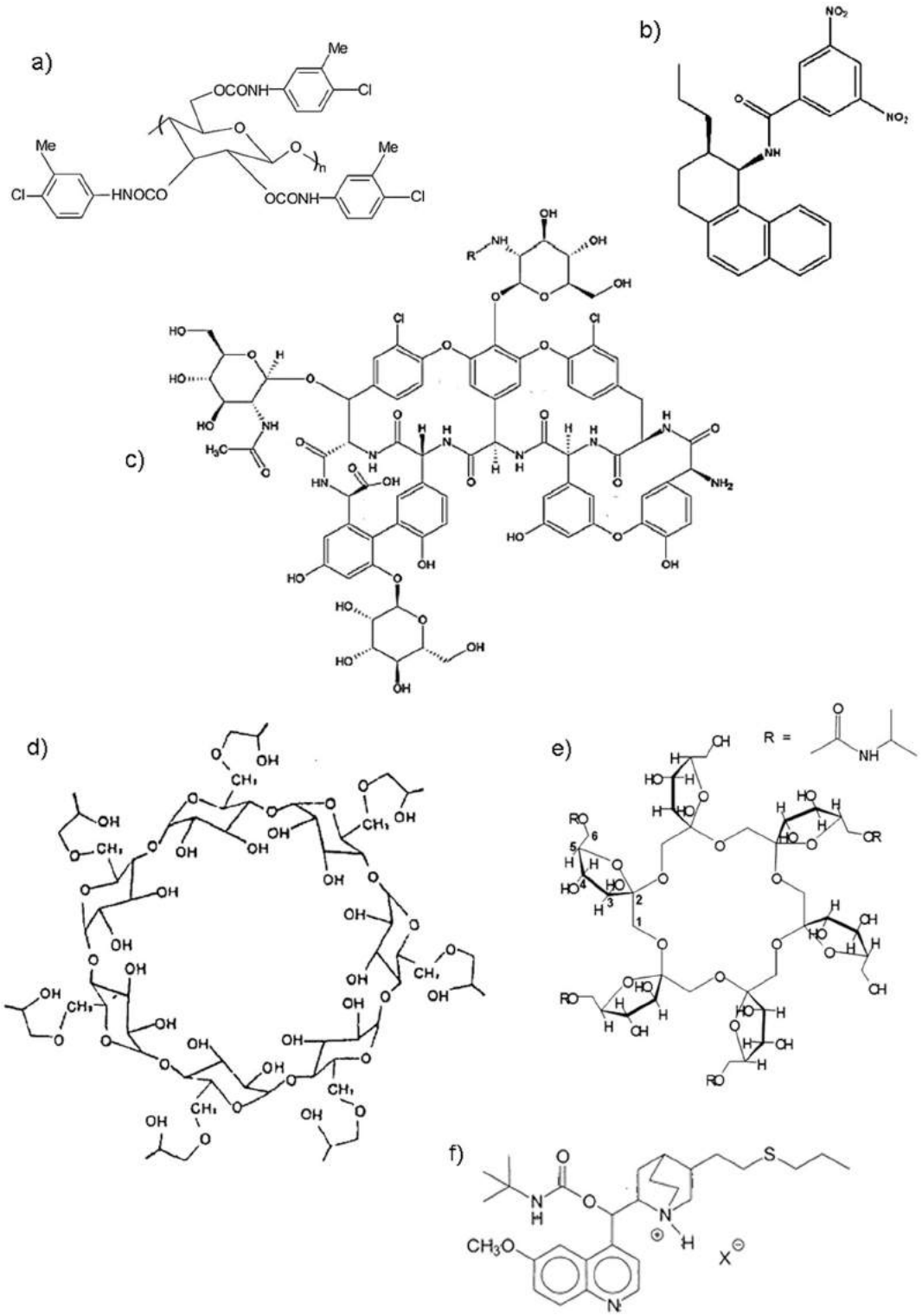

Fig. 2 Chemical structures of chiral selectors employed for the preparation of core–shell CSPs. (a) Cellulose tris(4-chloro-3-methylphenylcarbamate); (b) Whelk-O1; (c) teicoplanin; (d) cyclodextrin; (e) cyclofructan functionalized with the isopropyl carbamate group (CF6-P); (f) quinine carbamate derivative.

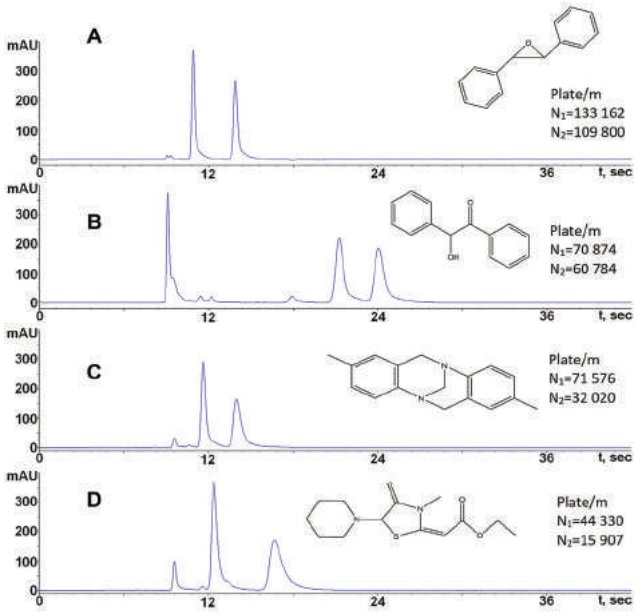

Fig. 3 Fast enantioseparations of the enantiomers of *trans*-stilbene oxide (A), benzoin (B), Tröger's base (C), and etozoline (D) performed on a 100 × 4.6 mm column packed with 3.6 μm SPPs functionalized with amylose tris(3,5-dimethylphenylcarbamate). Mobile phase: hexane/2-propanol 90 : 10 (case A and B) and methanol (case C and D). Flow rate: 5 mL min^{-1}. Reprinted with permission from ref. 19.

4.4 Cyclodextrin CSPs

Hydroxypropyl-β-cyclodextrin was used by Armstrong and co-workers to functionalize 2.7 μm SPPs, whose performance was compared to that of the two columns packed with 5 and 3 μm FPPs functionalized with the same chiral selector.[26] Small polar molecules such as nucleic acid bases, nucleotides, water soluble vitamins, β-blockers and salicylic acids were separated in the HILIC mode. Compared to FPP-based columns, the chiral SPP one exhibited better selectivities. No remarkable loss of efficiency was observed when the core–shell column was operated at high flow rates. Ultrafast separations were performed in less than 1 min.

This SPP-based CSP was also employed by Barhate and co-workers[22] to perform the ultrafast separation (analysis times <1 min) of fluorinated and desfluorinated pharmaceuticals.

4.5 Derivatized cyclofructan CSPs

Spudeit *et al.*[21] chemically bonded isopropyl cyclofructan 6 (CF6-P) to 2.7 μm SPPs. The column packed with this CSP was compared with other two FPP columns (5 and 3 μm particle sizes) with the same chemistry. The columns were operated under polar organic and normal phase modes for the separation of four pairs of enantiomers, including those of amlodipine and fipronil. The three columns showed comparable enantiomeric selectivity under constant mobile phase conditions, even though the SPP column was characterized by a higher surface density of the chiral selector. In contrast, the resolution measured on the SPP column was noticeably larger than that on the FPP columns. Shorter analysis times and wider optimal flow rates were achievable on the SPP-based column. Moreover, following these authors, the efficiency was enhanced thanks to a good packing quality. However, in the paper there is apparently not enough experimental

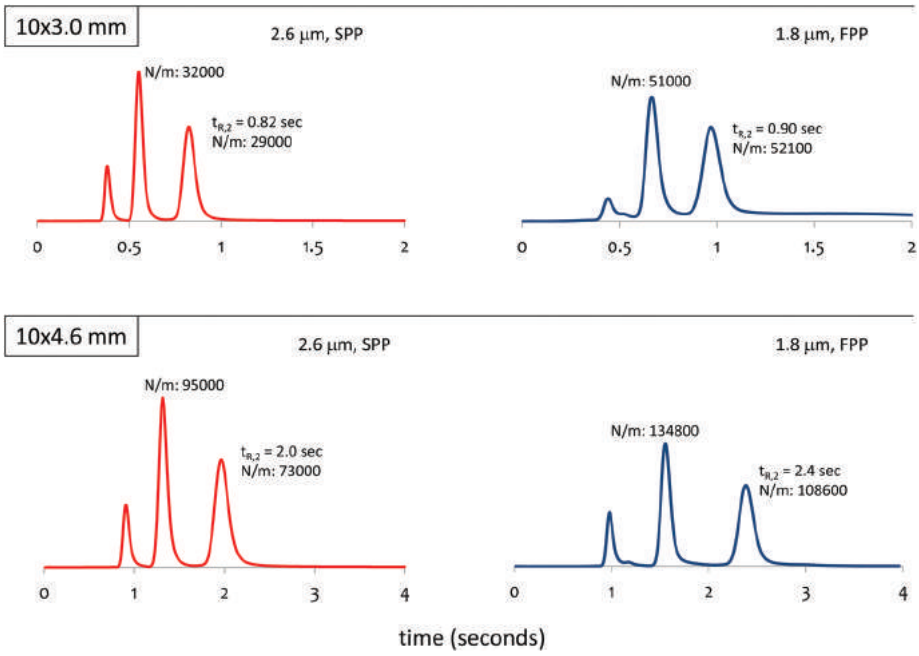

Fig. 4 Ultrafast enantioseparations on 10 × 3.0 mm (top) and 10 × 4.6 mm columns (bottom) packed with both 1.8 μm fully porous and 2.6 μm core–shell Whelk-O1 particles. Mobile phase 90 : 10, Hex/EtOH + 1% MeOH. Flow rate: 8 mL min^{-1}. The number of theoretical plates per meter and the retention time of the more retained enantiomer are indicated in each chromatogram. Unpublished data from ref. 27.

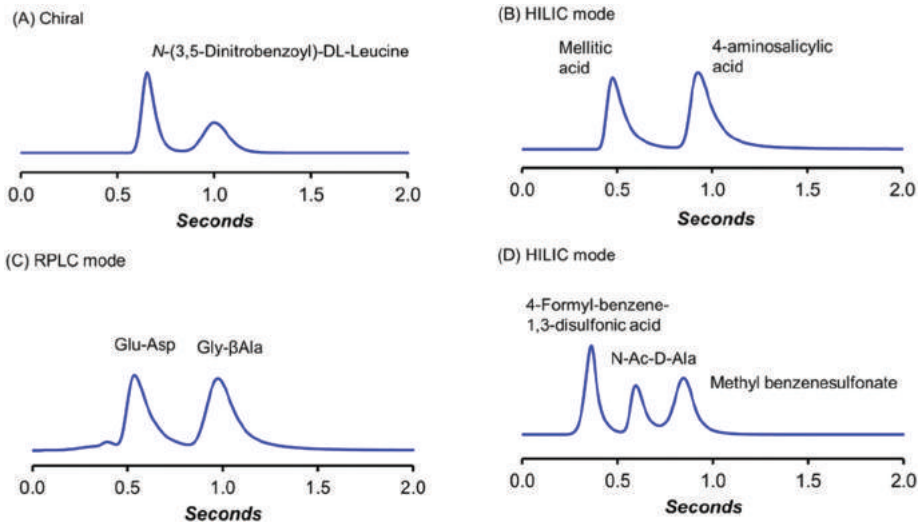

Fig. 5 Sub-second chromatography on various stationary phases using 50 × 4.6 mm I.D. columns: (A) SPP quinine (mobile phase 70 : 30, ACN/20 mM NH_4CO_2H, flow rate: 5 mL min^{-1}); (B) SPP silica (are indicated 94 : 6, ACN/15 mM $NH_4CH_3CO_2$, flow rate: 5 mL min^{-1}); (C) SPP teicoplanin (mobile phase 42 : 58, ACN/20 mM NH_4CO_2H, flow rate 5 mL min^{-1}); (D) SPP teicoplanin (mobile phase 70 : 30 ACN/water, flow rate 5 mL min^{-1}). Reprinted with permission from ref. 25.

information to support this hypothesis. The SPP-based CF6-P CSP was efficiently employed to perform the ultrafast separation of fluorinated and desfluorinated pharmaceuticals.[22]

Native cyclofructan 6 was employed as the chiral selector bonded to 2.7 μm SPP by Dolzan *et al.*[24] The performance of the column packed with these particles was evaluated under HILIC conditions and compared with that of the two FPP columns packed with 5 and 3 μm particles functionalized with the same chiral selector. This is the work where the functionalization of SPPs was found to lead to a lower surface density of the chiral selector than that of FPPs. The chiral core–shell column performed well in terms of analysis times and exhibited both higher optimal flow rates and efficiency than fully porous columns. However, the van Deemter curve measured on the 2.7 μm SPP column showed a comparable slope at high flow rates as that of the 3 μm FPP one, indicating that mass transfer was not advantageous on the former column. Following the authors, this was most likely due to a slow adsorption/desorption kinetics in the adsorbed water multilayer (typical of the HILIC mode).

Cyclofructan SPP-based CSPs were successfully employed to perform ultrafast separations (some of these in the sub-second domain) of achiral and chiral small molecules in different chromatographic modes.[20,25]

4.6 Ion and ligand exchange CSPs

The first ever report on SPP-based CSPs was that of Lindner and coworkers in 2011.[17] They reported about the preparation of a cinchona alkaloid based anion exchanger CSP on 2.7 μm SPPs. The column was employed for the separation of amide type amino acid derivatives.

A quinine-based CSP on 2.7 μm SPPs was employed by Armstrong and coworkers to perform sub-second separations of amino acid derivatives.[25]

5. Future directions

The reason for the great success of SPPs in achiral LC is that they have provided a reasonable compromise between two opposite tendencies. It is indeed well known that the tendency to improve analytical throughputs by using columns packed with smaller and smaller particles is limited by technical constraints, such as the very high pressures needed to operate these columns and the system extra-column volume. The future development of SPPs, even the chiral ones, towards particles of smaller diameters will necessarily require the availability of equipment with minimal extra-column volumes, that is also able to provide a very high back-pressure in the normal mode.

Another field where the development of a highly efficient chiral stationary phase for ultrafast separations is expected to have a tremendous impact is in supercritical fluid chromatography (SFC). Unlike what happened in LC, the technological advancement of SFC equipment has been much slower. The technical specifications of most of the instruments available nowadays on the market for SFC (*e.g.*, extra-column volume, maximum back-pressure/maximum flow-rate achievable, *etc.*) are indeed significantly worse than those for the instrumentation routinely employed in LC. Admittedly, with the packing particles already available, minor improvements in the characteristics of SFC equipment (for instance, a reduction in the volume of the detector cell that in many commercial instruments is excessively large) would permit the immediate achievement of extraordinary results in the direction of highest throughputs and ultrafast chiral separations.[71]

6. Conclusions

Chiral SPPs represent one of the most interesting advancements in the field of high-throughput ultrafast enantioseparations.

They were introduced as CSPs for LC more than five years ago. The scope was to exploit, in chiral liquid separations also, the advantages offered by core–shell particles and widely demonstrated in the literature (in particular, for the *b*- and *c*-terms of the van Deemter equation). Since then, different research groups all over the world have contributed to the development of these phases, to the resolution of many issues in their preparation and to the understanding of their properties in chiral separations.

It follows that the idea of using chiral core–shell particles for the preparation of highly efficient chiral columns is not a new one. Several research teams have been devoted to making pioneering publications in the field of chiral chromatography, as it has been mentioned in the present publication. It should also be mentioned that most recently a patent in this area has been filed, including selectors already described in some of the previous publications.[72]

The consistent employment of chiral SPPs for the fast separation of several classes of compounds is more recent. It culminated in the latest demonstration by Armstrong's group of sub-second chiral separations achieved on chiral SPPs of a different nature.

However, to conclude from all this that SPPs are the ideal (or, possibly, the only) support to prepare highly efficient CSPs for ultrafast enantioseparations is in our opinion not obvious. To fully exploit the intrinsic advantages of SPPs even in the field of chiral separations some not trivial practical and theoretical aspects need further investigation. In particular, the achievement of efficient packed beds of polar SPPs, by high-pressure slurry packing, is significantly more difficult than that of hydrophobic C_{18} core–shell particles. Thus, one of the greatest advantages (possibly the greatest one) of C_{18} core–shell particles – namely, their ability to give extraordinarily well packed beds – is not said to be a characteristic of polar SPPs too.

In addition, in our opinion it is necessary to deeply understand if and how the surface density of a chiral selector impinges on the kinetics of adsorption–desorption, especially by considering that the chemical functionalization of chiral SPPs is apparently inherently different from that of FPPs.

The impact of both an inefficient packing and a slow adsorption–desorption kinetics on the column efficiency can be extremely negative in terms of the column performance especially at high flow rates.

As a conclusive remark, we point out that without this information the comparison of the kinetic performance of the chiral core–shell and fully porous particles lacks any scientifically sound basis. This becomes particularly important when the comparison is used to generalize concepts beyond the performance analysis of the application explicitly executed.

Acknowledgements

The authors thank the Italian University and Scientific Research Ministry (Grant PRIN 2012ATMNJ_003) and the Laboratory Terra&Acqua Tech, member of the Energy and Environment Cluster, Technopole of Ferrara of Emilia-Romagna High Technology Network. Dr Valentina Costa from the University of Ferrara is acknowledged for technical support.

References

1 J. J. Kirkland, J. J. DeStefano and T. J. Langlois, *Am. Lab.*, 2007, 18–21.
2 J. J. DeStefano, S. A. Schuster, J. M. Lawhorn and J. J. Kirkland, *J. Chromatogr., A*, 2012, **1258**, 76–83.
3 C. G. Horváth, B. A. Preiss and S. R. Lipsky, *Anal. Chem.*, 1967, **39**, 1422–1428.
4 J. J. Kirkland, F. A. Truszkowski, C. H. Dilks Jr. and G. S. Engel, *J. Chromatogr., A*, 2000, **890**, 3–13.
5 A. Cavazzini, F. Gritti, K. Kaczmarski, N. Marchetti and G. Guiochon, *Anal. Chem.*, 2007, **79**, 5972–5979.
6 N. Marchetti, A. Cavazzini, F. Gritti and G. Guiochon, *J. Chromatogr., A*, 2007, **1163**, 203–211.
7 F. Gritti, A. Cavazzini, N. Marchetti and G. Guiochon, *J. Chromatogr., A*, 2007, **1157**, 289–303.
8 N. Marchetti and G. Guiochon, *J. Chromatogr., A*, 2007, **1176**, 206–216.
9 G. Guiochon and F. Gritti, *J. Chromatogr., A*, 2011, **1218**, 1915–1938.
10 F. Gritti, I. Leonardis, J. Abia and G. Guiochon, *J. Chromatogr., A*, 2010, **1217**, 3819–3843.
11 R. Hayes, A. Ahmed, T. Edge and H. Zhang, *J. Chromatogr., A*, 2014, **1357**, 36–52.
12 P. Jandera, T. Hàjek and M. Staňkovà, *Anal. Bioanal. Chem.*, 2016, **407**, 139–151.
13 N. Tanaka and D. V. McCalley, *Anal. Chem.*, 2016, **88**, 279–298.
14 A. Cavazzini, N. Marchetti, R. Guzzinati, M. Pierini, A. Ciogli, D. Kotoni, I. D'Acquarica, C. Villani and F. Gasparrini, *Trends Anal. Chem.*, 2014, **63**, 95–103.
15 L. Sciascera, O. Ismail, A. Ciogli, D. Kotoni, A. Cavazzini, L. Botta, T. Szczerba, J. Kocergin, C. Villani and F. Gasparrini, *J. Chromatogr., A*, 2015, 160–168.
16 A. Cavazzini, L. Pasti, A. Massi, N. Marchetti and F. Dondi, *Anal. Chim. Acta*, 2011, **706**, 205–222.
17 R. J. Reischl, L. Hartmanova, M. Carrozzo, M. Huszar, P. Frühauf and W. Lindner, *J. Chromatogr., A*, 2011, **1218**, 8379–8387.
18 K. Lomsadze, G. Jibuti, T. Farkas and B. Chankvetadze, *J. Chromatogr., A*, 2012, **1234**, 50–55.
19 Q. Kharaishvili, G. Jibuti, T. Farkas and B. Chankvetadze, *J. Chromatogr., A*, 2016, **1467**, 163–168.
20 D. C. Patel, Z. S. Breitbach, M. F. Wahab, C. L. Barhate and D. W. Armstrong, *Anal. Chem.*, 2015, **87**, 9137–9148.
21 D. A. Spudeit, M. D. Dolzan, Z. S. Breitbach, W. E. Barber, G. A. Micke and D. W. Armstrong, *J. Chromatogr., A*, 2014, **1363**, 89–95.
22 C. L. Barhate, Z. S. Breitbach, E. Costa Pinto, E. L. Regalado, C. J. Welch and D. W. Armstrong, *J. Chromatogr., A*, 2015, **1426**, 241–247.

23 D. C. Patel, M. F. Wahab, D. W. Armstrong and Z. S. Breitbach, *J. Chromatogr., A*, 2016, **1467**, 2–18.
24 M. D. Dolzan, D. A. Spudeit, Z. S. Breitbach, W. E. Barber, G. A. Micke and D. W. Armstrong, *J. Chromatogr., A*, 2014, **1365**, 124–130.
25 M. F. Wahab, R. M. Wimalasinghe, Y. Wang, C. L. Barhate, D. C. Patel and D. W. Armstrong, *Anal. Chem.*, 2016, **88**, 8821–8826.
26 R. W. Wimalasinghe, C. A. Weatherly, Z. S. Breitbach and D. W. Armstrong, *J. Liq. Chromatogr. Relat. Technol.*, 2016, **39**, 459–464.
27 O. H. Ismail, L. Pasti, A. Ciogli, C. Villani, J. Kocergin, S. Anderson, F. Gasparrini, A. Cavazzini and M. Catani, *J. Chromatogr., A*, 2016, **1466**, 96–104.
28 F. Gritti and G. Guiochon, *J. Chromatogr., A*, 2012, **1221**, 2–40.
29 U. D. Neue, in *HPLC Columns: Theory, Technology and Practice*, Wiley-VCH, 1997.
30 D. Cabooter, F. Lynen, P. Sandra and G. Desmet, *J. Chromatogr., A*, 2007, **1157**, 131–141.
31 O. H. Ismail, M. Catani, L. Pasti, A. Cavazzini, A. Ciogli, C. Villani, D. Kotoni, F. Gasparrini and D. S. Bell, *J. Chromatogr., A*, 2016, **1454**, 86–92.
32 M. Catani, O. H. Ismail, A. Cavazzini, A. Ciogli, C. Villani, L. Pasti, D. Cabooter, G. Desmet, F. Gasparrini and D. S. Bell, *J. Chromatogr., A*, 2016, **1454**, 78–85.
33 F. Gritti and G. Guiochon, *J. Chromatogr., A*, 2014, **1332**, 35–45.
34 F. Gritti and G. Guiochon, *J. Chromatogr., A*, 2012, **1221**, 2–40.
35 G. Desmet, K. Broeckhoven, J. De Smet, S. Deridder, G. V. Baron and P. Gzil, *J. Chromatogr., A*, 2008, **1188**, 171–188.
36 G. Desmet and S. Deridder, *J. Chromatogr., A*, 2011, **1218**, 32–45.
37 S. Deirdder, M. Catani, A. Cavazzini and G. Desmet, *J. Chromatogr., A*, 2016, **1456**, 137–144.
38 S. Bruns, T. Müllner, M. Kollmann, J. Schachtner, A. Höltzel and U. Tallarek, *Anal. Chem.*, 2010, **82**, 6569–6575.
39 S. Bruns and U. Tallarek, *J. Chromatogr., A*, 2011, **1218**, 1849–1860.
40 A. Cavazzini, G. Nadalini, V. Malanchin, V. Costa, F. Dondi and F. Gasparrini, *Anal. Chem.*, 2007, **79**, 3802–3809.
41 K. Miyabe, Y. Matsumoto and G. Guiochon, *Anal. Chem.*, 2007, **79**, 1970–1982.
42 J. C. Giddings, *Dynamics of Chromatography*, Marcel Dekker, New York, 1965.
43 F. Dondi, A. Cavazzini and M. Remelli, *Adv. Chromatogr.*, 1998, **38**, 51–74.
44 A. Cavazzini, M. Remelli, F. Dondi and A. Felinger, *Anal. Chem.*, 1999, **71**, 3453–3462.
45 G. Guiochon, A. Felinger, D. G. Shirazi and A. M. Katti, *Fundamentals of Preparative and Nonlinear Chromatography*, Academic Press, Elsevier, 2nd edn, 2006.
46 I. Quiñones, A. Cavazzini and G. Guiochon, *J. Chromatogr., A*, 2000, **877**, 1–11.
47 G. Desmet, *LC GC Eur.*, 2008, **21**, 310–317.
48 K. Kaczmarski, *J. Chromatogr., A*, 2011, **1218**, 951–958.
49 J. H. Knox and H. P. Scott, *J. Chromatogr.*, 1983, **282**, 297–313.
50 J. H. Knox and L. McLaren, *Anal. Chem.*, 1964, **36**, 1477–1482.
51 K. Kaczmarski, A. Cavazzini, P. Szabełski, D. Zhou, X. Liu and G. Guiochon, *J. Chromatogr., A*, 2002, **962**, 57–67.
52 K. Miyabe, *Anal. Sci.*, 2011, **27**, 1007–1017.
53 F. Gritti and G. Guiochon, *J. Chromatogr., A*, 2014, **1348**, 87–96.
54 S. Bruns, J. P. Grinias, L. E. Blue, J. W. Jorgenson and U. Tallarek, *Anal. Chem.*, 2012, **84**, 4496–4503.
55 F. Gritti and G. Guiochon, *J. Chromatogr., A*, 2010, **1217**, 6350–6365.
56 A. Cavazzini, F. Dondi, A. Jaulmes, C. Vidal-Madjar and A. Felinger, *Anal. Chem.*, 2002, **74**, 6269–6278.
57 A. Felinger, A. Cavazzini, M. Remelli and F. Dondi, *Anal. Chem.*, 1999, **71**, 4472–4479.
58 P. Jandera, V. Bačkovská and A. Felinger, *J. Chromatogr., A*, 2001, **919**, 67–77.
59 L. Pasti, N. Marchetti, R. Guzzinati, M. Catani, V. Bosi, F. Dondi, A. Sepsey, A. Felinger and A. Cavazzini, *TrAC, Trends Anal. Chem.*, 2016, 63–68.
60 M. C. Pietrogrande, A. Cavazzini and F. Dondi, *Rev. Anal. Chem.*, 2000, **19**, 124–154.
61 F. Gritti, T. Farkas, J. Heng and G. Guiochon, *J. Chromatogr., A*, 2011, **1218**, 8209–8221.
62 H. Lin and C. Horváth, *Chem. Eng. Sci.*, 1981, **36**, 47–55.
63 C. Horváth and H. J. Lin, *J. Chromatogr.*, 1978, **149**, 43–70.
64 H. Poppe, J. C. Kraak, J. F. K. Huber and J. H. M. v. Berg, *Chromatographia*, 1981, **14**, 515–523.
65 F. Gritti, M. Martin and G. Guiochon, *Anal. Chem.*, 2009, **81**, 3365–3384.
66 A. de Villiers, H. Lauer, R. Szucs, S. Goodall and P. Sandra, *J. Chromatogr., A*, 2006, **1113**, 84–91.
67 F. Gritti and G. Guiochon, *Chem. Eng. Sci.*, 2010, **65**, 6310–6319.
68 S. Rocchi, S. Fanali, T. Farkas and B. Chankvetadze, *J. Chromatogr., A*, 2014, **1363**, 363–371.
69 S. Fanali, G. D'Orazio, T. Farkas and B. Chankvetadze, *J. Chromatogr., A*, 2012, **1269**, 136–142.
70 X. Wu, L. You, W. Hao, M. Su, Y. Gu and L. Shen, *J. Chromatogr., A*, 2013, **1299**, 78–84.
71 E. L. Regalado and C. J. Welch, *J. Sep. Sci.*, 2015, **38**, 2826–2832.
72 D. W. Armstrong and Z. S. Breitbach, New ultrahigh efficiency, superficially porous particle chiral phases for liquid chromatography, *WO* 20160/11425, (PCT/US2015/041026), 2016.

Paper II

Journal of Chromatography A, 1520 (2017) 91–102

Contents lists available at ScienceDirect

Journal of Chromatography A

journal homepage: www.elsevier.com/locate/chroma

Future perspectives in high efficient and ultrafast chiral liquid chromatography through zwitterionic teicoplanin-based 2-μm superficially porous particles

Omar H. Ismail [a,*], Michela Antonelli [a], Alessia Ciogli [a], Claudio Villani [a], Alberto Cavazzini [b], Martina Catani [b], Simona Felletti [b], David S. Bell [c], Francesco Gasparrini [a,*]

[a] Dipartimento di Chimica e Tecnologie del Farmaco, "Sapienza" Università di Roma, P. le Aldo Moro 5, 00185 Roma, Italy
[b] Dipartimento di Scienze Chimiche e Farmaceutiche, Università di Ferrara, via L. Borsari 46, 44121 Ferrara, Italy
[c] MilliporeSigma/Supelco, 595 North Harrison Road, Bellefonte, PA 16823, USA

ARTICLE INFO

Article history:
Received 21 July 2017
Received in revised form 1 September 2017
Accepted 4 September 2017
Available online 6 September 2017

Keywords:
UHPC-Tzwitt
Superficially porous particles CSP
Very-high efficiency column
Ultra-fast/ultra-high performance chromatography

ABSTRACT

With the aim of pushing forward the limits of high efficient and ultrafast chiral liquid chromatography, a new Chiral Stationary Phase (CSP) has been prepared by covalently bonding the teicoplanin selector on 2.0 μm Superficially Porous Particles (SPPs). An already validated bonding protocol, which permits to achieve teicoplanin-based CSPs exhibiting zwitterionic behaviour, has been employed to prepare not only the 2.0 μm version of the CSP but also two other analogous CSPs based, respectively, on 2.7 μm SPPs and 1.9 μm Fully Porous Particles (FPPs). The kinetic performance of these CSPs has been compared through the analysis of both van Deemter curves and kinetic plots by employing in-house packed columns of 4.6 mm internal diameter and different lengths (20, 50 and 100 mm). In particular on the columns packed with 2.0 μm SPPs, extremely large efficiencies were observed for both achiral (>310,000 theoretical plates/meter, *N*/m; h_r: 1.61) and chiral compounds (>290,000 *N*/m; h_r: 1.72) in HILIC conditions. Thanks to their efficiency and enantioselectivity, these CSPs were successfully employed in ultrafast chiral separations. As an example, the enantiomers of haloxyfop were baseline resolved in about 3 s, with a resolution higher than 2.0, (flow rate: 8 mL/min) on a 2 cm long column packed with the 2.0 μm chiral SPPs.

1. Introduction

In the last decades, the technological progress and the continuous research of higher and higher column efficiency has led, on the one hand, to the development of stationary phases made of sub 2-μm fully porous particles (FPPs) and, since their introduction into the market in 2007 [1], to the employment of so-called second-generation superficially porous particles (SPPs, even referred to as core-shell or pellicular particles). Second-generation SPPs are made of a solid core surrounded by a porous layer which occupies about 75% of the overall particle volume. They have a particle diameter generally either 2.6 or 2.7 μm, depending on manufacturer [1–7]. In both approaches, the rationale is to decrease the contribution to band broadening due to intraparticle dispersion. As a consequence in achiral reversed-phase (RP) liquid chromatography, nowadays, the efficiency of modern chromatographic columns (be they packed with sub 2-μm FPPs or second-generation SPPs) easily reaches 300,000–350,000 theoretical plates per meter (*N*/m).

As a matter of fact, this extraordinary improvement of performance has instead only partially touched the field of chiral separations. Essentially up to 2010 [8], CSPs were prepared on FPPs with particle diameter of 3–5 μm. Improvements in the preparation of high efficient CSPs have lagged behind due to (i) the difficulty to adapt traditional techniques of surface modification to the preparation of small particles; (ii) the tendency of small particles to aggregate during chemical modification with consequent inefficient/poor packing; (iii) the low mechanical resistance and long-term stability of particles functionalized with chiral selector at the high flow rates/high pressure required to drive the flow through the packed bed in ultra-high performance liquid chromatography (UHPLC); (iv) the lack of fundamental studies of mass transfer in CSPs [9].

* Corresponding authors.
E-mail addresses: omar.ismail@uniroma1.it (O.H. Ismail), francesco.gasparrini@uniroma1.it (F. Gasparrini).

http://dx.doi.org/10.1016/j.chroma.2017.09.008
0021-9673/

Starting from 2010, Gasparrini and coworkers firstly reported on the use of brush-type CSPs prepared on sub-2 μm FPPs for the high efficient separation of enantiomers in the second-time scale [8,10–12]. In 2011, thanks to the work by Lindner and coworkers, the first example on the use of second-generation SPPs for the preparation of a weak anion-exchanger CSP was presented [13]. The first work aimed at evaluating the kinetic performance of chiral SPPs and FPPs dates 2012, when Chankvetadze et al. compared polysaccharide-based CSPs prepared on both kinds of particles [14]. The conclusion of this work was that columns packed with SPPs exhibited not only higher enantioselectivity (at comparable selector loading), but also both better kinetic performance at high flow-rate and larger enantioresolution than those made of FPPs. The systematic study of the performance of chiral SPPs and FPPs has been performed by Armstrong and coworkers who characterized many different types of CSPs (such as, cyclodextrins, cyclofructan-6, macrocyclic antibiotics, etc.) prepared on both supports [15–20]. In agreement with the conclusions drawn by Chankvetadze et al. [14], in these studies chiral SPPs were found to be more efficient from a kinetic viewpoint and thus more suitable for the transition to ultrafast chiral separations than their FPP counterparts. In principle the same basic concepts for which achiral hydrophobic SPPs outperform the fully porous ones (incidentally, a better packing quality, a reduced longitudinal diffusion and a smaller solid liquid mass transfer resistance), have been considered at the base of the better behavior of chiral SPPs.

More recently, some of the authors of this work, partially challenged this vision [21]. Basically, they tackled the idea that chiral SPPs exhibit superior performance, from the kinetic point of view, than fully porous ones. Unexpected results were indeed found by comparing the behavior of brush-type Whelk-O1 CSPs made on 2.6 μm SPPs, on the one hand, with that of both 1.8 and 2.5 μm FPPs, on the other [21]. In their study, Ismail et al. found the columns packed with FPPs to exhibit better performance than those made of SPPs, especially for the second eluted enantiomer. Following these authors, therefore, a deeper investigation of the effect of several factors on the chromatographic performance is needed to assess the superiority of either particle type. In particular, Ismail et al. mention the need to carefully investigate the effect of chiral selector surface density on the adsorption/desorption kinetics [8,21]. The latter observation seems particularly important since, as reported by many authors [15,18,21], significant differences in the surface density of chiral selectors were observed during functionalization of SPPs and FPPs even if the same experimental protocol was employed in both cases. Nevertheless, this effect has never been systematically investigated.

In this work, a deep evaluation of the kinetic and thermodynamic performance of three columns prepared respectively on 2.0 μm Halo® SPPs (here referred to as UHPC-SPP-Halo-Tzwitt 2.0), 2.7 μm Halo® SPPs (UHPC-SPP-Halo-Tzwitt 2.7) and 1.9 μm monodispersed Titan® FPPs (UHPC-FPP-Titan-Tzwitt 1.9) [22] is presented. In all cases, the teicoplanin selector was bonded to the particle so to guarantee to the CSP a zwitterionic character. The comparison between the three columns is based on the evaluation of both van Deemter curves and kinetic plots.

2. Theory

The efficiency of a column is usually evaluated through the well-known van Deemter equation (1), which correlates the plate height, H, to the interstitial velocity μ_{int} (i.e., the velocity of the fluid truly moving inside the column). In its basic formulation [23,24], the van Deemter equation is written as:

$$H = A + B/\mu_{int} + C\mu_{int} \quad (1)$$

Table 1
Physical properties of columns packed with zwitterionic teicoplanin-based CSPs (SPP-2.0, 2.7 μm and FPP-1.9 μm).

	SPP-Halo 2.0	SPP-Halo 2.7	FPP-Titan 1.9
L.xI.D. (mm)	100 × 4.6 20 × 4.6	100 × 4.6	100 × 4.6 20 × 4.6
d_p (μm)	2.0	2.7	1.9
Pore size (Å)	90	90	120
Surface area (m^2)	125	123	282
Selector loading (μmol/m^2)	0.45	0.47	0.27
Total porosity (ε_t)	0.54	0.53	0.65

where A represents the eddy dispersion, B the longitudinal diffusion and C the solid-liquid mass transfer resistance. The interstitial velocity is defined by:

$$\mu_{int} = \frac{\Phi}{\pi r^2 \varepsilon_e} \quad (2)$$

being Φ the flow rate, r the column radius and ε_e the external porosity ($\varepsilon_e = \frac{V_e}{V_{col}}$, with V_e the interstitial volume and V_{col} the geometrical volume of the column).

In addition to van Deemter plots, the kinetic performance of columns can be also evaluated through the kinetic plots. They provide the highest plate number, N, achievable in the shortest time possible while working at the maximum pressure of the system, ΔP_{max} [25]. Hold up time, t_0, versus N plots can be used to quickly estimate which column offers the fastest separation for a fixed efficiency or the highest N value that can be obtained in a given analysis time. Other forms of kinetic plots can be used to correlate either the column length, L, or the retention time, t_R, to N.

The following equations are employed for the conversion of experimentally determined linear velocity μ_0:

$$\mu_0 = \frac{L}{t_0} \quad (3)$$

and H values in kinetic plots:

$$N = \frac{\Delta P_{max}}{\eta}\left[\frac{K_0}{\mu_0 H}\right] \quad (4)$$

$$t_0 = \frac{\Delta P_{max}}{\eta}\left[\frac{K_0}{\mu_0^2}\right] \quad (5)$$

$$t_R = \frac{t_0}{(k' + 1)} \quad (6)$$

being η the viscosity of the mobile phase, K_0 the column permeability and k' the retention factor.

ΔP_{max} values were set at 600 bar for the UHPC-SPP-Halo-Tzwitt 2.7 column and to 1000 bar for both the UHPC-SPP-Halo-Tzwitt 2.0 and UHPC-FPP-Titan-Tzwitt 1.9 columns.

3. Experimental

3.1. Materials and chemicals

All chemicals were purchased from Sigma-Aldrich (St. Louis, Mo, USA). HPLC gradient grade solvents were filtered before use on 0.2 μm Omnipore filters (Merck Millipore, Darmstadt, Germany). Chiral samples were from Sigma-Aldrich (St. Louis, Mo, USA). Titan® monodispersed silica (pore size 120 Å, particle size 1.9 μm and specific surface area 282 $m^2\ g^{-1}$), Halo® 2.0 and 2.7 μm (90 Å, 125 and 123 m^2/g, respectively) and teicoplanin selector were provided by Merck Sigma–Aldrich (St. Louis, MO, USA). All physical properties of CSPs were summarized in Table 1. Empty stainless steel columns, 20, 50 and 100 mm × 4.6 mm (L × I.D.), were from IsoBar Systems by Idex (Wertheim-Mondfeld, Germany).

3.2. Instruments

The UHPLC chromatographic system used for all achiral tests in HILIC was an UltiMate 3000 RS system (Thermo Fisher Dionex Sunnyvale, California), equipped with a dual gradient RS pump, an in-line split loop Well Plate Sampler, a thermostatted RS Column Ventilated Compartment (temperature range 5–110 °C) and a diode array detector (Vanquish detector) with a low dispersion 2.0 μL flow cell. In addition, a second DAD detector with a 2.5 μL flow cell was employed for flow-rates higher than 4.0 mL/min. Vanquish and DAD detector, both, were set at a filter time constant of 0.002 s, a data collection rate of 100 Hz and a response time of 0.04 s. Inlet and outlet viper tubes (2 × 350 mm × 0.10 mm I.D.) were employed. Data acquisition and processing were performed with Chromeleon 6.8 software from Thermo Fisher. The extra-column peak variance (calculated through peak moments) was 3.94 μL^2 at a flow-rate of 1.0 mL/min. Data acquisition, data handling and instrument control were performed by Chromeleon software.

3.3. Preparation of chiral stationary phases

All columns were packed with CSPs synthesized according to the same Supelco proprietary bonding protocol immobilizing teicoplanin selector onto SPP-Halo 2.0 μm and 2.7 μm and monodispersed FPP-Titan-120 1.9 μm silica particles, leading to the zwitterionic chiral stationary phases named UHPC-SPP-Halo-Tzwitt 2.0, UHPC-SPP-Halo-Tzwitt 2.7 UHPC-FPP-Titan-Tzwitt 1.9, respectively. UHPC-FPP-Titan-Tzwit 1.9 μm silica particles were prepared by adjusting the synthetic procedure (medium density selector) in order to achieve comparable retention as the SPP CSPs. All CSPs were slurry packed with a pneumatically driven Haskel pump (roughly ΔP_{max} 950 bar) into stainless steel columns. Elemental analysis (C, H, N) of the different CSPs were used to extract values of selector loading and surface coverage. UHPC-SPP-Halo-Tzwitt 2.0 particles: 5.75%C, 0.74%H and 0.63%N, corresponding to 56 μmol of selector per gram of silica and to 0.45 μmol of selector per m^2 (based on N); UHPC-SPP-Halo-Tzwitt 2.7 particles: 6.05%C, 0.79%H and 0.66%N, corresponding to 59 μmol of selector per g of silica and to 0.47 μmol of selector per m^2 (based on N); UHPC-FPP-Titan-Tzwitt 1.9 particles: 8.19%C, 1.06%H and 0.92%N, corresponding to 85 μmol of selector per g of silica and to 0.27 μmol of selector per m^2 (based on N). As expected, the two SPP CSPs showed a lower loading (μmol/g) of selector but a higher surface density of teicoplanin (μmol/m^2) in comparison with the 1.9 μm FPPs (Table 1).

3.4. Methodology

All separations were performed in Hydrophilic Interaction Liquid Chromatography (HILIC) conditions by using a mobile phase made by ACN/H_2O 85:15 + 20 mM $HCOONH_4$ (^spH = 7.5). Injected volumes were 0.5-1.0 μL. For data evaluation, the values of resolution (R_s) and efficiency (N/m) were calculated according to the European Pharmacopeia using peak width at half height ($w_{0.5}$). Hold up time was estimated by injection of naphthalene. All data were processed with Origin 8.0.

3.4.1. Pycnometry measurement

Thermodynamic hold-up volume (V_0^{pyc}) was determined by static pycnometry:

$$V_0^{pyc} = \frac{w_{CHCl3} - w_{THF}}{\rho_{CHCl3} - \rho_{THF}} \quad (7)$$

where w and ρ are the mass of the column and the solvent density, respectively [26,27].

3.4.2. ISEC measurement

Inverse size exclusion chromatography (ISEC) was performed to determine both external, ε_e, and ε_p particle porosity, wide range of polystyrene standards (molecular weight between 500 and 3.6×10^6 Da) was injected into the columns, using neat THF as the mobile phase [28,29]. Total porosity, ε_t, was calculated as the ratio V_{col} between V_0^{pyc} and

Results of ISEC measurements are reported in Table 1S.

3.4.3. Frictional heating effect

For the sake of completeness, the column inlet and outlet temperatures were measured at the maximum flow-rates employed: 6.0 and 8.0 mL/min on the 5 and 2-cm long columns, respectively, by using thermocouples (accuracy: 0.1 °C) placed at the column inlet and outlet. The temperature of the ventilated column oven was set at 35 °C (the same temperature used for all the experiments reported in the paper). A ΔT of 7.5 and 3.2 °C on the 5 and 2-cm long columns, respectively, was recorded. These ΔTs are not dramatic (due to the very reduced length of columns employed in these experiments), and their effects on column performance are very reduced.

4. Results and discussion

4.1. Physical and geometric characterization of columns

In order to have a complete characterization of columns, the specific and the column permeability (K_{sf} and K_0, respectively) were calculated from the linear velocity vs. ΔP_{col} linear plots (Fig. 1). For this study, 100 × 4.6 mm (L × I.D.) columns were employed. As known, the linear velocity μ_0 and pressure drop ΔP_{col} are correlated by the Darcy's law with the equation: $K_0 = \frac{\mu_0 \eta L}{\Delta P}$ [30]. The column permeability (K_0) was 0.499, 0.500 and 1.00 × 10^{-14} m^2 for the UHPC-Halo-SPP-Tzwitt 2.0, the UHPC-Titan-FPP-Tzwitt 1.9 and the UHPC-Halo-SPP-Tzwitt 2.7 column, respectively (Fig. 1A). As expected, the column packed with 2.7 μm SPPs showed the highest K_0 value due to the larger particle diameter. This means that this column generates, at the same flow rate, a lower back-pressure (almost twice smaller) than the other two (Fig. 1B). Finally, the total porosity (ε_t) of columns was calculated through ISEC analysis. The two columns packed with SPPs, as expected, exhibited very similar ε_t values, consistently lower than the UHPC-Titan-FPP-Tzwitt 1.9 column. These data are summarized into Table 1S.

4.2. van Deemter analysis of achiral samples

All analysis, including van Deemter plots, were made on a Dionex Ultimate 3000RS with flow rates ranging from 0.2 mL/min up to 4.0 mL/min with a maximum operating pressure of 550 bar. This wide range of flow rates has permitted to achieve a complete view on the kinetic performance of the whole set of columns. The first evaluation was made using a mixture of the achiral solutes naphthalene (hold-up volume marker), thiourea, uracil and adenosine. In this work, all H values were not corrected for the extra-column variance since its contribution to band broadening was found to be negligible. van Deemter plots have been expressed as H as a function of μ_{inter} (Fig. 2), μ_0 (Fig. 1S) or flow rate depending on need; μ_{inter}, which takes into account the external porosity of each column, was used to have a correct comparison between columns packed with SPP and FPP CSPs. In Fig. 2A, the van Deemter plots of thiourea (k': 0.62–0.65) on the three columns are shown. Clearly, the column packed with UHPC-SPP-Halo-Tzwitt 2.0 CSP provides the best efficiency with more than 311,000 N/m, corresponding to a plate height H = 3.21 μm (h_r: 1.60) at a flow rate of 1.5 mL/min (μ_{inter} = 3.63 mm/s). Also

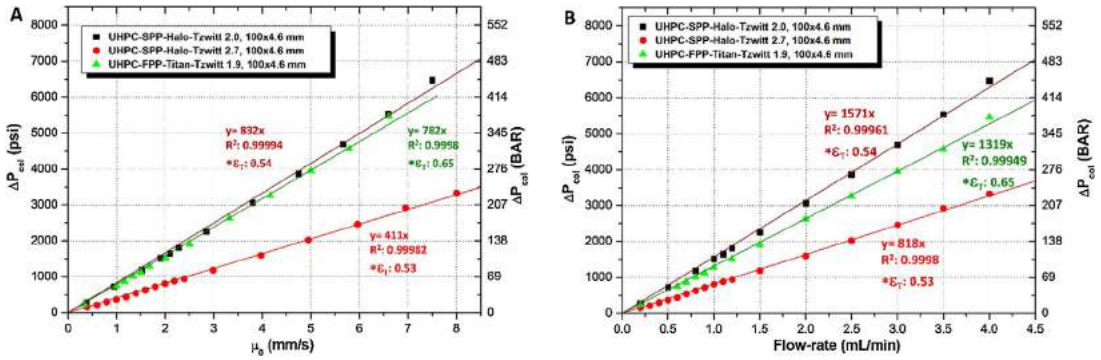

Fig. 1. A) Backpressure ΔP_{col} vs. flow-rate plots on UHPC-SPP-Halo-Tzwitt 2.0 μm (Black square), UHPC-SPP-Halo-Tzwitt 2.7 μm (Red circle) and UHPC-FPP-Titan-Tzwitt 1.9 μm (Green triangle). B) Backpressure ΔP_{col} vs. μ_0 plots on the UHPC-SPP-Halo-Tzwitt 2.0 μm (Black square), UHPC-SPP-Halo-Tzwitt 2.7 μm (Red circle) and UHPC-FPP-Titan-Tzwitt 1.9 μm (Green triangle). Eluent: ACN/H_2O 85:15 + 20 mM $HCOONH_4$, η: 0.41 × 10^{-3} Pa s, T: 35 °C. (For interpretation of the references to colour in this figure legend, the reader is referred to the web version of this article.)

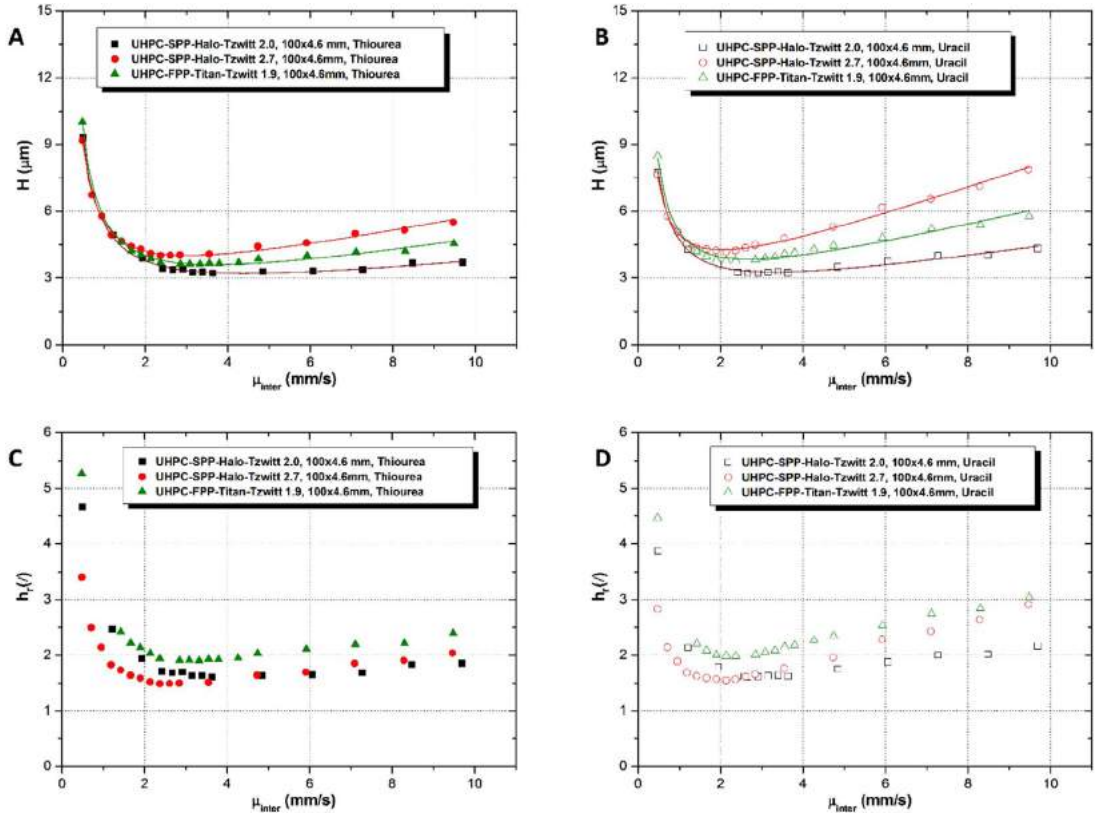

Fig. 2. A) and B) van Deemter plots (H vs μ_{inter}) for thiourea (k' = 0.6) and uracil (k' = 1.0), respectively, on the UHPC-SPP-Halo-Tzwitt 2.0 μm (Black square), UHPC-SPP-Halo-Tzwitt 2.7 μm (Red circle) and UHPC-FPP-Titan-Tzwitt 1.9 μm (Green triangle). C) and D) Plots of the reduced plate height, h_r vs. μ_{inter} on thiourea and uracil, respectively. Eluent: ACN/H_2O 85:15 + 20 mM $HCOONH_4$, T: 35 °C. (For interpretation of the references to colour in this figure legend, the reader is referred to the web version of this article.)

the column packed with UHPC-FPP-Titan-Tzwitt 1.9 CSP showed remarkable efficiency, with 277,000 N/m (H = 3.61 μm, h_r: 1.90) at a flow rate of 1.4 mL/min (μ_{inter} = 3.32 mm/s). The lowest efficiency was observed on the column packed with UHPC-SPP-Halo-Tzwitt 2.7 CSP, with less than 250,000N/m (H = 4.03 μm, h_r: 1.49) at a flow rate of 1.1 mL/min (μ_{inter} = 2.60 mm/s) (Table 2). Moreover, looking at the shape of plots, it can be observed that the C-branch of the van Deemter curve for the 2.0 μm SPP column is lower than both those of the 1.9 μm FPP and the 2.7 μm SPP columns. This characteristic is of fundamental importance for UHPLC separations since a flatter C-branch permits to increase the flow rate without significant loss of efficiency. Indeed, moving from the optimal flow rate to 3.0 mL/min, efficiency drops were 4.7%, 25% and 15% respectively for the UHPC-SPP-Halo-Tzwitt 2.0, the UHPC-SPP-Halo-Tzwitt 2.7 and UHPC-FPP-Titan-Tzwitt 1.9 columns. The van Deemter curves on the three columns for a test probe with a moderate retention (uracil, k': 0.99–1.03) are reported in Figs. 2B, 1SA and 1SC. Also in this case, at a flow rate of 1.2 mL/min, 311,000 N/m were recorded on the UHPC-SPP-Halo-Tzwitt 2.0 column, resulting in significantly higher efficiency than on both the UHPC-SPP-Halo-Tzwitt 2.7 column (30%) and the UHPC-FPP-Titan-Tzwitt 1.9 one (15%), respectively.

Considering a molecule with an higher retention factor, such as adenosine (k': 1.82–2.07) (see Fig. 1SB and D), the gap in terms of optimal flow rate becomes even larger in favor of the UHPC-SPP-Halo-Tzwitt 2.0 column, which shows an optimal flow rate

Table 2
Experimental van Deemter analysis data under Hilic conditions on UHPC-SPP-Halo-Tzwitt 2.0 μm, UHPC-SPP-Halo-Tzwitt 2.7 μm and UHPC-FPP-Titan-Tzwitt 1.9 μm. Eluent: ACN/H_2O 85:15 + 20 mM $HCOONH_4$, T: 35 °C.

UHPC-SPP-Halo-Tzwitt 2.0							
Sample	k' (/)	H_{min} (μm)	h_{min} (/)	N/m	$\mu_{0,opt}$ (mm/s)	$\mu_{inter,opt}$ (mm/s)	Flow-rate$_{opt}$ (mL/min)
Thiourea	0.62	3.21	1.60_5	311 280	2.85	3.63	1.5
Uracil	0.99	3.22	1.61	310 660	2.28	2.91	1.2
Adenosine	1.82	3.71	1.85	269 750	2.28	2.91	1.2
UHPC-SPP-Halo-Tzwitt 2.7							
Sample	k' (/)	H_{min} (μm)	h_{min} (/)	N/m	$\mu_{0,opt}$ (mm/s)	$\mu_{inter,opt}$ (mm/s)	Flow-rate$_{opt}$ (mL/min)
Thiourea	0.62	4.03	1.49	248 090	2.20	2.60	1.1
Uracil	0.99	4.19	1.55	238 920	1.59	1.89	0.8
Adenosine	1.93	4.50	1.67	222 040	1.00	1.18	0.5
UHPC-FPP-Titan-Tzwitt 1.9							
Sample	k' (/)	H_{min} (μm)	h_{min} (/)	N/m	$\mu_{0,opt}$ (mm/s)	$\mu_{inter,opt}$ (mm/s)	Flow-rate$_{opt}$ (mL/min)
Thiourea	0.66	3.61	1.90	276 780	2.34	3.32	1.4
Uracil	1.06	3.77	1.98	265 220	1.68	2.37	1.0
Adenosine	2.10	4.20	2.21	238 300	1.34	1.90	0.8

respectively 1.5 and 2.4 times higher than those of the UHPC-FPP-Titan-Tzwitt 1.9 and the UHPC-SPP-Halo-Tzwitt 2.7 columns. In Figs. 2C, D, 1SC and D, the reduced van Deemter plots are reported. Reduced plate height $h_r \left(= \frac{H}{d_p}\right)$ permits to properly evaluate the kinetic performance of columns packed with silica particles of size. Extremely low h_r values were found with thiourea (1.49, 1.60 and 1.90 on the UHPC-SPP-Halo-Tzwitt 2.7, the UHPC-SPP-Halo-Tzwitt 2.0 and the UHPC-FPP-Titan-Tzwitt 1.9 columns, respectively), proving the goodness of the packing process obtained for all columns.

4.3. Kinetic performance (achiral compounds)

The kinetic plot method was used to have a complete overview of the kinetic performance limits of all columns. This method shows the highest efficiency achievable by a column in the shortest time, working at the maximum pressure reachable by the instrument. Kinetic plots method is the best choice to have a clear and proper comparison of kinetic performance of different columns (also with different geometries) in various analytical conditions (HPLC, UHPLC or SFC). The t_0 *vs. N* kinetic plot is the original one introduced by Giddings in 1965 [31]. This is the starting point for other forms of kinetic plots, such as the so-called Poppe plot [32,33]. This plot permits to have a clearer view on the C-term of van Deemter equation. In this work, for the preparation of kinetic plots, the maximum operating pressure was set at 600 bar for columns packed with 2.7 μm SPP CSP (silica pressure limit) and 1000 bar (maximum operative pressure in most common UHPLC systems) for those packed with 2.0 μm SPP and 1.9 μm FPP CSPs. In Fig. 3, the kinetic plots for the three columns are reported. Fig. 3A (t_0 *vs N*) shows that the use of the UHPC-SPP-Halo-Tzwitt 2.0 column is worthwhile up to 190,000 plates. After this value, the best choice would be the UHPC-FPP-Titan-Tzwitt 1.9 column and beyond $N = 226{,}000$ the UHPC-SPP-Halo-Tzwitt 2.7 column gives the best kinetic performance, due to its very high permeability and low operating pressure. The same trend is observed in the Poppe plot (t_0/N *vs N*, Fig. 3B) and t_R*vs N* plot, on uracil, (Fig. 3C), where the column packed with the 2.0 μm SPP CSP overcomes the columns packed with the other two CSPs in the bottom left corner of the graph, which represents the maximum separation speed with realistic column length. In these two plots, where the data of uracil (*k'*: 0.99-1.03) are reported, it is evident how the UHPC-Halo-Tzwitt 2.0 column exceeds, in terms of kinetic performance, the other two columns in every area of the plot thanks to its low C-term (1.8 and 2.1 times lower than that of the UHPC-FPP-Titan-Tzwitt 1.9 and the UHPC-SPP-Halo-Tzwitt 2.7 columns, respectively). *L* vs *N* plots (Fig. 3D) confirm the same trend. Indeed, by assuming an efficiency of 45,000 plates as the target value, one sees that a 18 cm long column packed with 2.0 μm SPPs can be used (at 1000 bar) against the 24 cm required by the UHPC-FPP-Titan-Tzwitt 1.9 column and the 28 cm of the UHPC-SPP-Halo-Tzwitt 2.7 one (but at 600 bar). Finally, the same kinetic behavior was observed, considering adenosine (*k'*: 1.82–2.07) as the probe (Fig. 2S). In this case, the C-term critically affects kinetic plots. Indeed the UHPC-SPP-Halo-Tzwitt 2.7 column seems to be the less efficient from the kinetic point of view. On the other hand, the UHPC-SPP-Halo-Tzwitt 2.0 column performs better than the other two columns across the entire range of these plots.

Chromatograms showing the separation of a mixture of achiral probes naphthalene (hold-up volume marker), thiourea, uracil and adenosine, on all the three columns at their optimal flow rate (on thiourea) are shown in Fig. 4A. Since the optimal flow rate of the UHPC-SPP-Halo-Tzwitt 2.0 column is higher than those of the other columns, a reduction of almost 40% of analysis time could be achieved with this column. Fig. 4B and C shows the same chromatographic separations at higher flow rates (2.0 and 2.5 mL/min). The column packed with 2.0 μm SPPs exhibits the lower drops in efficiency and resolution when compared with the other two columns as a confirmation of the flat C-branch of its van Deemter curve. Indeed, by considering thiourea, moving from the optimal flow-rate to 2.5 mL/min produced efficiency loss of 3%, 10% and 12% respectively on the UHPC-SPP-Halo-Tzwitt 2.0, the UHPC-FPP-Titan-Tzwitt 1.9 and UHPC-SPP-Halo-Tzwitt 2.7 columns. If one considers adenosine, the efficiency drop became even more evident, going from 23% to 27% and then to 42% for the three columns (considered in the same order as before). This efficiency loss is reflected in corresponding resolution values, which decrease in the same order (Table 3). In Fig. 4D all chromatograms are reported as a function of *k'*. As it can be noticed, analytes have almost the same retention factors on the two SPP CSPs, while they are 6–10% higher on the FPP one (see above).

4.4. van Deemter analysis of chiral compounds

The kinetic profile of the different columns was completed by measuring van Deemter plots of the racemic chiral molecule 2-(4-chloro-phenoxy)-propionic acid (Fig. 5). The column packed with UHPC-SPP-Halo-Tzwitt 2.0 particles showed outstanding perfor-

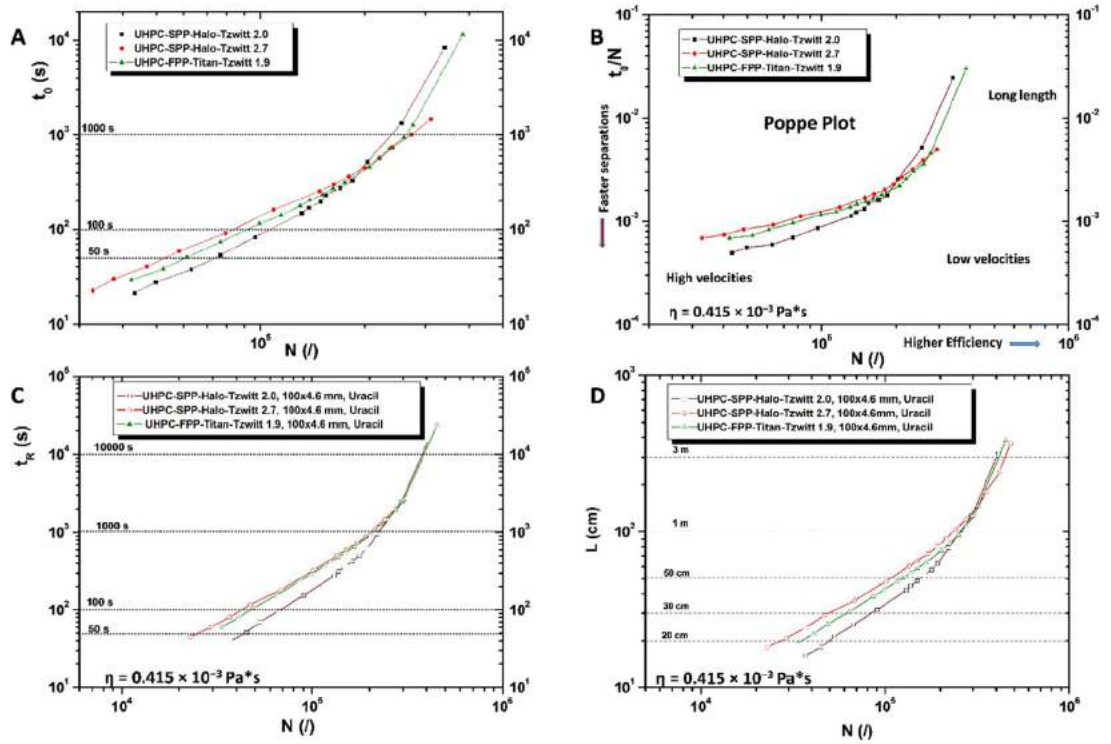

Fig. 3. Kinetic plots showing a comparison of the three different columns under HILIC conditions, mobile phase: ACN/H_2O 85:15 + 20 mM $HCOONH_4$; $\eta = 0.41 \times 10^{-3}$ Pa s; $T = 35\,^{\circ}C$. (A) t_0 vs N plot, (B) t_0/N vs Nplot, (C) Uracil t_R vs N plot and (D) L vs N plot on uracil. $\Delta P_{max} = 1000$ bar was set for the UHPC-SPP-Halo-Tzwitt 2.0 μm (Black square) and UHPC-FPP-Titan-Tzwitt 1.9 μm (Green triangle), but a $\Delta P_{max} = 600$ bar was used for the UHPC-SPP-Halo-Tzwitt 2.7 μm (Red circle). (For interpretation of the references to colour in this figure legend, the reader is referred to the web version of this article.)

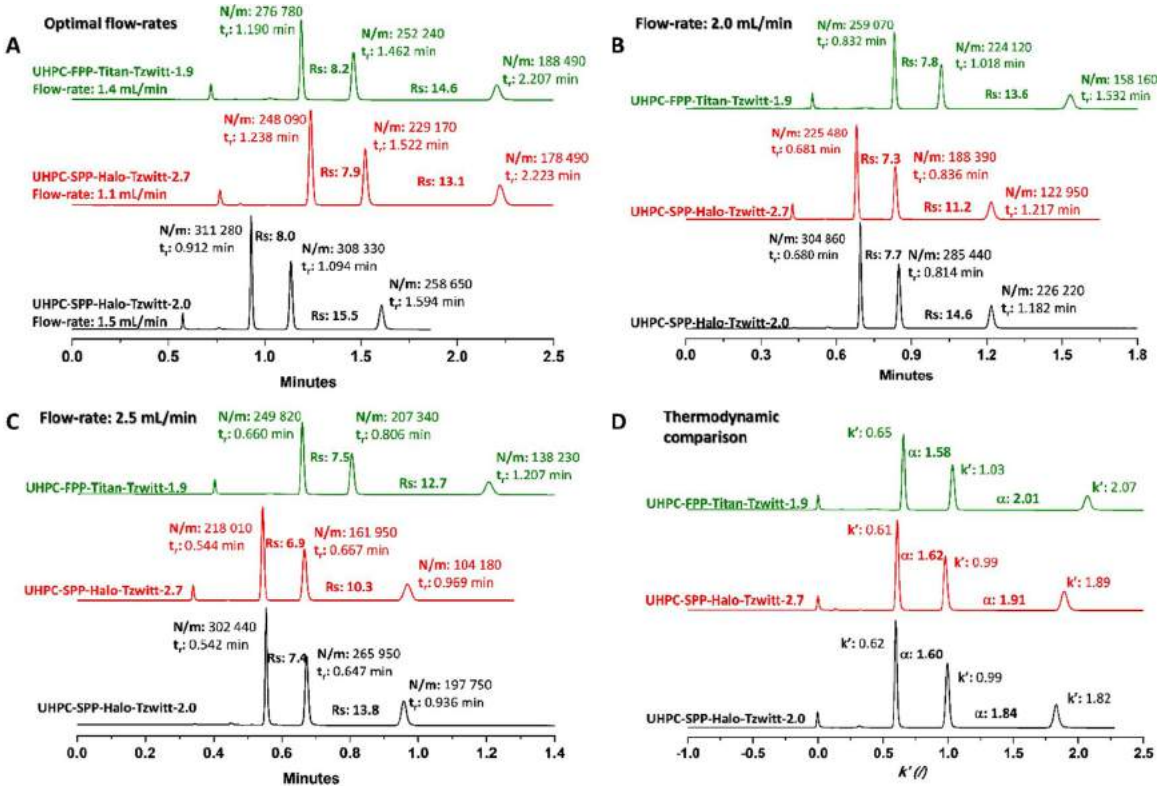

Fig. 4. Separations of the achiral probes naphthalene (hold-up volume marker), thiourea, uracil and adenosine on the UHPC-SPP-Halo-Tzwitt 2.0 μm (Black line), UHPC-SPP-Halo-Tzwitt 2.7 μm (Red line) and UHPC-FPP-Titan-Tzwitt 1.9 μm (Green line) at their optimal flow-rates (A), at flow-rate: 2.0 mL/min (B) and at 2.5 mL/min (C). Graph (D) shows the same chromatograms as a function of the retention factor (k'). Eluent: ACN/H_2O 85:15 + 20 mM $HCOONH_4$, T: 35 °C. (For interpretation of the references to colour in this figure legend, the reader is referred to the web version of this article.)

Table 3
Percentage of efficiency and resolution loss moving from the optimal flow-rate of each column up to flow-rate = 2.5 mL/min.

Column	Efficiency loss% [Φ_{opt} vs Φ 2.5 mL/min]			Resolution loss% [Φ_{opt} vs Φ 2.5 mL/min]	
	N/m Thiourea	N/m Uracil	N/m Adenosine	$Rs_{[Thiourea-Uracil]}$	$Rs_{[Uracil-Adenosine]}$
UHPC-SPP-Halo-Tzwitt 2.0	−3%	−14%	−23%	−7%	−11%
UHPC-SPP-Halo-Tzwitt 2.7	−12%	−30%	−42%	−13%	−21%
UHPC-FPP-Titan-Tzwitt 1.9	−10%	−18%	−27%	−9%	−13%

mance. Almost 300,000 N/m (H = 3.42 μm, h_r = 1.71) were recorded for the first eluted enantiomer and roughly 280,000 plates/m for the second one, at optimal flow rates of 0.9 and 0.7 mL/min, respectively. The column packed with 1.9 μm FPPs generated more than 260,000 N/m (H = 3.82 μm, h_r = 2.01) at 0.7 mL/min for the first eluted enantiomer. As expected, the column packed with the UHPC-SPP-Halo-Tzwitt 2.7 particles was the less efficient, by producing 211,000 N/m for the first eluted enantiomer (H = 4.74 μm, h_r = 1.76) at a flow rate of 0.5 mL/min. This gap in terms of efficiency is clearly pointed out in Fig. 5B and C, where N/m is reported as a function of flow rates for both enantiomers for each column. An efficiency gain of about 11% and more than 40% on the second eluted enantiomer is achievable with the UHPC-SPP-Halo-Tzwitt 2.0 column if compared to the UHPC-FPP-Titan-Tzwitt 1.9 and UHPC-SPP-Halo-Tzwitt 2.7 ones (Fig. 5C), respectively. Moreover, the UHPC-SPP-Halo-Tzwitt 2.0 column still exhibits a flatter C-branch also for the separation

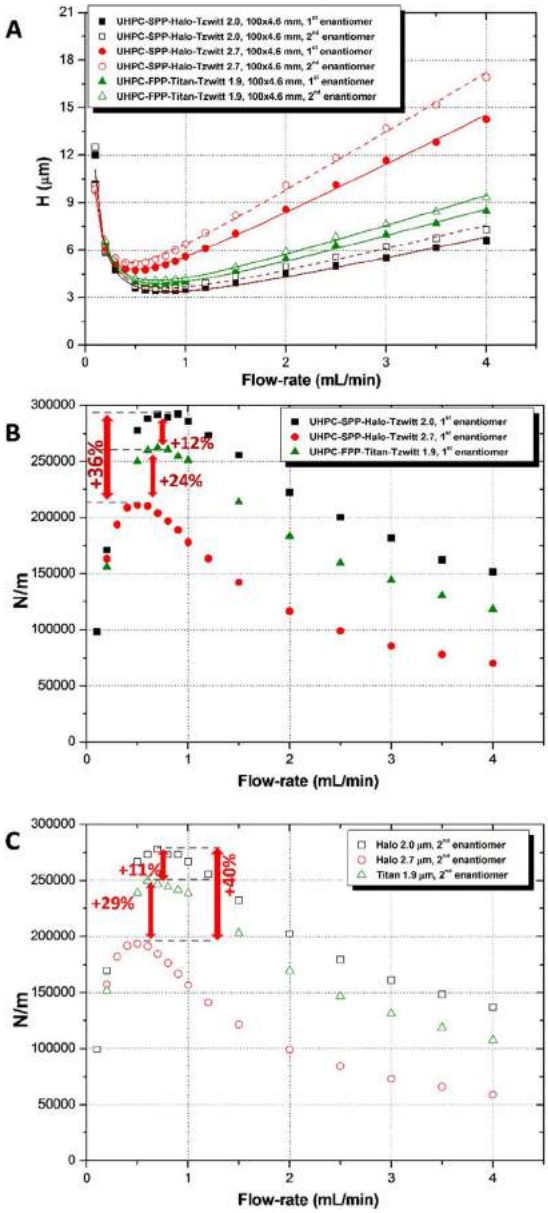

UHPC-SPP-Halo-Tzwitt 2.0

Sample	k' (/)	H_{min} (μm)	h_{min} (/)	N/m	Flow-rate$_{opt}$ (mL/min)
1° enantiomer	2.21	3.42	1.71	292 220	0.9
2° enantiomer	2.80	3.60	1.80	278 060	0.7

UHPC-SPP-Halo-Tzwitt 2.7

Sample	k' (/)	H_{min} (μm)	h_{min} (/)	N/m	Flow-rate$_{opt}$ (mL/min)
1° enantiomer	2.09	4.74	1.76	211 060	0.5
2° enantiomer	2.88	5.16	1.91	193 720	0.5

UHPC-FPP-Titan-Tzwitt 1.9

Sample	k' (/)	H_{min} (μm)	h_{min} (/)	N/m	Flow-rate$_{opt}$ (mL/min)
1° enantiomer	2.61	3.82	2.01	261 950	0.7
2° enantiomer	3.29	4.00	2.11	249 900	0.6

Fig. 5. A) van Deemter plots of 1st (solid lines) and 2nd (dashed lines) eluted enantiomers of 2-(4-chloro-phenoxy)-propionic acid on the UHPC-SPP-Halo-Tzwitt 2.0 μm (Black square), UHPC-SPP-Halo-Tzwitt 2.7 μm (Red circle) and UHPC-FPP-Titan- Tzwitt 1.9 μm (Green triangle). B) N/m of the 1st eluted enantiomer vs. flow-rate plots on the three columns. C) N/m of the 2nd eluted enantiomer vs. flow-rate plots on the three columns Eluent: ACN/H_2O 85:15 + 20 mM $HCOONH_4$, T: 35 °C. (For interpretation of the references to colour in this figure legend, the reader is referred to the web version of this article.)

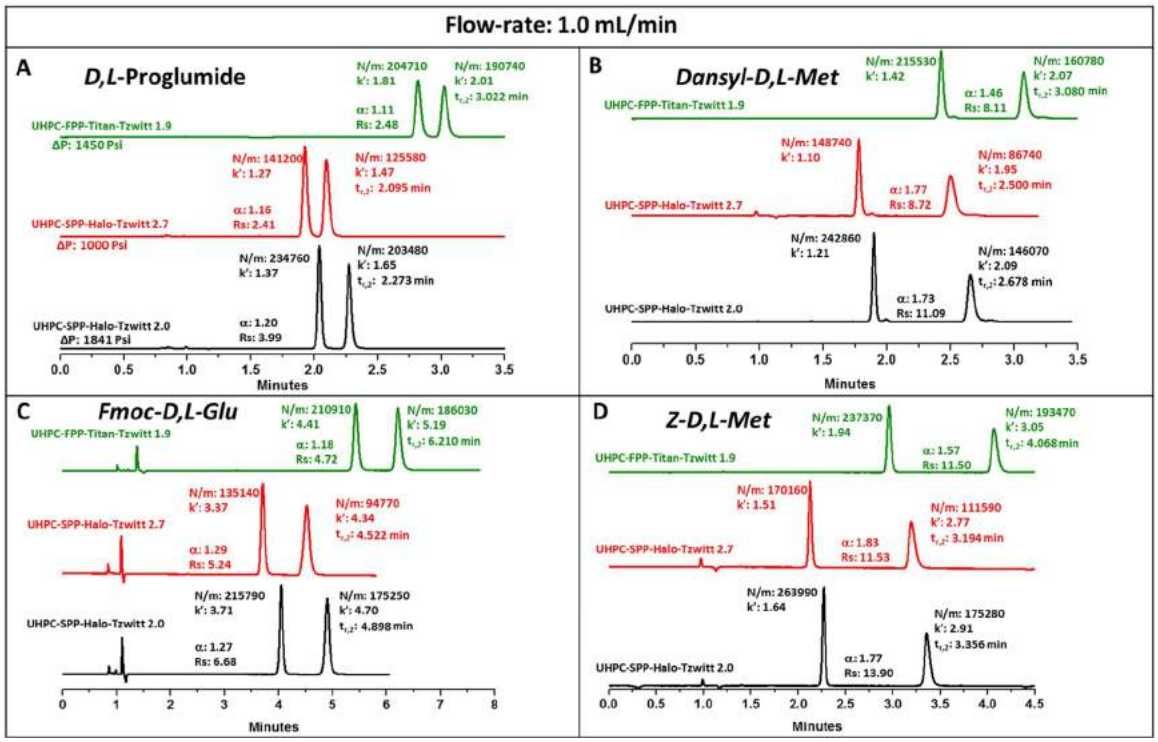

Fig. 6. Separations of the racemic analytes on the UHPC-SPP-Halo-Tzwitt 2.0 μm (Black line), UHPC-SPP-Halo-Tzwitt 2.7 μm (Red line) and UHPC-FPP-Titan-Tzwitt 1.9 μm (Green line) at flow-rate: 1.0 mL/min. (A) D,L-Proglumide, (B) Dansyl-D,L-Methionine, (C) Fmoc-D,L-Glutamine, (D) *Z*-D,L-Methionine. Eluent: ACN/H_2O 85:15 + 20 mM $HCOONH_4$, *T*: 35 °C. (For interpretation of the references to colour in this figure legend, the reader is referred to the web version of this article.)

of chiral samples. This is an essential advantage of this column for UHPLC enantioseparations, as it will be shown in the following.

4.5. Applications to chiral compounds

4.5.1. Kinetic performance (chiral compounds)

After evaluation of physical and kinetic properties, all columns were tested for practical applications. A broad range of chiral compounds (including N-derivatized amino acids, agrochemical and drugs or drug-like molecules) was employed under HILIC conditions. All kinetic data are summarized in Table 2S and Fig. 3S. As expected, the most efficient column was the UHPC-SPP-Halo-Tzwitt 2.0, followed by the UHPC-FPP-Titan-Tzwitt 1.9 and the UHPC-SPP-Halo-Tzwitt 2.7. Indeed, looking at the bar plot in Fig. 3S, an average 35% loss of efficiency for the first eluted enantiomer was observed on the UHPC-SPP-Halo-Tzwitt 2.7 column in comparison to the UHPC-SPP-Halo-Tzwitt 2.0 one.

Chromatograms of four different chiral samples recorded at 1.0 mL/min on the three columns are shown in Fig. 6. Roughly 265,000 *N*/m were recorded on the UHPC-SPP-Halo-Tzwitt 2.0 column for the first eluted enantiomer of *Z*-D,L-Met (Fig. 6D). Smaller efficiencies were observed on the UHPC-FPP-Titan-Tzwitt 1.9 column (−10%) and UHPC-SPP-Halo-Tzwitt 2.7 one (−36%).

Moreover in Fig. 3S, *N*/m values for 15 pairs of racemic samples recorded at a flow rate of 1.0 mL/min are reported as a bar plot. In most cases, the column packed with 2.0 μm particles provides the highest efficiency for the first eluted enantiomer (see Fig. 3S A). On the opposite, the UHPC-FPP-Titan-Tzwitt 1.9 column has shown larger efficiency for the second eluted enantiomer (see Fig. 3S B). The effect is more pronounced for the N-derivatized amino acids with medium-high retention factors. These findings seem to suggest the existence of different adsorption/desorption kinetics on the two columns, which could be correlated to the different surface density of chiral selector on particles (see above). However, further experimental and theoretical investigations are necessary to explain this behavior and to deeply understand the adsorption mechanism occurring on both SPP and FPP CSPs.

4.5.2. Thermodynamics and resolution (R_S)

Retention and enantioselectivity values for several chiral probes on the three CSPs are listed in Table 4 and Fig. 4S. From these data it is evident that the two SPP CSPs have similar retention behavior, while the UHPC-FPP-Titan-Tzwitt 1.9 column showed higher retention factors. Very similar enantioselectivity was observed on the two SPP CSPs (average value about 1.5). They were about 10% higher than those observed on the FPP CSP (Fig. 4S). This difference could be related to the higher density of the teicoplanin selector on the two SPP silica in comparison to the fully porous one (see above).

As far as resolution is concerned, the UHPC-SPP-Halo-Tzwitt 2.0 column showed the highest resolution values for 12 out of 15 samples (Fig. 7A). For instance, the UHPC-SPP-Halo-Tzwitt 2.0 column exhibited a resolution value of about 4.0 for D,L-Proglumide (Fig. 6A), which is 40% and 37% higher than those observed on the UHPC-SPP-Halo-Tzwitt 2.7 and UHPC-FPP-Titan-Tzwitt 1.9 columns, respectively. In Fig. 7B, the ratio between resolution values and retention times of the second eluted enantiomers is reported. This plot clearly shows the very high resolution power of the UHPC-SPP-Halo-Tzwitt 2.0 column in comparison to both the UHPC-SPP-Halo-Tzwitt 2.7 and the UHPC-FPP-Titan-Tzwitt 1.9 columns.

4.6. Very/ultra-high speed and ultra-high performance chiral separations

van Deemter analysis revealed the ability of these columns to work easily at flow rates higher than optimal ones. The behavior of these CSPs was thus investigated up to 6.0 mL/min flow rate (so-called very-high speed regime), by employing 50 × 4.6 mm in house

Table 4
Chromatographic data for chiral separations obtained on UHPC-SPP-Halo-Tzwitt 2.0 (Col. 1), UHPC-SPP-Halo-Tzwitt 2.7 (Col. 2) and UHPC-FPP-Titan-Tzwitt 1.9 (Col. 3) at flow-rate: 1.0 mL/min. Column geometry: 100 × 4.6 mm L.xI.D. Eluent: ACN/H_2O 85:15 + 20 mM $HCOONH_4$, T: 35 °C.

Sample	k'$_2$ (/)			α (/)			Rs (/)		
Name	Col. 1	Col. 2	Col. 3	Col. 1	Col. 2	Col. 3	Col. 1	Col. 2	Col. 3
N-Fmoc-D-L-Ala	3.18	2.83	2.96	1.61	1.57	1.39	7.73	6.37	6.75
N-Fmoc-D-L-Phe	1.31	1.33	1.46	1.15	1.27	1.15	2.67	3.45	2.91
N-Fmoc-D-L-Glu	4.70	4.34	5.19	1.27	1.29	1.18	6.68	5.24	4.72
N-Fmoc-D-L-Leu	1.22	1.29	1.42	1.40	1.29	1.42	5.84	5.65	5.34
N-BOC-D-L-Met	1.99	1.89	2.14	1.42	1.45	1.30	8.50	7.13	6.21
Dansyl-D-L-Met	2.09	1.95	2.07	1.73	1.77	1.46	11.09	8.72	8.11
Dansyl-D-L-Phe	1.33	1.24	1.52	1.15	1.17	1.11	2.72	2.30	2.08
Z-D,L-Phe	1.91	1.88	2.21	1.19	1.30	1.20	4.24	4.88	4.46
Z-D,L-Met	2.91	2.77	3.05	1.77	1.83	1.57	13.90	11.53	11.50
Z-D,L-Ala	4.33	4.02	4.47	1.54	1.65	1.44	12.54	10.38	10.12
Mandelic Acid	11.44	9.65	11.90	2.97	2.73	2.38	27.82	21.96	24.99
D,L-4,5-Dihydro orotic Acid	25.53	20.59	25.80	1.42	1.34	1.29	11.78	8.71	8.87
D,L-Proglumide	1.65	1.47	2.01	1.20	1.16	1.11	3.99	2.41	2.48
Haloxyfop	1.46	1.20	1.42	1.78	1.67	1.39	11.58	7.50	6.72
Ketorolac	4.80	4.30	4.44	1.40	1.37	1.26	9.61	7.03	6.33

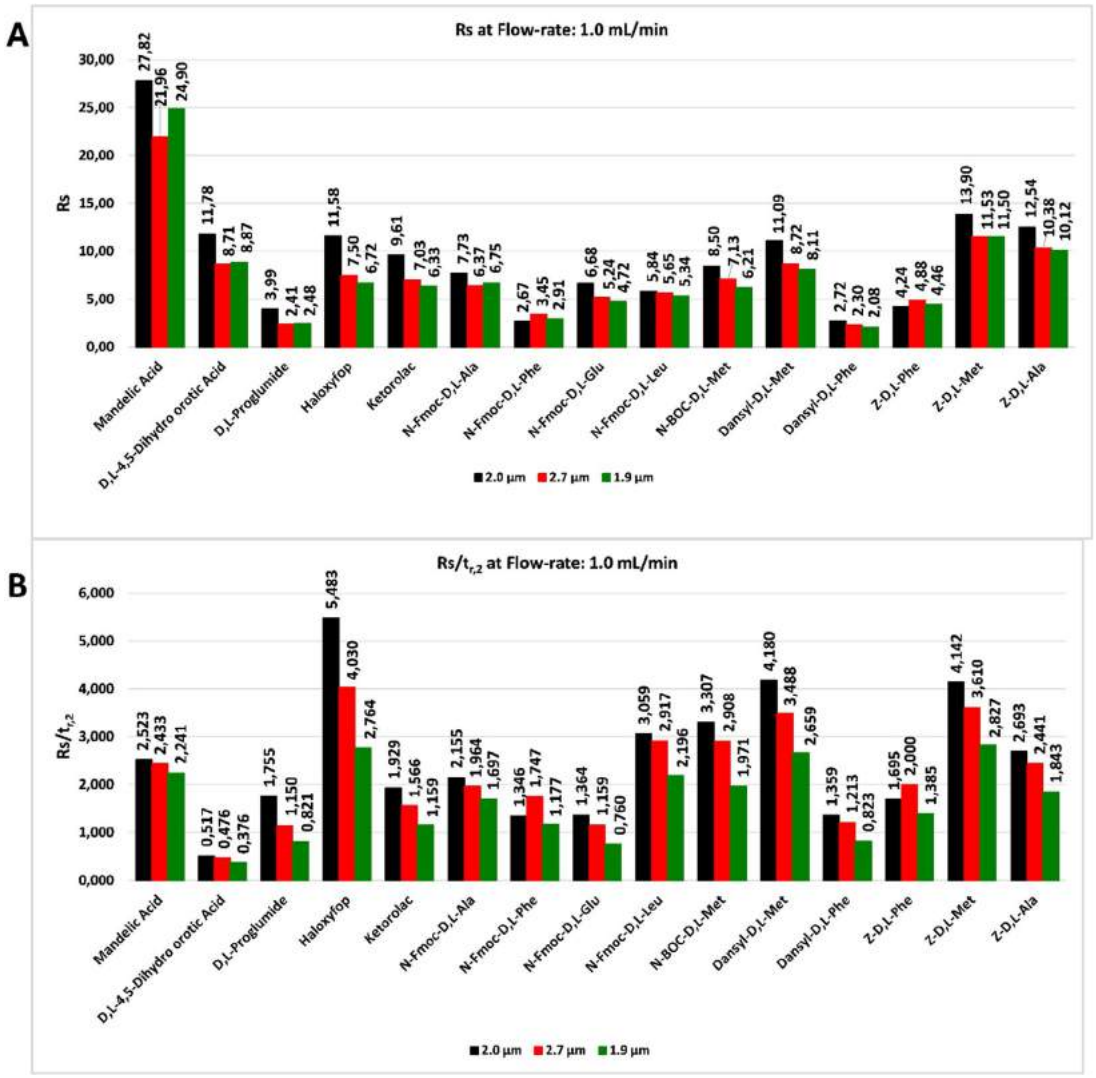

Fig. 7. Bar plots of resolution (R_s) and $R_s/t_{R,2}$ obtained for different analytes on the UHPC-SPP-Halo-Tzwitt 2.0 µm (Black), UHPC-SPP-Halo-Tzwitt 2.7 µm (Red) and UHPC-FPP-Titan-Tzwitt 1.9 µm (Green) at flow-rate: 1.0 mL/min. Eluent: ACN/H_2O 85:15 + 20 mM $HCOONH_4$, *T*: 35 °C. (For interpretation of the references to colour in this figure legend, the reader is referred to the web version of this article.)

packed columns and different chiral samples were tested (Fig. 5S). Fig. 8 shows the separation of a mixture of enantiomers of haloxyfop and ketorolac at flow rates ranging from 1.0 to 6.0 mL/min. The resolution drop was about 45% on both the UHPC-SPP-Halo-Tzwitt 2.0 and the UHPC-FPP-Titan-Tzwitt 1.9 columns and higher than 50% on the UHPC-SPP-Halo-Tzwitt 2.7 one (see Table 5). An average

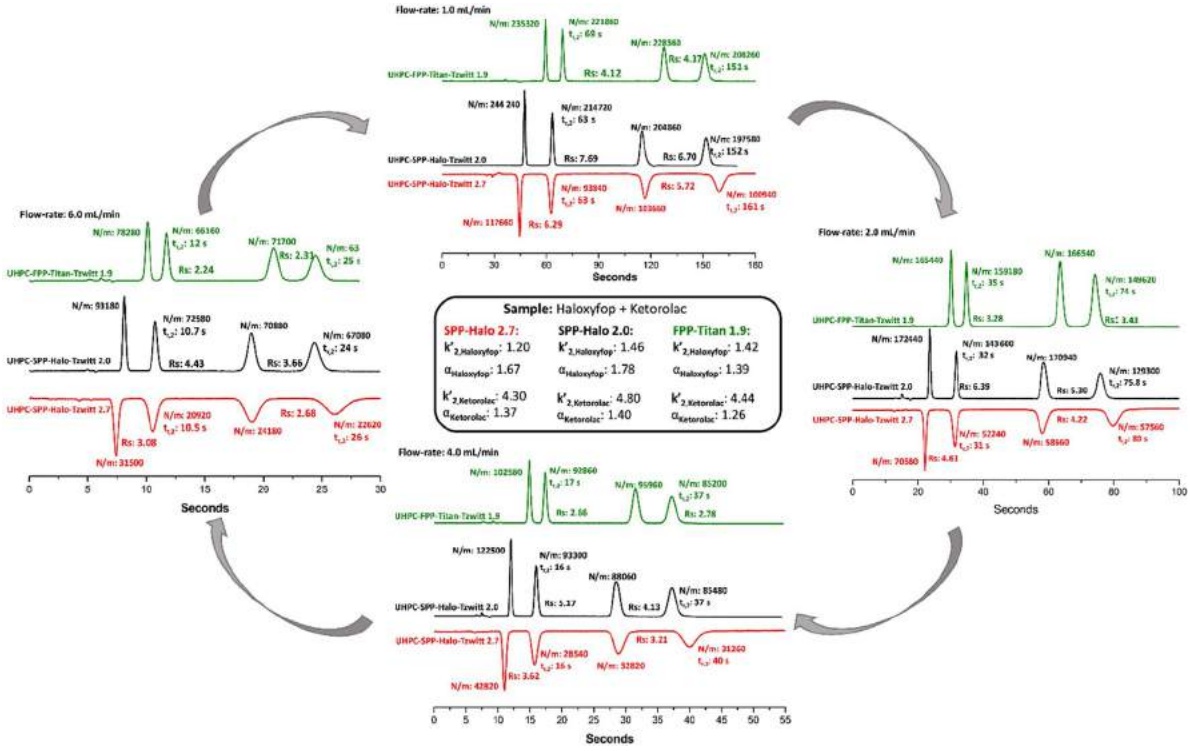

Fig. 8. Very-High speed/Ultra-High Performance separations of the enantiomers of Haloxyfop and Ketorolac, at different flow-rates, on UHPC-SPP-Halo-Tzwitt 2.0 μm (Black line), UHPC-SPP-Halo-Tzwitt 2.7 μm (Red line) and UHPC-FPP-Titan-Tzwitt 1.9 μm (Green line) packed in 50 × 4.6 mm columns. *k'* and α values reported in figure were calculated at flow-rate: 1.0 mL/min. Eluent: ACN/H_2O 85:15 + 20 mM $HCOONH_4$, *T*: 35 °C. (For interpretation of the references to colour in this figure legend, the reader is referred to the web version of this article.)

Table 5
Percentage of efficiency and resolution loss on 5-cm and 2-cm long columns (4.6 mm I.D.) moving from the flow-rate: 1.0 mL/min up to flow-rate: 6.0 (on the 50 × 4.6 mm) and 8.0 mL/min (on the 20 × 4.6 mm columns).

Flow-rate 1.0 mL/min vs. 6.0 mL/min (50 × 4.6 mm)/8.0 mL/min (20 × 4.6 mm)							
LxI.D.	CSP	Resolution drop (−%)		Efficiency drop (−%)			
		Haloxyfop	Ketorolac	1° enantiomer Haloxyfop	2° enantiomer Haloxyfop	1° enantiomer Ketorolac	2° enantiomer Ketorolac
50 × 4.6 mm	SPP-Halo 2.0	42	45	62	66	65	66
	SPP-Halo 2.7	51	53	73	78	77	78
	FPP-Titan 1.9	46	47	67	70	69	70
20 × 4.6 mm	SPP-Halo 2.0	44	52	61	69	74	72
	FPP-Titan 1.9	50	52	69	72	73	66

loss in efficiency of more than 60% was observed on both the UHPC-SPP-Halo-Tzwitt 2.0 and UHPC-FPP-Titan-Tzwitt 1.9 columns. On the other hand, a dramatic efficiency loss of about 80% was recorded on the UHPC-SPP-Halo-Tzwitt 2.7 column.

To further assess the potential of the two CSPs, exhibiting the best behavior under Ultra-High-Speed and Ultra-High-Performance regimes (namely, the UHPC-SPP-Tzwitt-Halo 2.0 and the UHPC-FPP-Tzwitt-Titan 1.9), two additional 20 × 4.6 mm columns were in house packed with these phases. Various chiral samples were tested, at flow rates as high as 8.0 mL/min (Fig. 6S). The separation of a mixture of haloxyfop and ketorolac is reported in Fig. 9. Ultra-fast separations were obtained on both columns. 73 s and 61 s were necessary to achieve the complete separation at 1.0 mL/min on the UHPC-FPP-Tzwitt-Titan 1.9 column and on the UHPC-SPP-Tzwitt-Halo 2.0 one, respectively, with efficiencies higher than 200,000 *N*/m and resolutions close to 4.0. Increasing the flow rate at 8.0 mL/min, the separation of the mixture was completed in roughly 8 s. Remarkably, by considering only the enantiomers of haloxyfop they were resolved in only 4.0 and 3.4 s on the UHPC-FPP-Titan-Tzwitt 1.9 and UHPC-SPP-Halo-Tzwitt 2.0 columns, respectively. High efficiency values close to 60,000 N/m were obtained also at this flow rate on the UHPC-FPP-Titan-Tzwitt 1.9 column, whereas the UHPC-SPP-Halo-Tzwitt 2.0 one showed about 76,000 *N*/m (Table 5). It is important to observe that the combination of high efficiency and high enantioselectivity allowed to maintain excellent R_s values also in ultrafast regimes. Indeed, the UHPC-FPP-Titan-Tzwitt 1.9 column showed R_s values of about 1.6 while the UHPC-SPP-Halo-Tzwitt 2.0 column exhibited R_s values higher than 2.0.

5. Conclusions

This work has demonstrated that the zwitterionic teicoplanin based CSP prepared on 2.0 μm SPPs is very promising towards the development of high efficient and ultrafast liquid chromatography. The columns packed with this CSP exhibited excellent performance (300,000 *N*/m), very close to that obtained in RP achiral chromatography. These columns were also characterized by extremely fast mass transfer (very flat C-branch of van Deemter equation). Therefore, they could be employed in ultrafast separation (up to 8 mL/min flow rate) without dramatically loosing performance. As a proof of concept example of the feasibility of ultrafast and high performance

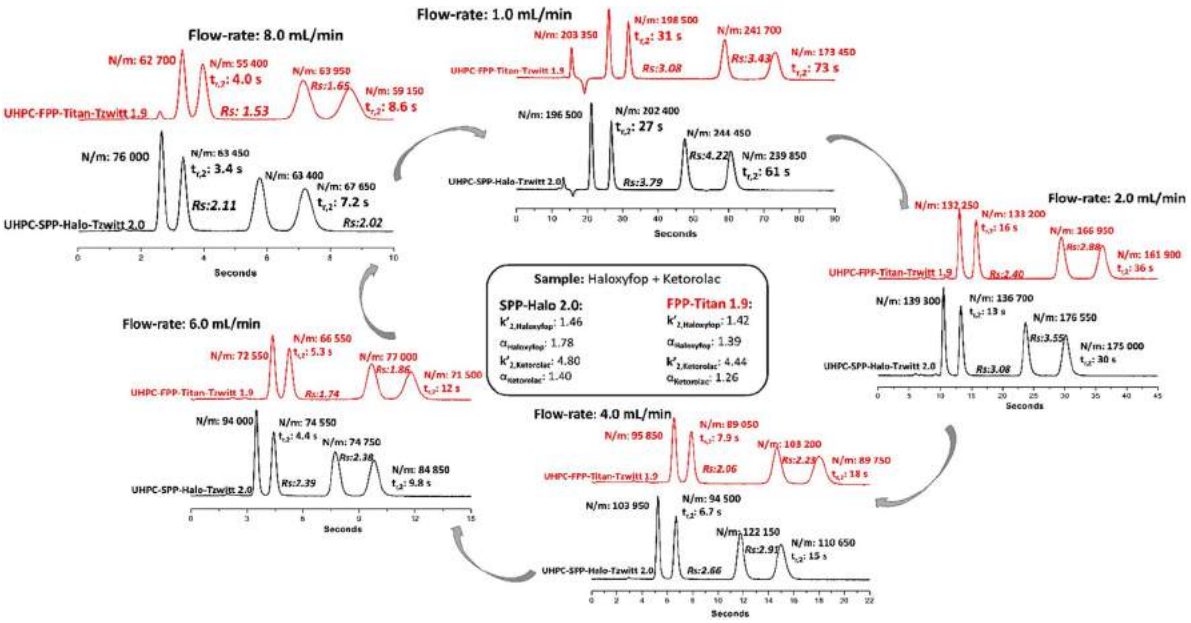

Fig. 9. Ultra-High speed/Ultra-High Performance separations of the enantiomers of Haloxyfop and Ketorolac, at different flow-rates, on UHPC-SPP-Halo-Tzwitt 2.0 μm (Black line) and UHPC-FPP-Titan-Tzwitt 1.9 μm (Green line) packed in 20 × 4.6 mm columns. *k'* and α values reported in figure were calculated at flow-rate: 1.0 mL/min. Eluent: ACN/H_2O 85:15 + 20 mM $HCOONH_4$, *T*: 35 °C. (For interpretation of the references to colour in this figure legend, the reader is referred to the web version of this article.)

chiral separations on these columns, haloxyfop enantiomers were baseline resolved (resolution equal to 2) in only 3 s.

In a forthcoming paper, the effect of chiral selector surface density on the adsorption/desorption kinetics will be investigated by preparing a series of chiral particles (both SPP and FPP) with the same base chemistry and different loading of chiral selector. In our opinion, indeed, this parameter has a dramatic effect on the efficiency of the chiral stationary phase and its optimization will allow to prepare CSPs significantly more efficient towards ultrafast applications.

Acknowledgements

This work was conducted with financial support from Sapienza University of Rome, Italy (DR n. 3210/16 of 16/12/2016). The authors thank Dr. E. Bianchini, Department of Chemistry and Pharmaceutical Sciences, University of Ferrara, for elemental analysis measurements.

Appendix A. Supplementary data

Supplementary data associated with this article can be found, in the online version, at http://dx.doi.org/10.1016/j.chroma.2017.09.008.

References

[1] J.J. Kirkland, J.J. DeStefano, T.J. Langlois, Characteristics of superficially-porous silica particles for fast HPLC: some performance comparisons with sub-2-μm particles, Am. Lab. (2007) 18–21.
[2] J.J. DeStefano, S.A. Schuster, J.M. Lawhorn, J.J. Kirkland, Performance characteristics of new superficially porous particles, J. Chromatogr. A 1258 (2012) 76–83.
[3] G. Guiochon, F. Gritti, Shell particles trials, tribulations and triumphs, J. Chromatogr. A 1218 (2011) 1915–1938.
[4] A. Cavazzini, F. Gritti, K. Kaczmarski, N. Marchetti, G. Guiochon, Mass-transfer kinetics in a shell packing material for chromatography, Anal. Chem. 79 (2007) 5972–5979.
[5] N. Marchetti, A. Cavazzini, F. Gritti, G. Guiochon, Gradient elution separation and peak capacity of columns packed with porous shell particles, J. Chromatogr. A 1163 (2007) 203–211.
[6] F. Gritti, A. Cavazzini, N. Marchetti, G. Guiochon, Comparison between the efficiencies of columns packed with fully and partially porous C18-bonded silica materials, J. Chromatogr. A 1157 (2007) 289–303.
[7] N. Marchetti, G. Guiochon, High peak capacity separations of peptides in reversed-phase gradient elution liquid chromatography on columns packed with porous shell particles, J. Chromatogr. A 1176 (2007) 206–216.
[8] G. Cancelliere, A. Ciogli, I. D'Acquarica, F. Gasparrini, J. Kocergin, D. Misiti, M. Pierini, H. Ritchie, P. Simone, C. Villani, Transition from enantioselective high performance to ultra-high performance liquid chromatography: a case study of a brush-type chiral stationary phase based on sub-5-micron to sub-2-micron silica particles, J. Chromatogr. A 1217 (2010) 990–999.
[9] M. Catani, O.H. Ismail, F. Gasparrini, M. Antonelli, L. Pasti, N. Marchetti, S. Felletti, A. Cavazzini, Recent advancements and future directions of superficially porous chiral stationary phases for ultrafast high-performance enantioseparations, Analyst 142 (2017) 555–566.
[10] D. Kotoni, A. Ciogli, C. Molinaro, I.D. Acquarica, J. Kocergin, T. Szczerba, H. Ritchie, C. Villani, F. Gasparrini, Introducing enantioselective ultrahigh-pressure liquid chromatography (eUHPLC): theoretical inspections and ultrafast separations on a new sub-2-μm whelk-O1 stationary phase, Anal. Chem. 84 (2012) 6805–6813.
[11] D. Kotoni, A. Ciogli, I. D'Acquarica, J. Kocergin, T. Szczerba, H. Ritchie, C. Villani, F. Gasparrini, Enantioselective ultra-high and high performance liquid chromatography: a comparative study of columns based on the Whelk-O1 selector, J. Chromatogr. A 1269 (2012) 226–241.
[12] A. Cavazzini, N. Marchetti, R. Guzzinati, M. Pierini, A. Ciogli, D. Kotoni, I. D'Acquarica, C. Villani, F. Gasparrini, Enantioseparation by ultra-high-performance liquid chromatography, TrAC – Trends Anal. Chem. 63 (2014) 95–103.
[13] R.J. Reischl, L. Hartmanova, M. Carrozzo, M. Huszar, P. Frühauf, W. Lindner, Chemoselective and enantioselective analysis of proteinogenic amino acids utilizing N-derivatization and 1-D enantioselective anion-exchange chromatography in combination with tandem mass spectrometric detection, J. Chromatogr. A 1218 (2011) 8379–8387.
[14] K. Lomsadze, G. Jibuti, T. Farkas, B. Chankvetadze, Comparative high-performance liquid chromatography enantioseparations on polysaccharide based chiral stationary phases prepared by coating totally porous and core-shell silica particles, J. Chromatogr. A 1234 (2012) 50–55.
[15] D.A. Spudeit, M.D. Dolzan, Z.S. Breitbach, W.E. Barber, G.A. Micke, D.W. Armstrong, Superficially porous particles vs. fully porous particles for bonded high performance liquid chromatographic chiral stationary phases: isopropyl cyclofructan 6, J. Chromatogr. A 1363 (2014) 89–95.
[16] M.D. Dolzan, D.A. Spudeit, Z.S. Breitbach, W.E. Barber, G.A. Micke, D.W. Armstrong, Comparison of superficially porous and fully porous silica supports used for a cyclofructan 6 hydrophilic interaction liquid chromatographic stationary phase, J. Chromatogr. A 1365 (2014) 124–130.
[17] C.L. Barhate, Z.S. Breitbach, E. Costa Pinto, E.L. Regalado, C.J. Welch, D.W. Armstrong, Ultrafast separation of fluorinated and desfluorinated pharmaceuticals using highly efficient and selective chiral selectors bonded to superficially porous particles, J. Chromatogr. A 1426 (2015) 241–247.
[18] D.C. Patel, Z.S. Breitbach, M.F. Wahab, C.L. Barhate, D.W. Armstrong, Gone in seconds: praxis, performance, and peculiarities of ultrafast chiral liquid

chromatography with superficially porous particles, Anal. Chem. 87 (2015) 9137–9148.
[19] D.C. Patel, M.F. Wahab, D.W. Armstrong, Z.S. Breitbach, Advances in high-throughput and high-efficiency chiral liquid chromatographic separations, J. Chromatogr. A 1467 (2016) 2–18.
[20] M.F. Wahab, R.M. Wimalasinghe, Y. Wang, C.L. Barhate, D.C. Patel, D.W. Armstrong, Salient sub-second separations, Anal. Chem. 88 (2016) 8821–8826.
[21] O.H. Ismail, L. Pasti, A. Ciogli, C. Villani, J. Kocergin, S. Anderson, F. Gasparrini, A. Cavazzini, M. Catani, Pirkle-type chiral stationary phase on core-shell and fully porous particles: are superficially porous particles always the better choice toward ultrafast high-performance enantioseparations? J. Chromatogr. A 1466 (2016) 96–104.
[22] O.H. Ismail, A. Ciogli, C. Villani, M. De Martino, M. Pierini, A. Cavazzini, D.S. Bell, F. Gasparrini, Ultra-fast high-efficiency enantioseparations by means of a teicoplanin-based chiral stationary phase made on sub-2μm totally porous silica particles of narrow size distribution, J. Chromatogr. A 2016 (1427) 55–68.
[23] F. Gritti, G. Guiochon, Mass transfer kinetics, band broadening and column efficiency, J. Chromatogr. A 1221 (2012) 2–40.
[24] M. Catani, O.H. Ismail, A. Cavazzini, A. Ciogli, C. Villani, L. Pasti, C. Bergantin, D. Cabooter, G. Desmet, F. Gasparrini, D.S. Bell, Rationale behind the optimum efficiency of columns packed with new 1.9 μm fully porous particles of narrow particle size distribution, J. Chromatogr. A 2016 (1454) 78–85.
[25] G. Desmet, D. Clicq, P. Gzil, Geometry-independent plate height representation methods for the direct comparison of the kinetic performance of LC supports with a different size or morphology, Anal. Chem. 77 (2005) 4058–4070.
[26] G. Gritti, Y. Kazakevich, G. Guiochon, Effect of the surface coverage of endcapped C18-silica on the excess adsorption isotherms of commonly used organic solvents from water in reversed phase liquid chromatography, J. Chromatogr. A 1169 (2007) 111–124.
[27] F. Gritti, Y. Kazakevich, G. Guiochon, Measurement of hold-up volumes in reverse-phase liquid chromatography: definition and comparison between static and dynamic methods, J. Chromatogr. A 1161 (2007) 157–169.
[28] M. Al-Bokari, D. Cherrak, G. Guiochon, Determination of the porosities of monolithic columns by inverse size-exclusion chromatography, J. Chromatogr. A 975 (2002) 275–284.
[29] O.H. Ismail, A. Pasti, A. Cavazzini, C. Ciogli, D. Villani, F. Kotoni, D.S. Bell, Experimental evidence of the kinetic performance achievable with columns packed with new 1.9 μm fully porous particles of narrow particle size distribution, J. Chromatogr. A 1454 (2016) 86–92.
[30] C.A. Cramers, J.A. Rijks, C.P.M. Schutjes, Factors determining flow rate in chromatographic columns, Chromatographia 14 (1981) 439–444.
[31] J.C. Giddings, Comparison of theoretical limit of separating speed in gas and liquid chromatography, Anal. Chem. 37 (1965) 60–63.
[32] U.D. Neue, Kinetic plots made easy, LC-GC Eur. 22 (2009) 570.
[33] H. Poppe, Some reflections on speed and efficiency of modern chromatographic methods, J. Chromatogr. A 778 (1997) 3–21.

Paper III

Analytical and Bioanalytical Chemistry (2018) 410:2457–2465
https://doi.org/10.1007/s00216-017-0842-4

TRENDS

New frontiers and cutting edge applications in ultra high performance liquid chromatography through latest generation superficially porous particles with particular emphasis to the field of chiral separations

Martina Catani[1] · Simona Felletti[1] · Omar H. Ismail[2] · Francesco Gasparrini[2] · Luisa Pasti[1] · Nicola Marchetti[1] · Chiara De Luca[1] · Valentina Costa[1] · Alberto Cavazzini[1]

Received: 30 October 2017 / Revised: 5 December 2017 / Accepted: 15 December 2017 / Published online: 16 January 2018

Abstract

About ten years after their introduction to the market (happened in 2006), the so-called second generation superficially porous particles (SPPs) have undoubtedly become the benchmark as well as, very often, the preferred choice for many applications in liquid chromatography (LC), when high efficiency and fast separations are required. This trend has interested practically all kinds of separations, with the only exception of chiral chromatography (at least so far). The technology of production of base SPPs is advanced, relatively simple and widely available. The deep investigation of mass transfer mechanisms under reversed-phase (RP) and normal-phase (NP) conditions for achiral separations has shown the advantages in the use of these particles over their fully porous counterparts. In addition, it has been demonstrated that SPPs are extremely suitable for the preparation of efficient packed beds through slurry packing techniques. However, the research in this field is in continual evolution. In this article, some of the most advanced concepts and modern applications based on the use of SPPs, embracing in particular ultrafast chiral chromatography and the design of SPPs with engineered pore structures or very reduced particle diameter, are revised. We describe modern trends in these fields and focus on those aspect where further innovation and research will be required.

Keywords Superficially porous particles (SPPs) · Sub-2 µm SPPs · 2.0 µm chiral SPPs · Highly ordered radially oriented mesopore SPPs · Highly efficient ultrafast (chiral) separations

Introduction

One of the main challenges facing chromatographers is developing high efficient and fast separation methods. A fundamental aspect of this process is the choice of the liquid-chromatography (LC) column, in particular regarding the physico-chemical and geometric characteristics of packing particles. Their size and morphology (either fully or superficially porous) indeed dramatically affect the kinetic performance of columns not only by modifying the volume available for the diffusion of molecules but also through the "quality" of the resulting packed bed [1–3].

As a matter of fact, for a long time, the main approach followed by column manufacturers to improve the efficiency of separation has been to prepare columns made of particles with smaller and smaller diameter. Sub-2 μm spherical fully porous particles (FPPs) are nowadays widely commercialized and routinely employed. The downside of this approach is in the very high pressure required to use these columns at their full potential (up to 1200-1500 bars or more) [4], since pressure drop along the column increases by a square function of the inverse of particle size [5].

In 2006, the so-called second generation superficially porous particles (SPPs) – alternatively named core-shell, fused-core^{TM} or porous shell particles – were launched [6]. Since then, columns packed with SPPs invaded the market,

✉ Martina Catani
martina.catani@unife.it

✉ Alberto Cavazzini
cvz@unife.it

[1] Department of Chemistry and Pharmaceutical Sciences, University of Ferrara, via L. Borsari 46, 44121 Ferrara, Italy

[2] Department of Drug Chemistry and Technology, "Sapienza" University of Rome, P.le Aldo Moro 5, 00185 Rome, Italy

representing an effective and concrete alternative to sub-2 μm FPPs in terms of efficiency and speed of separation, but orignating much less back pressure [7]. As an example, columns packed with C_{18} 2.7 μm SPPs provide efficiencies close to those of columns of the same geometry packed with 1.7 μm fully porous C_{18} particles but operating at a backpressure that is 50-75% smaller than that of FP particles [8, 9].

Second-generation SPPs are made of a nonporous solid silica core surrounded by a porous silica shell, exactly as the pellicular particles introduced in the sixties by Horváth and Lipsky [10]. The main advantage of these particles with respect to first generation ones is their higher loading capacity achieved thanks to a specific design, where the porous zone occupies roughly 3/4 of the total particle volume [11].

The rationale behind the introduction of a solid core into the particle was not only to improve solid-liquid mass transfer (c_s-term of the van Deemter equation) by shortening the diffusion path length across the particle but also to reduce the contribution of longitudinal diffusion (b-term of the van Deemter equation) by decreasing the pore volume accessible to analyte molecules [8, 12–14]. Later on, it turned out that SPPs are characterized by very low eddy diffusion (a-term of the van Deemter equation, accounting for any kind of flow inhomogeneity and unevenness in the packed bed), which largely contributes to the overall efficiency of a column [8, 15].

A countless number of papers and reviews have been published describing the fundamentals, developments and applications of SPPs in areas as different as food chemistry, biological applications, environmental chemistry, "omics" sciences, bi-dimensional chromatography, etc. [8, 11, 16–24]. Readers interested in these topics are addressed to specific literature.

On the other hand, in this paper, we focus on some of the most interesting solutions and ideas proposed to push further the limits of performance and the field of applications of SPPs. These innovations embrace different fields and sectors of activities. First of all, they pertain to high efficient and ultrafast chiral chromatography, where results that were unimaginable even only a few years ago have been recently achieved [16, 25–28]. For instance, several examples of chiral separations performed in less than one second with chiral SPPs as stationary phases have been published. Even if some fundamental aspects need further understanding [16, 25], these works represent the turning point between an old concept of chiral separations by LC and a new one based on columns exhibiting perfomance (in terms of efficiency and speed of separation) very similar to those of chips employed for high-speed enantioseparations [29]. We may reasonably expect in the next few years the appearence on the market of many chiral stationary phases based on these concepts, since the technology of production of chiral SPP particles is mature enough to find its way into commercial products.

In other less fortunate cases, very innovative and promising concepts of SPPs are still at the level of prototypes. Among these, it is worth to mention the so-called highly ordered radially oriented mesopore (ROM) SPPs [30, 31]. Engineered to achieve superior kinetic performance thanks to their highly ordered mesopore network, these SPPs have however exhibited some issues in terms of chemical and long term stability, limiting the extensive evaluation of their potential for high efficient separations. Another remarkable example of precursors is represented by SPPs of very reduced diameter (down up to 1.1 μm) and porous layer thickness. In this case, the major barrier to large scale production and commercialization has been essentially practical, coming from actual limits of even state-of-art instrumentation, whose extra column void volume is incompatible with the efficiency of these particles. Admittedly, also the slurry packing of smallest SPPs (1.1 μm) into very narrow tubes presents important difficulties [32, 33].

Chiral SPPs: the future of high efficient and ultrafast enantioseparations?

The employment of high efficient particles – either sub-2 μm fully porous or second-generation superficially ones – in chiral LC has been relatively recent. This delay, with respect to achiral separations, depends on different reasons. They include both practical issues and theoretical problems. Among the former, the most relevant ones are the difficulty to adapt in some cases pre-existing methods in use for the functionalization of larger chiral FPPs to very small particles; particle agglomeration during synthesis; the non uniform coating of chiral particles. On the other hand, from a theoretical viewpoint, the lack of complete understanding of the complex mass transfer phenomena in chiral chromatography is a relevant limitation to the development of very efficient chiral particles [1, 16, 34]. Last but not least, conservative commercial strategies by the most important producers of chiral columns may also be advocated to explain the delay.

As a matter of fact, until 2011, SPPs were not used as base material for the preparation of chiral stationary phases (CSPs) [35, 36] (for the sake of information completeness, the first report on the use of 1.9 μm fully porous chiral particles is dated 2010 [37, 38]). Since then, different classes of CSPs have been produced as porous shell materials and the debate about pros and cons of chiral SPPs over FPPs has begun. Chankvetadze and his group were most active in the preparation of polysaccharide-based

superficially porous CSPs [39, 40]. Their studies about the comparison of kinetic performance between these CSPs and their fully porous counterparts of comparable content of chiral selector and particle size led to the conclusion that SPP chiral columns can provide higher separation factors, higher efficiency and flatter van Deemter curves.

The most complete works on the evaluation of the performance of SPPs in chiral chromatography are those from Armstrong's group [28, 41–46]. Armstrong and coworkers have evaluated, from a kinetic viewpoint, a wide class of chiral selectors prepared on 2.7 μm SPPs including cyclofructan-6 and β-cyclodextrin, macrocyclic antibiotics (teicoplanin, teicoplanin aglycone and vancomycin) and quinine-based ones. In agreement with Chankvetadze's findings, they also have demonstrated that chiral SPPs perform systematically better than fully porous ones under RP, NP, hydrophilic interaction (HILIC) and polar organic mode LC. Remarkably, the employment of very short columns (5 mm long) packed with chiral SPPs and operated at a very high flow rate, permitted to achieve ultrafast enantioseparations (sub-second timescale) [27]. At the same time, also Gasparrini and coworkers reported about the possibility of performing sub-second separations by using SPPs functionalized with Whelk-O1 chiral selector [1, 16]. As an example, Fig. 1 shows some remarkable cases where – thanks to the use of high flow rates (up to 8 ml/min) and very short columns (length 5-10 mm) packed with latest generation chiral particles – separations of enantiomers in less than one second were achieved (see figure caption for details).

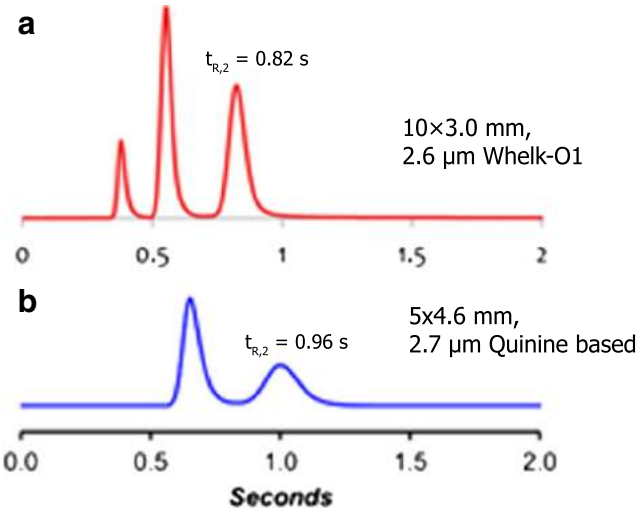

Fig. 1 Ultrafast enantioseparations of **a** *trans*-stilbene oxide enantiomers on a 10×3.0 mm column packed with 2.6 μm Whelk-O1 SPPs, MP: hexane/ethanol 90:10 %(v/v)+1% methanol, flow rate: 8 mL/min; **b** N-(3,5-dinitrobenzoyl)- DL-leucine enantiomers on a 5×4.6 mm column packed with 2.7 μm Quinine based SPPs, MP: acetonitrile/20 mM ammonium formate 70:30%(v/v), flow rate: 5 mL/min. (Modified with permissions from Refs. [16] and [27], respectively)

These proof-of-concept experiments demonstrate the state of the art of chiral LC and allow to predict a great future for this technology in the field of ultrafast enantioseparations. However, in spite of these very promising results, it is the opinion of the authors of this paper that there are still some fundamental aspects that require a deeper investigation to truly understand the potential and limits of these particles. They concern essentially two interconnected aspects. The first one is about the importance of the adsorption-desorption kinetics on the performance of modern, ultra-high effient chiral LC columns [47, 48]. In particular, questions such as:

- if (and how) the adsorption-desorption kinetics varies by changing the surface density of chiral selector;
- if (and how) the surface density of chiral selector varies across the particle diameter (this is particularly important when considering the comparison between chiral SPPs and FPPs);
- if (and how) the chemical environment surrounding the chiral moiety anchored to the surface affects the adsorption-desorption kinetics (physico-chemical properties of bare silicas can be very different);

need serious consideration. To date these points have been only marginally addressed in the literature.

The other aspect that needs more fundamental work is about the very complex problem of evaluating the contribution of eddy dispersion to band broadening and the factors on which it depends [49]. It concerns, clearly, also the study of packing of particles into chromatographic columns and how it possibly changes depending on the surface characteristics of particles themselves [50]. According to the experience of the authors of this work, packing apolar or polar particles (such as chiral ones), be they FPPs or SPPs, [16, 25] can be intrinsically different. Even the most advanced approaches to study mass transfer in chiral chromatography, indeed, cannot provide independent estimations of contributions to band broadening coming from eddy dispersion and adsorption-desorption kinetics [51].

These considerations show that the apparently obvious statement according to which columns packed with chiral SPPs must outperform those made of chiral FPPs in terms of efficiency (in agreement with what happens in achiral RP LC) [43, 44], must be taken with great caution. Indeed, some experimental facts showing that the above mentioned generalization cannot be always applied have been reported. Ismail et al. [1], for instance, compared the efficiency of chiral columns for ultrafast high-efficient separations packed with both Whelk-O1 SPPs (2.6 μm) and FPPs (1.8 and 2.5 μm). Contrary to initial expectations they found that, especially for the more retained enantiomer, the efficiency of the column packed with SPPs was worse than

that of the 1.8 μm FPP column and quasi-comparable to that of the column made of 2.5 μm FPPs [16]. The authors reported about the possible combination of both a slower adsorption-desorption kinetics and a larger eddy dispersion in the column packed with chiral SPPs as the reasons to explain this behavior. On the one hand, they correlated the unusual low perfomance of SPPs to the larger surface density of chiral selector found on the SPPs (+ 20%) with respect to the fully porous ones (even if particles were prepared under identical experimental conditions) and, on the other hand, to the empirical difficulties encountered during the packing of chiral SPPs.

Quite recently, the same group pushed beyond the limit of high efficient chiral particles, by featuring the first example of a (teicoplanin-based) CSP prepared on 2.0 μm SPPs [26]. The kinetic performance of the column packed with this new particles was compared to that of other two columns packed with 2.7 μm SPPs and 1.9 μm FPPs of narrow particle size distribution (Titan^{TM} particles), functionalized with the same chiral selector. At the minimum of the van Deemter curve, the new 2.0 μm SPP CSP was found to overcome the other two for the separation of both achiral and chiral compounds in HILIC conditions, with efficiency close to 300,000 plates/meter. On the opposite, at higher flow rates, even with the new 2.0 μm teicoplanin-based SPP column a significant loss of performance (especially for the second eluted enantiomer) was observed. This finding is consistent with the observation made with Whelk-O1 CSPs (see before).

To conclude this paragraph, Fig. 2 reports another extraordinary example, in addition to those given in Fig. 1, of the outstanding results that can be achieved with the new 2.0 μm teicoplanin-based SPPs. This figure shows the separation of a mixture of haloxyfop and ketorolac enantiomers in about 8 seconds with a resolution larger than 2.0 (see figure caption for details) [26]. Incidentally, we mention here that teicoplanin and teicoplanin-based derivatives have been for a long time considered "slow" selectors, unsuitable for high efficient and ultrafast separations.

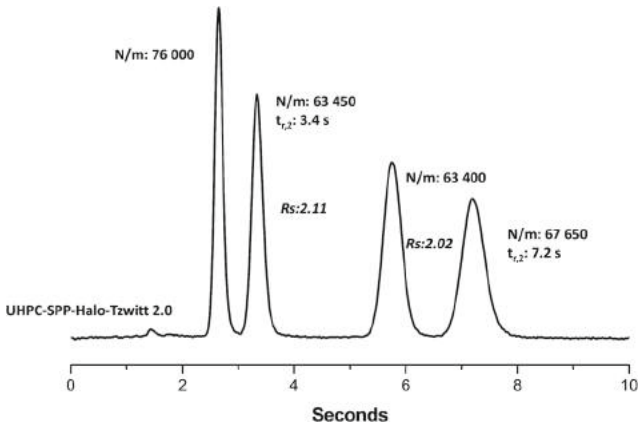

Fig. 2 Ultrafast enantioseparation of a racemic mixture containing haloxyfop (firstly eluted pair of peaks) and ketorolac (secondly eluted pairs of peaks) on a 20×4.6 mm (L×I.D.) column packed with 2.0 μm teicoplanin SPPs. Modified with permission from [26]

Highly ordered radially oriented mesopore SPPs: reaching unexplored efficiency limits through engineered particles

In 2016, an innovative approach named pseudomorphic transformation (PMT) micelle templating has been described to produce a new type of SPPs characterized by: (i) narrower particle size; (ii) thinner porous layer with high surface area; and, most importantly, (iii) a pore network made of highly ordered radially oriented mesopores [30]. PMT process is based on the dispersion of non-porous silica particles (which will form the core) in a silica-dissolving alkaline solution with self-organizing surfactant molecules. Fig. 3 reports SEM images of ROM-SPPs (squares *a* and *c*) and traditional SPPs (squares *b* and *d*). Cross-section views (Fig. 3c and d) show how the presence of ROM limits diffusion only to the radial direction. This is thus fundamentally different from the randomly distributed and tortuous diffusion pathways in conventional SPPs (Fig. 3d). Prototype columns packed ROM-SPPs with an overall diameter of 5 μm have been demonstrate to produce minimum reduced plate height values about 0.5-1 units lower than those achievable with fully porous and traditional SPPs of the same particle size, respectively. This represents the lowest value reported for analytical columns [30].

In a remarkable theoretical study by Deridder et al. [31], computational fluid dynamics (CFD) was used to compare mass transfer properties and band broadening in perfectly ordered beds made of: ROM-SPPs; traditional SPPs; and, finally, FPPs. To allow for a fair comparison, the same particle arrangement, the same values for the mobile zone and porous zone diffusion coefficients, as well as the same retention factor have been assumed for the three particle types. The results of this study can be summarized with the help of Fig. 4, where the theoretical van Deemter curves obtained for the three types of particles are reported. The advantage in terms of mass transfer given by ROM-SPPs is evident. The ordered pore structure allow these particles to outperform the others, thanks to a dramatic reduction of the *b*-term contribution.

Deridder et al. demonstrated the longitudinal diffusion to be independent of the retention factor. It remained at its minimal value (corresponding to that of unretained molecules) instead of increasing with retention, as it happens for particles with isotropic internal diffusion. This depends on the fact that when retained molecules reside in the porous layer of ROM-SPPs, their diffusion in the

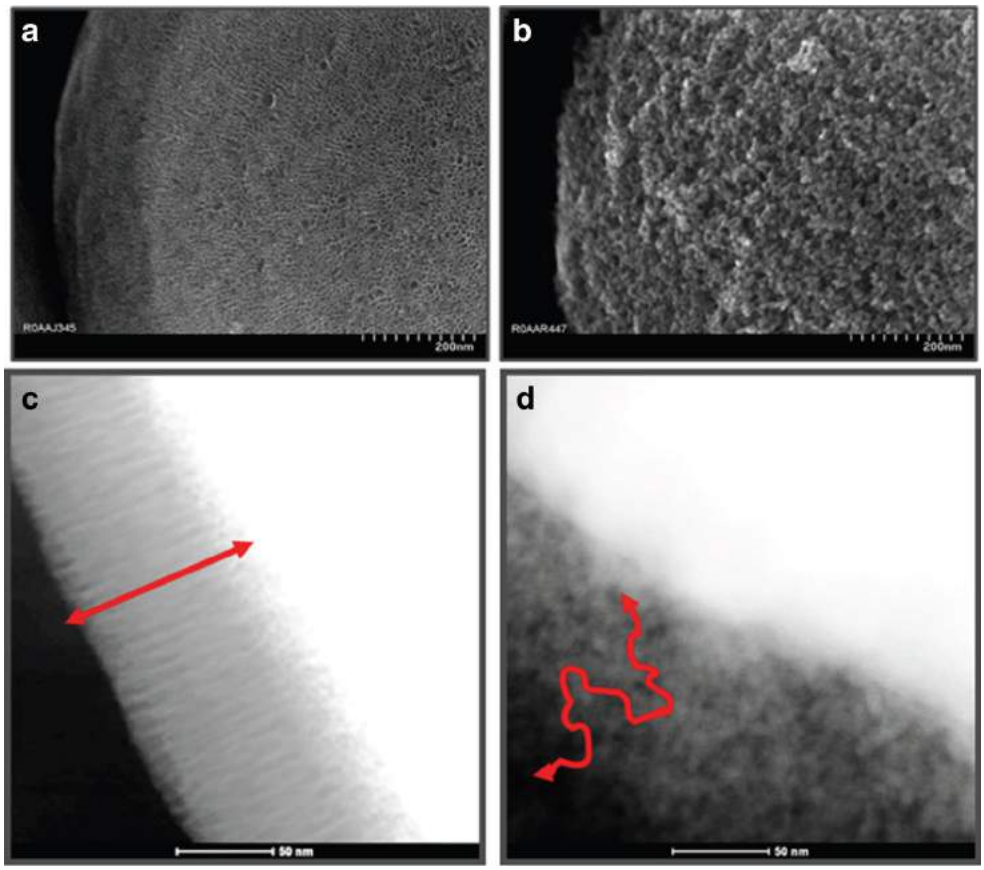

Fig. 3 High resolution SEM images of a ROM-SPP (**a**, **c**) and a SPP (**b**, **d**). Pictures (**c**) and (**d**) are cross-section views of the mesoporous network, showing the differences between the diffusion pathways in the two types of particles. Taken with permission from [30]

circumferential direction is completely blocked. Therefore, the only remaining route available for diffusion is the interstitial volume between particles. This advantage in the *b*-term is achieved without affecting the c_s-term, which does not increase, as it should be expected. Another important aspect that would affect the performance of ROM-SPPs is the geometrical shape of mesopores. From a theoretical point of view, Gritti has demonstrated that conical shaped mesopores would produce roughly 80% lower c_s-term than cylindrical ones [52].

In spite of these important advantages, the development of ROM-SPPs apparently is not any longer supported, due to (no better specified) both chemical stability problems and low mechanical resistance.

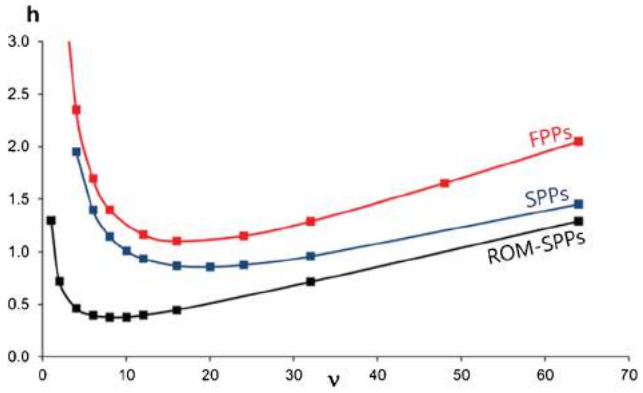

Fig. 4 Theoretical reduced van Deemter curves (h vs. ν, being h the reduced plate height and ν the reduced interstitial velocity) for packed beds made of FPPs (red data), traditional SPPs (blue data) and ROM-SPPs (black data). Modified with permission from [31]

Sub-2 μm SPPs: when instrumental constraints are the bottleneck to reaching highest efficiency

The reduction of the particle size to increase efficiency and favour faster separation has been pursued also with SPPs. Already a few years after the introduction of second generation SPPs in the format of 2.7 μm (Halo^{TM} particles), sub-2 μm SPPs were produced and commercialized. Very high efficiency and reduced analysis times were found by several authors by using columns packed with 1.7 μm SPPs [7, 17, 53–55]. Later on, the particle diameter of SPPs has been further decreased to 1.3 μm, which represents the smallest dimension of SPPs available to date in the market. Fekete et al. characterized columns packed with these particles from a kinetic viewpoint [4, 56]. They found exceptionally low reduced plate heights and high

peak capacities with cutting edge applications, especially in the field of fast separation of peptides. However, it appeared evident that instrumental constraints of even state of the art equipments prevent the full deployment of particle technology.

Figure 5 compares the van Deemter curves of Kinetex^{TM} SPPs of different sizes (including 1.3 μm ones). As it can be evinced from this plot, the minimum of the van Deemter curve for 1.3 μm particles is barely reached. This depends on the back-pressure limitations of commercial UHPLC equipments, which are not able to supply the pressure needed to push, through beds made of very small particles, the mobile phase at reasonably high linear velocities. As a matter of fact, for the current operating pressure limit, these particle format look advantageous only for the separation of large molecules (having a lower optimal velocity range than that of small molecules) both in isocratic and gradient elution mode [4, 56].

The reasearch was pushed forward by Blue and Jorgenson who featured the first example of 1.1 μm SPPs, the smallest SPP ever produced, through an innovative layer-by-layer synthetic approach [32, 33]. The information contained in Fig. 5 let us glimpse the highest potential of this material. Indeed, one might expect the van Deemter curve of 1.1 μm SPPs to be significantly lower than those of the other particle formats, potentially permitting to achieve incredibly high efficiency.

However, the expectation was not satisfied. Blue and Jorgenson report about the importance not only of an extremely precise control of experimental conditions for the synthesis of these particles but also of the slurry packing procedure, which can have a major impact on the efficiency of the column, in their case made of a 30 μm I.D. capillary. This last aspect, in particular, was claimed to be responsible for the performance observed with their capillaries, significantly lower than the theoretical values predictable for 1.1 μm particles.

In addition, the other very important instrumental factor limiting the development of this technology comes from the contribution to efficiency given by band broadening in the extra-column void volume (including injector, connections, column frits, detector, etc.) of modern UHPLC equipments, which is larger than that produced by particles of these intrinsic characteristics [57]. Finally, it is worth to mention that a practical problem of columns packed with very small particles is that they can behave as traps for particulate matter dissolved in the eluent, with important consequences on the lifetime of these columns if mobile phases and samples are not carefully filtered prior analysis.

Outlook

The technology not only of production but also of functionalization of SPPs to prepare very small particles with extremely enhanced properties in terms of mass transfer has come a long way. With the remarkable exception of RP achiral separations for particle not smaller than 1.7 μm, however, the potential of latest generation SPPs remains still largely unexplored due to a series of limitations, mainly instrumental ones, which have impeded the development of techniques and methods based on them.

The further advancement of the field requires an important contribution by LC instrument manufacturers for the production of equipments suitable to provide very large back pressure and, simultaneously, characterized by extremely low extra-column volume through innovative designs for detectors, injectors, column fittings, etc. This is particularly important (see below) for supercritical fluid chromatography (SFC), where the development of enhanced instrumentation is particularly necessary. Column manufacturers, on the other hand, should develop the technology to prepare very short columns with optimized

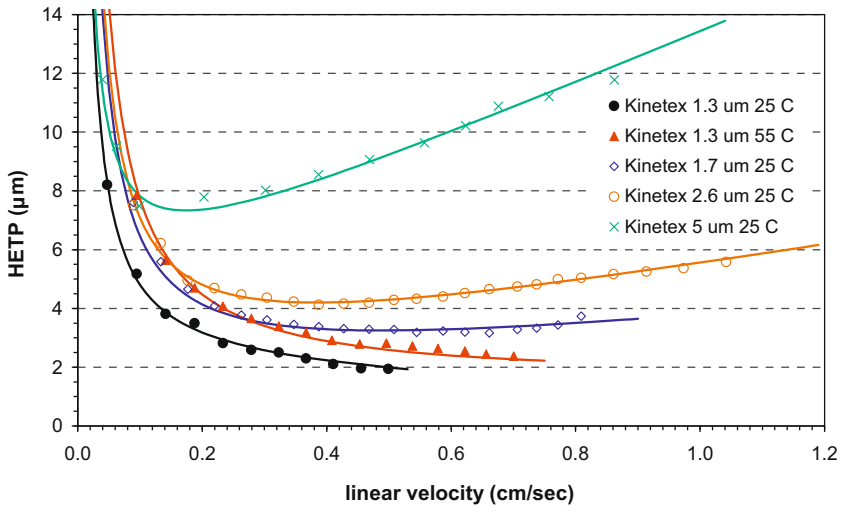

Fig. 5 Experimental van Deemter curves of butylparaben in reversed-phase conditions measured on columns packed with Kinetex 1.3, 1.7, 2.6 and 5 μm SPPs. Taken with permission from [4]

hardware (including column frits) to reduce extra-column band broadening. Advancement in 3D printing technology and CFD studies are fundamental to drive this change.

From a more theoretical viewpoint, an extension of our understanding of the packing process of slurry suspensions into chromatographic columns is necessary, by focusing in particular on the factors (including the rheology of particles, slurry density, etc. [49]) that affect it and which could have an impact on the performance of the resulting packed bed (e.g., through the *a*-term of the van Deemter equation).

In parallel, the investigation of the fundamentals of mass transfer is expected to provide information that will help the design of SPPs with still more advanced kinetic properties. For instance, the study of adsorption-desorption kinetics in chiral chromatography might suggest important indications on how to functionalize particles (e.g., in terms of density of chiral selector) for optimum performance.

It is precisely in the field of enantioseparations by LC that, in the nearest future, we can expect a real revolution thanks to the use of chiral SPPs of latest generation. Over the year, this field has fallen behind compared to achiral RP separations as regards ultrafast and high efficient separations. However, new developments in chiral particle technology let us predict an inversion of this trend. The market of chiral technology is already a very important one but it is expected to remarkably grow thanks to the new technology. In particular, extraordinary results and very fast enantioseparations are expected by the employment of latest generation chiral particles in SFC [58]. Moreover, chiral stationary phases made on SPPs could be suitable, thanks to their high efficiency, in the case of challenging enantiomeric separations (e.g., chiral impurity profiling), where an extremely low concentration of one enantiomer has to be detected [59].

Another field where chiral SPPs will find application is 2D-chromatography. Very short columns packed with SPPs can be efficiently used as second dimension for very fast separations in comprehensive applications [22].

Acknowledgements The authors thank Dr. Ercolina Bianchini of the University of Ferrara for technical support.

Compliance with Ethical Standards

Conflict of interests The authors declare that they have no conflict of interest.

References

1. Ismail OH, Catani M, Pasti L, Cavazzini A, Ciogli A, Villani C, et al. Experimental evidence of the kinetic performance achievable with columnspacked with new 1.9 μm fully porous particles of narrow particle size distribution. J Chromatogr A. 2016;1454:86–92.
2. Catani M, Ismail OH, Cavazzini A, Ciogli A, Villani C, Pasti L, et al. Rationale behind the optimum efficiency of columns packed with the new 1.9 μm fully porous particles of narrow particle size distribution. J Chromatogr A. 2016;1454:78–85.
3. Gritti F, Bell DS, Guiochon G. Particle size distribution and column efficiency. An ongoing debaterevived with 1.9 μm titan-C_{18} particles. J Chromatogr A. 2014;1355:179–92.
4. Fekete S, Guillarme D. Kinetic evaluation of new generation of column packed with 1.3 μm core-shell particles. J Chromatogr A. 2013;1308:104–13.
5. Neue UD. HPLC Columns: theory, technology and practice. Wiley-VCH. 1997.
6. Kirkland JJ, Langlois TJ. US Patent application 20070189944 a1. 2007.
7. Gritti F, Leonardis I, Shock D, Stevenson P, Shalliker A, Guiochon G. Performance of columns packed with the new shell particles, kinetex-C_{18}. J Chromatogr A. 2010;1217:1589–603.
8. Guiochon G, Gritti F. Shell particles, trials, tribulations and triumphs. J Chromatogr A. 2011;1218:1915–38.
9. Cavazzini A, Gritti F, Kaczmarski K, Marchetti N, Guiochon G. Mass-transfer kinetics in a shell packing materials for chromatography. Anal Chem. 2007;79:5972–79.
10. Horváth CG, Preiss BA, Lipsky SR. Fast liquid chromatogrpahy: an investigation of operating parameters and the separation of nucleotides on pellicular ion exchangers. Anal Chem. 1967;39:1422–28.
11. González-Ruiz V, Olives AI, Martín MA. Core-shell particles lead the way to renewing high-performance liquid chromatography. TrAC. 2015;64:17–28.
12. Guiochon G, Gritti F. Theoretical investigation of diffusion along columns packed with fully and superficially porous particles. J Chromatogr A. 2011;1218:3476–88.
13. van Deemter JJ, Zuiderweg FJ, Klinkenberg A. Longitudinal diffusion and resistance to mass transfer as causes of nonideality in chromatography. Chem Eng Sci. 1956;5:271–83.
14. Gritti F, Cavazzini A, Marchetti N, Guiochon G. Comparison between the efficiencies of columns packed with fully and partially porous C_{18}-bonded silica materials. J Chromatogr A. 2007;1157:289–303.
15. Daneyko A, Hlushkou D, Baranau V, Khirevic S, Seidel-Morgenstern A, Tallarek U. Computational investigation of longitudinal diffusion, eddy dispersion, and trans-particle mass transfer in bulk, random packings of core-shell particles with varied shell thickness and shell diffusion coefficient. J Chromatogr A. 2015;1407:139–56.
16. Catani M, Ismail OH, Gasparrini F, Antonelli M, Pasti L, Marchetti N, et al. Recent advancements and future directions of superficially porous chiral stationary phases for ultrafast high-performance enantioseparations. Analyst. 2017;142:555–66.
17. Gritti F, Leonardis I, Abia J, Guiochon G. Physical properties and structure of fine core-shell particles used as packing materials for chromatography. Relationship between particle characteristics and column performance. J Chromatogr A. 2010;1217:3819–43.
18. Preti R. Core-shell columns in high-performance liquid chromatography: food analysis applications. International Journal of Analytical Chemistry. 2016;2016:1–9.
19. Gritti F, Guiochon G. Speed-resolution properties of columns packed with new 4.6 μm kinetex-C_{18} core-shell particles. J Chromatogr A. 2013;1280:35–50.
20. Oláh E, Fekete S, Fekete J, Ganzler K. Comparative study of new shell-type, sub-2 μm fully porous and monolith stationary phases, focusing on mass transfer resistance. J Chromatogr A. 2010;1217:3642–53.
21. Hayes R, Ahmed A, Edge T, Zhang H. Core-shell particles: preparation, fundamentals and applications in high performance liquid chromatography. J Chromatogr A. 2014;1357:36–52.

22. Jandera P, Hàjek T, Staňkovà M. Monolithic and core-shell columns in comprehensive two-dimensional HPLC: a review. Anal Bioanal Chem. 2016;407:139–51.
23. Marchetti N, Guiochon G. High peak capacity separations of peptides in reversed-phase gradient elution liquid chromatography on columns packed with porous shell particles. J Chromatogr A. 2007;1176:206–16.
24. Marchetti N, Guiochon JNFG. High peak capacity separations of peptides in reversed-phase gradient elution liquid chromatography on columns packed with porous shell particles. Anal Chem. 2008;80:2756–67.
25. Ismail OH, Pasti L, Ciogli A, Villani C, Kocergin J, Anderson S, et al. Pirkle-type chiral stationary phase on core–shell and fully porousparticles: are superficially porous particles always the better choice toward ultrafast high-performance enantioseparations? J Chromatogr A. 2016;1466:96–104.
26. Ismail OH, Antonelli M, Ciogli A, Villani C, Cavazzini A, Catani M, et al. Future perspectives in high efficient and ultrafast chiral liquid chromatography through zwitterionic teicoplanin-based 2-μm superficially porous particles. J Chromatogr A. 1520;2017:91–102.
27. Patel DC, Wahab MF, Armstrong DW, Breitbach ZS. Salient sub-second separations. Anal Chem. 2016;88:8821–26.
28. Patel DC, Breitbach ZS, Wahab MF, Barhate CL, Armstrong DW. Gone in seconds: praxis, performance and peculiarities of ultrafast chiral liquid chromatography with superficially porous particles. Anal Chem. 2015;87:9137–48.
29. Thurmann S, Lotter C, Heiland JJ, Chankvetadze B, Belder D. Chip-based high-performance liquid chromatography for high-speed enantioseparations. Anal Chem. 2015;87:5568–76.
30. Wei TC, Mack A, Chen W, Liu J, Dittmann M, Wang X, et al. Synthesis, characterization and evaluation of a superficially porous particle with unique, elongated pore channels normal to the surface. J Chromatogr A. 2016;1440:55–65.
31. Deridder S, Catani M, Cavazzini A, Desmet G. A theorethical study on the advantage of core-shell particles with radially-oriented mesopores. J Chromatogr A. 2016;1456:137–44.
32. Blue LE, Jorgenson JW. 1.1 μm superficially porous particles for liquid chromatography. Part I: synthesis and particle structure characterization. J Chromatogr A. 2011;1218:7989–95.
33. Blue LE, Jorgenson JW. 1.1 μm superficially porous particles for liquid chromatography. Part II: column packing and chromatographic performance. J Chromatogr A. 2015;1380:71–80.
34. Cavazzini A, Pasti L, Massi A, Marchetti N, Dondi F. Recent applications in chiral high performance liquid chromatography: a review. Anal Chim Acta. 2011;706:205–22.
35. Reischl RJ, Hartmanova L, Carrozzo M, Huszar M, Frühauf P, Lindner W. Chemoselective and enantioselective analysis of proteinogenic ammino acids utilizing N-derivatization and 1-D enantioselective anion-exchange chromatography in combination with tandem mass spectrometry. J Chromatogr A. 2011;1218:8379–87.
36. Lai X, Tang W, Ng SC. Novel cyclodextrin chiral stationary phases for high performance liquid chromatography enantioseparation: Effect of cyclodextrin type. J Chromatogr A. 2011;1218:5597–601.
37. Cancelliere G, Ciogli A, D'Acquarica I, Gasparrini F, Kocergin J, Misiti D, et al. Transition from enantioselective high performance to ultra-high performance liquid chromatography: a case study of a brush-type chiral stationary phase based on sub-5-micron to sub-2-micron silica particles. J Chromatogr A. 2010;1217:990–9.
38. Cavazzini A, Marchetti N, Guzzinati R, Pierini M, Ciogli A, Kotoni D, et al. Enantioseparation by ultra-high-performance liquid chromatography. TrAC. 2014;63:95–103.
39. Lomsadze K, Jibuti G, Farkas T, Chankvetadze B. Comparative high-performance liquid chromatography enantioseparations on polysaccharide based chiral stationary phases prepared by coating totally porous and core-shell silica particles. J Chromatogr A. 2012;1234:50–55.
40. Kharaishvili Q, Jibuti G, Farkas T, Chankvetadze B. Further proof to the utility of polysaccharide-based chiral selectors in combination with superficially porous silica particles as effective chiral stationary phases for separation of enantiomers in high-performance liquid chromatography. J Chromatogr A. 2016;1467:163–8.
41. Spudeit DA, Dolzan MD, Breitbach ZS, Barber WE, Micke GA, Armstrong DW. Superficially porous particles vs. fully porous particles for bonded high performance liquid chromatography chiral stationary phases: isopropyl cyclofructan 6. J Chromatogr A. 2014;1363:89–95.
42. Barhate CL, Breitbach ZS, Pinto EC, Regalado EL, Welch CJ, Armstrong DW. Ultrafast separation of fluorinated and desfluorinated pharmaceuticals using highly efficient and selective chiral selectors bonded to superficially porous particles. J Chromatogr A. 2015;1426:241–7.
43. Patel DC, Wahab MF, Armstrong DW, Breitbach ZS. Advances in high-throughput and high-efficiency chiral liquid chromatographic separations. J Chromatogr A. 2016;1467:2–18.
44. Patel DC, Wahab MF, Armstrong DW, Breitbach ZS. Superficially porous particles vs. fully porous particles for bonded high performance liquid chromatographic chiral stationary phases: isopropyl cyclofructan 6. J Chromatogr A. 2014;1365:124–30.
45. Wimalasinghe RM, Weatherly CA, Breitbach ZS, Armstrong DW. Hydroxypropyl beta cyclodextrin bonded superficially porous particlebased HILIC stationary phases. J Liq Chromatogr Rel Tech. 2016;39:459–64.
46. Patel DC, Breitbach ZS, Yu J, Nguyen KA, Armstrong DW. Quinine bonded to superficially porous particles for high-efficiency and ultrafast liquid and supercritical fluid chromatography. Anal Chim Acta. 2017;963:164–74.
47. Pasti L, Marchetti N, Guzzinati R, Catani M, Bosi V, Dondi F, et al. Microscopic models of liquid chromatography: from ensemble-averaged information to resolution of fundamental viewpoint at single-molecule level. TrAC. 2016;81:63–68.
48. Dondi F, Cavazzini A, Remelli M. The stochastic theory of chromatography. Adv Chromatogr. 1998;38:51–74.
49. Bruns S, Franklin EG, Grinias JP, Godinho JM, Jorgenson JW, Tallarek U. Slurry concentration effects on the bed morphology and separation efficiency of capillaries packed with sub-2 μm particles. J Chromatogr A. 2013;1318:189–97.
50. Wahab MF, Patel DC, Wimalasinghe RM, Armstrong DW. Fundamental and practical insights on the packing of modern high-efficiency analytical and capillary columns. Anal Chem. 2017;89:8177–91.
51. Gritti F, Guiochon G. Mass transfer mechanism in chiral reversed phase liquid chromatography. J Chromatogr A. 2014;1332:35–45.
52. Gritti F. Impact of straight, unconnected, radially-oriented, and tapered mesopores on column efficiency: a theoretical investigation. J Chromatogr A. 1485;2017:70–81.
53. Fekete S, Ganzler K, Fekete J. Efficiency of the new sub-2 μm core-shell (Kinetex^{TM}) column in practice, applied for small and large molecule separation. J Pharm Biomed Anal. 2011;54:482–90.
54. Omamogho JO, Hanrahan JP, Tobin J, Glennon JD. Structural variation of solid core and thickness of porous shell of 1.7 μm core–shell silica particles on chromatographic performance: narrow bore columns. J Chromatogr A. 2011;1218:1942–53.

55. Gritti F, Guiochon G. Mass transfer resistance in narrow-bore columns packed with 1.7 μm particles in very high pressure liquid chromatography. J Chromatogr A. 2010;1217:5069–83.
56. Sanchez AC, Friedlander G, Fekete S, Anspach J, Guillarme D, Chitty M, et al. Pushing the performance limits of reversed-phase ultra high performance liquid chromatography with 1.3 μm core-shell particles. J Chromatogr A. 2013;1311:90–97.
57. Broeckhoven K, Desmet G. The future of UHPLC: towards higher pressure and/or smaller particles? TrAC. 2014;63:65–75.
58. Sciascera L, Ismail OH, Ciogli A, Kotoni D, Cavazzini A, Botta L, et al. Expanding the potential of chiral chromatography for high-throughput screening of large compound libraries by means of sub-2 μm Whelk-O 1 stationary phase in supercritical fluid conditions. J Chromatogr A. 2015;1383:160–8.
59. Mazzoccanti G, Ismail OH, D'Acquarica I, Vilani C, Manzo C, Wilcox M, et al. Cannabis through the looking glass: chemo- and enantio-selective separation of phytocannabinoids by enantioselective ultra high performance supercritical fluid chromatography. Chem Commun. 2017;53:12262–5.

Paper IV

molecules

MDPI

Article

The Way to Ultrafast, High-Throughput Enantioseparations of Bioactive Compounds in Liquid and Supercritical Fluid Chromatography

Omar H. Ismail [1], Simona Felletti [2], Chiara De Luca [2], Luisa Pasti [2], Nicola Marchetti [2], Valentina Costa [2], Francesco Gasparrini [1], Alberto Cavazzini [2] and Martina Catani [2,*]

[1] Department of Drug Chemistry and Technology, "Sapienza" University of Rome, P. le Aldo Moro 5, 00185 Rome, Italy; omar.ismail@uniroma1.it (O.H.I.); francesco.gasparrini@uniroma1.it (F.G.)

[2] Department of Chemistry and Pharmaceutical Sciences, University of Ferrara, via L. Borsari 46, 44121 Ferrara, Italy; simona.felletti@unife.it (S.F.); chiara.deluca@unife.it (C.D.L.); psu@unife.it (L.P.); nicola.marchetti@unife.it (N.M.); valentina.costa@unife.it (V.C.); cvz@unife.it (A.C.)

* Correspondence: ctnmtn@unife.it; Tel.: +39-0532-455389

Received: 2 October 2018; Accepted: 17 October 2018; Published: 20 October 2018

Abstract: Until less than 10 years ago, chiral separations were carried out with columns packed with 5 or 3 μm fully porous particles (FPPs). Times to resolve enantiomeric mixtures were easily larger than 30 min, or so. Pushed especially by stringent requirements from medicinal and pharmaceutical industries, during the last years the field of chiral separations by liquid chromatography has undergone what can be defined a "true revolution". With the purpose of developing ever faster and efficient method of separations, indeed, very efficient particle formats, such as superficially porous particles (SPPs) or sub-2 μm FPPs, have been functionalized with chiral selectors and employed in ultrafast applications. Thanks to the use of short column (1–2 cm long), packed with these extremely efficient chiral stationary phases (CSPs), operated at very high flow rates (5–8 mL/min), resolution of racemates could be accomplished in very short time, in many cases less than 1 s in normal-, reversed-phase and HILIC conditions. These CSPs have been found to be particularly promising also to carry out high-throughput separations under supercritical fluid chromatography (SFC) conditions. The most important results that have been recently achieved in terms of ultrafast, high-throughput enantioseparations both in liquid and supercritical fluid chromatography with particular attention to the very important field of bioactive chiral compounds will be reviewed in this manuscript. Attention will be focused not only on the latest introduced CSPs and their applications, but also on instrumental modifications which are required in some cases in order to fully exploit the intrinsic potential of new generation chiral columns.

Keywords: ultra-high performance liquid chromatography (UHPLC); supercritical fluid chromatography (SFC); ultrafast enantioseparations; bioactive chiral compounds

1. Introduction

Separation of chiral compounds has always been one of the most challenging applications of liquid chromatography (LC). Since enantiomers have the same chemo-physical properties, conventional approaches used to separate achiral molecules cannot be adopted for chiral separations. For this reason, for over thirty years, research activities in the field of LC enantioseparations have been essentially focused on the development of novel chiral stationary phases (CSPs), able to resolve the largest number of enantiomeric pairs. Different CSPs have been, thus, developed by functionalizing 3 or 5 μm fully porous particles (FPPs) with different chiral selectors including polysaccharides, macrocyclic glycopeptides, Pirkle-type ones, ion-exchangers, cyclofructans [1]. However, during the last ten years the attention of scientists has been moved from the research for ever better enantioselectivity to the

efficiency of enantioseparations and, most importantly, speed factors [2,3]. This change of direction has been essentially driven by pressing requirements from medicinal and pharmaceutical industries for the development of faster and more efficient methods. Indeed, elution of enantiomers from chiral columns packed with 3 or 5 μm FPPs typically requires 5 to 30 min at least. Since chiral separations are fundamental in many stages of drug development (i.e., high-throughput screenings of large libraries of chiral molecules, monitoring steps), it follows that they could represent a time-consuming and limiting step of the production process, if too slow.

In the last few years, technological progress in materials and particle manufacturing has allowed to introduce, in chiral chromatography, very efficient particle formats, such as sub-2 μm FPPs and second-generation superficially porous particles (SPPs), routinely used as stationary phases for achiral reversed-phase (RP) C_{18} columns. At early stages, improvements in preparation of CSPs have been limited for many years essentially by the following reasons: (i) the complex adaptation of surface modification methods from larger to smaller particles; (ii) the tendency of small particles to aggregation during chemical modification; (iii) low mechanical resistance and stability of small particles functionalized with chiral selectors when operated at high flow rates/pressures; (iv) the lack of fundamental studies in chiral LC [4].

The introduction of packed columns made of new generation particles has represented the most important innovation in the field of chiral LC, allowing to reach efficiencies comparable to those typical of RP achiral separations (in the order of 300,000 plates/m) [5–7]. Thanks to the very good kinetic performance of these particles, it is possible to increase the flow rate without remarkable loss of efficiency, opening the way to fast (or ultrafast) high-throughput enantioseparations.

The first report on the use of sub-2 μm FPPs in chiral LC was published in 2010 by Gasparrini and coworkers [8–11]. They packed columns with 1.9 μm FPPs functionalized with a Pirkle-type chiral selector that allowed to obtain the separation of different pairs of enantiomers in a range of 15–40 s. In 2011, Lindner and coworkers prepared the first CSP by using second-generation SPPs functionalized with a weak anion exchanger chiral selector [12]. During the following year, Chankvetadze et al. published the first work in which sub-2 μm FPPs and sub-3 μm SPPs, functionalized with the same polysaccharide chiral selector, were compared [13]. The most comprehensive work aimed at investigating kinetic performance of columns packed with both sub-2 μm FPPs and second-generation SPPs is that by Armstrong's group. They compared CSPs based on different chiral selectors (i.e., polysaccharides, cyclofructans, macrocyclic glycopeptides) operated in different chromatographic modes, including RP, hydrophilic interaction chromatography (HILIC), polar organic mode (POM) [2,14–18]. Results of these investigations have shown that chiral SPPs outperform their FP counterparts in every chromatographic mode. Following these authors, the reasons behind the better performance of chiral SPPs are the same as those already extensively demonstrated for achiral hydrophobic SPPs [19], namely a reduced longitudinal diffusion, smaller solid-liquid mass transfer resistance and better packing quality (hence, smaller eddy dispersion).

Even though it is true that SPPs, due to their geometrical characteristics, allow for the reduction of all those effects associated with diffusion inside particles, the same concepts cannot be taken for granted in chiral chromatography. By comparing columns packed with FPPs (2.5 and 1.8 μm) and SPPs (2.6 μm) functionalized with Whelk-O1 chiral selector operated in normal phase mode, for instance, some of the authors of this work found that, unexpectedly, the column packed with the latter CSP provide worse kinetic performance than FPP ones [6]. This has been related essentially to two main reasons [4]. The first one is an higher contribution of eddy dispersion, most likely coming from some difficulties encountered during the packing process of chiral SPPs. This suggests that slurry packing polar SPPs (such as chiral ones) could be more difficult than for hydrophobic ones for which, on the other hand, it has been largely demonstrated a smaller contribution of eddy diffusion if compared to FP counterparts. Another important point is that in chiral chromatography an additional source of band broadening must be considered, that is adsorption-desorption kinetics. This term is usually neglected in achiral RP separations (except in the case of large proteins) since kinetics is very

fast. Oppositely, it can be one of the main factors contributing to poor kinetic performance in chiral chromatography [20,21]. In particular, the authors suggests the importance of a deeper investigation of the impact of bonding density of chiral selector, base silica characteristics, surface heterogeneity, etc. on the adsorption-desorption kinetics [4,22,23].

However, development in column technology, on the one hand, and instrumental design, on the other, have permitted to decrease analysis time in chiral chromatography from tenths of minute to less than one second (ultrafast enantioseparations). The key point has been to pack columns of very short length (5–20 mm long) with these new generation CSPs (be either SPPs or sub-2 μm FPPs) and operate them at the highest flow rate achievable by state-of-the-art equipments.

The scope is this review is to give an overview of the evolution of chiral chromatography towards ultrafast enantioseparations of chiral bioactive molecules in the last three years. Not only the recent achievements in the field of LC will be reviewed but also those obtained in supercritical fluid chromatography (SFC), where new generation CSPs have been more recently introduced. Particular attention will be also focused on instrumental modifications required on chromatographic equipments in order to fully exploit the intrinsic potential of new generation chiral columns.

2. Theory Background

Separation efficiency is conventionally evaluated in terms of number of theoretical plates, N, or plate height, H:

$$H = \frac{L}{N} \tag{1}$$

being L the length of the column. The smaller H (higher N), the higher the efficiency.

In order to compare the efficiency of columns packed with different particle geometries, instead of H, its adimensional quantity, the reduced plate height, h, can be used. h is defined as follows:

$$h = \frac{H}{d_p} \tag{2}$$

being d_p the mean diameter of the particles forming the packed bed. Since inside particle there is absence of flow, the right velocity to refer to, when evaluating kinetic performance, is the interstitial velocity, u_e:

$$u_e = \frac{F_v}{\pi r_c^2 \epsilon_e} \tag{3}$$

where F_v is the flow rate, r_c the radius of the column and ϵ_e the interstial porosity (referred only to the portion of column where there is effectively flow). The adimensional quantity used to express mobile phase velocity is the reduced velocity, ν:

$$\nu = \frac{u_e d_p}{D_m} \tag{4}$$

where D_m is the molecular diffusion coefficient of the analyte in the bulk mobile phase. h and ν are correlated by means of the well known van Deemter equation:

$$h = a(\nu) + \frac{b}{\nu} + c_s\nu + c_{ads}\nu + h_{extra} + h_{heat} \tag{5}$$

where $a(\nu)$ represents the contribution to band broadening of eddy dispersion, b is the longitudinal diffusion, c_s the solid-liquid mass transfer resistance, c_{ads} the adsorption-desorption kinetics, h_{extra} extra-column band broadening and h_{heat} an additional source of band spreading due to frictional heating effects between the eluent at high flow velocity and packed beds made of very fine particles (such as sub-2 μm FPPs).

One of the main approaches used to increase column efficiency is to reduce particle diameter since H is proportional to $2d_p$. However, the main drawback of the use of such fine particles is that significant backpressure can be generated by the packed bed even at moderate flow rates, so that columns packed with these particles can be only used on Ultra-High Performance (or Pressure) Liquid Chromatography (UHPLC) instruments able to reach up to 1200–1500 bars. In 2006 SPPs have been introduced. The presence of the solid core reduces the volume accessible for analytes to diffuse inside the particle. As a consequence, it has been demonstrated that columns packed with sub-3 μm SPPs produce, at least in achiral RPLC, efficiencies comparable to those of sub-2 μm FPPs but at significantly lower backpressure [4,24–27]. However, mass transfer contributions in chiral chromatography have been barely investigated before, mainly due to the complexity of estimation of each band broadening contributions. Deeper studies are especially needed in order to quantify the effect of c_{ads} on column efficiency [4].

3. Recent Achievements in Ultrafast, High-Throughput UHPLC Enantioseparations

In this section the most important results in terms of ultrafast, high-throughput enantioseparations obtained in UHPLC conditions will be discussed. For the sake of simplicity, applications have been divided according to the type of particle used.

3.1. CSPs Based on FPPs

As mentioned before, the first example of new generation CSPs has been developed by Gasparrini and co-workers by bonding a Pirkle-type chiral selector to sub-2 μm FPPs [8]. The choice of this class of chiral selector to start the transition from enantioselective HPLC to UHPLC finds its rationale on the ease of functionalization of even small particles (absence of particle aggregation and clogging during their synthesis) and on the supposed fast mass transfer kinetics properties of CSPs based on this class of selectors [11,28].

The same group has obtained the enantioseparation of *trans*-stilbene oxide enantiomers in 0.9 s on a 10 × 3.0 mm (L × I.D.) column packed with 1.8 μm FPPs functionalized with a Pirkle-type (more specifically, Whelk-O1) chiral selector. Flow rate was set at the maximum value deliverable by the equipment (8 mL/min) [6].

Barhate et al. found efficiencies up to 210,000 N/m with columns packed with 1.9 μm Titan® particles characterized by a narrow particle size distribution (nPSD), with a reative standard deviation smaller than 10%, functionalized with teicoplanin, teicoplanin aglycone and vancomycin. They were able to separate different classes of bioactive chiral compounds including aminoacids, β-blockers and pharmaceuticals with analysis time in some cases smaller than 40 s on 50 × 4.6 mm (L × I.D.) columns (see Figure 1) [29].

Ismail et al. recently employed a proprietary bonding protocol to obtain the zwitterionic version of teicoplanin and vancomycin CSPs bonded to 1.9 μm Titan® FPPs [30]. Thanks to the zwitterionic character of these phases, chiral Active Pharmaceutical Ingredients (APIs) have been separated from inorganic anions, which are usually unretained or even excluded from traditional versions of macrocyclic glycopeptide CSPs, due to electrostatic repulsion. Moreover, the same authors obtained the separation of Haloxyfop enantiomers in 4 s (F_v = 8 mL/min) on a 20 × 4.6 mm (L × I.D.) column packed with the 1.9 μm FPPs zwitterionic teicoplanin CSP [5]. The introduction of these particles has rekindled the debate about the possible correlation between column efficiency and PSD. Until 1970's, common belief was that, unless PSD is larger than 40%, its influence on column performance is negligible [31–34]. More recently, some authors found that PSD has an effect on column efficiency as long as its RSD ranges from 5% to 20% [35,36]. As a marginal remark, excellent kinetic performance (h_{min} = 1.7 corresponding to an efficiency of 300,000 N/m) has been also observed for the separation of achiral compounds on columns packed with C_{18} Titan® particles [6,7,37,38].

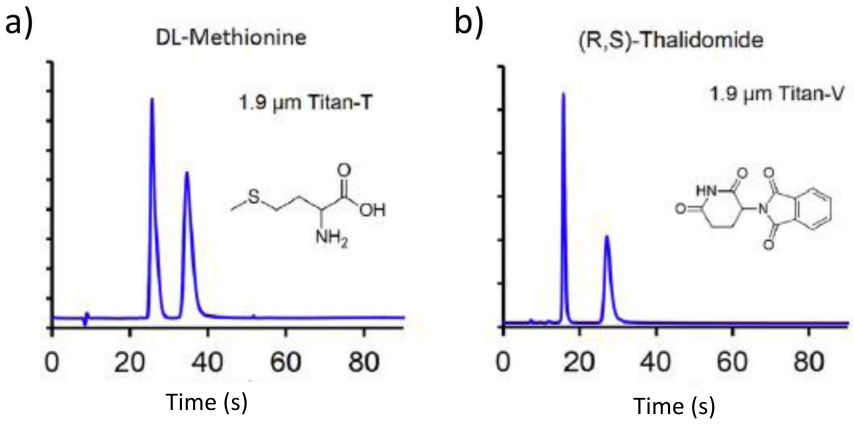

Figure 1. Examples of fast separations on 50 × 4.6 mm (L × I.D.) columns packed with nPSD 1.9 µm FPP CSP. (**a**) chiral selector: teicoplanin, compound: DL-methionine, mobile phase: water/methanol 30%:70% (*v*/*v*), F_v = 2 mL/min; (**b**) chiral selector: vancomycin, compound: (*R*, *S*)-thalidomide, mobile phase: 100% methanol, F_v = 3 mL/min. Modified with permission from reference [29].

The growing interest in high-throughput analysis has led to the development of solutions able to overcome the instrumental limitation imposed by autosamplers, whose typical injection cycle time is 20 s or even more. One of the most used approaches is MISER (Multiple Injections in a Single Experimental Run), whcih allows not only to reduce analysis times but also to produce a repetitive chromatogram that facilitates the interpretation of results when large number of samples must be analyzed. A 5 × 4.6 mm (L × I.D.) column packed with 1.9 µm nPSD particles functionalized with vancomycin chiral selector has been used for the MISER analysis of enantiopurity of the drug thalidomide with injection cycle time of only 10.5 s. This approach can be used for the analysis of an entire microwell plate in very short times [39].

Columns packed with sub-2 µm chiral FPPs have been demonstrated to be suitable for the use as second dimension for 2D achiral × chiral separations. Due to the slowness of elution, the employment of chiral columns for this type of analysis has always been very limited in the past. On the other hand, Barhate et al. excellently employed a 50 × 4.6 mm (L × I.D.) column packed with 1.9 µm teicoplanin FPPs for the baseline resolution of two isomers coeluting in the first achiral dimension [40].

Remarkably, some authors have also obtained very fast separations with FPPs with dimensions higher than sub-2 µm. Khundadze et al. were able to separate chiral sulfoxide derivatives in less than 3 s (F_v = 4.5 mL/min) on a 10 × 2.0 mm packed with 3 µm phenylhexyl FPPs to which a cellulose derivative was bonded. In this specific case, temperature was increased up to 70 °C in order to improve mass transfer and decrease retention times of the second eluted enantiomer [41].

A 5 µm FPP cellulose-based CSP was packed into the first example of microfluidic pressure-driven separation device that allowed the separation of different racemic mixtures, including also pharmaceuticals such as fluvastatin and rimadyl extract, under different chromatographic conditions. Very short separation times down to 5 s were achieved with reduced plate of about 2.2 on a 12 mm long channel [42].

3.2. CSPs Based on SPPs

The most comprehensive works aimed at evaluating the potential of sub-3 µm SPPs towards ultrafast, high-throughput enantioseparations are those published by Armstrong's group. In a first report of 2015, they functionalized 2.7 µm SPPs with different chiral selectors (including teicoplanin, cyclofructans and cyclodextrins). These CSPs were then packed into columns of 50 or 100 mm length and operated under different chromatographic modes (i.e., RP, HILIC and polar organic mode to name but a few) to separate 60 pairs of enantiomers. Separations in the range of 4–40 s have been obtained [2].

Moreover, the same CSPs have been used to separate fluorinated APIs from their desfluoro analogs with analysis times smaller than 55 s in both reversed phase and polar organic mode [15].

Fast separations (under 1.5 s) of chiral sulfoxides have been obtained by Chankvetadze's group by using a 20 × 2.0 mm (L × I.D.) column packed with 2.6 μm SPPs functionalized with a cellulose derivative [41].

Analysis times have been recently further decreased under the second time scale and examples of ultrafast enantioseparations using sub-3 μm SPPs have been reported by different authors. *Trans*-stilbene oxide enantiomers have been separated in 0.82 s (F_v = 8 mL/min) on a 10 × 3.0 mm (L × I.D.) column packed with Whelk-O1 2.6 μm SPPs by our research group [4]. Sub-second separations (F_v = 7.5 mL/min) of lorazepam and oxazepam enantiomers have been obtained by Armstrong and coworkers on a 10 × 3.0 mm (L × I.D.) column packed with 2.7 μm SPPs [43]. The same research group reported also on the enantioseparation of different biologically active compounds on 5 mm columns packed with 2.7 μm SPPs CSPs. Analysis times as low as 0.66 s have been obtained with a flow rate of 5 mL/min [17].

Columns packed with 2.7 μm SPPs functionalized with teicoplanin have been demonstrated to be suitable for the enantiopurity analysis of the entire verubecestat route [18]. Verubecestat is used in the treatment of Alzheimer's disease. The analytical technical package of validated methods currently in use to evaluate the enantiomeric excess during its production requires two separation modes (both LC and SFC), five different chiral columns and four different mobile phases. Barhate et al. developed an alternative method in which analysis are performed only in RPLC mode. The enantiopurity of all intermediates was assessed by using a 2.7 μm teicoplanin SPPs CSP while another macrocyclic glycopeptide column made on the same particle format was found to be the most suitable for the analysis of the final API. This new approach, requiring only two chiral columns and mobile phases on a conventional HPLC system, simplifies the transfer to manufacturing facilities, significantly reducing waste of time.

A 100 × 4.6 mm (L × I.D.) column packed with a novel CSP based on 2.7 μm SPPs functionalized with hydroxypropyl β-cyclodextrins was used to separate five β-blockers (carvedilol, alprenolol, acebutolol,nadolol and atenolol) in less than 1 min (F_v = 1 mL/min) under HILIC conditions [44].

The same CSP packed into a 30 × 4.6 mm (L × I.D.) column was used for achiral × chiral 2D separations [40]. The use of a fast (separation times in the range of 26–52 s) and efficient chiral column as second dimension allowed to perform multiple heart-cutting analysis of fluorophenylacetic acid isomers (see Figure 2). This technique is different from the common comprehensive 2D-LC, where the entire first dimension is injected into the second one. In multiple heart-cutting mode only few selected portions of the first dimension chromatogram are cut and analysed in the second dimension. Each cut is stored into a loop system while waiting for the second dimension to be available for the next injection. This approach has been also employed by Lämmerhofer's group in ref. [45] with an ion exchange chiral column made on 2.7 μm SPPs as second dimension to analyze 25 amino acids (20 of which were proteinogenic) in a single run with 130 min total run time.

The same group recently developed a chiral × chiral 2D-LC method based on two columns packed with 2.7 μm SPPs functionalized with the same chiral selector but with different configuration (quinine and quinidine carbamates) [46]. By means of this approach, highly ordered chromatograms can be obtained that can be used to get important information about the stereochemistry of peptides or unknown complex samples (such as nonribosomal peptides and therapeutic proteins) during pharmaceutical development or impurity analysis.

Thanks to the improvements in particle manufacturing and technology, the reduction of particle size to favour higher efficiencies and faster separations has been sought also with SPPs. Very high efficiencies can be achievable with packed beds made of SPPs with diameter smaller than 2.6–2.7 μm at the cost of increased backpressure. In literature there are only few reports on the use of small SPPs in chiral chromatography, however it is expected that the number of papers will increase in the next future. Ismail et al. reported on the use of 2.0 μm SPPs functionalized with teicoplanin and

operated in HILIC mode [5]. They were able to obtain the enantioseparation of haloxyfop enantiomers in 3.4 s (F_v = 8 mL/min) with very high efficiencies ($h_{min} \simeq 1.7$) on a 20 × 4.6 mm (L × I.D.) column packed with the novel teicoplanin CSP. Patel et al. performed ultrafast enantioseparations of different compounds on a 10 × 3.0 mm (L × I.D.) column packed with 1.9 µm SPPs functionalized with quinine. The simultaneous separation of DNB-phenylglycine and 2-phenylpropionic acid enantiomers has been obtained in less than 1 s (F_v = 7.85 mL/min) [43]. Even smaller SPPs (1.5 µm diameter) functionalized with teicoplanin have been used by Min et al. for the enantioseparation of different pairs of amino acids achieving high resolution and selectivity [47]. For instance, norvaline enantiomers were separated with a resolution factor of 4 and a selectivity higher than 9.

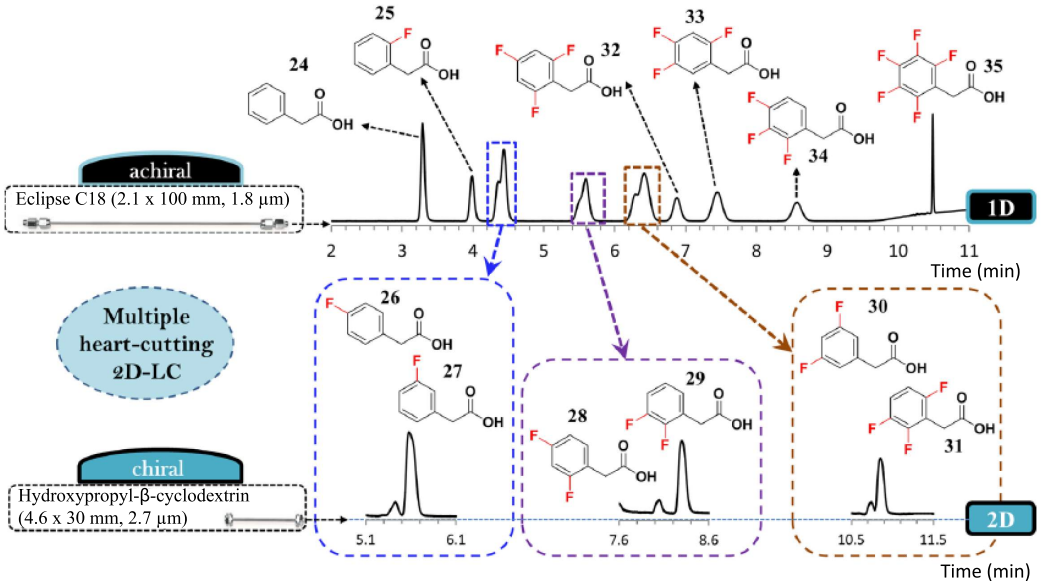

Figure 2. Multiple heart-cutting 2D-LC method for separation of a complex mixture of fluorophenylacetic acid isomers. Flow rates employed were F_v = 0.5 mL/min for the first achiral dimension and 1 mL/min for the second chiral one. Modified with permission from ref. [40].

3.3. Instrumental Limitations

When working with ultrafast, high efficiency enantioseparations, important disadvantages could come from instrumental limitations. The extra-column variance of the equipment must be reduced by using short and narrow tubings, low-volume detector cells (2–3 µL) and ultra-low dispersion injectors. Another important aspect to be considered is the speed of autosamplers. 15–20 s injection cycle times can represent an obstacles for high-troughput separations [3]. Due to increasing number of applications in which separation times are in the order of few seconds, new, faster autosampler need to be designed.

Also sampling frequency of diode array detectors is another parameter that needs to be optimized. If it is not appropriate, many signals might be lost. According to a recent study published by Wahab et al. [17], the maximum sampling frequency achievable on current instrumentations is high enough for commercially available high efficiency columns. However, due to the continuous improvements in design of new materials for ultrafast chromatography, it is predictable that higher sampling rates might be shortly required [48].

4. Advances in Ultrafast, High-Throughput SFC Enantioseparations

SFC has been largely used in the past for the purification of chiral compounds, due to its green character, versatility and ease of removal of carbon dioxide (CO_2) from collected fractions. However, less than ten years ago, thanks to the introduction of latest generation SFC equipments and

the improvement in particle technology, the attention of scientists has been moved towards the use of SFC for analytical purposes. In particular, thanks to the unique properties of supercritical fluid CO_2, SFC allows to run faster separations than in LC without remarkable loss of efficiency and with reduced backpressure. For these reasons, SFC seems to be a promising technique in the field of high speed enantioseparations [49].

Different examples of sub-minute separations of different chiral pharmaceuticals (including chlortalidone and 5-methyl-5-phenylhydantoin) have been performed by Barhate et al. by using 50 × 4.6 mm (L × I.D.) columns packed with nPSD 1.9 µm FPPs functionalized with teicoplanin and teicoplanin aglycone [29]. Also some of the authors of this work reported on remarkable results in terms of fast separations in SFC by using both teicoplanin 1.9 µm Titan® FPPs and Whelk-O1 1.8 µm FPPs packed into 20 and 50 × 4.6 (L × I.D.) columns, respectively [50,51]. The latter column has also been excellently used for the screening of a large library of compounds (including antidepressant, *β*-blockers and antibiotics, see Figure 3) under fast gradient elution conditions (total analysis time 9 min, including column re-equilibration) with a score of 63% positively resolved couples of enantiomers [51].

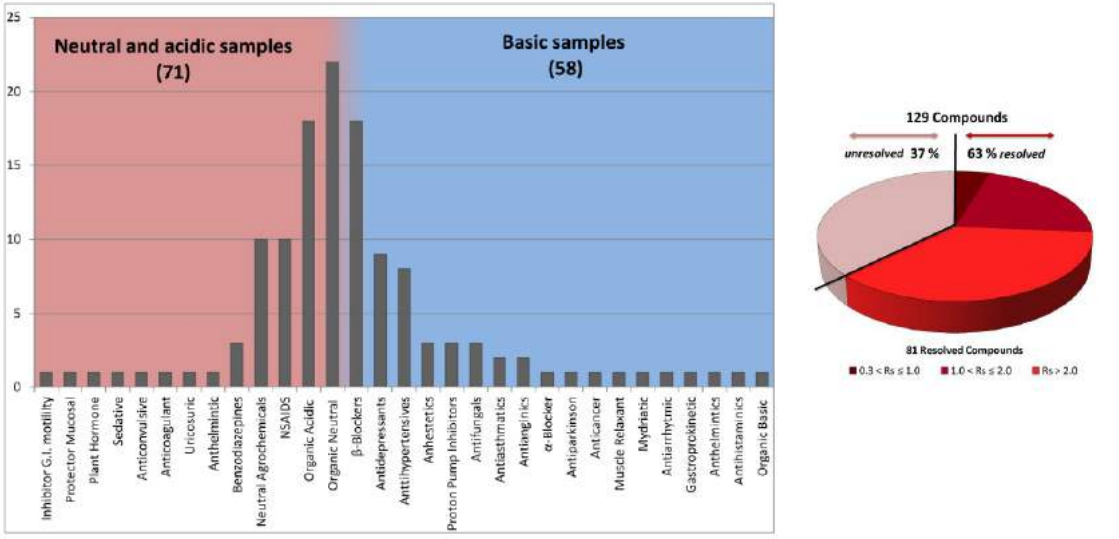

Figure 3. Classification of the different molecules analyzed during fast gradient screening (left); pie chart reporting numerical proportion of resolved enantiomers with different resolution values ($R_s = 2(t_{R,2} - t_{R,1})/(w_{0.5,2} + w_{0.5,1})$, being t_R retention time and $w_{0.5}$ peak width at half height. Modified with permission from ref. [51].

Even faster separations have been obtained by Armstrong's group by running separations of different amino acids at a flow rate of 20 mL/min on a 30 × 4.6 mm (L × I.D.) column packed with 2.7 µm SPPs. Elution times in the range of 6–8 s have been observed [52].

Instrumental Limitations

The achievement of ultrafast, high efficiency enantioseparations in SFC is currently limited by the excessively large extra-column volume of state-of-the-art SFC equipments. Technological advancements in SFC instrumentation have been much slower with respect to what happened in LC.

Different authors have demonstrated that tremendous improvements in column efficiency could be achieved by properly optimizing the plumbing of commercially available SFC equipments. Berger firstly went through this issue by replacing tubings (170 µm ID) and flow cell (13 µL internal volume) with 120 µm I.D. tubings of shortest possible length and a 2 µL internal volume cell. With this setup, the extra-column variance was reduced up to 6–9 μL^2 and fast enantioseparations (up to less than 8 s, see Figure 4) of different pharmaceuticals have been obtained with 50 mm long columns

packed with both Whelk-O1 1.8 µm FPPs and amylose-based 1.6 µm FPPs, with efficiencies as high as 280,000 N/m [53,54].

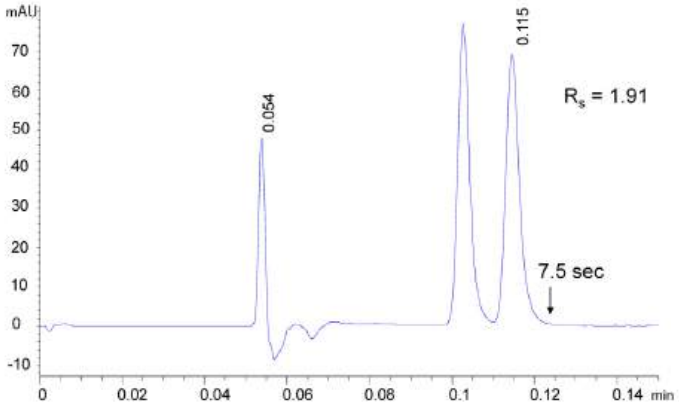

Figure 4. Fast SFC separation of *trans*-stilbene oxide enantiomers on a 50 × 3.0 mm (L × I.D.) column packed with 1.6 µm FPPs functionalized with amylose, F_v = 4.65 mL/min, mobile phase: CO_2/methanol 70%:30% (*v*/*v*), 40 °C. Reproduced with permission from ref. [54].

More recently, Ismail et al. performed a series of technical adjustments on a commercial SFC instrument (of a different brand from that used by Berger) by replacing (i) tubings with narrower capillaries; (ii) the 8 µL flow cell with a 3 µL one; (iii) the injector with a 200 nL fixed-loop external one and (iv) the column oven with a in-house designed one. The latter adjustment, in particular, was crucial for the reduction of the extra-column variance by more than 97% (from 85 to slightly more than 2 μL^2, measured at 2 mL/min) from the as-shipped configuration to the optimized one [55]. This has been possible thanks to the presence at even low flow rates (1.5–4 mL/min) of fully-developed turbulent flow regime inside capillaries of proper length and I.D.. Unmatched kinetic performance of roughly 300,000 N/m have been obtained on a 100 × 3.0 mm (L × I.D.) column packed with Whelk-O1 1.8 µm FPPs.

5. Final Remarks

The introduction of very efficient particle formats, such as sub-2 µm FPPs and sub-3 µm SPPs, functionalized with chiral selectors has represented the most important innovation in the field of chiral chromatography towards ultrafast, high-throughput enantioseparations. However, the continuous evolution in particle design and material technology will lead lo the development of smaller and smaller particles which will require the availability of equipments able to tolerate very high pressures and with minimal extra-column volumes. Technical improvements are especially required on SFC instruments, since extra-column contribution of state-of-the-art equipment is too large with respect to variance of a very narrow peak eluted from high efficiency columns.

New generation CSPs are expected to be increasingly applied as chromatographic supports for miniaturized platforms and microchips and multidimensional applications. In parallel, faster autosamplers will be needed in order to perform very fast screenings.

From a more fundamental point of view, deeper studies of mass transfer phenomena in chiral chromatography are necessary in order to understand the impact of adsorption-desorption kinetics on column efficiency, its possible correlation with bonding denisty and if this term could respresent a kinetic limit to ultrafast enantioseparations.

Author Contributions: Conceptualization and writing, M.C.; Data curation, O.H.I.; Writing-review, M.C., S.F. and C.D.L.; Editing, N.M. and V.C., Supervision, L.P., F.G. and A.C. All authors have read and approved the final version of the manuscript.

Funding: This research received no external funding.

Conflicts of Interest: The authors declare no conflict of interest.

References

1. Cavazzini, A.; Pasti, L.; Massi, A.; Marchetti, N.; Dondi, F. Recent applications in chiral high performance liquid chromatography: A review. *Anal. Chim. Acta* **2011**, *706*, 205–222.
2. Patel, D.C.; Breitbach, Z.S.; Wahab, M.F.; Barhate, C.L.; Armstrong, D.W. Gone in seconds: Praxis, performance and peculiarities of ultrafast chiral liquid chromatography with superficially porous particles. *Anal. Chem.* **2015**, *87*, 9137–9148.
3. Ciogli, A.; Ismail, O.H.; Mazzoccanti, G.; Villani, C.; Gasparrini, F. Enantioselective ultra high performance liquid and supercritical fluid chromatography: The race to the shortest chromatogram. *J. Sep. Sci.* **2018**, *41*, 1307–1318.
4. Catani, M.; Ismail, O.H.; Gasparrini, F.; Antonelli, M.; Pasti, L.; Marchetti, N.; Felletti, S.; Cavazzini, A. Recent advancements and future directions of superficially porous chiral stationary phases for ultrafast high-performance enantioseparations. *Analyst* **2017**, *142*, 555–566.
5. Ismail, O.H.; Antonelli, M.; Ciogli, A.; Villani, C.; Cavazzini, A.; Catani, M.; Felletti, S.; Bell, D.S.; Gasparrini, F. Future perspectives in high efficient and ultrafast chiral liquid chromatography through zwitterionic teicoplanin-based 2 μm superficially porous particles. *J. Chromatogr. A* **2017**, *1520*, 91–102.
6. Ismail, O.H.; Catani, M.; Pasti, L.; Cavazzini, A.; Ciogli, A.; Villani, C.; Kotoni, D.; Gasparrini, F.; Bell, D.S. Experimental evidence of the kinetic performance achievable with columns packed with the new 1.9 μm fully porous particles Titan C_{18}. *J. Chromatogr. A* **2016**, *1454*, 86–92.
7. Catani, M.; Ismail, O.H.; Cavazzini, A.; Ciogli, A.; Villani, C.; Pasti, L.; Cabooter, D.; Desmet, G.; Gasparrini, F.; Bell, D.S. Rationale behind the optimum efficiency of columns packed with the new 1.9 μm fully porous particles Titan C_{18}. *J. Chromatogr. A* **2016**, *1454*, 78–85.
8. Cancelliere, G.; Ciogli, A.; D'Acquarica, I.; Gasparrini, F.; Kocergin, J.; Misiti, D.; Pierini, M.; Ritchie, H.; Simone, P.; Villani, C. Transition from enantioselective high performance to ultra-high performance liquid chromatography: A case study of a brush-type chiral stationary phase based on sub-5-micron to sub-2-micron silica particles. *J. Chromatogr. A* **2010**, *1217*, 990–999.
9. Kotoni, D.; Ciogli, A.; Molinaro, C.; D'Acquarica, I.; Kocergin, J.; Szczerba, T.; Ritchie, H.; Villani, C.; Gasparrini, F. Introducing enantioselective Ultrahigh-Pressure Liquid Chromatography (eUHPLC): Theoretical inspections and ultrafast separations on a new sub-2-μm Whelk-O1 stationary phase. *Anal. Chem.* **2012**, *84*, 6805–6813.
10. Kotoni, D.; Ciogli, A.; D'Acquarica, I.; Kocergin, J.; Szczerba, T.; Ritchie, H.; Villani, C.; Gasparrini, F. Enantioselective ultra-high and high performance liquid chromatography: A comparative study of columns based on the Whelk-O1 selector. *J. Chromatogr. A* **2012**, *1269*, 226–241.
11. Cavazzini, A.; Marchetti, N.; Guzzinati, R.; Pierini, M.; Ciogli, A.; Kotoni, D.; D'Acquarica, I.; Villani, C.; Gasparrini, F. Enantioseparation by ultra-high-performance liquid chromatography. *Trends Anal. Chem.* **2014**, *63*, 95–103.
12. Reischl, R.J.; Hartmanova, L.; Carrozzo, M.; Huszar, M.; Frühauf, P.; Lindner, W. Chemoselective and enantioselective analysis of proteinogenic amino acids utilizing N-derivatization and 1-D enantioselective anion-exchange chromatography in combination with tandem mass spectrometric detection. *J. Chromatogr. A* **2011**, *1218*, 8379–8387.
13. Lomsadze, K.; Jibuti, G.; Farkas, T.; Chankvetadze, B. Comparative high-performance liquid chromatography enantioseparations on polysaccharide based stationary phases prepared by coating totally porous and core-shell silica particles. *J. Chromatogr. A* **2012**, *1234*, 50–55.
14. Spudeit, D.A.; Dolzan, M.D.; Breitbach, Z.S.; Barber, W.E.; Micke, G.A.; Armstrong, D.W. Superficially porous particles vs. fully porous particles for bonded high performance liquid chromatographic chiral stationary phases: Isopropyl cyclofructan 6. *J. Chromatogr. A* **2014**, *1363*, 89–95.
15. Barhate, C.L.; Breitbach, Z.S.; Pinto, E.C.; Regalado, E.L.; Welch, C.J.; Armstrong, D.W. Ultrafast separation of fluorinated and desfluorinated pharmaceuticals using highly efficient and selective chiral selectors bonded to superficially porous particles. *J. Chromatogr. A* **2015**, *1426*, 241–247.
16. Patel, D.C.; Wahab, M.F.; Armstrong, D.W.; Breitbach, Z.S. Advances in high-throughput and high-efficiency chiral liquid chromatographic separations. *J. Chromatogr. A* **2016**, *1467*, 2–18.

17. Patel, D.C.; Wahab, M.F.; Armstrong, D.W.; Breitbach, Z.S. Salient sub-second separations. *Anal. Chem.* **2016**, *88*, 8821–8826.
18. Barhate, C.L.; Lopez, D.A.; Makarov, A.A.; Bu, X.; Morris, W.J.; Lekhal, A.; Hartman, R.; Armstrong, D.W.; Regalado, E.L. Macrocyclic glycopeptide chiral selectors bonded to core-shell particles enables enantiopurity analysis of the entire verubecestat synthetic route. *J. Chromatogr. A* **2018**, *1539*, 87–92.
19. Guiochon, G.; Gritti, F. Shell particles, trials, tribulations and triumphs. *J. Chromatogr. A* **2011**, *1218*, 1915–1938.
20. Gritti, F.; Guiochon, G. Mass transfer mechanism in chiral reversed phase liquid chromatography. *J. Chromatogr. A* **2014**, *1332*, 35–45.
21. Gritti, F.; Guiochon, G. Possible resolution gain in enantioseparations afforded by core-shell particle technology. *J. Chromatogr. A* **2014**, *1348*, 87–96.
22. Catani, M.; Felletti, S.; Ismail, O.H.; Gasparrini, F.; Pasti, L.; Marchetti, N.; Luca, C.D.; Costa, V.; Cavazzini, A. New frontiers and cutting edge applications in ultra high performance liquid chromatography through latest generation superficially porous particles with particular emphasis to the field of chiral separations. *Anal. Bioanal. Chem.* **2018**, *410*, 2457–2465.
23. Felletti, S.; De Luca, C.; Ismail, O.H.; Pasti, L.; Costa, V.; Gasparrini, F.; Cavazzini, A.; Catani, M. On the effect of chiral selector loading and mobile phase composition on adsorption properties of latest generation fully- and superficially-porous Whelk-O1 particles for high-efficient ultrafast enantioseparations. *J. Chromatogr. A* **2018**, doi:10.1016/j.chroma.2018.10.022.
24. Gritti, F.; Farkas, T.; Heng, J.; Guiochon, G. On the relationship between band broadening and the particle-size distribution of the packing material in liquid chromatography: Theory and practice. *J. Chromatogr. A* **2011**, *1218*, 8209–8221.
25. Cavazzini, A.; Gritti, F.; Kaczmarski, K.; Marchetti, N.; Guiochon, G. Mass-Transfer Kinetics in a Shell Packing Material for Chromatography. *Anal. Chem.* **2007**, *79*, 5972–5979.
26. Marchetti, N.; Cavazzini, A.; Gritti, F.; Guiochon, G. Gradient elution separation and peak capacity of columns packed with porous shell particles. *J. Chromatogr. A* **2007**, *1163*, 203–211.
27. Gritti, F.; Cavazzini, A.; Marchetti, N.; Guiochon, G. Comparison between the efficiencies of columns packed with fully and partially porous C18-bonded silica materials. *J. Chromatogr. A* **2007**, *1157*, 289–303.
28. Catani, M.; Ismail, O.H.; Felletti, S.; Gasparrini, F.; Pasti, L.; Costa, V.; Cavazzini, A. Pirkle-type chiral stationary phases for ultra-high performance ultra-fast enantioseparations. *Am. Pharm. Rev.* **2017**, *20*, 44–48.
29. Barhate, C.L.; Wahab, M.F.; Breitbach, Z.S.; Bell, D.S.; Armstrong, D.W. High efficiency, narrow particle size distribution, sub-2 μm based macrocyclic glycopeptide chiral stationary phases in HPLC and SFC. *Anal. Chim. Acta* **2015**, *898*, 128–137.
30. Ismail, O.H.; Antonelli, M.; Ciogli, A.; De Martino, M.; Catani, M.; Villani, C.; Cavazzini, A.; Ye, M.; Bell, D.S.; Gasparrini, F. Direct analysis of chiral active pharmaceutical ingredients and their counterions by ultra high performance liquid chromatography with macrocyclic glycopeptide-based chiral stationary phases. *J. Chromatogr. A* **2018**, doi:10.1016/j.chroma.2018.09.029.
31. Snyder, L.R. Column efficiency in liquid-solid adsorption chromatography. H.E.T.P. (height equivalent to a theoretical plate) values as a function of separation conditions. *Anal. Chem.* **1967**, *39*, 698–704.
32. Done, J.N.; Knox, J.H. The Performance of Packings in High Speed Liquid Chromatography II. ZIPAX®. The Effect of Particle Size. *J. Chromatogr. Sci.* **1972**, *10*, 606–612.
33. Halász, I.; Naefe, M. Influence of column parameters on peak broadening in high-pressure liquid chromatography. *Anal. Chem.* **1972**, *44*, 76–84.
34. Endele, R.; Halász, I.; Unger, K. Influence of the particle size (5–35 μm) of spherical silica on column efficiency in HPLC. *J. Chromatogr. A* **1974**, *99*, 377–393.
35. Cabooter, D.; Fanigliulo, A.; Bellazzi, G.; Allieri, B.; Rottigni, A.; Desmet, G. Relationship between the particle size distribution of commercial fully porous and superficially porous high-performance liquid chromatography column packings and their chromatographic performance. *J. Chromatogr. A* **2010**, *1217*, 7074–7081.
36. Reising, A.E.; Godinho, J.M.; Hormann, K.; Jorgenson, J.W.; Tallarek, U. Larger voids in mechanically stable, loose packings of 1.3 μm frictional, cohesive particles: Their reconstruction, statistical analysis, and impact on separation efficiency. *J. Chromatogr. A* **2016**, *1436*, 118–132, doi:10.1016/j.chroma.2016.01.068.
37. Gritti, F.; Bell, D.S.; Guiochon, G. Particle size distribution and column efficiency. An ongoing debate revived with 1.9 μm Titan-C_{18} particles. *J. Chromatogr. A* **2014**, *1355*, 179–192.

38. Gritti, F.; Guiochon, G. The rationale for the optimum efficiency of columns packed with new 1.9 μm fully porous Titan-C_{18} particles. A detailed investigation of the intra-particle diffusivity. *J. Chromatogr. A* **2014**, *1355*, 164–178.
39. Kawatzki, K.; Barhate, C.L.; Regalado, E.L.; Mann, B.F.; Marshall, N.; Moore, J.C.; Welch, C.J. Overcoming "speed limits" in high throughput chromatographic analysis. *J. Chromatogr. A* **2017**, *1499*, 211–216.
40. Barhate, C.L.; Regalado, E.L.; Contrella, N.D.; Lee, J.; Jo, J.; Makarov, A.A.; Armstrong, D.W.; Welch, C.J. Ultrafast Chiral Chromatography as the Second Dimension in Two-Dimensional Liquid Chromatography Experiments. *Anal. Chem.* **2017**, *89*, 3545–3553.
41. Khundadze, N.; Pantsulaia, S.; Fanali, C.; Farkas, T.; Chankvetadze, B. On our way to sub-second separations of enantiomers in high-performance liquid chromatography. *J. Chromatogr. A* **2018**, *1572*, 37–43.
42. Thrumann, S.; Lotter, C.; Heiland, J.J.; Chankvetadze, B.; Belder, D. Chip-based high-performance liquid chromatography for high-speed enantioseparations. *Anal. Chem.* **2015**, *87*, 5568–5576.
43. Patel, D.C.; Wahab, M.F.; O'Haver, T.C.; Armstrong, D.W. Separations at the speed of sensors. *Anal. Chem.* **2018**, *90*, 3349–3356.
44. Wimalasinghe, R.M.; Weatherly, C.A.; Breitbach, Z.S.; Armstrong, D.W. Hydroxypropyl beta cyclodextrin bonded superficially porous particlebased HILIC stationary phases. *J. Liq. Chromatogr. Relat. Technol.* **2016**, *39*, 459–464.
45. Woiwode, U.; Neubauer, S.; Lindner, W.; Buckenmaier, S.; Lämmerhofer, M. Enantioselective multiple heartcut two-dimensional ultra-high-performance liquid chromatography method with a Coreshell chiral stationary phase in the second dimension for analysis of all proteinogenic amino acids in a single run. *J. Chromatogr. A* **2018**, *1562*, 69–77.
46. Woiwode, U.; Reischl, R.J.; Buckenmaier, S.; Lindner, W.; Lämmerhofer, M. Imaging peptide and protein chirality via amino acid analysis by chiral × chiral two-dimensional correlation liquid chromatography. *Anal. Chem.* **2018**, *90*, 7963–7971.
47. Min, Y.; Sui, Z.; Liang, Z.; Zhang, L.; Zhang Y. Teicoplanin bonded sub-2 μm superficially porous particles for enantioseparation of native amino acids. *J. Pharm. Biomed. Anal.* **2015**, *114*, 247–253.
48. Felinger, A.; Kilár, A.; Boros, B. The myth of data acquisition rate. *Anal. Chim. Acta* **2015**, *854*, 178–182.
49. Patel, D.C.; Wahab, M.F.; O'Haver, T.C.; Armstrong, D.W. Recent achievements and future challenges in supercritical fluid chromatography for the enantioselective separation of chiral pharmaceuticals. *Chromatographia* **2018**, 1–11, doi:10.1007/s10337-018-3606-1.
50. Ismail, O.H.; Ciogli, A.; Villani, C.; Martino, M.D.; Pierini, M.; Cavazzini, A.; Bell, D.S.; Gasparrini, F. Ultra-fast high-efficiency enantioseparations by means of a teicoplanin-based chiral stationary phase made on sub-2 μm totally porous silica particles of narrow size distribution. *J. Chromatogr. A* **2016**, *1427*, 55–68.
51. Sciascera, L.; Ismail, O.; Ciogli, A.; Kotoni, D.; Cavazzini, A.; Botta, L.; Szczerba, T.; Kocergin, J.; Villani, C.; Gasparrini, F. Expanding the potential of chiral chromatography for high-throughput screening of large compound libraries by means of sub-2 μm Whelk-O1 stationary phase in supercritical fluid conditions. *J. Chromatogr. A* **2015**, *1383*, 160–168.
52. Patel, D.C.; Breitbach, Z.S.; Yu, J.; Nguyen, K.A.; Armstrong, D.W. Quinine bonded to superficially porous particles for high-efficiency and ultrafast liquid and supercritical fluid chromatography. *Anal. Chim. Acta* **2017**, *963*, 164–174.
53. Berger, T.A. Kinetic performance of a 50 mm long 1.8 μm chiral column in supercritical fluid chromatography. *J. Chromatogr. A* **2016**, *1459*, 136–144.
54. Berger, T.A. Preliminary kinetic evaluation of an immobilized polysaccharide sub-2 μm column using a low dispersion supercritical fluid chromatograph. *J. Chromatogr. A* **2017**, *1510*, 82–88.
55. Ismail, O.H.; Losacco, G.L.; Mazzoccanrti, G.; Ciogli, A.; Villani, C.; Catani, M.; Pasti, L.; Anderson, S.; Cavazzini, A.; Gasparrini, F. Unmatched kinetic performance in enantioselective supercritical fluid chromatography by combining latest generation Whelk-O1 chiral stationary phases with a low-dispersion in-house modified equipment. *Anal. Chem.* **2018**, *90*, 10828–10836.

Paper V

Journal of Chromatography A, 1579 (2018) 41–48

Contents lists available at ScienceDirect

Journal of Chromatography A

journal homepage: www.elsevier.com/locate/chroma

On the effect of chiral selector loading and mobile phase composition on adsorption properties of latest generation fully- and superficially-porous Whelk-O1 particles for high-efficient ultrafast enantioseparations

Simona Felletti [a], Chiara De Luca [a], Omar H. Ismail [b], Luisa Pasti [a], Valentina Costa [a], Francesco Gasparrini [b], Alberto Cavazzini [a,*], Martina Catani [a,*]

[a] Department of Chemistry and Pharmaceutical Sciences, University of Ferrara, via L. Borsari 46, 44121 Ferrara, Italy
[b] Department of Drug Chemistry and Technology, "Sapienza" University of Rome, P. le Aldo Moro 5, 00185 Rome, Italy

ARTICLE INFO

Article history:
Received 17 July 2018
Received in revised form 9 October 2018
Accepted 14 October 2018
Available online 15 October 2018

Keywords:
Chiral stationary phases
Whelk-O1 selector
Superficially porous particles
Sub-2μm fully porous particles
Adsorption isotherms

ABSTRACT

The adsorption isotherms of *trans*-stilbene oxide (TSO) enantiomers have been measured under a variety of normal phase (NP) mobile phases (MPs) on three Whelk-O1 chiral stationary phases (CSPs), prepared respectively on 1.8 μm and 2.5 μm fully porous particles (FPPs) and 2.6 μm superficially porous particles (SPPs). Specific loading of chiral selector (moles per square meter) of the two FPPs was about 20% smaller than that of SPPs (even if they were prepared under exactly the same experimental conditions).

Regardless of particle size or format, adsorption was described by means of a Bilangmuir model with ethanol/hexane MPs. On the other hand, in pure hexane, the Tóth isotherm was employed. Interestingly, it was found that selective and nonselective Henry's constants vary in opposite directions by increasing the percentage of strong MP modifier (between 3 and 10%, v/v). Saturation capacity of SPPs (referred only to the porous zone of the particle) was remarkably smaller than those of FPPs. On the other hand, binding constants on both selective and nonselective sites were significantly larger on SPPs. Finally, a correlation between the specific loading of chiral selector and the binding constants of enantiomers was suggested by data, which can be important also to understand the kinetic behavior of these particles in chiral ultrafast applications.

1. Introduction

The design and development of high efficient particles, either sub-2μm fully porous (FPPs) [1–3] or (second-generation) superficially porous (SPPs) ones [4–12], functionalized with chiral selectors, have represented the most important innovation in the last decade in the field of chiral separations by liquid chromatography. Not only have they allowed for the preparation of packed columns with extraordinary kinetic performance – altogether comparable to that of typical reversed-phase (RP) achiral separations [13–15] – but they also have permitted to decrease the analysis time by up to three orders of magnitude (from tenths of minutes to fractions of seconds) [16,17,5,18,19,14,1,12,20,2,13,3,4].

Many remarkable examples showing the very large potential of new generation particles toward high-efficient ultrafast (sub-seconds) enantioseparations have been published [1–12]. Essentially, in all of these studies the key has been to use very short prototype columns (either 10 or even 5 mm long) operated at the maximum flow rate allowed by the equipment (between 5 and 8 mL/min depending on the brand of the instrument). At very large flow rates, the so-called mass transfer term, or *c*-term, of the van Deemter equation dominates over the other mechanisms of band broadening (longitudinal diffusion and eddy dispersion). Differently from what happens in RP achiral chromatography, in chiral chromatography this term accounts not only for diffusion of molecules through the particles of the packed bed (where flow is absent) but also for the adsorption–desorption kinetics. Adsorption–desorption kinetics is negligible in RP achiral chromatography unless very large molecules (such as proteins or large polypeptides) are considered. It has been indeed demonstrated that for small molecules adsorption–desorption is very fast [21,22]. On

* Corresponding authors.
E-mail addresses: cvz@unife.it (A. Cavazzini), ctnmtn@unife.it (M. Catani).

https://doi.org/10.1016/j.chroma.2018.10.022
0021-9673/

the opposite, the enantiorecognition process can be slow, even if the extent largely depends on the type of chiral selector employed. For instance, it is generally accepted that brush-type chiral selectors, such as the Whelk-O1 type, are "fast" while other kinds of selectors, including macrocyclic glycopeptides and polysaccharides, are "slow". This information basically comes from molecular spectroscopic investigation (firstly, by NMR). Therefore, it is not unusual that experimental conditions under which it was obtained can be significantly different from those typical of liquid chromatography. Not just because spectroscopic measurements are (very often) performed in homogeneous systems, where both chiral selectors and analytes are in solution, but also since solvents employed in these measurements can be very different from typical eluents used in liquid chromatography. Thus, these measurements does not account for the effect of several variables that may affect chiral recognition in heterogenous systems (i.e., when the chiral selector is tethered to the surface), such as the chemical composition of the surface around chiral selector, the surface density of chiral selector, pore size and morphology, their accessibility, the competitive effect for adsorption by so-called strong mobile phase (MP) modifiers, etc.

For the reasons explained above, however, these considerations assume great importance for latest generation sub-2μm fully porous and second-generation superficially porous particles. This is particularly so when one wants to compare superficially- and fully-porous particles (functionalized with the same chiral selector) in terms of kinetic performance. The common reasoning [8,23–27] about the alleged superiority, in terms of efficiency, of the former type of particles over their fully porous counterpart is based on the same considerations employed in achiral RP chromatography, namely that eddy dispersion, longitudinal diffusion and solid-liquid mass transfer are smaller on chiral SPPs than on FPPs. Therefore, these conclusions either completely neglect the role of adsorption–desorption kinetics or they implicitly assume that adsorption–desorption kinetics is identical on both kinds of particles. On the other hand, many authors report that functionalization of SPPs and FPPs systematically leads to different specific loading, or density (μmol/m^2) of chiral selectors on the two types of particles, even if their chemical modification is performed under exactly the same experimental conditions [1,13,8,11,5].

With the purpose of shedding light on some of these aspects, in this work the adsorption isotherms of *trans*-stilbene oxide (TSO) enantiomers have been measured under normal phase (NP) conditions on three different Whelk-O1 chiral stationary phases (CSPs). Two of them were prepared on FPPs (2.5 and 1.8 μm particle diameter, respectively) and the other one on 2.6 μm SPPs [1,13]. The investigation of adsorption isotherms is fundamental not only to characterize surface heterogeneity (in terms of adsorption energy distribution) but also to investigate if, e.g., the bonding density has an effect on the binding constants of enantiomers and enantioselectivity of CSPs. In addition, since adsorption–desorption kinetics is strongly influenced by thermodynamic equilibria [28], this information can also be useful to understand the chromatographic behavior of fully- and superficially-porous particles at high flow rates [1,29,30,2,31].

2. Theory

The equilibrium-dispersive (ED) model has often been used to describe chromatographic separations characterized by efficient mass transfer [28]. In this model, instantaneous equilibrium between mobile (MP) and stationary phase (SP) is assumed. Since both thermodynamics of phase equilibria and mass transfer kinetics change with experimental conditions, the only parameter that is conserved during a chromatographic separation (in absence of chemical reaction) is the mass of the injected sample. Therefore, a differential mass balance equation can be written that, for the ED model, includes an apparent lumped dispersion term (D_a) accounting for all the contributions to band broadening observed in linear chromatography:

$$\frac{\partial C_i}{\partial t} + F\frac{\partial q_i}{\partial t} + u\frac{\partial C_i}{\partial z} = D_{a,i}\frac{\partial^2 C_i}{\partial z^2} \tag{1}$$

where the index i indicates ith component of the system. In this equation, C_i and q_i are the concentrations of analyte in MP and SP, respectively, t represents the temporal coordinate and z the spatial one. Finally, u is the MP linear velocity and F the phase ratio:

$$F = \frac{1-\epsilon_t}{\epsilon_t} \tag{2}$$

being ϵ_t the total porosity of the packed bed given by the ratio between the hold-up, V_0, and the geometric volume, V_{col}, of the column. The apparent dispersion coefficient is calculated through the efficiency of the chromatographic peak under analytical conditions:

$$D_{a,i} = \frac{uL}{2N_i} \tag{3}$$

where N is the number of theoretical plates and L the column length. In the case of enantiomeric separations ($i = 1, 2$), the system will be described by two partial differential equations, which are coupled through a competitive isotherm equation, $q_i = f(C_1, C_2)$ (see later on).

2.1. Inverse Method for determination of isotherms

The direct numerical resolution of the system of mass balance equations requires the knowledge of the isotherm. This can be, for instance, evaluated through (competitive) frontal analysis. Contrary, in the so-called Inverse Method (IM) [32–34], isotherm parameters are derived through a procedure based on the iterative resolution of system of mass balance equations (once an isotherm model has been chosen). Isotherm parameters are calculated by minimizing the differences between experimental and calculated chromatograms. Schematically, IM requires the following steps: (i) recording of some experimental overloaded profiles; (ii) selection of an isotherm model (the shape of overloaded profiles guides this process [28]) and guess of initial parameters; (iii) resolution of system of mass balance equations with the adsorption isotherm just selected (to get a calculated chromatogram); (iv) comparison between calculated overloaded profiles and experimental ones; (v) tuning of isotherm parameters until calculated and experimental profiles match as much as possible. Numerical optimization of isotherm parameters was made by means of the super-modified simplex method described in [32,35].

To solve the system of mass balance equations, obviously proper initial and boundary conditions must be defined. In this work, the following initial

$$C_i(z, t=0) = 0 \quad i = 1, 2 \tag{4}$$

and boundary

$$C_i(z=0, t) = \begin{cases} C_{i,0} & 0 \le t \le t_{inj} \quad i = 1, 2 \\ 0 & t > t_{inj} \end{cases} \tag{5}$$

conditions were taken describing, respectively, that at $t = 0$ the column is equilibrated with pure eluent (Eq. (4)) and that the injection profile is a rectangular pulse of concentration $C_{i,0}$ ($i = 1, 2$) during the injection time, t_{inj} (Eq. (5)).

2.2. Isotherm models

2.2.1. Langmuir isotherm

The Langmuir model is the most frequently used to describe adsorption in liquid chromatography. Based on the Langmuir model, the adsorption surface is assumed to be paved by only one type of adsorption sites (homogeneous adsorption). In addition, adsorption is monolayer and no lateral interactions between adsorbed molecules are possible. In the case the Langmuir isotherm is used to model chiral separations, not only it is assumed that nonselective interactions have a negligible contribution to retention of enantiomers but also that energies of all possible enantioselective interactions are close enough that they can be averaged. Accordingly, a single adsorption energy and a single adsorption constant can be defined, which characterize all adsorption sites on the surface. (Obviously, average energies and constants are different for the two enantiomers). The competitive Langmuir model applied to the separation of two enantiomers (denoted hereafter 1 and 2) is written as:

$$q_i = \frac{q_s b_i c_i}{1 + b_1 c_1 + b_2 c_2} \quad i = 1, 2 \tag{6}$$

where q_s is the saturation capacity (equal for both enantiomers [28]) and b_i is the adsorption equilibrium (binding) constant. The product between q_s and b_i defines the so-called Henry's constant of adsorption, a_i (that is the initial slope of the isotherm). Retention factor (under linear condition), k, and Henry's constant are connected by:

$$k = \frac{t_R - t_0}{t_0} = aF \tag{7}$$

where t_R and t_0 are respectively the retention and hold-up time measured under linear conditions.

2.2.2. Tóth isotherm

This isotherm describes heterogeneous adsorption. In particular, it assumes a continuous and possibly wide adsorption energy distribution. Width depends on the value of the so-called heterogeneity parameter, ν ($0 < \nu < 1$). The smaller ν the wider the adsorption energy distribution function. For binary competitive systems, the Tóth isotherm is:

$$q_i = \frac{q_s b_i c_i}{[1 + (b_1 c_1 + b_2 c_2)^{\nu}]^{1/\nu}} \quad i = 1, 2 \tag{8}$$

2.2.3. Bilangmuir isotherm

The Bilangmuir model, finally, accounts for a bimodal adsorption energy distribution due to the presence of two different adsorption sites that, in case of chiral separations, are considered selective (responsible for diastereomeric or enantioselective interactions) and nonselective (where both enantiomers behave identically) [36]. This model has been often successfully applied to describe adsorption processes of enantiomers on CSPs [32,37,38]. The competitive 2-component adsorption isotherm is:

$$q_i = \frac{q_{sel} b_{i,sel} c_i}{1 + b_{1,sel} c_1 + b_{2,sel} c_2} + \frac{q_{nsel} b_{nsel} c_i}{1 + b_{nsel}(c_1 + c_2)} \quad i = 1, 2 \tag{9}$$

where subscripts *sel* and *nsel* refer to selective and nonselective sites, respectively [28,32,39,40].

3. Materials and methods

3.1. Columns and materials

All solvents and reagents were purchased from Sigma Aldrich (St. Louis, MI, USA). Kromasil fully porous silica particles (2.5 and 1.8 μm particle size, 100 Å pore size, 323 m^2/g specific surface area) were from Akzo-Nobel (Bohus, Sweden). Accucore second-generation superficially porous silica particles (2.6 μm, 80 Å pore size, 130 m^2/g specific surface area, radius of core over particle radius, $\rho = 0.63$) were from Thermo Fisher Scientific (Waltham, MA, USA). Whelk-O1 selector was generously donated by Regis Technologies Inc. (Morton Grove, IL, USA). Synthesis and preparation of Whelk-O1 CSPs are reported in Ref. [1]. 100 and 150 mm × 4.6 mm empty stainless steel columns were from IsoBar Systems by Idex (Erlangen, Germany).

3.2. Equipment

All measurements were performed on an Agilent 1100 Series Capillary LC system equipped with a binary solvent pump, a column thermostat and a photodiode array detector. An external manual injector (Rheodyne 8125, equipped with either 5 or 50 μL fixed-loops) was used for sample injections. Detector calibration was performed by sequentially injecting 50 μL TSO racemic solutions (concentration from 0.05 g/L to 5 g/L) without the column. This volume was large enough to observe concentration plateau. Wavelength: 280 nm.

3.3. Experimental conditions

Adsorption isotherms were measured at five different hexane/ethanol MP compositions: 90/10, 92/8, 95/5, 97/3 and 100/0% (v/v). Temperature was 35 °C. TSO racemic mixture injected concentrations were: 3, 10, 20, 40, and 50 g/L. Injection volume was 5 μL.

4. Results and discussion

Table 1 reports some of the physico-chemical characteristics of particles and columns employed in this work [1,30,2]. Fully porous particles were used to prepare the columns named FPP-1.8 and FPP-2.5; the column called SPP-2.6 was packed with core–shell particles (see Table 1). Information on particle diameter, specific surface area and pore size comes from manufacturers. Bonding density was determined through elemental analysis (more information under SI). As expected, bonding densities per gram of base silica are larger on FPPs (for which essentially the same value was obtained regardless of particle size) than on SPPs. On the other hand, specific bonding density (μmol/m^2) is significantly larger (by almost 20%) on SPPs than that of FPPs. This last finding has been observed also with other chiral selectors [13] and by other authors [8,5]. However, in other cases [7] the opposite was reported so that no generaliza-

Table 1
Acronyms of columns employed in this work and their dimensions (length times internal diameter). Chemico-physical characteristics of particles: base silica brand, particle diameter, d_p, specific surface area, A_s, pore size, bonding density (given both as μmol per gram of base silica and μmol per square meter) and particle porosity, ϵ_p.

Column acronym	Dimensions	Silica brand	d_p	A_s	Pore size	Bonding density		ϵ_p
	(L × I.D., mm)		(μm)	(m^2/g)	(Å)	(μmol/g)	(μmol/m^2)	
FPP-1.8	100 × 4.6	Kromasil	1.8	323	100	394.6	1.22	0.414
FPP-2.5	150 × 4.6	Kromasil	2.5	323	100	391.2	1.21	0.438
SPP-2.6	150 × 4.6	Accucore	2.6	130	80	189.8	1.46	0.251

Table 2
Bilangmuir isotherm parameters calculated through Inverse Method at different percentage of strong MP modifier.

MP	Column	Selective site			Nonselective site	
(% EtOH)		q_{sel} (g/L)	$b_{1,sel}$ (L/g)	$b_{2,sel}$ (L/g)	q_{nsel} (g/L)	b_{nsel} (L/g)
10	FPP-1.8	42	0.010	0.063	100	0.012
	FPP-2.5	42	0.011	0.071	96	0.013
	SPP-2.6	22	0.022	0.095	50	0.015
8	FPP-1.8	38	0.011	0.071	101	0.012
	FPP-2.5	41	0.013	0.082	102	0.013
	SPP-2.6	22	0.025	0.105	39	0.019
5	FPP-1.8	40	0.011	0.090	104	0.015
	FPP-2.5	36	0.011	0.111	105	0.017
	SPP-2.6	22	0.024	0.128	50	0.020
3	FPP-1.8	33	0.012	0.142	106	0.018
	FPP-2.5	30	0.013	0.170	108	0.020
	SPP-2.6	15	0.025	0.212	49	0.027

tion can be made. It is worth noting that functionalization of both SPPs and FPPs was performed under identical experimental conditions (and repeated several times). Nevertheless, specific bonding density was different. Among the hypotheses that can be formulated to explain why this happens, the different reactivity of surface silanol groups on the two kinds of particles or the different accessibility of intraparticle space (during particle functionalization) are the most likely. Particle porosity, ϵ_p, was measured as reported under SI. ϵ_p, describing the fraction of empty pores per particle, is consistent with values of specific bonding density.

To investigate whether the different specific bonding density of chiral selector entails changes on the CSPs, the adsorption isotherms of the enantiomers of a probe compound, TSO, were measured under NP conditions. Measuring the isotherms is the only approach to characterize the surface in terms of adsorption sites and their abundance. This information, on the other hand, cannot be gathered through measurements performed under linear conditions (i.e., by means of retention factors) [32,28,41–45].

Isotherms were measured through IM. Different competitive adsorption models were considered, including the simplest Langmuir, the Bilangmuir and the Tóth isotherm. Based on the statistical evaluation of results according to Fisher's test, IM has shown that the most suitable model to describe the separation of TSO enantiomers on Whelk-O1 CSPs is the Bilangmuir isotherm for all MP compositions but 100% hexane (see later on). In Fig. 1, overloaded profiles obtained through IM calculations with a Bilangmuir isotherm (continuous lines) are overlapped to experimental peaks (with points). As it can be seen, in all cases the agreement between experimental and calculated peaks is very consistent.

Table 2 lists the Bilangmuir isotherm parameters as a function of the percentage of ethanol in MP (from 10 to 3%, v/v) for the three columns used in this work.

4.1. 1.8 and 2.5 μm FPPs

The first thing that can be observed by data in Table 2 is that both binding constants and saturation capacity on selective (q_{sel}) and nonselective (q_{nsel}) sites are very similar on the columns packed with FPPs (FFP-2.5 and FFP-1.8). This is, therefore, consistent with the loading of chiral selector measured through elemental analysis (see Table 1). On another viewpoint, it is a confirmation that preparation of Whelk-O1 CSPs, even when based on particles of very reduced dimensions, is a very reproducible and robust process. Finally, it offers a sound thermodynamic explanation for the observation that not only retention (see k_1 values on the third column of Table 3) but also selectivity (fourth column of the same

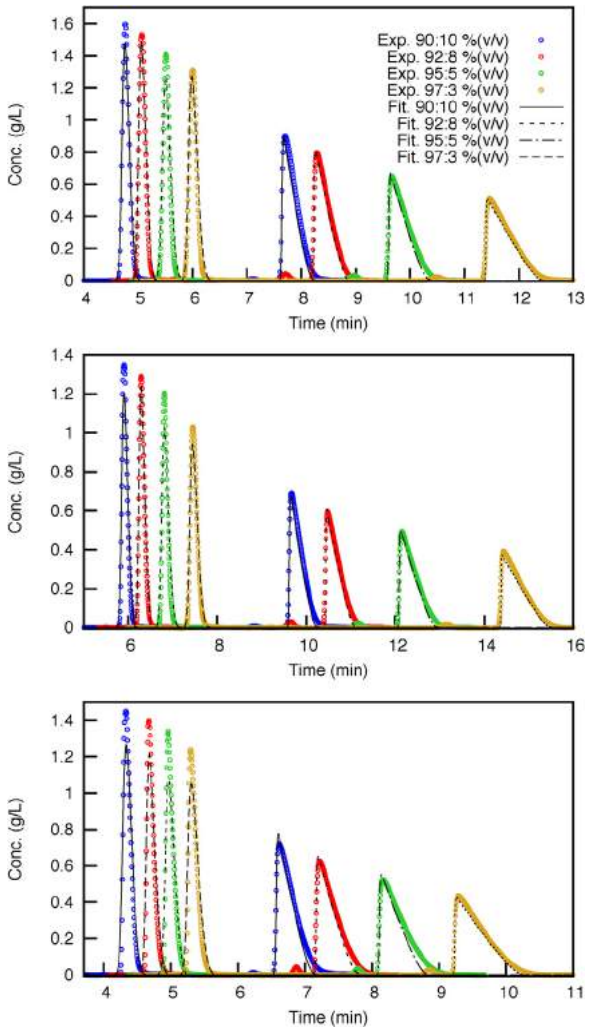

Fig. 1. Experimental (empty circles) and calculated (full lines) overloaded profiles of TSO enantiomers on FPP-1.8 (top), FPP-2.5 (middle) and SPP-2.6 (bottom) columns measured at 90:10 (blue), 92:8 (red), 95:5 (green) and 97:3 (yellow) % (v/v) of hexane/ethanol. Injected concentration: 40 g/L. (For interpretation of the references to color in this figure legend, the reader is referred to the web version of the article.)

Table 3
Retention factor of first eluted enantiomer (k_1) and apparent (α_{app}) and true (α_{true}) selectivity. See text for more details.

Eluent (% EtOH)	Column	k_1	α_{app}	α_{true}
10	FPP-1.8	0.6	2.6	6.3
	FPP-2.5	0.7	2.5	6.4
	SPP-2.6	0.5	2.5	4.4
8	FPP-1.8	0.7	2.7	6.5
	FPP-2.5	0.8	2.7	6.3
	SPP-2.6	0.6	2.7	4.2
5	FPP-1.8	0.8	2.9	8.2
	FPP-2.5	0.9	2.8	10.0
	SPP-2.6	0.7	2.8	5.3
3	FPP-1.8	1.0	3.1	11.6
	FPP-2.5	1.0	3.0	13.2
	SPP-2.6	0.8	3.0	8.5

Table) measured at the different MPs under linear conditions are essentially equal on the columns packed with FPPs. Following Forn-

stedt et al. [42,41], selectivity measured through retention factors will be denoted by the symbol α_{app}:

$$\alpha_{app} = \frac{k_2}{k_1} \quad (10)$$

where the subscript *app* serves to underline that, when measured this way, enantioselectivity comes from a combination of both selective and nonselective interactions. Therefore, it is an apparent value. On the other hand, the so-called "true" enantioselectivity (α_{true}), based only on enantioselective contributions, can be estimated once isotherm parameters are known (see later on). For the sake of clarity, it is worth clarifying the use of the term "true" applied to the concept of liquid chiral separations on CSPs. As it was pointed out before, chemically modified (chiral) surfaces are intrinsically heterogeneous in terms of their morphology, chemical composition and "solvation" status (which strongly depends on the mobile phase composition). SP and FP porous silica types, in addition, are different and thus also the morphology of the modified silica surface. All of these variables/conditions may have an effect on an experimentally observed enantioselectivity. The word "true", therefore, must not use be considered as an "absolute" concept. It merely describes, under specific conditions, the contribution of the stereoselective and non-stereoselective portfolio of "intermolecular" interactions taking place at the solvated and stereochemically modified silica surface with the chiral analytes.

4.1.1. The effect of the strong MP modifier amount on binding constant and saturation capacity. Excess isotherms

By considering how binding constants and saturation capacity change by changing the amount of ethanol (Table 2), some interesting features can be evidenced. Firstly, one may see that selective binding constants for the first eluted enantiomer ($b_{1,sel}$) are essentially independent on the amount of ethanol (they are between 0.010 and 0.013 L/g). On the other hand, increasing ethanol percentage provokes a significant decreasing not only of the enantioselective binding of the more retained enantiomer ($b_{2,sel}$ decreases by almost 60% by moving from 3 to 10% ethanol, v/v in MP), but also of nonselective binding, even if to a smaller extent (b_{nsel} decreases of about 35% for the same change in MP composition). The other interesting observation is about the behavior of saturation capacity with the percentage of ethanol. Surprisingly, indeed saturation capacities of selective sites, q_{sel}, and of nonselective ones, q_{nsel}, exhibit opposite trends. While q_{sel} decreases by almost 30% by decreasing the percentage of ethanol in MP from 10 to 3% (v/v) (by roughly passing from 42 to 30 g/L), q_{nsel} increases by roughly 10% (from about 98 to 110 g/L). Therefore, the overall effect on retention of selective sites is that, by increasing the amount of ethanol in MP, the Henry's constant of adsorption (see Eq. (7)) of the first enantiomer ($a_1 = q_{sel}b_{1,sel}$) slightly increases while that of the second one ($a_2 = q_{sel}b_{2,sel}$) decreases. In addition, nonselective contributions lead to a decrease of retention due to the simultaneous reduction of both binding constant and saturation capacity. The combination of both selective and nonselective contributions leads to the trend observed in Fig. 1 (see figure caption for details), where retention decreases with increasing ethanol in MP.

Fig. 2 reports the excess isotherm for ethanol/hexane binary mixtures on the three chiral CSPs employed in this work. Details on how excess isotherms were measured are given under SI. Excess isotherms allow to describe the preferential adsorption of ethanol on the stationary phase in function of the bulk MP composition. Basically, the interpretation of these plots reveals that the composition of the stationary phase can be considered constant (and thus independent on the bulk MP composition) only when percentage of ethanol in MP exceeds 10–15% (v/v) (i.e., when excess isotherms decrease almost linearly with increasing ethanol amount). In this region, our understanding is that ethanol has saturated all polar

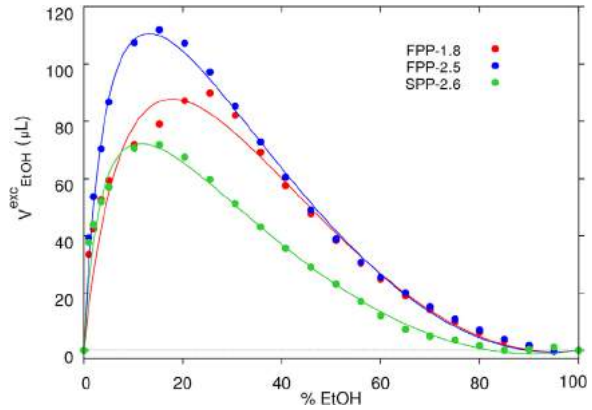

Fig. 2. Excess adsorption isotherms on the three columns employed in this work (see text for details), expressed as excess volume of ethanol adsorbed on the stationary phase (V^{exc}_{EtOH}) as a function of percentage (v/v) of EtOH (% EtOH) in the mobile phase. Experimental (full circles), fitted curves (full lines). (For interpretation of the references to color in this figure legend, the reader is referred to the web version of the article.)

sites on the surface. It is where a "true" NP chromatographic behavior is effective and retention decreases – following the increase of the strong MP modifier – due to the increasing competition for adsorption on the polar surface by MP modifier molecules [46,47,33,48,49]. On the other hand, in the initial part of isotherms, the composition of stationary phase is not constant but changes with the amount of ethanol in MP. Herein more complex, so-called "mixed-mode" mechanisms can be active which can explain the observed features. Excess isotherms could therefore offer a thermodynamic-based interpretation to the behavior of binding constant and saturation capacity previously observed. Existence of mechanisms affecting retention in opposite ways can also be at the origin of the well known but little understood phenomenon in chiral liquid chromatography, that is the inversion of elution order of enantiomers by changing either MP composition or modifier [50–52].

4.2. Comparison between FPPs and 2.6 µm SPPs

The same general dependence of both saturation capacity and binding constant on the strong MP modifier has been observed also for the chiral SPPs, as shown by data in Table 2.

On the other hand, if one compares fully- and superficially-porous particles at the same MP composition, it can be seen that SPPs are characterized by larger selective and nonselective binding than FPPs. This therefore seems to correlate with the specific loading of chiral selector, which is larger on SPPs than on FPPs (see Table 1).

This could be due to the fact that high selector loading may be responsible, as expected, for an higher contribution of selective sites but, on the other hand, it could also lead to the formation of different structures of chiral selector bonded to the surface that can interact with enantiomers in different manners. This sort of clusters or aggregates between two or more chiral selectors could possibly behave also as nonselective sites. Another hypothesis that can be made is about the existance of secondary interactions between enantiomers and chemical neighborhood of the chiral selector that can be different on FPPs or SPPs. However, it is difficult to predict what happens at a molecular level and which kinds of interactions can be involved. More physically-sound explanations can be deduced by performing more specific measurements (e.g. solid NMR) [53].

This finding is of remarkable interest when considering the employment of these particles in high-efficient ultrafast separa-

Table 4
Tóth isotherm parameters calculated through Inverse Method with a MP made of pure hexane.

Column	q_s (g/L)	b_1 (L/g)	b_2 (L/g)	ν
FPP-1.8	94	0.110	0.589	0.71
FPP-2.5	96	0.128	0.697	0.71
SPP-2.6	30	0.289	1.425	0.81

tions for which they have been originally designed. It is evident indeed that a larger binding constant provokes (on average) longer adsorption–desorption times, which negatively impacts on the *c*-term of the van Deemter equation [1,2,28].

The other interesting observation comes from the comparison of saturation capacities. It is evident, indeed, that they are significantly lower (roughly −40%) on superficially – than on fully-porous particles. It is worth noting that saturation capacity values reported for SPPs are referred only to the porous zone of particles (see details under SI) so that, in principle, one should not expect this large difference. Therefore a possible explanation could be the significantly smaller particle porosity and the following reduced access to intraparticle volume, of SPPs than FPPs (Table 1).

Data reported in Table 2, finally, allows also to calculate the so-called "true" enantioselectivity (see before) defined by [42]:

$$\alpha_{true} = \frac{b_{2,sel}}{b_{1,sel}} \tag{11}$$

α_{true} values are reported in Table 3 next to their corresponding α_{app}s (see Eq. (10)). It is interesting to observe that in all cases true enantioselectivity is larger on fully porous particles. This is due to the large binding constant of first eluted enantiomer on selective sites of SPPs, which is on average more than twice as large as that on FPPs.

4.3. Adsorption equilibria with pure hexane

In the last part of this study the behavior of TSO enantiomers with a MP made of pure hexane has been investigated. As it was previously mentioned, in this case the Bilangmuir model did not allow an accurate fitting of overloaded profiles. This means that an heterogeneous model based on the existence of only two different adsorption sites is not satisfactory to account for the heterogeneity of the surface when ethanol is not a MP component. As a matter of fact, the competitive adsorption by ethanol makes the surface "more homogenous" by masking the most polar sites of the surface. Fig. 3 shows the experimental overloaded band profiles (points) obtained on the three columns with pure hexane MP (see figure captions for more information). As it can be seen, especially for second eluted peaks, tailing is much more pronounced than with binary MPs (see Fig. 3). In the same figures, continuous lines represent the overloaded peaks calculated by solving the IM by means of the Tóth isotherm (Eq. (8)), which assumes a continuous adsorption energy distribution function. Table 4 summarizes the isotherm parameters obtained in this case. Even if, from a theoretical viewpoint, the adsorption model used with pure hexane is very different from that employed with binary MPs, the main information derivable from these parameters is consistent with that obtained with the simpler Bilangmuir isotherm. First of all, indeed, isotherm parameters for the two CSPs made of FPPs are very close each other. In addition, by comparing FPPs and SPPs, it can be observed that, for both enantiomers, binding constants are larger on SPPs, while saturation capacity is smaller. This thus confirms the intrinsic difference between chiral fully- and superficially-porous Whelk-O1 particles.

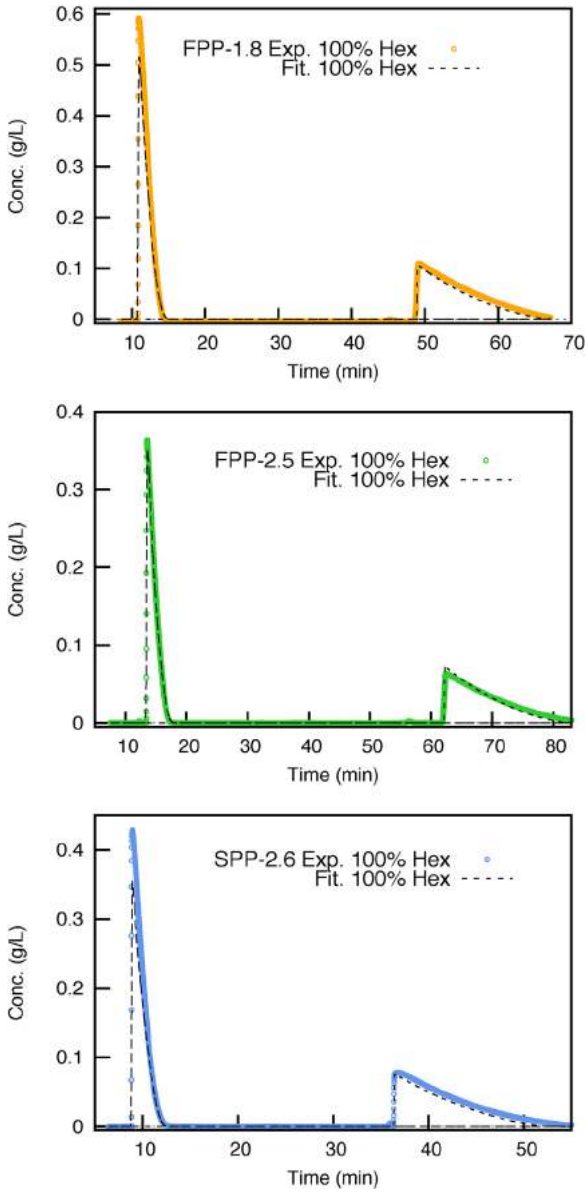

Fig. 3. Experimental (empty circles) and calculated (full line) overloaded profiles of TSO enantiomers on FPP-1.8 (top), FPP-2.5 (middle) and SPP-2.6 (bottom) columns measured at 100% hexane MP. Injected concentration: 40 g/L.

5. Conclusions

The investigation of adsorption isotherms of enantiomers on new generation CSPs is a fundamental tool for the deep characterization of the adsorption properties of these phases and possibly for finding correlations between their chemico-physical characteristics (bonding density of chiral selector, porosity, etc.) and thermodynamic quantities that directly affect the enantiorecognition process (such as binding constants on selective and nonselective sites, saturation capacity, adsorption energy distribution function, etc.).

This approach may help to investigate some very important unanswered questions such as whether chiral recognition process is the same on fully- or superficially-porous particles (functionalized with the same chiral selector), how enantiorecognition changes by changing experimental variables (e.g. mobile phase composition), if and how loading of chiral selector affects enantiorecognition, etc.

Combined with studies on the efficiency of these CSPs and mass transfer through them, this information can help not only to understand the complexity of enantioseparations but also to drive further the development of particles, either fully- or superficially-porous, with enhanced kinetic and thermodynamic properties.

Acknowledgement

Authors acknowledge dr. Ercolina Bianchini of the University of Ferrara for technical support.

Appendix A. Supplementary data

Supplementary data associated with this article can be found, in the online version, at https://doi.org/10.1016/j.chroma.2018.10.022.

References

[1] O.H. Ismail, L. Pasti, A. Ciogli, C. Villani, J. Kocergin, S. Anderson, F. Gasparrini, A. Cavazzini, M. Catani, Pirkle-type chiral stationary phase on core–shell and fully porous particles: are superficially porous particles always the better choice toward ultrafast high-performance enantioseparations? J. Chromatogr. A 1466 (2016) 96–104.
[2] M. Catani, O.H. Ismail, F. Gasparrini, M. Antonelli, L. Pasti, N. Marchetti, S. Felletti, A. Cavazzini, Recent advancements and future directions of superficially porous chiral stationary phases for ultrafast high-performance enantioseparations, Analyst 142 (2017) 555–566.
[3] M. Catani, S. Felletti, O.H. Ismail, F. Gasparrini, L. Pasti, N. Marchetti, C.D. Luca, V. Costa, A. Cavazzini, New frontiers and cutting edge applications in ultra high performance liquid chromatography through latest generation superficially porous particles with particular emphasis to the field of chiral separations, Anal. Bioanal. Chem. (2018), http://dx.doi.org/10.1007/s00216-017-0842-4.
[4] D.C. Patel, Z.S. Breitbach, M.F. Wahab, C.L. Barhate, D.W. Armstrong, Gone in seconds: praxis, performance and peculiarities of ultrafast chiral liquid chromatography with superficially porous particles, Anal. Chem. 87 (2015) 9137–9148.
[5] C.L. Barhate, Z.S. Breitbach, E. Costa Pinto, E.L. Regalado, C.J. Welch, D.W. Armstrong, Ultrafast separation of fluorinated and desfluorinated pharmaceuticals using highly efficient and selective chiral selectors bonded to superficially porous particles, J. Chromatogr. A 1426 (2015) 241–247.
[6] D.C. Patel, M.F. Wahab, D.W. Armstrong, Z.S. Breitbach, Advances in high-throughput and high-efficiency chiral liquid chromatographic separations, J. Chromatogr. A 1467 (2016) 2–18.
[7] M.D. Dolzan, D.A. Spudeit, Z.S. Breitbach, W.E. Barber, G.A. Micke, D.W. Armstrong, Comparison of superficially porous and fully porous silica supports used for a cyclofructan 6 hydrophilic interaction liquid chromatographic stationary phase, J. Chromatogr. A 1365 (2014) 124–130.
[8] D.A. Spudeit, M.D. Dolzan, Z.S. Breitbach, W.E. Barber, G.A. Micke, D.W. Armstrong, Superficially porous particles vs. fully porous particles for bonded high performance liquid chromatographic chiral stationary phases: isopropyl cyclofructan 6, J. Chromatogr. A 1363 (2014) 89–95.
[9] M.F. Wahab, R.M. Wimalasinghe, Y. Wang, C.L. Barhate, D.C. Patel, D.W. Armstrong, Salient sub-second separations, Anal. Chem. 88 (2016) 8821–8826.
[10] R.M. Wimalasinghe, C.A. Weatherly, Z.S. Breitbach, D.W. Armstrong, Hydroxypropyl beta cyclodextrin bonded superficially porous particle-based HILIC stationary phases, J. Liq. Chromatogr. Relat. Technol. 39 (2016) 459–464.
[11] K. Lomsadze, G. Jibuti, T. Farkas, B. Chankvetadze, Comparative high-performance liquid chromatography enantioseparations on polysaccharide based stationary phases prepared by coating totally porous and core–shell silica particles, J. Chromatogr. A 1234 (2012) 50–55.
[12] Q. Kharaishvili, G. Jibuti, T. Farkas, B. Chankvetadze, Further proof to the utility of polysaccharide-based chiral selectors in combination with superficially porous silica particles as effective chiral stationary phases for separation of enantiomers in high-performance liquid chromatography, J. Chromatogr. A 1467 (2016) 163–168.
[13] O.H. Ismail, M. Antonelli, A. Ciogli, C. Villani, A. Cavazzini, M. Catani, S. Felletti, D.S. Bell, F. Gasparrini, Future perspectives in high efficient and ultrafast chiral liquid chromatography through zwitterionic teicoplanin-based 2 μm superficially porous particles, J. Chromatogr. A 1520 (2017) 91–102.
[14] O.H. Ismail, M. Catani, L. Pasti, A. Cavazzini, A. Ciogli, C. Villani, D. Kotoni, F. Gasparrini, D.S. Bell, Experimental evidence of the kinetic performance achievable with columns packed with the new 1.9 μm fully porous particles Titan c_{18}, J. Chromatogr. A 1454 (2016) 86–92.
[15] M. Catani, O.H. Ismail, A. Cavazzini, A. Ciogli, C. Villani, L. Pasti, D. Cabooter, G. Desmet, F. Gasparrini, D.S. Bell, Rationale behind the optimum efficiency of columns packed with the new 1.9 μm fully porous particles titan C_{18}, J. Chromatogr. A 1454 (2016) 78–85.
[16] C.L. Barhate, D.A. Lopez, A.A. Makarov, X. Bu, W.J. Morris, A. Lekhal, R. Hartman, D.W. Armstrong, E.L. Regalado, Macrocyclic glycopeptide chiral selectors bonded to core–shell particles enables enantiopurity analysis of the entire verubecestat synthetic route, J. Chromatogr. A 1539 (2018) 87–92.
[17] L. Sciascera, O. Ismail, A. Ciogli, D. Kotoni, A. Cavazzini, L. Botta, T. Szczerba, J. Kocergin, C. Villani, F. Gasparrini, Expanding the potential of chiral chromatography for high-throughput screening of large compound libraries by means of sub-2 μm Whelk-O1 stationary phase in supercritical fluid conditions, J. Chromatogr. A (2015) 160–168.
[18] D. Kotoni, A. Ciogli, I. D'Acquarica, J. Kocergin, T. Szczerba, H. Ritchie, C. Villani, F. Gasparrini, Enantioselective ultra-high and high performance liquid chromatography: a comparative study of columns based on the Whelk-O1 selector, J. Chromatogr. A 1269 (2012) 226–241.
[19] O.H. Ismail, A. Ciogli, C. Villani, M.D. Martino, M. Pierini, A. Cavazzini, D.S. Bell, F. Gasparrini, Ultra-fast high-efficiency enantioseparations by means of a teicoplanin-based chiral stationary phase made on sub-2 μm totally porous silica particles of narrow size distribution, J. Chromatogr. A 1427 (2016) 55–68.
[20] L. Bezhitashvili, A. Bardavelidze, T. Ordjonikidze, L. Chankvetadze, M. Chity, T. Farkas, B. Chankvetadze, Effect of pore-size optimization on the performance of polysaccharide-based superficially porous chiral stationary phases for the separation of enantiomers in high-performance liquid chromatography, J. Chromatogr. A 1482 (2017) 32–38.
[21] F. Gritti, G. Guiochon, Mass transfer kinetics, band broadening and column efficiency, J. Chromatogr. A 1221 (2012) 2–40.
[22] A. Felinger, Determination of rate constants for heterogeneous mass transfer kinetics in liquid chromatography, J. Chromatogr. A 1126 (2006) 120–128.
[23] D.C. Patel, Z.S. Breitbach, J. Yu, K.A. Nguyen, D.W. Armstrong, Quinine bonded to superficially porous particles for high-efficiency and ultrafast liquid and supercritical fluid chromatography, Anal. Chim. Acta 963 (2017) 164–174.
[24] A. Cavazzini, F. Gritti, K. Kaczmarski, N. Marchetti, G. Guiochon, Mass-transfer kinetics in a shell packing material for chromatography, Anal. Chem. 79 (2007) 5972–5979.
[25] N. Marchetti, A. Cavazzini, F. Gritti, G. Guiochon, Gradient elution separation and peak capacity of columns packed with porous shell particles, J. Chromatogr. A 1163 (2007) 203–211.
[26] F. Gritti, A. Cavazzini, N. Marchetti, G. Guiochon, Comparison between the efficiencies of columns packed with fully and partially porous C18-bonded silica materials, J. Chromatogr. A 1157 (2007) 289–303.
[27] G. Guiochon, F. Gritti, Shell particles, trials, tribulations and triumphs, J. Chromatogr. A 1218 (2011) 1915–1938.
[28] G. Guiochon, A. Felinger, D.G. Shirazi, A.M. Katti, Fundamentals of Preparative and Nonlinear Chromatography, second ed., Academic Press, Elsevier, 2006.
[29] F. Gritti, G. Guiochon, Possible resolution gain in enantioseparations afforded by core–shell particle technology, J. Chromatogr. A 1348 (2014) 87–96.
[30] F. Gritti, G. Guiochon, Mass transfer mechanism in chiral reversed phase liquid chromatography, J. Chromatogr. A 1332 (2014) 35–45.
[31] K. Kaczmarski, A. Cavazzini, P. Szabelski, D. Zhou, X. Liu, G. Guiochon, Application of the general rate model and the generalized Maxwell–Stefan equation to the study of the mass transfer kinetics of a pair of enantiomers, J. Chromatogr. A 962 (2002) 57–67.
[32] A. Felinger, D.M. Zhou, G. Guiochon, Determination of the single component and competitive adsorption isotherms of the 1-indanol enantiomers by the inverse method, J. Chromatogr. A 1005 (2003) 35–49.
[33] M. Catani, R. Guzzinati, N. Marchetti, L. Pasti, A. Cavazzini, Exploring fluorous affinity by liquid chromatography, Anal. Chem. 87 (2015) 6854–6860.
[34] P. Vajda, A. Cavazzini, A. Felinger, Adsorption equilibria of proline in hydrophilic interaction chromatography, J. Chromatogr. A 1217 (2010) 5965–5970.
[35] E. Morgan, K.W. Burton, Optimization using the super-modified simplex method, Chemom. Intell. Lab. 8 (1990) 97–107.
[36] A. Cavazzini, M. Remelli, F. Dondi, Stochastic theory of two-site adsorption chromatography by the characteristic function method, J. Microcolumn Sep. 9 (1997) 295–302.
[37] P. Jandera, V. Bačkovská, A. Felinger, Analysis of the band profiles of the enantiomers of phenylglycine in liquid chromatography on bonded teicoplanin columns using the stochastic theory of chromatography, J. Chromatogr. A 919 (2001) 67–77.
[38] D. Zhou, K. Kaczmarski, A. Cavazzini, X. Liu, G. Guiochon, Modeling of the separation of two enantiomers using a microbore column, J. Chromatogr. A 1020 (2003) 199–217.
[39] A. Cavazzini, F. Dondi, A. Jaulmes, C. Vidal-Madjar, A. Felinger, Monte Carlo model of nonlinear chromatography: correspondence between the microscopic stochastic model and the microscopic Thomas kinetic model, Anal. Chem. 74 (2002) 6269–6278.
[40] A. Cavazzini, M. Remelli, F. Dondi, A. Felinger, Stochastic theory of multiple-site linear adsorption chromatography, Anal. Chem. 71 (1999) 3453–3462.
[41] T. Fornstedt, P. Sajonz, G. Guiochon, A closer study of chiral retention mechanisms, Chirality 10 (1998) 375–381.
[42] G. Götmar, T. Fornstedt, G. Guiochon, Apparent and true enantioselectivity in enantioseparations, Chirality 12 (2000) 558–564.
[43] G. Götmar, T. Fornstedt, M. Andersson, G. Guiochon, Influence of the solute hydrophobicity on the enantioselective adsorption of beta-blockers on a cellulase protein used as the chiral selector, J. Chromatogr. A 905 (2001) 3–17.

[44] F. Gritti, G. Guiochon, Critical contribution of nonlinear chromatography to the understanding of retention mechanism in reversed-phase liquid chromatography, J. Chromatogr. A 1099 (2005) 1–42.
[45] A. Cavazzini, K. Kaczmarski, P. Szabełski, D.M. Zhou, X.D. Liu, G. Guiochon, Modeling of the separation of the enantiomers of 1-phenyl-1-propanol on cellulose tribenzoate, Anal. Chem. 73 (2001) 5704–5715.
[46] N. Marchetti, L. Caciolli, A. Laganà, F. Gasparrini, L. Pasti, F. Dondi, A. Cavazzini, Fluorous affinity chromatography for enrichment and determination of perfluoroalkyl substances, Anal. Chem. 84 (2012) 7138–7145.
[47] A. Cavazzini, N. Marchetti, R. Guzzinati, L. Pasti, A. Ciogli, F. Gasparrini, A. Laganá, Understanding mixed-mode retention mechanisms in liquid chromatography with hydrophobic stationary phases, Anal. Chem. 86 (2014) 4919–4926.
[48] F. Gritti, Y.V. Kazakevich, G. Guiochon, Effect of the surface coverage of endcapped C_{18}-silica on the excess adsorption isotherms of commonly used organic solvents from water in reversed phase liquid chromatography, J. Chromatogr. A 1169 (2007) 111–124.
[49] S. Bocian, P. Vajda, A. Felinger, B. Buszewski, Solvent excess adsorption on the stationary phases for reversed-phase liquid chromatography with polar functional groups, J. Chromatogr. A 1204 (2007) 35–41.
[50] K. Balmér, P.O. Lagerström, B.A. Persson, G. Schill, Reversed retention order and other stereoselective effects in the separation of amino alcohols on Chiralcel OD, J. Chromatogr. 592 (1992) 331–337.
[51] S. Ma, S. Shen, H. Lee, M. Eriksson, X. Zeng, J. Xu, K. Fandrick, N. Yee, C. Senanayake, N. Grinberg, Mechanistic studies on the chiral recognition of polysaccharide-based chiral stationary phases using liquid chromatography and vibrational circular dichroism: reversal of elution order of N-substituted alpha-methyl phenylalanine esters, J. Chromatogr. A 1216 (2009) 3784–3793.
[52] L. Chankvetadze, N. Ghibradze, M. Karchkhadze, L. Peng, T. Farkas, B. Chankvetadze, Enantiomer elution order reversal of fluorenylmethoxycarbonyl-isoleucine in high-performance liquid chromatography by changing the mobile phase temperature and composition, J. Chromatogr. A 1218 (2011) 6554–6560.
[53] R. Guzzinati, E. Sarti, M. Catani, V. Costa, A. Pagnoni, A. Martucci, E. Rodeghero, D. Capitani, M. Pietrantonio, A. Cavazzini, L. Pasti, Formation of supramolecular clusters at the interface of Zeolite X following the adsorption of rare-earth cations and their impact on the macroscopic properties of the Zeolite, ChemPhysChem (2018), http://dx.doi.org/10.1002/cphc.201800333.

Paper VI

Chromatographia
https://doi.org/10.1007/s10337-018-3606-1

REVIEW

Recent Achievements and Future Challenges in Supercritical Fluid Chromatography for the Enantioselective Separation of Chiral Pharmaceuticals

Simona Felletti[1] · Omar H. Ismail[2] · Chiara De Luca[1] · Valentina Costa[1] · Francesco Gasparrini[2] · Luisa Pasti[1] · Nicola Marchetti[1] · Alberto Cavazzini[1] · Martina Catani[1]

Received: 5 July 2018 / Revised: 28 August 2018 / Accepted: 3 September 2018

Abstract
During the last years, supercritical fluid chromatography (SFC) has attracted a continuously growing number of users. Thanks to the introduction of state-of-the-art equipment, this technique has allowed to run three-to-five times faster separations than in high-performance liquid chromatography (HPLC) on columns packed with particles of comparable dimension, at lower pressure drops and without loss of efficiency. Thanks to its high versatility, its high-throughput screening capability, and "green" character of the mobile phase, SFC has become particularly attractive for the separation of chiral drugs in pharmaceutical industries. In this review, we will consider the latest applications of SFC for the analysis of compounds of pharmaceutical interest and/or with biological activity essentially covering main achievements of the last 3 years. We also focus on some very recent, remarkable applications of SFC in ultrafast enantioseparations on chiral columns of the latest generation. Technical improvements needed on commercial equipment to increase the competitiveness of SFC towards highly efficient enantioseparations are discussed.

Keywords Supercritical fluid chromatography (SFC) · Chiral chromatography · Enantioseparations · Pharmaceuticals · Ultrafast enantioseparations

Introduction

Most of the molecules that play a key role in living organisms (such as amino acids, nucleic acids, sugars, pharmaceuticals) are chiral [1, 2]. Since biological interactions are strictly stereospecific, the two enantiomers may exhibit a completely different biological activity. It has been demonstrated that, in many cases, while one enantiomer is effectively active as therapeutic, the other one could be totally inactive or even toxic for the human body or the environment. As a consequence, identification of possible impurities and full characterization of chiral active pharmaceutical ingredients (APIs) are crucial steps for the development of drug substances. For this reason, the availability of high-performance analytical methods is fundamental at any stage of the production of pharmaceuticals or biomedical products, whose commercialization is strictly monitored by specific guidelines recommended by regulatory agencies [3–5].

Chromatography represents the most powerful technique nowadays in use for the separation of chiral compounds for both analytical and preparative purposes. Even if chiral high- (or ultra-high-) performance liquid chromatography (HPLC/UHPLC) still remains the first choice for the separation of enantiomers, during the last years, the attention of separation scientists has moved towards alternative methods, in particular supercritical fluid chromatography (SFC). This technique is based on the same principles as those of LC and, as a matter of fact, it makes use of the same software, hardware, and very similar instrumentation. The main difference is the replacement of common liquids used as mobile phases in LC with mixtures of high-pressurized carbon dioxide (CO_2) mixed with another solvent (most often methanol

Published in Chromatographia's 50th Anniversary Commemorative Issue.

✉ Martina Catani
ctnmtn@unife.it

[1] Department of Chemistry and Pharmaceutical Sciences, University of Ferrara, via L. Borsari 46, Ferrara 44121, Italy

[2] Department of Drug Chemistry and Technology, "Sapienza" University of Rome, P. le Aldo Moro 5, Rome 00185, Italy

Published online: 08 September 2018

or other alcohols). The use of CO_2 above its critical point leads to several advantages from a chromatographic viewpoint. Thanks to a lower viscosity and higher diffusion coefficients, chromatographic separations in SFC can be carried out at high flow rates without remarkable loss of efficiency and with very limited pressure drop along the column.

The development of SFC as a separation method has been somehow slow and discontinuous. The first report on the use of supercritical fluids in chromatography traces back to the 1960s [6], but, at that time, this approach did not attract much attention within the analytical community, having to compete with a well-established and traditional technique as GC. Twenty years later, neat supercritical fluid CO_2 found use, especially with open tubular columns but also with packed ones [7–14]. Despite promising kinetic performance, the widespread use of SFC has been limited by different factors. First, due to the GC-like conception of using a single fluid as mobile phase, this technique has been restricted mainly to the analysis of nonpolar compounds (the eluting strength of CO_2 is comparable to that of pentane). Other issues come from instrumental limitations such as the lack of UV sensitivity. During the 90s, SFC has started to be considered a competitive chromatographic method, especially for the purification of chiral compounds. Moreover, the introduction of a co-solvent opened the door for the analysis of polar molecules [15].

However, it is after 2010 that SFC has seriously started attracting a growing number of users not only for preparative applications but also for analytical purposes. In that period, latest generation SFC equipments have been commercialized with different technical improvements that enhanced reproducibility, sensitivity, and reliability of the system. As a matter of fact, in state-of-the-art equipments, extra-column variance is still dramatically larger (70–100 μL^2) than in modern UHPLC equipment (1–2 μL^2). As it will be shown later on, this is a main issue when using very efficient columns of reduced internal diameter packed with fine particles [16–18].

In general, the use of supercritical fluid CO_2/co-solvent mixtures has gained popularity over the last years as a "green" alternative to normal-phase or reversed-phase (NP or RP) LC separations. Another advantage is that, differently from LC, polar and hydrophobic stationary phases can be operated in SFC with the same mobile phase, representing a powerful orthogonal method for different analytical applications, especially for chiral separations, as described in past detailed review papers [14, 15, 19].

This review is not intended to be a comprehensive overview of SFC covering all the aspects of this technique from fundamentals of separation to instrumental aspects. Many detailed works [14, 15, 18–22] have been recently published to which the interested reader is referred to. Scope of this paper is to provide an overview of the most recent advances in chiral SFC, covering literature of the past 3 years. In particular, we will focus on the last applications reported in the literature for rapid high-throughput separation of chiral pharmaceuticals and on the last achievements in ultrafast (sub-minute) chiral SFC separations. A short section on the use of SFC for preparative applications is also included in the last part of the manuscript.

SFC in a Glance

In SFC, the mobile phase is a supercritical fluid. This is a particular state of matter reached when temperature and pressure are near or above the critical point. For pure CO_2, which is the most common supercritical fluid used in chromatography, these values are $T_c = 31$ °C and $P_c = 74$ bar. Fluids exhibit particular properties in supercritical conditions that are intermediate between those of gases and liquids. In particular, density is similar to that of liquids, viscosity is comparable to that of gases, and diffusivity is midway. For these reasons, SFC is considered an intermediate separation technique between gas chromatography (GC) and HPLC. As a marginal remark, the term SFC is also often extended to applications in which temperature is kept below than the critical one, since there is no phase transition when pressure is maintained above 74 bar.

Neat supercritical fluid CO_2 is a nonpolar solvent, comparable to pentane. However, it is rarely used as single eluent. Organic modifiers, such as methanol or other alcohols, are routinely used as co-solvents. Their introduction not only increases the polarity of the mobile phase, hence the solvating power, but it also affects density of the mobile phase. In addition, several different additives (e.g., trifluoroacetic acid, triethylamine, and ammonium acetate) are often added to the mobile phase, enhancing solvating power or favoring ion-pairing with charged analytes. Also water is used sometimes as a ternary mixture, allowing for the elution of the most polar compounds, such as peptides and amphoteric molecules [21].

Density plays a key role on different chromatographic parameters in SFC. First, molecular interactions, and hence retention, but also viscosity, diffusivity, and mobile phase velocity are strongly influenced by changes in density. Density profile along the column is affected by any change in pressure and temperature. A significant variation in density could have a detrimental effect on column efficiency due to the formation of radial temperature gradients when CO_2 is operated under high compressibility conditions [18]. For the reason above, modern SFC instruments are designed to ensure isothermal or adiabatic conditions of the column and a strict control of pressure. Moderate temperature and high pressure ensure a higher density of fluid, further contributing to maintain the conditions away from the critical point

(where the situation is the worst). In addition, the use of co-solvents greatly reduces compressibility.

Recent Applications of SFC for the Analysis of Pharmaceuticals Divided by the Type of Chiral Stationary Phase

Polysaccharide-Based CSPs

The most employed class of CSPs used in SFC is that based on immobilized polysaccharide derivatives [14, 15, 23]. The widespread use of cellulose- and amylose-based CSPs can be ascribed especially to their large applicability and their high loadability. This latter characteristic has represented the main reason for the success of these CSPs for preparative purposes in the past [15, 24].

However, in the last few years, 3 or 5 µm fully porous particles (FPPs) polysaccharide-based CSPs have been mainly used for analytical purposes. Recent works also report the use of 2.5 µm polysaccharide FPPs [25–27]. In the following, the main applications of polysaccharide CSPs in SFC will be revised.

High-Throughput Screenings

In a recent paper, different cellulose- and amylose-based 3 µm FPPs CSPs have been successfully employed for high-throughput screening of 20 pharmaceuticals (including ketoprofen, ibuprofen, and epinephrine) in only 4 min, followed by 2 min of column equilibration [28]. The mobile phases used were CO_2/methanol or CO_2/2-propanol mixtures plus a combined additive of trifluoroacetic acid and diethylamine. The simultaneous presence of both the two organic modifiers was found to be beneficial for the enhancement of enantioselectivity.

Retention mechanism of 13 pairs of enantiomers belonging to the same structural family (phenylthiohydantoin-amino acids) has been studied on two different polysaccharide stationary phases (Chiralpak AD-H, amylose-based and Chiralpak OD-H, and cellulose-based) at five different temperatures ranging from 5 up to 40 °C [29]. The mobile phase used was CO_2/methanol 90:10 %v/v. Some structural changes seem to affect both CSPs above 20–30 °C. Below this limit, it was found that retention is substantially unaffected by temperature changes on the cellulose-based column. On the contrary, remarkable differences in retention factors have been observed on the Chiralpak AD-H by changing temperature. According to the authors of this work, this result suggests the presence of more heterogeneous chiral sites on the amylose-based CSP than on the cellulose one. However, another reason that could explain the observed behavior may be the higher rigidity of cellulose-based CSPs with respect to amylose-based ones.

To enhance the possibility to carry out high-throughput analysis, multiple injections in a single experimental run (MISER) chromatographic technique has been applied in SFC with a 10 × 4.0 mm (L × I.D.) Chiralpak AD-3 column packed with 3 µm FPPs. This high-throughput method is based on multiple injections within a single chromatographic run to produce a continuous trace of chromatograms. The separation of Tröger's base enantiomers in an entire 96-well microplate of samples has been performed in 33 min (Fig. 1) [30]. However, this approach is currently limited by the speed of autosamplers. Faster instrument control softwares are required to extensively apply MISER SFC to rapid enantiopurity screenings of a large number of samples.

Determination of Enantiopurity of APIs and Their Intermediates

One of the most challenging tasks for pharmaceutical industries is the reduction of the number of separation modes required for the analysis of an API and its intermediates. Due to its versatility, SFC appears one of the most appealing chromatographic methods for this purpose.

Barhate et al. have investigated a large number of chromatographic CSPs by both RPLC and SFC for the determination of enantiomeric excess of verubecestat (employed in clinical trials for the treatment of Alzheimer's disease) and its intermediates [31]. The best results have been obtained in RPLC using a teicoplanin-based CSP made on 2.7 µm superficially porous particles (SPPs), but cellulose-based chiral columns produced very promising results in SFC for the determination of enantiopurity of the entire verubecestat synthetic route.

Bu et al. have also recently applied SFC for the analysis of poor UV absorbing drugs and synthetic intermediates with charged aerosol detection (CAD) [32]. Enantiomeric excess has been determined under both gradient and isocratic elution conditions, and compared with results obtained with UV detection. A strong correlation between UV and CAD responses under isocratic conditions was observed, while, under gradient conditions, higher absolute errors between the two measures were registered, due to the fact that high amount of organic modifier enhances CAD response of later eluting compounds. In the same work, the practical use of SFC-CAD has been investigated for high-throughput parallel screening of chemo- and bio-catalytic reactions for the quick identification of desired reaction conditions. Twenty-four different hydrolase enzymes were screened in parallel on a well plate and the two isomeric monoacid products were separated on a Chiralpak AD-3 column in less than 2 h.

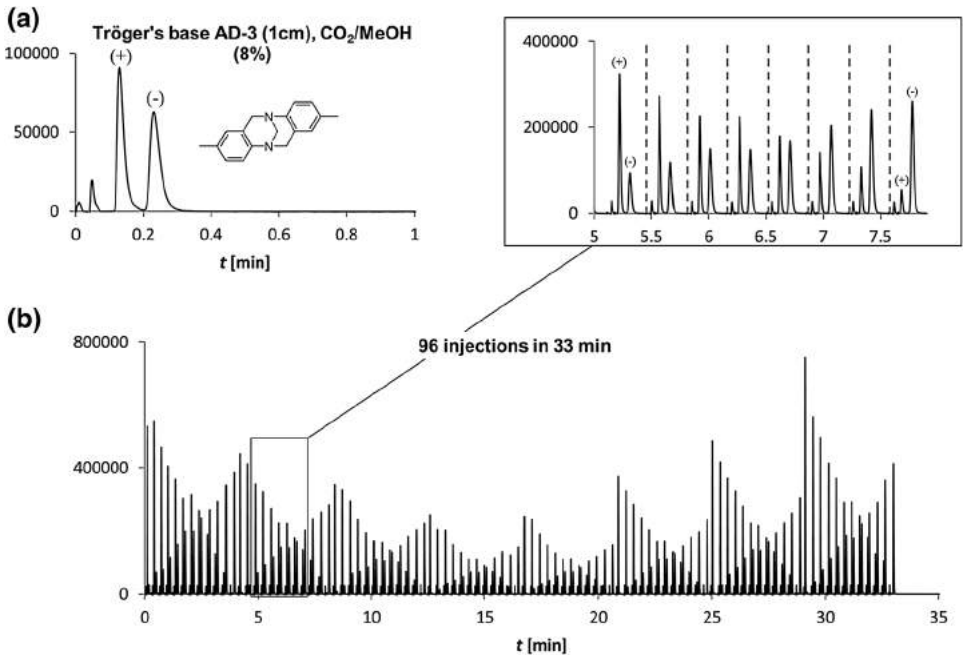

Fig. 1 **a** Separation of Tröger's base enantiomers on a 10 × 4.0 mm (L × I.D.) Chiralpak AD-3 column packed with 3 µm FPPs functionalized with an amylose derivative. **b** Injection of a 96-well plate with MISER approach on the same column. Tröger's base concentrations between 0.4 and 1 mg/mL. Reproduced with permission from Ref. [30]

Comparison Between Chiral SFC and HPLC

Different studies have been recently conducted to compare retention mechanism of enantiomers on polysaccharide-based CSPs in SFC and different LC conditions.

West et al. have compared retention of 24 chiral sulfoxides on seven different polysaccharide CSPs with CO_2 /methanol mixtures as mobile phase, proving that chlorinated cellulose CSPs are better in terms of both retention and enantioselectivity towards molecules containing a chiral sulfur atom [33]. By means of molecular modeling measurements, the authors of this paper demonstrated that molecules that could adopt a folded U-shaped conformation were most efficiently discriminated compared to linear ones. Moreover, SFC was compared to polar organic mode (POM) HPLC. It was found that the chiral selector must adopt a different conformation in the two operating modes. However, SFC outperformed POM HPLC in terms of enantioresolution.

Recently, retention mechanisms of different pairs of enantiomers on polysaccharide CSPs have been explored in both SFC and NPLC conditions. It has been demonstrated that the transposability of methods from NPLC to SFC can be challenging in some cases, mainly due to different interactions (hydrogen bonding and accessibility of chiral cavities) contributing to retention in the two chromatographic modes [34, 35]. Separations in NPLC resulted in shorter retention times and higher enantioresolution for the separation of dihydropyridine derivatives, especially if bearing two chiral centers [36]. Indeed, scope of this work was the investigation of chromatographic conditions transfer from NPLC to SFC (this explains reported larger retention times in SFC). Despite higher retention times, selectivity was not consistently better in SFC, meaning that the additional retention was due to nonspecific interactions of enantiomers with the CSP.

Vera et al. have compared selectivity of a Lux Cellulose-1 towards retention of FMOC-protected amino acids in SFC, NPLC, and RPLC conditions [37]. In terms of retention, SFC lies in the middle between RPLC and NPLC. Although RPLC gave comprehensively the best enantioresolution, the introduction of 2% formic acid as additive in CO_2/methanol mixture used in SFC provided comparable results in shorter run time, allowing for a better resolution per unit of time.

Chiral SFC–MS Methods

Even if RPLC–MS is still considered the gold standard for the analysis of serum, urine, and plasma samples, in the last years, SFC has been efficiently hyphenated with mass spectrometry giving very promising results.

A reliable SFC–MS/MS method for the separation of amphetamine enantiomers in biological samples has been developed and validated for the first time by Hegstad et al in Ref. [38]. R- and S-amphetamine enantiomers were baseline resolved using a Chiralpak AD-3 column and CO_2/2-propanol+0.2% cyclohexylamine as mobile phase. This method has been routinely used for the analysis of several human urine samples representing a reliable tool to discriminate between legal use of amphetamine as therapeutic (in most countries, only the S-enantiomer is prescribed) and illegal use (as racemic mixture).

Jenkinson et al. have recently developed a new SFC–MS/MS method for the analysis of metabolites of vitamin D in human serum [39]. The separation has been achieved in 6 min on a Lux Cellulose column using CO_2/methanol+0.1% formic acid as eluent. Concentrations of metabolites measured on 41 routine human serum samples have been found to be in accordance with those measured by means of UHPLC-MS/MS. In addition, structurally similar metabolites, differing only for the position or direction of an hydroxyl group, have been resolved and quantified by means of the optimized SFC–MS/MS method.

A 3 µm FPPs Chiralpak IA was efficiently used to separate panthenol enantiomers in cosmetic formulations (such as creams, body lotions, and exfoliants) [40]. Since only the D-enantiomer of panthenol is active as therapeutic, reliable methods to assess enantiopurity of formulated cosmetics are required. The column was employed in SFC conditions (CO_2 with 11% methanol as mobile phase) with both UV and MS detection. The online coupling improved sensitivity (LOQ as low as 0.5 µg/mL), since underivatized panthenol has a poor signal in UV.

Multidimensional Chromatography

Chiral SFC has also been applied as the second dimension in highly selective multidimensional chromatography approaches to assess purity of chiral APIs. A first (achiral) RPLC dimension is needed to assess the amount of impurities and related substances, while the second (chiral) dimension is used to evaluate the possible presence of undesired enantiomers [41]. Such a system has been applied for the quantitative analysis of an API, its metabolites, and their corresponding enantiomers in a mouse hepatocyte treated sample using Chiralpak IB-3 and AD-3 columns (Fig. 2) [42].

Other Applications

Immobilized amylose-based CSPs have been proved to be useful for the separation of basic biologically active compounds, whose separation has always been challenging in SFC [43]. The authors of this work investigated the effect of co-solvent, temperature, and backpressure on the enantioseparation of 27 different compounds bearing a basic moiety including amphetamine, cathinone, benzofury, and amino-naphthol derivatives. It was found that adding bases (or the mixture of base and acid) to the mobile phase has a beneficial effect on peak shape and enantioresolution.

Polysaccharide-based CSPs have been also successfully used for the separation of chiral compounds with biological activity such as pesticides containing sulfur or phosphorous atoms [44], fungicides (i.e., fenbuconazole) in foods [45], and herbicides (i.e., napropramide) [46].

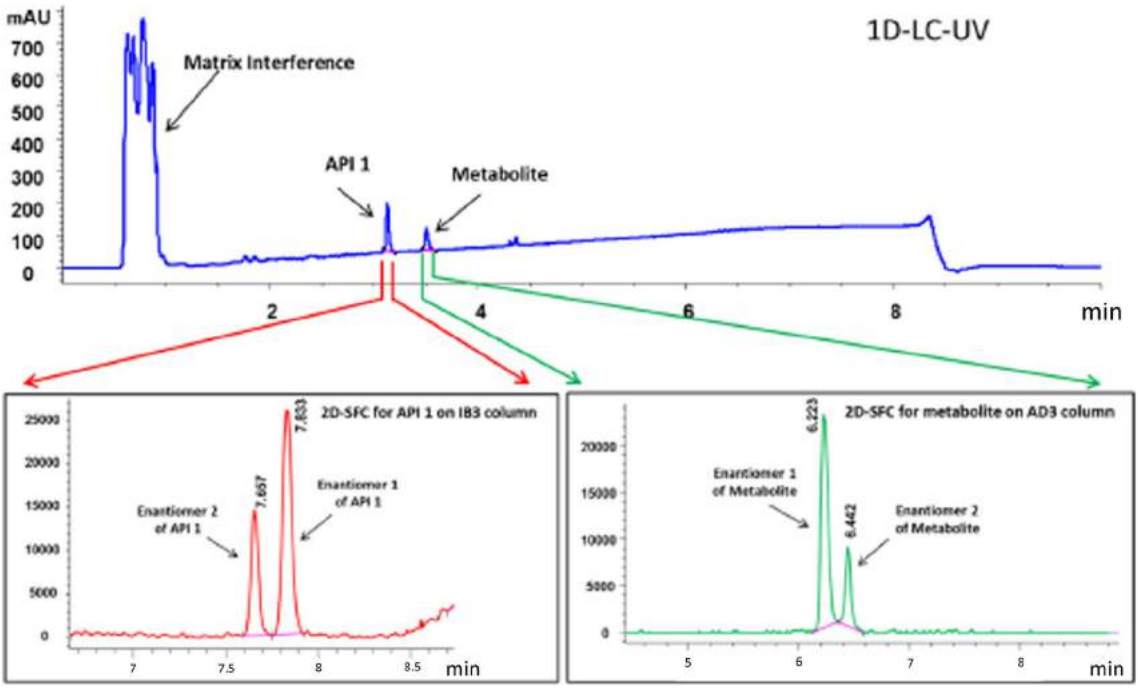

Fig. 2 2D LC-SFC analysis of an API and its metabolite. First dimension: achiral RPLC (top); second dimension: chiral SFC (bottom). Reproduced with permission from Ref. [42]

Pirkle-type CSPs

Pirkle-type (or brush-type) chiral selectors are among the most versatile, allowing for the separation of a broad range of compounds. They represent the first class of CSPs that has been prepared on sub-2µm format [47–49]. One of the main advantages of these CSPs is that they exist in both the enantiomeric versions. Using columns functionalized with the same chiral selector but with opposite configuration, it is possible to reverse the elution order of enantiomers (the so-called "Inverted Chirality Columns Approach", ICCA). This method has been recently applied by Mazzoccanti et al. to determine the enantiomeric excess of phytocannabinoids in marijuana samples for therapeutic use [50]. Indeed, many problems can be faced when working with Cannabis plant extracts. Not only are they highly complex mixtures but also the minor enantiomer is not always available as reference sample. Moreover, in many cases, it can partially coelute with the main enantiomer. Two complementary—(S,S) and (R,R)—Whelk-O1 CSPs made on sub-2µm FPPs have been employed in SFC conditions (CO_2/methanol, 98:2 %v/v) to determine the enantiomeric excess of (-)-Δ^9-THC in medicinal marijuana (Bedrocan®). Thanks to ICCA protocol, besides the major enantiomer ((−)-4 peak in Fig. 3), a not negligible concentration (0.13%) of the (+)-enantiomer ((+)-4 peak in Fig. 3) has been detected. The enantiomeric excess was estimated to be 99.73%.

The same sub-2µm FPP (S,S)-Whelk-O1 CSP has been used for the high-throughput screening of a large library of 129 pharmaceutical compounds with different chemicophysical properties including β-blockers, antidepressants, anticancers, and benzodiazepines, to name but a few [51]. The overall screening was completed in 24 h under fast gradient elution (9 min total analysis time, including column reconditioning) using a mixture of CO_2/methanol as mobile phase with a success rate of 63%. Even basic racemic mixtures, whose separation is traditionally challenging on Whelk-O1 CSPs prepared on larger particles, have been resolved with the sub-2µm CSP used in this work.

Macrocyclic Glycopeptide CSPs

Macrocyclic glycopeptide CSPs allow for the separation of underivatized amino acids. This class of CSP has been rarely used in SFC to date.

Recently, however, a 5 µm teicoplanin CSP (Chirobiotic T2) has been efficiently employed for the separation of D,L-enantiomers of underivatized phenylalanine (Phe), tyrosine (Tyr), and tryptophan (Trp) amino acids. Baseline separations have been obtained in less than 7 min using CO_2 and 40% of organic modifier made of a mixture of methanol/water (90:10 %v/v) [52]. LOD in the range of 0.5–2.0 µg/mL allowed for the determination of D-enantiomers up to 0.2%. This method has been applied for the determination of enantiopurity of five commercial food supplements confirming the absence of impurities in all of them. The authors have also investigated the possibility to simultaneously determine D,L-Phe and D,L-Tyr by coupling a diol achiral column (first dimension) with the Chirobiotic T2 (second dimension). The separation was obtained in about 15 min.

Cyclofructan-based CSPs

Recently developed cyclofructan-based 2.7 µm SPP CSPs have been employed by Armstrong and coworkers to investigate the transposability of chromatographic methods from NPLC to SFC for the enantioseparation of 21 α-aryl ketones [53]. The mobile phase used in NPLC was a mixture of heptanol/ethanol with percentages ranging from 95:5 to 99:1 %v/v. The same compositions have been transposed to SFC

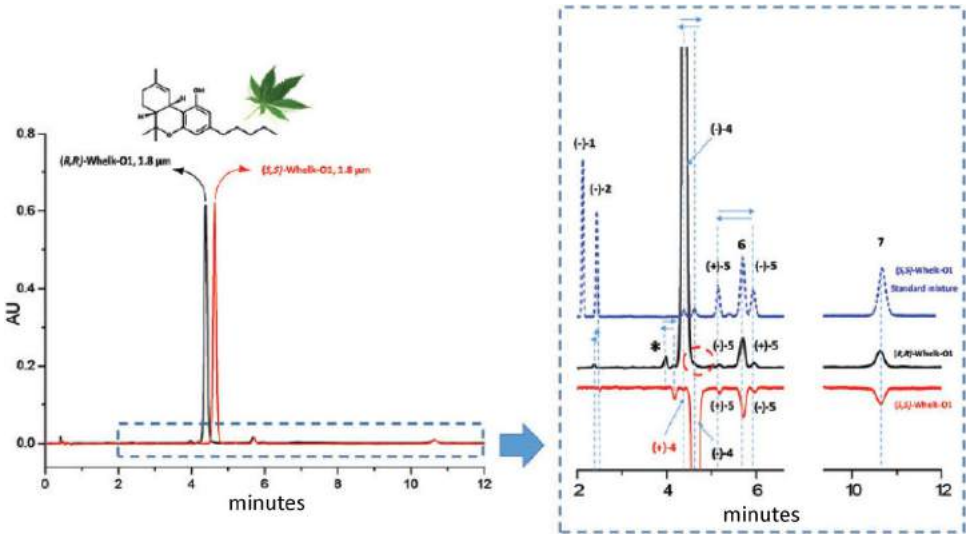

Fig. 3 Chromatograms of a Bedrocan® ethanol extract analyzed by applying the ICCA protocol. A zoom of the chromatogram between 2 and 6 min is shown in the inset together with the separation of a standard mixture of six-component cannabinoids (dotted chromatogram). The asterisk denotes a chiral unknown impurity. Reproduced from Ref. [50] with permission from The Royal Society of Chemistry

by replacing heptanol with CO_2. 17 of the 21 compounds have been baseline separated in NP conditions, while 10 out to 21 compounds via SFC. Even if the latter allowed for lower analysis time, HPLC provided better resolutions due to greater enantioselectivity values.

Ion-Exchange CSPs

The use of ion-exchange CSPs in SFC is very recent. Lajkó et al. have first used Cinchona alkaloid-based ZWIX(+) and ZWIX(-) CSPs for the enantioseparation of N_α-Fmoc proteinogenic amino acids [54]. The effect of methanol content in the mobile phase and different additives (water, acids, and bases) has been investigated to optimize separation conditions. The addition of water led to the formation of carbonic acid, imparting acidic character to the mobile phase. It was also found that a reduction of temperature has a beneficial effect on enantioresolution, meaning that chiral recognition mechanism is enthalpically controlled.

The chromatographic behavior of the ZWIX(+) column in both HPLC and SFC conditions was compared for the separation of acidic, basic, and zwitterionic species [55]. In general, SFC provided a better enantioresolution than HPLC, but there is evidence that separation mechanism is completely different. By constantly increasing the amount of organic modifier (methanol) in SFC, it was found that the ion-exchange mechanism is strongly influenced by the formation of transient acidic species (carbonic acid mono methyl ester). Finally, it was proved that basic additives are not strictly necessary when using the zwitterionic column, and they could have an effect only on basic analytes.

Towards High-Efficiency Ultrafast SFC Enantioseparations

The recent achievements in particle manufacturing have allowed to prepare very efficient particle formats, such as SPPs or sub-2µm FPPs, functionalized with chiral selectors. The introduction of these new CSPs packed into columns of very short length has represented a real breakthrough in the field of UHPLC enantioseparations, not only in terms of efficiency (comparable to those of achiral RPLC) but also in terms of speed of separation (analysis time < 1 s) [31, 48, 51, 56–67].

Since SFC allows to run chromatographic separations at higher flow rates than LC without remarkable loss of efficiency [68], the use of new generation CSPs under these conditions seems to be a promising approach to achieve even faster separations.

Some of the authors of this work have recently obtained very fast enantioseparations using both Teicoplanin and Whelk-O1 CSPs under SFC conditions [51, 59].

In the first case, Teicoplanin was bonded to 1.9 µm FPPs and packed into a 20 × 4.6 mm (L × I.D) column operated at 4 mL/min. The enantiomers of Ketorolac have been resolved in less than 70 s on a chiral selector which has been considered a "slow" one [59].

In the second case, using a 50 × 4.6 mm (L × I.D) column packed with 1.8 µm FPPs functionalized with Whelk-O1, the separation of abscisic acid enantiomers has been obtained in less than 45 s (flow rate 3.5 mL/min) with a resolution (R_s) of 2.2 (see Fig. 4a) [51].

Very remarkable results in terms of ultrafast enantioseparations have been reported by Armstrong and coworkers. Sub-minute separations of different pairs of enantiomers

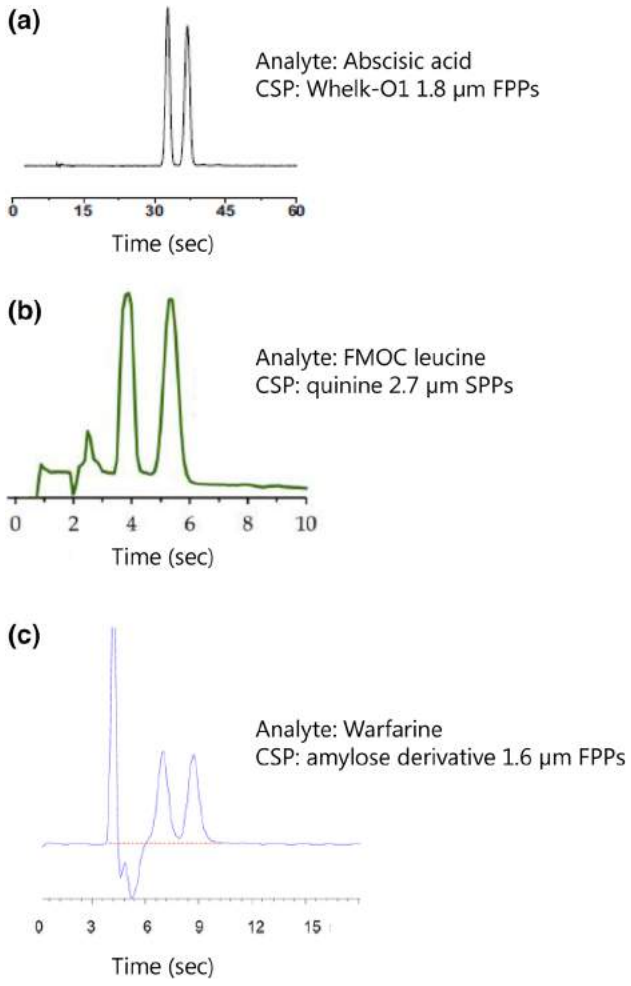

Fig. 4 Examples of ultrafast enantioseparations obtained in SFC. **a** Abscisic acid enantiomers. Column: 50 × 4.6 mm (L × I.D), Whelk-O1 1.8 µm FPPs. Flow rate: 3.5 mL/min. Instrument: Waters Acquity UPC^2. Modified with permission from Ref. [51]. **b** FMOC leucine enantiomers. Column: 30 × 4.6 (L × I.D), quinine-based 2.7 µm SPPs. Flow rate: 20 mL/min. Instrument: Jasco SFC-2000-7. Modified with permission from Ref. [70]. **c** Warfarin enantiomers. Column: 50 × 3 mm (L × ID), amylose-based 1.6 µm FPPs. Flow rate: 3.75 mL/min. Instrument: low-dispersion-modified Agilent 1260 Infinity SFC. Modified with permission from Ref. [72]

of pharmaceutical interest have been obtained on teicoplanin and teicoplanin aglycone CSPs made on 1.9 µm FPPs packed into 50 × 4.6 mm (L × ID) columns at a flow rate of 7 mL/min [69]. Moreover, using a 30 × 4.6 (L × I.D) column packed with 2.7 µm SPPs functionalized with a quinine derivative, they were able to obtain the separation of different amino acids in 6–8 s with a flow rate of 20 mL/min [70]. An example is shown in Fig. 4b.

However, the use of new generation CSPs in SFC is often partially limited by some instrumental issues. The excessively large extra-column band broadening of current SFC instruments has a detrimental effect on the overall chromatographic performance.

Berger has recently modified a commercial 1260 Infinity SFC from Agilent Technology, by replacing standard tubing (170 µm ID) and flow cell (13 µL internal volume) with 120 µm ID tubing (of shortest possible length) and a 2 µL internal volume cell [71]. The extra-column dispersion was reduced to about 6–9 μL^2. With the new configuration, he was able to achieve more than 280,000 plates/m (reduced HETP of 1.93) by employing a prototype 50 × 4.6 mm (L × ID) column packed with 1.8 µm Whelk-O1 FPPs. In addition, he reported about the ultrafast separations of 5-methyl 5-phenyl hydantoin enantiomers in roughly 10 s (flow rate 5 mL/min).

Using the same instrumental setup, he has been the first to operate a sub-2µm-immobilized polysaccharide CSP in SFC conditions [72]. Using a 50 × 3 mm (L × ID) column packed with an amylose-based CSPs made on 1.6 µm FPPs, he was able to obtain the ultrafast separation of warfarin enantiomers in less than 10 s (flow rate 3.75 mL/min) with a resolution of 1.5 (see Fig. 4c).

Recently, some of the authors of this work have modified a commercial Waters Acquity UPC^2 SFC instrument by a series of technical adjustments including the replacement of (i) standard tubings with shorter and narrower capillaries; (ii) the 8 µL flow cell with a 3 µL one; (iii) the injection system with a 200 nL fixed-loop external one; (iv), finally, using an ad hoc designed external column oven [73]. The extra-column variance was reduced from about 85 μL^2 (original configuration) to slightly more than 2 μL^2 (optimized configuration) measured at 2.0 mL/min. Kinetic performance of a 50 × 4.6 mm (L × ID) column packed with 1.8 µm Whelk-O1 FPPs operated on the optimized SFC instrument has been compared with that obtained on a commercial UHPLC instrument (Waters Acquity I-Class) with extra-column variance of 1 μL^2. At the minimum of the van Deemter curve, SFC provided a gain of 10% on the efficiency of the second enantiomer (285,000 N/m *vs.* 260,000 N/m recorded in UHPLC) in roughly 50% shorter analysis time. The expression ultra-high-performance SFC (UHPSFC) can be properly used under these conditions.

In addition, Barhate et al. have demonstrated that, when running ultrafast SFC separations, some unexpected results could be observed [74]. These deviations, not detected in LC, are mostly due to the noise generated by backpressure regulators and the presence of low viscosity eluent inside connection tubings. The latter is responsible for the development of possible turbulent flow inside tubings which could change both retention time and peak shape.

Preparative SFC for the Purification of Chiral Pharmaceuticals

Preparative SFC is routinely used for the purification of chiral drugs in pharmaceutical industries [14]. This technique offers several advantages over preparative LC such as higher productivity, thanks to the possibility of using higher flow rates, lower organic solvent consumption, reduced impact on the environment, and faster solvent removal. In terms of stationary phases, polysaccharide-based ones are the most used for preparative applications owing to their high loadability [75]. However, scale-up from analytical to preparative conditions is more complex in SFC than in LC due to the high compressibility of the mobile phase. Indeed, this may cause possible variations in density, pressure, and temperature that possibly modify the adsorption process on the stationary phase. Besides these variables, also the content of organic modifier is an important parameter that needs to be taken into account. Most of the time, optimization procedures are based on the variation of one of these parameters, while all the others are kept constant. For this reason, ultrafast enantioseparation methods are increasingly required during screening processes. However, different parameters could present interaction effects. To face this problem, chemometric approaches, such as design of experiment (DOE), are increasingly used to find the optimal experimental conditions for purification purposes, taking into account the simultaneous effect of different variables [76–78].

Perspectives

Due to the unique properties of supercritical fluid CO_2, SFC can be considered not only a "greener" alternative to HPLC but also an orthogonal and, in some cases, more versatile method of separation. This is particularly important for high-throughput screenings at the beginning of the production of new drugs, when the number of unknown impurities could be relevant.

One of the fields in which SFC will be increasingly used is in multidimensional applications, especially RPLC × SFC achiral–chiral separations. However, particular attention has to be put on the interface between the first RPLC dimension

and the SFC one, especially to avoid the injection of large volumes of water. Different approaches have been already proposed. Particularly interesting is the use of collection loops [79] or active modulators [80] that seem to be able to solve some of the issues encountered in this coupling [81].

Thanks to the introduction of latest generation CSPs made on sub-3µm SPPs and sub-2µm FPPs packed into short columns (2–5 cm), the first examples of enantioseparations in less than one minute or even in the order of seconds have been obtained also in SFC. This is a very promising field in which SFC could be expected to emerge as a gold technique. However, as demonstrated in recent works [71–73], some technical optimizations aimed at the reduction of extra-column band broadening are needed on commercial equipments. This can be obtained not only by replacing standard tubings with small capillaries but also using low-dispersion ovens and flow cells in the order of nanoliters. These improvements will increase competitiveness of UHPSFC towards UHPLC.

From a fundamental point of view, the investigation of mass transfer phenomena in SFC is necessary to understand how diffusion coefficients possibly change with pressure and temperature and their effect on column efficiency. Moreover, due to the lower mobile phase viscosity, turbulent flow effects have been clearly demonstrated through capillaries connecting the injector system to the column and the column to the detector. From an experimental point of view, this is accompanied by a nonlinear dependence of system back-pressure on the flow rate (contrary to what happens when the Darcy's law is applicable). When turbulence is developing, increasingly growing inertial effects become dominant and the relationship between flow and pressure is not linear any longer [82]. The main consequence of turbulence is the improvement in mass transfer [83] even if, on the other hand, experimental findings show that, through a packed bed, turbulence is much more difficult to develop (at least at the flow rates commonly employed in SFC). These findings could be the basis to renew the interest in chiral open tubular columns for SFC applications, since, through them, maintaining of turbulent regime should be possible. These concepts were proposed more than 50 years ago in the fundamental work of J. C. Giddings [83] when, however, technology was not advanced enough to permit their practical realization. The use of open tubular chiral columns on low-dispersion SFC equipments could lead to unmatched kinetic performance in chromatography.

Compliance with ethical standards

Conflict of interest The authors declare that they have no conflict of interest.

Ethical approval This article does not contain any studies with human participants or animals performed by any of the authors.

References

1. Nikolai LN, McClure EL, Macleod SL, Wong CS (2006) Stereoisomer quantification of the beta-blocker drugs atenolol, metoprolol, and propranolol in wastewaters by chiral high-performance liquid chromatography-tandem mass spectrometry. J Chromatogr A 1131:103–109
2. Sanganyado E, Lu Z, Fu Q, Schlenk D, Gan J (2017) Chiral pharmaceuticals: a review on their environmental occurrence and fate processes. Water Res 124:527–542
3. Liu JT, Liu RH (2002) Enantiomeric composition of abused amine drugs: chromatographic methods of analysis and data interpretation. J Biochem Biophys Methods 54:115–146
4. Nguyen LA, He H, Pham-Huy C (2006) Chiral drugs: an overview. J Biochem Biophys Methods 2:85–100
5. International conference on harmonization, IQ32A (R2): Impurities in new drug substances (2006)
6. Klesper E, Corwin AH, Turner DA (1962) High pressure gas chromatography above critical temperatures. J Org Chem 27:700–701
7. Novotny M, Springston SR, Paeden PA, Fjeldsted JC, Lee ML (1981) Capillary supercritical fluid chromatography. Anal Chem 53:407A–411A
8. Paeden PA, Fjeldsted JC, Springston SR, Lee ML, Novotny M (1982) Instrumental aspects of capillary supercritical fluid chromatography. Anal Chem 54:1090–1093
9. Springston SR, Novotny M (1981) Kinetic optimization of capillary supercritical fluid chromatography using carbon dioxide as the mobile phase. Chromatographia 14:679–684
10. Paeden PA, Lee ML (1983) Theoretical treatment of resolving power in open tubular column supercritical fluid chromatography. J Chromatogr 259:1–16
11. Gere DR, Board R, McManigill D (1982) Supercritical fluid chromatography with small particle diameter packed columns. Anal Chem 54:736–740
12. Crowther JB, Henion JD (1985) Supercritical fluid chromatography of polar drugs using small-particle packed columns with mass spectrometric detection. Anal Chem 57:2711–2716
13. Schwarz HE (1987) LC-GC 5:14–22 Kindly provide article title for reference [13].
14. Desfontaine V, Guillarme D, Francotte E, Nováková L (2015) Supercritical fluid chromatography in pharmaceutical analysis. J Pharm Biomed Anal 113:56–71
15. Lemasson E, Bertin S, West C (2016) Use and practice of achiral and chiral supercritical fluid chromatography in pharmaceutical analysis and purification. J Sep Sci 39:212–233
16. Perrenoud AGG, Veuthey JL, Guillarme D (2012) Comparison of ultra-high performance supercritical fluid chromatography and ultra-high performance liquid chromatography for the analysis of pharmaceutical compounds. J Chromatogr A 1266:158–167
17. Berger TA, Berger BK (2013) Separation of natural food pigments in saponified and un-saponified paprika oleoresin by ultra high performance supercritical fluid chromatography (UHPSFC). Chromatographia 76:591–601
18. Poole, C.F. (ed.) (2017) Supercritical fluid chromatography, 1st Edition. Elsevier, New York
19. Kalíková K, Šlechtová T, Vozka J, Tesařová E (2014) Supercritical fluid chromatography as a tool for enantioselective separation; a review. Anal Chim Acta 821:1–33
20. Lesellier E, West C (2015) The many faces of packed column supercritical fluid chromatography—a critical review. J Chromatogr A 1382:2–46
21. Tarafder A (2016) Metamorphosis of supercritical fluid chromatography to sfc: an overview. TrAC 81:3–10
22. Vozka J, Kalíková K, Roussel C, Armstrong DW, Tesařová E (2013) An insight into the use of dimethylphenyl carbamate

cyclofructan 7 chiral stationary phase in supercritical fluid chromatography: the basic comparison with HPLC. J Sep Sci. 81:1711–1719
23. Mangelings D, Heyden YV (2008) Chiral separations in sub- and supercritical fluid chromatography. J Sep Sci 31:1252–1273
24. Cavazzini A, Kaczmarski K, Szabelski P, Zhou D, Liu X, Guiochon G (2002) Modeling of the separation of the enantiomers of 1-phenyl-1-propanol on cellulose tribenzoate. J Chromatogr A 73:5705–5715
25. Li L (2016) Direct enantiomer determination of methorphan by HPLC-MS and SFC-MS. Forensic Chem 2:82–85
26. Carnes S, O'Brien S, Szewczak A, Tremeau-Cayel L, Rowe WF, McCord B, Lurie IS (2017) Comparison of ultra high performance supercritical fluid chromatography, ultra high performance liquid chromatography, and gas chromatography for the separation of synthetic cathinones. J Sep Sci 40:3545–3556
27. Hegstad S, Havnen H, Helland A, Falch BMH, Spigset O (2017) Enantiomeric separation and quantification of citalopram in serum by ultra-high performance supercritical fluid chromatography-tandem mass spectrometry. J Chromatogr B 1061–1062:103–109
28. Nováková L, Douša M (2017) General screening and optimization strategy for fast chiral separations in modern supercritical fluid chromatography. Anal Chim Acta 950:199–210
29. Khater S, Canault B, Azzimani T, Bonnet P, West C (2018) Thermodynamic enantioseparation behavior of phenylthiohydantoin-amino acid derivatives in supercritical fluid chromatography on polysaccharide chiral stationary phases. J Sep Sci 41:1450–1459
30. Kawatzki K, Biba M, Regalado EL, Welch CJ (2016) Miser chiral supercritical fluid chromatography for high throughput analysis of enantiopurity. J. Chromatogr. A 1429:374–379
31. Barhate CL, Lopez DA, Makarov AA, Bu X, Morris WJ, Lekhal A, Hartman R, Armstrong DW, Regalado EL (2018) Macrocyclic glycopeptide chiral selectors bonded to core-shell particles enables enantiopurity analysis of the entire verubecestat synthetic route. J Chromatogr A 1539:87–92
32. Bu X, Regalado EL, Cuff J, Schafer W, Gong X (2016) Chiral analysis of poor uv absorbing pharmaceuticals by supercritical fluid chromatography-charged aerosol detection. J Supercrit Fluids 116:20–25
33. West C, Konjaria ML, Shashviashvili N, Lemasson E, Bonnet P, Kakava R, Volonterio A, Chankvetadze B (2017) Enantioseparation of novel chiral sulfoxides on chlorinated polysaccharide stationary phases in supercritical fluid chromatography. J Chromatogr A 1499:174–182
34. Khater S, Lozac'h MA, Adam I, Francotte E, West C (2016) Comparison of liquid and supercritical fluid chromatography mobile phases for enantioselective separations on polysaccharide stationary phases. J Chromatogr A 1467:463–472
35. Kalíková K, Martínková M, Schmidt MG, Tesařová E (2018) Cellulose tris-(3,5-dimethylphenylcarbamate)-based chiral stationary phase for the enantioseparation of drugs in supercritical fluid chromatography: comparison with HPLC. J Sep Sci 41:1471–1478
36. Hoguet V, Charton J, Hecquet PE, Lakhmi C, Lipka E (2018) Supercritical fluid chromatography versus high performance liquid chromatography for enantiomeric and diastereoisomeric separations on coated polysaccharides-based stationary phases: Application to dihydropyridone derivatives. J Chromatogr A 1549:39–50
37. Vera CM, Shock D, Dennis GR, Farrell W, Shalliker RA (2017) Comparing the selectivity and chiral separation of D- and L-fluorenylmethyloxycarbonyl chloride protected amino acids in analytical high performance liquid chromatography and supercritical fluid chromatography; evaluating throughput, economic and environmental impact. J Chromatogr A 1493:10–18
38. Hegstad S, Havnen H, Helland A, Spigset O, Frost J (2018) Enantiomeric separation and quantification of R/S-amphetamine in urine by ultra-high performance supercritical fluid chromatography tandem mass spectrometry. J Chromatogr B 1077–1078:7–12
39. Jenkinson C, Taylor A, Storbeck KH, Hewison M (2018) Analysis of multiple vitamin d metabolites by ultra-performance supercritical fluid chromatography-tandem mass spectrometry (UPSFC-MS/MS). J Chromatogr B 1087–1088:43–48
40. Khater S, West C (2015) Development and validation of a supercritical fluid chromatography method for the direct determination of enantiomeric purity of provitamin B5 in cosmetic formulations with mass spectrometric detection. J Pharm Biomed Anal 102:321–325
41. Venkatramani CJ, Al-Sayah M, Li G, Goel M, Girotti J, Zang L, Wigman L, Yehl P, Chetwyn N (2016) Simultaneous achiral-chiral analysis of pharmaceutical compounds using two-dimensional reversed phase liquid chromatography-supercritical fluid chromatography. Talanta 148:548–555
42. Goel M, Larson E, Venkatramani CJ, Al-Sayah M (2018) Optimization of a two-dimensional liquid chromatography-supercritical fluid chromatography-mass spectrometry (2D-LC-SFS-MS) system to assess in-vivo inter-conversion of chiral drug molecules. J Chromatogr B 1084:89–95
43. Geryk R, Kalíková K, Schmid MG, Tesařova E (2016) Enantioselective separation of biologically active basic compounds in ultra-performance supercritical fluid chromatography. Anal Chim Acta 932:98–105
44. Zhang L, Miao Y, Lin C (2018) Enantiomeric separation of six chiral pesticides that contain chiral sulfur/phosphorus atoms by supercritical fluid chromatography. J Sci Sep 41:1460–1470
45. Tao Y, Zheng Z, Yu Y, Xu J, Liu X, Wu X, Dong F, Zheng Y (2018) Supercritical fluid chromatographytandem mass spectrometry-assisted methodology for rapid enantiomeric analysis of fenbuconazole and its chiral metabolites in fruits, vegetables, cereals, and soil. Food Chem 241:32–39
46. Zhao L, Xie J, Guo F, Liu K (2018) Enantioseparation of napropamide by supercritical fluid chromatography: effects of the chromatographic conditions and separation mechanism. Chirality 30:661–669
47. Cavazzini A, Marchetti N, Guzzinati R, Pierini M, Ciogli A, Kotoni D, D'Acquarica I, Villani C, Gasparrini F (2014) Enantioseparation by ultra-high-performance liquid chromatography. Trends Anal Chem 63:95–103
48. Cancelliere G, Ciogli A, D'Acquarica I, Gasparrini F, Kocergin J, Misiti D, Pierini M, Ritchie H, Simone P, Villani C (2010) Transition from enantioselective high performance to ultra-high performance liquid chromatography: a case study of a brush-type chiral stationary phase based on sub-5-micron to sub-2-micron silica particles. J Chromatogr A 1217:990–999
49. Catani M, Ismail OH, Felletti S, Gasparrini F, Pasti L, Costa V, Cavazzini A (2017) Pirkle-type chiral stationary phases for ultra-high performance ultra-fast enantioseparations. Am Pharmaceut Rev 20
50. Mazzoccanti G, Ismail OH, D'Acquarica I, Villani CM, Wilcox CM, Cavazzini A, Gasparrini F (2017) Cannabis through the looking glass: chemo- and enantio-selective separation of phytocannabinoids by enantioselective ultra high performance supercritical fluid chromatography. Chem Commun 53:12262–12265
51. Sciascera L, Ismail O, Ciogli A, Kotoni D, Cavazzini A, Botta L, Szczerba T, Kocergin J, Villani C, Gasparrini F (2015) Expanding the potential of chiral chromatography for high-throughput screening of large compound libraries by means of sub-2 μm Whelk-O1 stationary phase in supercritical fluid conditions. J Chromatogr A 1383:160–168
52. Sánchez-Hernández L, Bernal JL, del Nozal MJ, Toribio L (2016) Chiral analysis of aromatic amino acids in food supplements usingsubcritical fluid chromatography and chirobiotic T2 column. J Supercrit Fluids 107:519–525

53. Breitbach AS, Lim Y, Xu QL, Kürti YL, Armstrong DW, Breitbach ZS (2016) Enantiomeric separations of α-aryl ketones with cyclofructan chiral stationary phases via high performance liquid chromatography and supercritical fluid chromatography. J Chromatogr A 1427:45–54
54. Lajkó G, Ilisz I, Tóth G, Fülöp F, Lindner W, Péter A (2015) Application of Cinchona alkaloid-based zwitterionic chiral stationary-phases in supercritical fluid chromatography for theenantioseparation of n_α-protected proteinogenic amino acids. J Chromatogr A 1415:134–145
55. Wolrab D, Frühauf P, Gerner C, Kohout M, Lindner W (2017) Consequences of transition from liquid chromatography to supercritical fluid chromatography on the overall performance of a chiral zwitterionic ion-exchanger. J Chromatogr A 1517:165–175
56. Rocchi S, Fanali C, Fanali S (2015) Use of a novel sub-2 µm silica hydride vancomycin stationary phase in nano-liquid chromatography. ii. Separation of derivatized amino acid enantiomers. Chirality 27:767–772
57. Barhate CL, Breitbach ZS, Costa Pinto E, Regalado EL, Welch CJ, Armstrong DW (2015) Ultrafast separation of fluorinated and defluorinated pharmaceuticals using highly efficient and selective chiral selectors bonded to superficially porous particles. J Chromatogr A 1426:241–247
58. Kotoni D, Ciogli A, D'Acquarica I, Kocergin J, Szczerba T, Ritchie H, Villani C, Gasparrini F (2012) Enantioselective ultra-high and high performance liquid chromatography: a comparative study of columns based on the Whelk-O1 selector. J Chromatogr A 1269:226–241
59. Ismail OH, Ciogli A, Villani C, Martino MD, Pierini M, Cavazzini A, Bell DS, Gasparrini F (2016) Ultra-fast high-efficiency enantioseparations by means of a teicoplanin-based chiral stationary phase made on sub-2 µm totally porous silica particles of narrow size distribution. J Chromatogr A 1427:55–68
60. Ismail OH, Catani M, Pasti L, Cavazzini A, Ciogli A, Villani C, Kotoni D, Gasparrini F, Bell DS (2016) Experimental evidence of the kinetic performance achievable with columns packed with the new 1.9 µm fully porous particles Titan C_{18}. J Chromatogr A 1454:86–92
61. Ismail OH, Pasti L, Ciogli A, Villani C, Kocergin J, Anderson S, Gasparrini F, Cavazzini A, Catani M (2016) Pirkle-type chiral stationary phase on coreshell and fully porousparticles: Are superficially porous particles always the better choice toward ultrafast high-performance enantioseparations? J Chromatogr A 1466:96–104
62. Kharaishvili Q, Jibuti G, Farkas T, Chankvetadze B (2016) Further proof to the utility of polysaccharide-based chiral selectors in combination with superficially porous silica particles as effective chiral stationary phases for separation of enantiomers in high-performance liquid chromatography. J Chromatogr A 1467:163–168
63. Catani M, Ismail OH, Gasparrini F, Antonelli M, Pasti L, Marchetti N, Felletti S, Cavazzini A (2017) Recent advancements and future directions of superficially porous chiral stationary phases for ultrafast high-performance enantioseparations. Analyst 142:555–566
64. Ismail OH, Antonelli M, Ciogli A, Villani C, Cavazzini A, Catani M, Felletti S, Bell DS, Gasparrini F (2017) Future perspectives in high efficient and ultrafast chiral liquidchromatography through zwitterionic teicoplanin-based 2µm superficially porous particles. J Chromatogr A 1520:91–102
65. Catani M, Felletti S, Ismail OH, Gasparrini F, Pasti L, Marchetti N, Luca CD, Costa V, Cavazzini A (2018) New frontiers and cutting edge applications in ultra high performance liquid chromatography through latest generation superficially porous particles with particular emphasis to the field of chiral separations. Anal Bioanal Chem 410:2457–2465
66. Patel DC, Breitbach ZS, Wahab MF, Barhate CL, Armstrong DW (2015) Gone in seconds: praxis, performance and peculiarities of ultrafast chiral liquid chromatography with superficially porous particles. Anal Chem 87:9137–9148
67. Spudeit DA, Dolzan MD, Breitbach ZS, Barber WE, Micke GA, Armstrong DW (2014) Superficially porous particles vs. fully porous particles for bonded high performance liquid chromatographic chiral stationary phases: Isopropyl cyclofructan 6. J Chromatogr A 1363:89–95
68. Regalado EL, Welch CJ (2015) Pushing the speed limit in enantioselective supercritical fluid chromatography. J Sep Sci 38:2826–2832
69. Barhate CL, Wahab MF, Breitbach ZS, Bell DS, Armstrong DW (2015) High efficiency, narrow particle size distribution, sub-2 µm based macrocyclic glycopeptide chiral stationary phases in HPLC and SFC. Anal Chim Acta 898:128–137
70. Patel DC, Breitbach ZS, Yu J, Nguyen KA, Armstrong DW (2017) Quinine bonded to superficially porous particles for high-efficiency and ultrafast liquid and supercritical fluid chromatography. Anal Chim Acta 963:164–174
71. Berger TA (2016) Kinetic performance of a 50 mm long 1.8 µm chiral column in supercritical fluid chromatography. J Chromatogr A 1459:136–144
72. Berger TA (2017) Preliminary kinetic evaluation of an immobilized polysaccharide sub-2 µm column using a low dispersion supercritical fluid chromatograph. J Chromatogr A 1510:82–88
73. Ismail OH, Losacco GL, Mazzoccanrti G, Ciogli A, Villani C, Catani M, Pasti L, Anderson S, Cavazzini A, Gasparrini F (2018) Unmatched kinetic performance in enantioselective supercritical fluid chromatography by combining latest generation Whelk-O1 chiral stationary phases with a low-dispersion in-house modified equipment. Anal Chem. https://doi.org/10.1021/acs.analchem.8b01907
74. Barhate CL, Wahab MF, Tognarelli DJ, Berger TA, Armstrong DW (2016) Instrumental idiosyncrasies affecting the performance of ultrafast chiral and achiral sub/supercritical fluid chromatography. Anal Chem 88:8664–8672
75. Speybrouck D, Lipka E (2016) Preparative supercritical fluid chromatography: a powerful tool for chiral separations. J Chromatogr A 1467:33–55
76. Galea C, Mangelings D, Vander Heyden Y (2015) Method development for impurity profiling in SFC: the selection of a dissimilar set of stationary phases. J Pharm Biomed Anal 111:333–343
77. Enmark M, Åsberg D, Leek H, Öhlén K, Klarqvist M, Samuelsson J, Fornstedt T (2015) Evaluation of scale-up from analytical to preparative supercritical fluid chromatography. J Chromatogr A 1425:280–286
78. Landagaray E, Vaccher C, Yous S, Lipka E (2016) Design of experiments for enantiomeric separation in supercritical fluid chromatography. J Pharm Biomed Anal 120:297–305
79. Sun M, Sandahl M, Turner C (2018) Comprehensive on-line two-dimensional liquid chromatography × supercritical fluid chromatography with trapping column-assisted modulation for depolymerised lignin analysis. J Chromatogr A 1541:21–30
80. Gargano AFG, Duffin M, Navarro P, Schoenmakers PJ (2016) Reducing dilution and analysis time in online comprehensive two-dimensional liquid chromatography by active modulation. Anal Chem 88:1785–1793
81. Francois I, Pereira AD, Lynen F, Sandra P (2008) Construction of a new interface for comprehensive supercritical fluid chromatography x reversed phase liquid chromatography (SFC × RPLC). J Sep Sci 1541:21–30
82. Pauw RD, Choikhet K, Desmet G, Broeckhoven K (2014) Occurrence of turbulent flow conditions in supercritical fluid chromatography. J Chromatogr A 1361:277–285
83. Giddings JC (1965) Dynamics of Chromatography. Marcel Dekker, New York

Paper VII

Journal of Chromatography A xxx (xxxx) xxx

Contents lists available at ScienceDirect

Journal of Chromatography A

journal homepage: www.elsevier.com/locate/chroma

Modeling the nonlinear behavior of a bioactive peptide in reversed-phase gradient elution chromatography

Chiara De Luca[a], Simona Felletti[a], Marco Macis[b], Walter Cabri[b], Giulio Lievore[a], Tatiana Chenet[a], Luisa Pasti[a], Massimo Morbidelli[c], Alberto Cavazzini[a,*], Martina Catani[a,*], Antonio Ricci[b]

[a] Dept. of Chemistry and Pharmaceutical Sciences, University of Ferrara, via L. Borsari 46, Ferrara 44121, Italy
[b] Fresenius Kabi iPSUM, via San Leonardo 23, Villadose, Rovigo 45010, Italy
[c] Dept. of Chemistry and Applied Biosciences, Institute for Chemical and Bioengineering, ETH Zurich, Vladimir-Prelog-Weg 1, Zurich 8093, Switzerland

ARTICLE INFO

Article history:
Received 22 October 2019
Revised 9 December 2019
Accepted 12 December 2019
Available online xxx

Keywords:
Pharmaceutical peptides
Gradient elution
Adsorption isotherms
Reversed-phase liquid chromatography (RP-LC)
Inverse method
Preparative chromatography

ABSTRACT

The thermodynamic behavior of octreotide, a cyclic octapeptide with important pharmaceutical functions, has been simulated under reversed-phase gradient elution conditions. To this end, adsorption behavior was firstly investigated in isocratic conditions, under a variety of water/acetonitrile + 0.02% (v/v) trifluoroacetic acid (TFA) mixtures as mobile phase by using a Langmuir isotherm. Organic modifier was varied in the range between 23 and 28% (v/v). Adsorption isotherms were determined by means of the so-called Inverse Method (IM) with a minimum amount of peptide. The linear solvent strength (LSS) model was used to find the correlation between isotherm parameters and mobile phase composition. This study contributes to enlarge our knowledge on the chromatographic behavior under nonlinear gradient conditions of peptides. In particular, it focuses on a cyclic octapeptide.

1. Introduction

Peptides represent a unique class of biochemical compounds. They are of primary importance in human physiology, being able to selectively interact with cells, receptors and other endogenous peptides and to induce specific biological reactions [1,2]. The interest on the use of peptides in pharmaceuticals (e.g., as antitumorals, anticoagulant, anti-hypertensive, antioxidant, antimicrobial drugs), nutraceuticals (for fortification of functional foods) and cosmetics (for skin health and care) is continuously increasing [3–7]. Due to their very high specificity, therapeutic peptides are competitive and advantageous over traditional drugs since they can be effective even at extremely low concentration [7,8]. Moreover, peptides do not accumulate in the human body nor in the environment after they have been excreted, minimizing possible toxic side effects.

From an industrial point of view, therapeutic peptides are produced by two main routes: recombinant synthesis [9] or chemical synthesis strategy [10].

The first one involves the use of suitable microorganisms to produce peptide of interest, through its trascription-transduction machinery [11]. The chemical synthesis approach can be further subdivided into two main strategies: Liquid Phase Peptide Synthesis (LPPS) and Solid Phase Peptide Synthesis (SPPS) [12]. In both cases, the approach involves the use of amino acids ortogonally protected as to enable the specific generation of the desired amino acid sequence through repetitive peptide bond formation. In any case, both recombinant and chemical synthesis do not generally produce target API peptide with an acceptable purity for market requirement. Purification is therefore needed to get the target peptide at the desired degree of purity for therapeutic and pharmaceutical scopes [5,13]. The downstream process (purification and recovery of the target peptide) takes up an important percentage of total manufacturing costs [14].

Preparative liquid chromatography is the most widely used technique for the purification of therapeutic peptides [15–18]. With the purpose of isolating finite amounts of pure compounds, in preparative (or nonlinear) chromatography large volumes of concentrated multicomponent feed are processed at a time. Under overloaded conditions, retention of analytes becomes concentration-dependent, being the adsorption isotherm of the analyte nonlinear. Thus, injected compounds are not eluted from the

* Corresponding author.
E-mail addresses: cvz@unife.it (A. Cavazzini), ctnmtn@unife.it (M. Catani).

https://doi.org/10.1016/j.chroma.2019.460789
0021-9673/

column as a series of Gaussian peaks but chromatograms appear as a complex mixture of tailed bands that may also change shape by increasing sample size. The problems encountered in nonlinear chromatography are extremely complex, not only owing to the effect of nonlinear adsorption isotherms on peak shapes, but also to the dependence of the amount of any component adsorbed on the concentrations of all the species in solution (competitive systems) [19–21]. Even though the theory of nonlinear chromatography has advanced to the point that quantitative predictions are possible, in preparative chromatography, working conditions are usually optimized through trial and error methods, which may cause significant waste of time and compound and thus money. As a matter of fact, when it comes to the separation/purification of (poly)peptides, some general guidelines can be applied to start with. However, the application of these protocols is not a guarantee that the process will be successful. Many aspects in this field require significant experimental and theoretical efforts to improve our understanding of the fundamentals of separation. For instance, the chromatographic behavior of two quasi-identical polypeptides under nonlinear conditions can dramatically change when even a single amino acid differs in their structure. It is well known that the adsorption model for the same peptide can also change not only by changing the mobile phase composition but also depending on the concentration of the peptide itself. But there are no means to predict if and how this will happen. There are, e.g., cases of polypeptides where the curvature of the adsorption isotherm inverts, by moving from one mobile phase modifier to another. Other times, by increasing the concentration of the polypeptide under investigation, the adsorption isotherm, initially Langmuirian, becomes S-shaped. The presence of an inflection point on the isotherm may strongly affect the shape of overloaded peaks. This explains why, in our opinion, it is so important to develop methodologies based on the measurement of adsorption isotherms. The investigation of adsorption behavior and phase equilibria involved in the separation of the target compound using a model-based approach is, therefore, the basis not only to investigate the feasibility of purification process via preparative chromatography but also to possibly provide information (e.g., maximum loading, affinity for the stationary phase) that may help to optimize large-scale purification [16,22–26]. This is particularly important in pharmaceutical manufacturing, where continuous (or semi-continuous) processes could alleviate the trade-off between yield and purity, typical of most batch (single-column) preparative chromatographic separations [27,28]. The first multi-column setup is the so-called simulated moving bed (SMB) process introduced in 1950 for isocratic binary separations of small molecules [19,29–32]. Since then, many different improved versions of continuous processes based on SMB concepts have been proposed to overcome some fundamental issues (process optimization, difficulty to deal with complex mixtures, gradient operation) and technical problems associated to the large number of columns to be operated simultaneously. The most important alternative to SMB is the multi-column counter-current solvent gradient purification (MCSGP) process, which combines linear gradients with the counter-current movement of mobile and stationary phases [33]. Originally realized with at least six columns, the process has modified in order to work with four [34], three columns [35] and more recently only two columns [36]. It has been demonstrated that the outcome of twin column MCSGP processes is easily predictable from batch chromatographic runs [37]. As a consequence, the results of investigation of thermodynamic equilibria influencing the separation in batch conditions can be used during process design to more efficiently move to continuous separations, which are extremely attractive for pharmaceutical industry to replace batch technologies [38–42].

In this work, the adsorption behavior of a therapeutic peptide, octreotide, has been investigated and modeled under reversed-phase liquid chromatography (RP-LC) gradient elution conditions. Octreotide is a cyclic octapeptide belonging to somatostatins [43,44]. Its industrial production can be obtained either with LPPS or SPPS approaches [45] and it is employed in the treatment of hepatocellular carcinoma, cirrhosis of the liver and to contrast some symptomps associated with metastatic carcinoid and Vasoactive Intestinal Peptide (VIP) tumors [46]. Adsorption isotherms of octreotide have been measured on a commercial C_{18} stationary phase by means of the so-called Inverse Method (IM) [19,47–54]. Goal of this work is to demonstrate how the adsorption behavior of octreotide under nonlinear gradient conditions can be predicted with a very low amount of compound and extremely reduced costs with respect to more traditionals techniques of isotherm determination, such as for instance frontal analysis.

2. Theory

2.1. Equilibrium-dispersive model of chromatography

The equilibrium-dispersive (ED) model of chromatography is mostly used to describe nonlinear chromatographic separations for molecules with low molecular weight [19]. This model assumes that mobile and stationary phases are in costant equilibrium and that all the contributions to band broadening (diffusion phenomena and finite rate of mass transfer kinetics) can be lumped into a unique apparent dispersion coefficient, D_a [19]:

$$D_a = \frac{uL}{2N} \tag{1}$$

where u is the mobile phase linear velocity, L the length of the column and N the number of theoretical plates.

The differential mass balance equation describing the accumulation of material in a thin slice of column of thickness ∂z in a ∂t time interval is [19]:

$$\frac{\partial C}{\partial t} + F\frac{\partial q}{\partial t} + u\frac{\partial C}{\partial z} = D_a\frac{\partial^2 C}{\partial z^2} \tag{2}$$

where C and q the concentrations of the analyte in the mobile and stationary phases. $F = (1-\epsilon_t)/\epsilon_t$ is the phase ratio and $\epsilon_t = V_0/V_{col}$ the total porosity of the column (with V_0 and V_{col} the thermodynamic void volume and the column voume, respectively).

In order to solve Eq. (2), an isotherm model ($q = f(C)$), expressing q as a function of C, must be chosen.

2.2. Modeling of overloaded profiles under gradient elution chromatography

In gradient elution RP-LC, the volume fraction (ϕ) of the organic modifier in the mobile phase is gradually increased during a chromatographic run. Differently from isocratic conditions, the adsorption isotherm of a species in gradient elution mode is ϕ- (and time-) dependent [53,55,56]. For this reason, it is usually considered that, even if the adsorption isotherm type is not affected by changes in mobile phase composition, its parameters are a function of ϕ [57].

In addition, the Linear Solvent Strength (LSS) model [58–60] is applied to describe the variation of retention factor with the mobile phase composition:

$$\ln k(\phi) = \ln k_0 - S\phi \tag{3}$$

with k_0 the retention factor extrapolated at $\phi = 0$ and S a coefficient characteristic of the system solute-mobile phase.

By considering a simple Langmuir isotherm model (under isocratic elution conditions):

$$q = \frac{aC}{1+bC} \tag{4}$$

Please cite this article as: C. De Luca, S. Felletti and M. Macis et al., Modeling the nonlinear behavior of a bioactive peptide in reversed-phase gradient elution chromatography, Journal of Chromatography A, https://doi.org/10.1016/j.chroma.2019.460789

where b and $a(= q_s b)$ are the equilibrium and Henry constants of adsorption, respectively (being q_s the saturation capacity), the dependence of isotherm parameters on ϕ could be obtained by combining Eq. (3) and the following relationship between k and a:

$$k = aF \tag{5}$$

It follows that:

$$a(\phi) = a_0\, e^{(-S\phi)} \tag{6}$$

where $a_0\ (= k_0/F)$ is the Henry constant (extrapolated) at $\phi = 0$.

If the range of variation of ϕ is sufficiently narrow, q_s can be considered constant [19,61,62] and, as a consequence, b and ϕ are correlated by the same relation as in Eq. (6):

$$b(\phi) = b_0\, e^{(-S\phi)} \tag{7}$$

where b_0 is the adsorption constant at $\phi = 0$.

By combining Eqs. (4), (6) and (7), the Langmuir isotherm describing the adsorption process under gradient elution conditions can be obtained:

$$q(\phi) = \frac{q_s\, b_0\, e^{(-S\phi)} C}{1 + b_0\, e^{(-S\phi)} C} \tag{8}$$

The mass balance equation (Eq. (2)) can be numerically solved by applying a finite difference method based on the so-called backward-backward scheme [19,63].

Lastly, boundary and initial conditions need to be defined in order to solve the mass balance equation. The Danckwerts-type boundary conditions have been applied [19,64,65] while the gradient in the inlet feed has been simulated as follows:

$$\phi(t,0) = \begin{cases} \phi_0 & 0 \le t \le t_{inj} \\ \phi_0 + \frac{\Delta\phi}{t_g}(t - t_{inj}) & t_{inj} \le t \le t_{inj} + t_g \\ \phi_0 + \Delta\phi & t \ge t_{inj} + t_g \end{cases} \tag{9}$$

where t_{inj} is the length of the rectangular injection profile, ϕ_0 is the initial fraction of organic modifier and t_g is the time of the gradient.

3. Experimental

Column and materials

All solvents were purchased from Sigma–Aldrich (St. Louis, MI, USA). A 150 × 4.6 mm Zorbax Sb-C18 column (5 µm particle size, 80 Å pore size) used to perform separations was from Agilent Technologies (Santa Clara, California, USA). Uracile (Sigma–Aldrich, St. Louis, MI, USA) was injected for the determination of the void volume of the column. Pure and crude (= not purified) mixtures of octreotide were from Fresenius Kabi iPSUM (Villadose, Rovigo, Italy). Crude sample is the product obtained after solid-phase synthesis.

Equipment All the measurements were carried out on an Agilent 1100 Series Capillary LC system equipped with a binary pump system, a column thermostat set at 35 °C and a photodiode array detector. A manually Rheodyne 8125 injecting valve was employed by using different loops to perform detector calibration (500 µ) and injections of overloaded profiles (5, 10, 20 µ). All the experimental profiles were recorded at UV wavelengths of 280 nm, at flow rate of 1 mL/min. Maximum absorbance was below 1000 mAU.

Measurement of overloaded profiles

Overloaded band profiles in both isocratic and gradient elution conditions have been recorded by injecting solutions of peptide with different concentrations: 0.1, 0.3, 0.6, 1.2, 2.0, 4.0 and 6.0 g/L.

Mobile phase A (MP-A) was a solution of 0.02% (v/v) trifluoroacetic acid (TFA) in water, while mobile phase B (MP-B) was 0.02% (v/v) TFA in acetonitrile (ACN). The gradient program was set as follows: (i) the column was firstly equilibrated with 10% (v/v) of MP-B; (ii) in a first linear ramp the percentage of MP-B was increased from 10% to 30% (v/v) over a gradient time, t_{g1}, of 12 min (gradient slope = 1.6% ACN/min); (iii) in a second steeper ramp MP-B was changed from 30% to 90% (v/v) in 3 min, t_{g2} (slope = 20% ACN/min).

Overloaded profiles under isocratic elution conditions were recorded in a range of MP-B from 23% to 28% (v/v). Solubility limit of the peptide in these conditions is 9.0 g/L.

Adsorption isotherm determination

Adsorption isotherms under isocratic elution conditions have been calculated by means of the so-called Inverse Method [19,47,51,66–68]. This method allows the determination of the adsorption isotherm in a few steps, requiring less amount of samples and solvents than other alternative techniques, such as frontal analysis [19,51,68]. The first necessary step is the calibration of the detector. In order to do this, the column has been replaced with a zero-dead-volume connector and 500 µL of each solution of peptide with different concentration have been injected into the system. This operation has been performed for each mobile phase composition. Not surprisingly, differences in detector response were negligible in the very small operative concentration range considered in this work. The maximum absorbance (*Abs*) of each plateau at 280 nm has been recorded and reported in a curve as a function of *C*. Then, (i) experimental profiles at the seven concentrations have been recorded in overloading conditions; (ii) overloaded profiles *Abs vs. t* have been converted into *C vs. t* through the slope of the calibration curve; (iii) an isotherm type and a guess of its initial parameters have been selected; (iv) a system of equations including the mass balance equation and the selected adsorption isotherm have been solved in order to obtain a calculated overloaded profile; (v) the calculated overloaded profile and the experimental *C vs. t* one have been compared; (vi) isotherm parameters have been iteratively changed until the calculated and experimental profiles match as much as possible (the numerical optimization was made by means of the Simplex method, minimizing the sum of the squares of the differences between simulated and experimental profiles) [47,66,69].

4. Results and discussion

Fig. 1 reports an experimental chromatogram recorded under gradient elution conditions by injecting 5 μL of the solution of crude octreotide. The main peak (t_R = 12.5 min) corresponds to

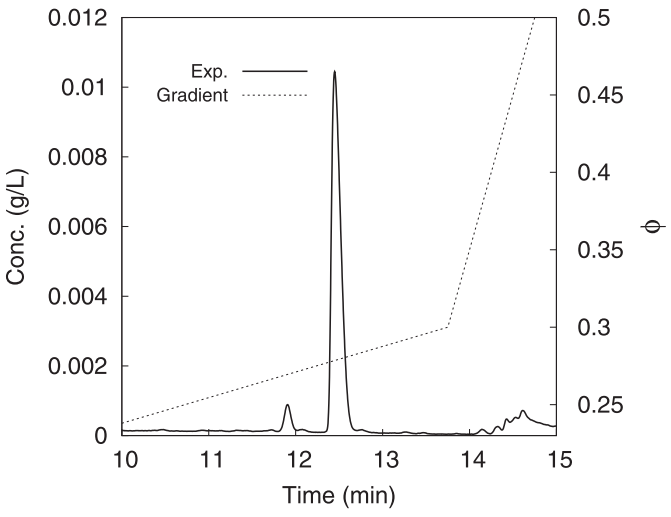

Fig. 1. Experimental gradient elution profile of the crude peptide. Injected concentration: 0.2 g/L; injected volume: 5 µL; wavelength: 280 nm.

Please cite this article as: C. De Luca, S. Felletti and M. Macis et al., Modeling the nonlinear behavior of a bioactive peptide in reversed-phase gradient elution chromatography, Journal of Chromatography A, https://doi.org/10.1016/j.chroma.2019.460789

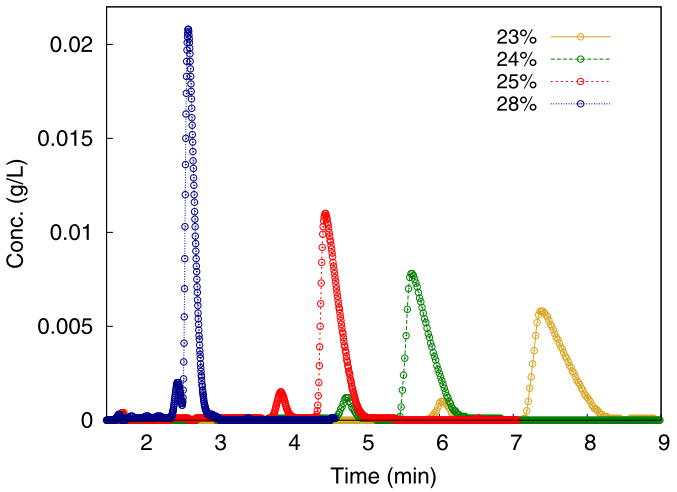

Fig. 2. Comparison between experimental profiles of the crude peptide measured at different volume fractions of organic modifier, ranging from $\phi = 0.23$ to $\phi = 0.28$. Injected concentration = 0.6 g/L; injected volume = 5 μL; wavelength: 280 nm.

the elution of peptide and the smaller one (t_R = 12.0 min) is an impurity from the synthesis.

Taking into account the dwell volume of the system, it was estimated that the elution of peptide takes place approximately around $\phi = 0.25$, therefore a range of ϕ between 0.23 and 0.28 has been chosen for experimental measurements.

Investigation of retention at infinite dilution

The investigation of chromatographic behavior of octreotide at infinite dilution demonstrated that its retention is profoundly affected by changes in the percentage of organic modifier. The dead volume has been determined through an unretained compound, uracil. Indeed, a variation of only roughly 5%, from $\phi = 0.23$ to $\phi = 0.28$, induced a 500% drop of retention factor (from 4.7 to 0.95, respectively, see Fig. 2).

Eq. (3) can be re-arranged according to the displacement model of retention in RP-LC [70]. This model predicts that retention of an hydrophobic molecules from an apolar stationary phase is accompanied by the displacement of a stoichiometric number of solvent molecules adsorbed on the surface [71]:

$$\log k = \log I + Z \times \log\left(\frac{1}{D_0}\right) \tag{10}$$

In this equation, which can be applied in a range where the concentration of organic solvent on the stationary phase is approximately constant, D_0 is the molar concentration of organic modifier, Z the number of molecules of organic solvent displaced by the analyte during retention and I is the value of k when D_0 is 1 M. Fig. 3 shows the variation of log k with $\log(1/D_0)$ for octreotide. From the slope of the linear regression line, the number of displaced molecules has been evaluated. Z resulted to be 8.2 $\pm$ 0.1. This value is significantly large if compared to the molecular weight of the compound, however very close to that obtained for a small polypeptide of comparable molecular mass [63].

Modeling of overloaded profiles under isocratic elution conditions

Adsorption isotherms of both crude and pure peptide solutions at each mobile phase composition have been determined by means of IM. Different adsorption isotherm models have been tested (Langmuir, BiLangmuir, Tóth). Among them, only the Langmuir model was found to satisfactorily fit experimental data. An excellent agreement was found between experimental and calculated peaks of pure and crude solutions of peptide (see Fig. 4). The amount of impurity is so small that it does not compete with peptide for adsorption and its retention time is not influenced by peptide concentration.

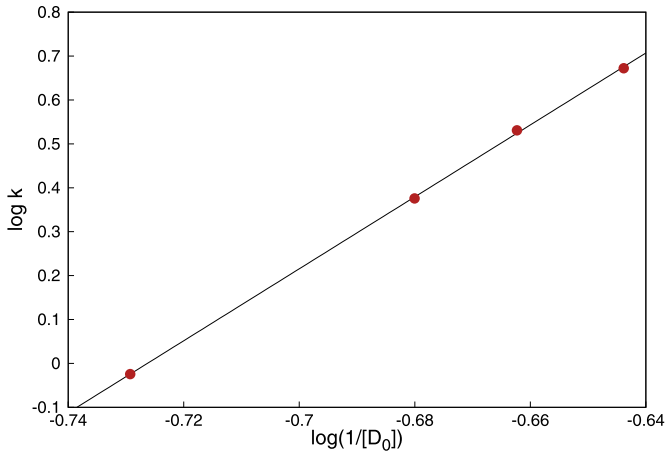

Fig. 3. Dependence of logarithm of retention factor (k) on logarithm of the inverse of ACN concentration (D_0) expressed in terms of molarity. The slope of the linear regression gives an indication of the number of displaced molecules (Z) equal to 8.2 $\pm$ 0.1. $R^2 = 0.999$.

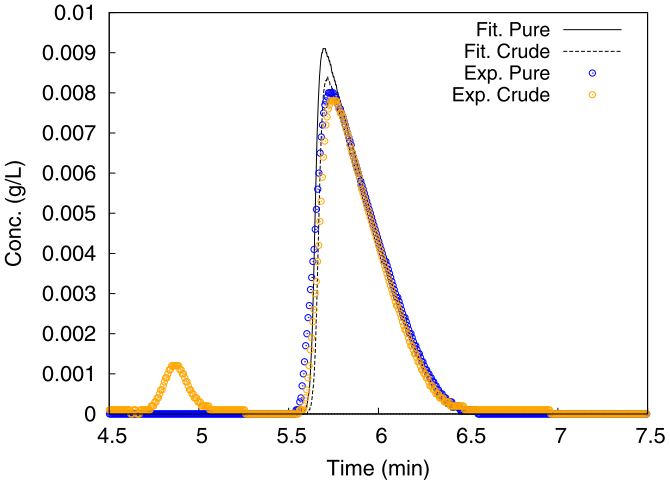

Fig. 4. Comparison between experimental peaks of crude (orange circles) and pure (blue circles) peptide and their corresponding calculated profiles. Dotted and solid lines corresponds to the fitting profiles of the crude and the pure peptide, respectively. $\phi = 0.24$, injected concentration = 0.6 g/L; injected volume = 5 µL; wavelength: 280 nm. (For interpretation of the references to colour in this figure legend, the reader is referred to the web version of this article.)

Table 1
Adsorption isotherm parameters obtained through IM with a Langmuir model at different mobile phase compositions.

ϕ	a	b (L/g)	q_s (g/L)
0.23	5.86	8.14	0.72
0.24	4.21	5.69	0.74
0.25	3.07	4.65	0.66
0.28	1.17	1.86	0.63

Fig. 5 compares some experimental and simulated overloaded profiles of the crude peptide recorded at $\phi = 0.24$ and various loading concentrations. Some small discrepancies in the front part of the peaks, especially for the two highest concentrations, could be due to the presence of kinetic phenomena that are neglected by the ED model. However, the rear parts of experimental and calculated profiles excellently match even at high concentrations.

The best isotherm parameters obtained at the different isocratic conditions investigated in this work are reported in Table 1. As it

Please cite this article as: C. De Luca, S. Felletti and M. Macis et al., Modeling the nonlinear behavior of a bioactive peptide in reversed-phase gradient elution chromatography, Journal of Chromatography A, https://doi.org/10.1016/j.chroma.2019.460789

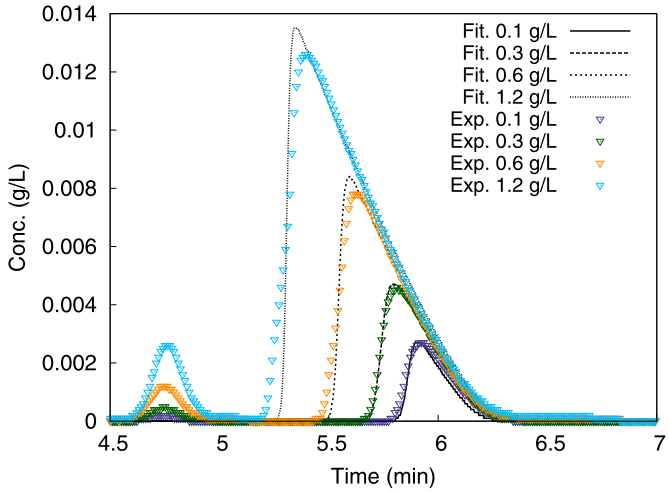

Fig. 5. Comparison between experimental and simulated peaks obtained with IM (Langmuir adsorption isotherm) for four different concentrations of the crude peptide in isocratic conditions (ϕ=0.24). Injected volume: 5 µL; wavelength: 280 nm.

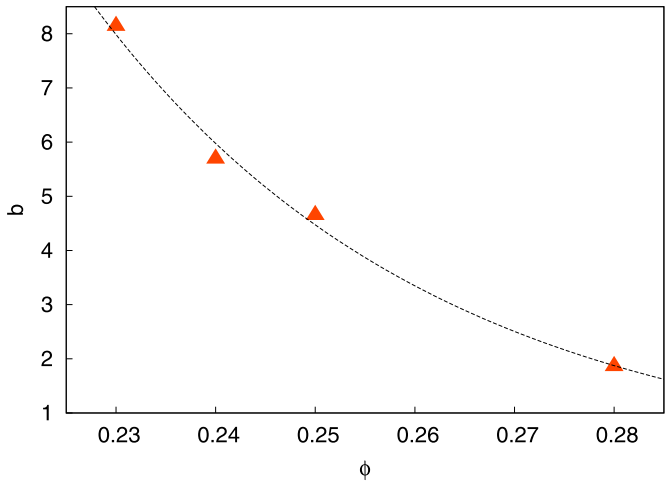

Fig. 6. Dependence of the equilibrium adsorption constant (b) on the fraction of organic modifier (ϕ) according to Eq. (7) (R^2=0.998).

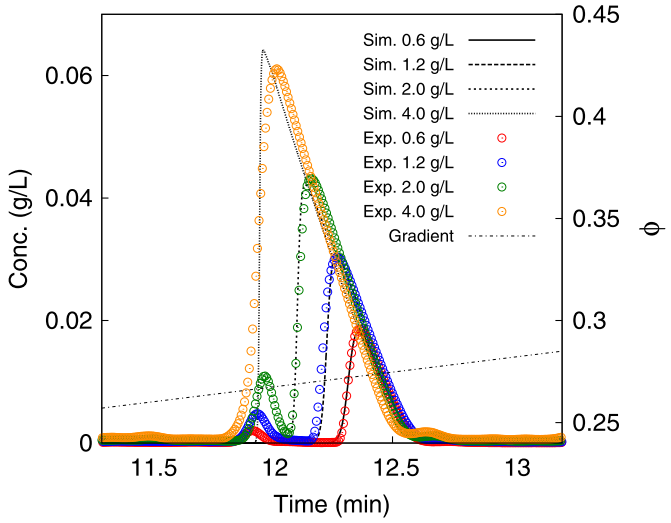

Fig. 7. Comparison between experimental and simulated peaks in gradient elution (Langmuir adsorption model) of four different concentrations of crude peptide. Injected volume: 5 µL; wavelength: 280 nm.

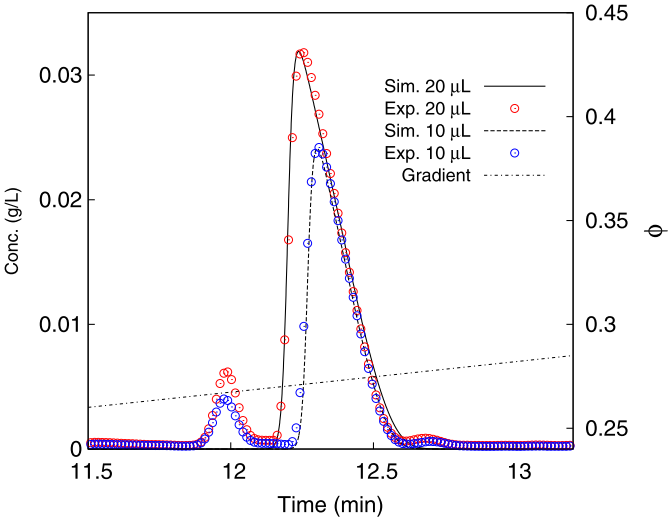

Fig. 8. Comparison between experimental and simulated peaks in gradient elution conditions. Injected concentrations: 0.5 g/L. Injected volume: 10 µL (blue) and 20 µL (red); wavelength: 280 nm. (For interpretation of the references to colour in this figure legend, the reader is referred to the web version of this article.)

can be evinced, q_s values are in a very good agreement, supporting the hypothesis of a small variation of q_s if this range of ϕ is significantly small. Moreover, the variation of b with ϕ follows the trend described by Eq. (7) (see Fig. 6). By fitting experimental data with an exponential equation, values of 29 and 6.3 $\times$ 10^3 L/g have been calculated for S and b_0, respectively. For the saturation capacity q_s the average value of 0.69 g/L was taken in the simulation of gradient elution experiments.

Modeling of overloaded profiles under gradient elution conditions

Substituting the above value of b_0, S and q_s in Eq. (8), the equilibrium-dispersive model with the feed conditions (Eq. (9)) can be solved to simulate gradient elution runs. As it can be observed from Fig. 7, where calculated profiles (solid lines) and experimental ones (coloured circles) are compared, a very good agreement between theoretical and experimental profiles has been obtained even at high concentrations.

In order to test model reliability and potential to predict conditions not considered in its development and parameter tuning, two more experimental runs at increasing loading volume have been considered, that is 10 and 20 µL. The match between experimental and predicted peaks was satisfactory (see Fig. 8). This means not only that the simple Langmuir model (based on the assumption that the adsorption surface is energetically homogeneous) is adequate to describe the adsorption mechanism of this peptide on this stationary phase but also, most importantly, that very small amount (μg) of peptide are sufficient to gather information on its adsorption equilibria and to model the separation under nonlinear gradient conditions.

5. Conclusions

Gradient preparative RP-LC is one of the most widely used technique for the purification of synthesized peptides. A reasonable approach to develop a purification method via preparative HPLC is based on the prior investigation of thermodynamic equilibria regulating retention of peptides on the stationary phase. This is practically translated into the calculation of their adsorption isotherms under different mobile phase compositions in a range of ϕ where elution takes place, in order to find the relationship between isotherm parameters and variation of organic modifier in the mobile phase.

Please cite this article as: C. De Luca, S. Felletti and M. Macis et al., Modeling the nonlinear behavior of a bioactive peptide in reversed-phase gradient elution chromatography, Journal of Chromatography A, https://doi.org/10.1016/j.chroma.2019.460789

Most of the times, the amount of available peptide is reduced or its cost is elevated. When this is the case, modern techniques of isotherm determination, based on theoretical hypotheses on the adsorption model and the simulation of peaks under overloaded conditions, can be efficiently employed to achieve the relevant information.

Declaration of Competing Interest

None.

CRediT authorship contribution statement

Chiara De Luca: Investigation, Visualization, Writing - original draft. **Simona Felletti:** Investigation, Visualization, Writing - original draft. **Marco Macis:** Resources, Supervision. **Walter Cabri:** Resources, Supervision. **Giulio Lievore:** Investigation, Validation. **Tatiana Chenet:** Data curation. **Luisa Pasti:** Formal analysis. **Massimo Morbidelli:** Supervision. **Alberto Cavazzini:** Supervision, Funding acquisition, Project administration, Resources, Writing - review & editing. **Martina Catani:** Conceptualization, Methodology, Visualization, Writing - original draft, Writing - review & editing. **Antonio Ricci:** Resources, Supervision, Funding acquisition.

Acknowledgments

The authors thank the Italian University and Scientific Research Ministry (grant PRIN 2017Y2PAB8_003, title: "Cutting edge analytical chemistry methodologies and bio-tools to boost precision medicine in hormone-related diseases"). The authors also acknowledge Fresenius Kabi iPSUM for the kind donation of octreotide and Dr. Marco Carmosino from the University of Ferrara for technical support.

References

[1] R.J.S. de Castro, H.H. Sato, Biologically active peptides: processes for their generation, purification and identification and applications as natural additives in the food and pharmaceutical industries, Food Res. Int. 74 (2015) 185–198.
[2] J.L. Lau, M.K. Dunn, Therapeutic peptides: historical perspectives, current development trends, and future directions, Bioorg. Med. Chem. 26 (2018) 2700–2707.
[3] D. Agyei, C.M. Ongkudon, C.Y. Wei, A.S. Chan, M.K. Danquah, Bioprocess challenges to the isolation and purification of bioactive peptides, Food Bioprod. Proc. 98 (2016) 244–256.
[4] K. Sikora, D. Neubauer, M. Jaśkiewicz, W. Kamysz, Citropin 1.1 trifluoroacetate to chloride counter-ion exchange in hcl-saturated organic solutions: an alternative approach, Int. J. Pept. Res. Therapeutics 24 (2018) 265–270.
[5] V. Sanz-Nebot, F. Benavente, I. Toro, J. Barbosa, Liquid chromatography-mass spectrometry approach for the characterization and purification of crude synthetic peptide hormones, Anal. Bioanal. Chem. 377 (2003) 306–315.
[6] S. Roux, E. Zékri, B. Rousseau, M. Paternostre, J.-C. Cintrat, N. Fay, Elimination and exchange of trifluoroacetate counter-ion from cationic peptides: a critical evaluation of different approaches, J. Pept. Sci. 14 (2008) 354–359.
[7] S. Marqus, E. Pirogova, T.J. Piva, Evaluation of the use of therapeutic peptides for cancer treatment, J. Biomed. Sci. 24 (2017) 21–36.
[8] R. Ali, R. Rani, S. Kumar, New peptide based therapeutic approaches, Semantic Scholar (2013).
[9] S. Wegmüller, S. Schmid, Recombinant peptide production in microbial cells, Curr. Org. Chem. 18 (2014) 1005–1019.
[10] S. Chandrudu, P. Simerska, I. Toth, Chemical methods for peptide and protein production, Molecules 18 (2013) 4373–4388.
[11] S. Chandrudu, P. Simerska, I. Toth, Overview of bacterial expression systems for heterologous protein production: from molecular and biochemical fundamentals to commercial systems, Appl. Microbiol. Biotechnol. 72 (2006) 211–222.
[12] T. Bruckerdorfer, O. Marder, F. Albericio, From production of peptides in milligram amounts for research to multi-tons quantities for drugs of the future, Curr. Pharm. Biotech. 5 (2004) 29–43.
[13] S. Bernardi, D. Gétaz, N. Forrer, M. Morbidelli, Modeling of mixed-mode chromatography of peptides, J. Chromatogr. A 1283 (2013) 46–52.
[14] C. Grossmann, G. Ströhlein, M. Morari, M. Morbidelli, Optimizing model predictive control of the chromatographic multi-column solvent gradient purification (MCSGP) process, J. Process Control 20 (2010) 618–629.
[15] B. Bobály, V. Mikola, E. Sipkó, Z. Márta, J. Fekete, Recovery of proteins affected by mobile phase trifluoroacetic acid concentration in reversed-phase chromatography, J. Chromat. Sci. 53 (2015) 1078–1083.
[16] T. Müller-Späth, G. Ströhlein, O. Lyngberg, D. Maclean, Enabling high purities and yields in therapeutic peptide purification using multicolumn countercurrent solvent gradient purification, Chem. Today 31 (2013) 56–61.
[17] L. Aumann, M. Morbidelli, A continuous multicolumn countercurrent solvent gradient purification (MCGSP) process, Biotech. Bioeng. 98 (2007) 1043–1055.
[18] D. Gétaz, N. Dogan, N. Forrer, M. Morbidelli, Influence of the pore size of reversed phase materials on peptide purification processes, J. Chromatogr. A 1218 (2011) 2912–2922.
[19] G. Guiochon, A. Felinger, A. Katti, D. Shirazi, Fundamentals of Preparative and Nonlinear Chromatography, 2nd Edition, Academic Press, Boston, MA, 2006.
[20] K. Kaczmarski, A. Cavazzini, P. Szabelsky, D. Zhou, X. Liu, G. Guiochon, Application of the general rate model and the generalized maxwell-stefan equation to the study of the mass transfer kinetics of a pair of enantiomers, J. Chromatogr. A 962 (2002) 57–67.
[21] A. Cavazzini, A. Felinger, K. Kaczmarski, P. Szabelski, G. Guiochon, Study of the adsorption equilibria of the enantiomers of 1-phenyl-1-propanol on cellulose tribenzoate using a microbore column, J. Chromatogr. A 953 (2002) 55–66.
[22] G. Carta, A. Jungbauer, Protein Chromatography: Process Development and Scale-Up, Wiley-VCH, 2010.
[23] D. Gétaz, G. Stroehlein, A. Butté, M. Morbidelli, J. Chromatogr, Model-based design of peptide chromatographic purification processes, 2013, J. Chromatogr. A 1284, 69–79.
[24] Y. Yue, S. Li, L. Feng, A. S.-M., P. Benner, Efficient model reduction of SMB chromatography by Krylov-subspace method with application to uncertainty quantification, 2014, Comput. Aided Chem. Eng. 33925–930
[25] P. Forssén, T. Fornstedt, Impact of column and stationary phase properties on the productivity in chiral preparative LC, J. Sep. Sci 41 (2018) 1346–1354.
[26] J.W. Lee, A. Seidel-Morgenstern, Model predictive control of simulated moving bed chromatography for binary and pseudo-binary separations: simulation study, IFAC Pap.Online 51 (2018) 530–535.
[27] S. Vogg, T. Müller-Späth, M. Morbidelli, Current status and future challenges in continuous biochromatography, Curr. Opin. Chem. Eng. 22 (2018) 138–144.
[28] D. Pfister, L. Nicoud, M. Morbidelli, Continuous biopharmaceutical processes, Cambridge Series in Chemical Engineering, 2018.
[29] M. Mazzotti, G. Storti, M. Morbidelli, Optimal operation of simulated moving bed units for nonlinear separation, J. Chromatogr. A 769 (1997) 3–24.
[30] E.R. Francotte, P. Richert, Applications of simulated moving-bed chromatography to the separation of the enantiomers of chiral drugs, J. Chromatogr. A 1997 (1997) 101–107.
[31] H. Schramm, M. Kaspereit, A. Kienle, A. Seidel-Morgenstern, Simulated moving bed process with cyclic modulation of the feed concentration, J. Chromatogr. A 1006 (2003) 77–86.
[32] T. Kröber, M.W. Wolff, B. Hundt, A. Seidel-Morgenstern, U. Reichl, Continuous purification of influenza virus using simulated moving bed chromatography, J. Chromatogr. A 1307 (2013) 99–110.
[33] G. Ströhlein, L. Aumann, M. Mazzotti, M. Morbidelli, A continuous, counter-current multi-column chromatographic process incorporating modifier gradients for ternary separations, J. Chromatogr. A 1126 (2006) 338–346.
[34] F. Steinebach, T. Müller-Späth, M. Morbidelli, Continuous counter-current chromatography for capture and polishing steps in biopharmaceutical products, Biotech. J. 11 (2016) 1126–1141.
[35] L. Aumann, M. Morbidelli, A semicontinuous 3-column countercurrent solvent gradient purification (MCSGP) process, Biotech. Bioeng. 99 (2008) 728–733.
[36] M. Krättli, F.S.M. Morbidelli, Online control of the twin-column countercurrent solvent gradient process for biochromatography, J. Chromatogr. A 1293 (2013) 51–59.
[37] S. Vogg, N. Ulmer, J. Souquet, H. Broly, M. Morbidelli, Experimental evaluation of the impact of intrinsic process parameters on the performance of a continuous chromatographic polishing unit (MCSGP), Biotechnol. J. 14 (2019) 1–8, doi:10.1002/biot.201800732.
[38] C. Heuer, E. Küsters, T. Plattner, A. Seidel-Morgenstern, Design of the simulated moving bed process based on adsorption isotherm measurements using a perturbation method, J. Chromatogr. A 827 (1998) 175–191.
[39] M. Ballerstein, D. Michaels, A. Seidel-Morgenstern, R. Weismantel, A theoretical study of continuous counter-current chromatography for adsorption isotherms with inflection points, Comput. Chem. Eng. 34 (2010) 447–459.
[40] S. Palani, L. Guerguieva, U. Rinas, A. Seidel-Morgenstern, G. Jayaraman, Recombinant protein purification using gradient-assisted simulated moving bed hydrophobic interaction chromatography. Part i: selection of chromatographic system and estimation of adsorption isotherms, J. Chromatogr. A 1218 (2011) 6396–6401.
[41] J. Nowak, D. Antos, A. Seidel-Morgenstern, Theoretical study of using simulated moving bed chromatography to separate intermediately eluting target compounds, J. Chromatogr. A 1253 (2012) 58–70.
[42] S. Li, L. Feng, P. Benner, A. Seidel-Morgenstern, Efficient optimization of simulated moving bed processes using reduced order models, Comput. Aided Chem. Eng. 30 (2012) 1232–1236.
[43] P.E. Battershill, S.P. Clissold, Octreotide. a review of its pharmacodynamic and pharmacokinetic properties, and therapeutic potential in conditions associated with excessive peptide secretion, Drugs 38 (1989) 658–702.
[44] S.W.J. Lamberts, A.J. van der Lely, W.W. de Herder, L.J. Hofland, Octreotide N. Engl. J. Med 334 (1996) 246–254.
[45] G. Sabatino, I. Guryanov, A. Rombecchi, J. Zanon, A. Ricci, W. Cabri, A.M. Papini, P. Rovero, Production of peptides as generic drugs: a patent landscape of octreotide, Expert Opin. Ther. Pat. 26 (2016) 4.

Please cite this article as: C. De Luca, S. Felletti and M. Macis et al., Modeling the nonlinear behavior of a bioactive peptide in reversed-phase gradient elution chromatography, Journal of Chromatography A, https://doi.org/10.1016/j.chroma.2019.460789

[46] C. Xidakis, D. Ljumovic, P. Manousou, G. Notas, V. Valatas, G. Kolios, E. Kouroumalis, Production of pro- and anti-fibrotic agents by rat kupffer cells: the effect of octreotide, Dig. Dis. Sci. 50 (2005) 935–941.
[47] M. Catani, R. Guzzinati, N. Marchetti, L. Pasti, A. Cavazzini, Exploring fluorous affinity by liquid chromatography, Anal. Chem. 87 (2015) 6854–6860.
[48] S. Felletti, C.D. Luca, O.H. Ismail, L. Pasti, V. Costa, F. Gasparrini, A. Cavazzini, M. Catani, On the effect of chiral selector loading and mobile phase composition on adsorption properties of latest generation fully- and superficially-porous whelk-O1 particles for high-efficient ultrafast enantioseparations, J. Chromatogr. A 1579 (2018) 41–48.
[49] S. Deridder, M. Catani, A. Cavazzini, G. Desmet, A theoretical study on the advantage of core-shell particles with radially-oriented mesopores, J. Chromatogr. A 1456 (2016) 137–144.
[50] O.H. Ismail, G.L. Losacco, G. Mazzoccanti, A. Ciogli, C. Villani, M. Catani, L. Pasti, S. Anderson, A. Cavazzini, F. Gasparrini, Unmatched kinetic performance in enantioselective supercritical fluid chromatography by combining latest generation whelk-o1 chiral stationary phases with a low-dispersion in-house modified equipment, Anal. Chem. 90 (2018) 10828–10836.
[51] A. Cavazzini, A. Felinger, G. Guiochon, Comparison between adsorption isotherm determination techniques and overloaded band profiles on four batches of monolithic columns, J. Chromatogr. A 1012 (2003) 139–149.
[52] L. Pasti, N. Marchetti, R. Guzzinati, M. Catani, V. Bosi, F. Dondi, A. Sepsey, A. Felinger, A. Cavazzini, Microscopic models of liquid chromatography: from ensemble-averaged information to resolution of fundamental viewpoint at single-molecule level, TrAC 81 (2016) 63–68.
[53] D. Åsberg, M. Leśko, M. Enmark, J. Samuelsson, K. Kaczmarski, T. Fornstedt, Fast estimation of adsorption isotherm parameters in gradient elution preparative liquid chromatography. i: the single component case, J. Chromatogr. A 1299 (2013) 64–70.
[54] D. Åsberg, M. Leśko, T. Leek, J. Samuelsson, K. Kaczmarski, T. Fornstedt, Estimation of nonlinear adsorption isotherms in gradient elution rp-lc of peptides in the presence of an adsorbing additive, Chromatographia 80 (2017) 961–966.
[55] D. Åsberg, J. Samuelsson, M. Leśko, A. Cavazzini, K. Kaczmarski, T. Fornstedt, Method transfer from high-pressure liquid chromatography to ultra-high-pressure liquid chromatography. II. temperature and pressure effects, J. Chromatogr. A 1401 (2015) 52–59.
[56] D. Antos, W. Piatkowski, K. Kaczmarski, Determination of mobile phase effect on single-component adsorption isotherm by use of numerical estimation, J. Chromatogr. A 874 (2000) 1–12.
[57] M. Leśko, D. Åsberg, M. Enmark, J. Samuelsson, T. Fornstedt, K. Kaczmarski, Choice of model for estimation of adsorption isotherm parameters in gradient elution preparative liquid chromatography, Chromatographia 78 (2015) 1293–1297.
[58] L.R. Snyder, M.A. Stadalius, High-Performance Liquid Chromatography: advances and perspectives, Vol. 4, Academic Press, New York, 1986.
[59] L.R. Snyder, J.W. Dolan, J.R. Gant, Systematic approach to optimizing resolution in reversed- phase liquid chromatography, with emphasis on the role of temperature, J. Chromatogr. 165 (1979) 3–30.
[60] P. Jandera, J. Churáček, Gradient elution in column liquid chromatography: theory and practice, Journal of Chromatography Library 31 (1985). Elsevier
[61] A. Felinger, G. Guiochon, Comparing the optimum performance of the different modes of preparative liquid chromatography, J. Chromatogr. A 796 (1998) 59–74.
[62] A. Felinger, G. Guiochon, Optimizing experimental conditions in overloaded gradient elution chromatography, Biotechnol. Prog. 12 (1996) 638–644.
[63] N. Marchetti, F. Dondi, A. Felinger, R. Guerrini, S. Salvadori, A. Cavazzini, Modeling of overloaded gradient elution of nociceptin/orphanin fq in revesed-phase liquid chromatography, J. Chromatogr. A 1079 (2005) 162–172.
[64] P.W. Danckwerts, Continuous flow systems: distribution of residence times, Chem. Eng. Sci. 2 (1953) 1–13.
[65] F. Gritti, A. Felinger, G. Guiochon, Overloaded gradient elution chromatography on heterogeneous adsorbents in reversed-phase liquid chromatography, J. Chromatogr. A 1017 (2003) 45–61.
[66] A. Felinger, D.M. Zhou, G. Guiochon, Determination of the single component and competitive adsorption isotherms of the 1-indanol enantiomers by the inverse method, J. Chromatogr. A 1005 (2003) 35–49.
[67] P. Vajda, A. Cavazzini, A. Felinger, Adsorption equilibria of proline in hydrophilic interaction chromatography, J. Chromatogr. A 1217 (2010) 5965–5970.
[68] J. Xu, L. Zhu, G. Xu, W. Yu, A.K. Ray, Determination of competitive adsorption isotherm of enantiomers on preparative chromatographic columns using inverse method, J. Chromatogr. A 1273 (2013) 49–56.
[69] E. Morgan, K.W. Burton, Optimization using the super-modified simplex method, Chemom. Intell. Lab. 8 (1990) 97–107.
[70] C. Horváth, High-Performance Liquid Chromatography: Advances and Perspectives, 2, Academic Press, 1986.
[71] X. Geng, F. Reigner, Stoichiometric displacement of solvent by non-polar solutes in reversed-phase liquid chromatography, J. Chromatogr. A 332 (1985) 147–168.

Please cite this article as: C. De Luca, S. Felletti and M. Macis et al., Modeling the nonlinear behavior of a bioactive peptide in reversed-phase gradient elution chromatography, Journal of Chromatography A, https://doi.org/10.1016/j.chroma.2019.460789

Paper VIII

Exploring stationary-phase diffusion and adsorption-desorption kinetics in Whelk-O1 and zwitterionic-teicoplanin chiral stationary phases

Simona Felletti,[†] Chiara De Luca,[†] Giulio Lievore,[†] Luisa Pasti,[†] Tatiana Chenet,[†] Omar H. Ismail,[†] Giulia Mazzoccanti,[‡] Francesco Gasparrini,[‡] Alberto Cavazzini,[*,†] and Martina Catani[*,†]

Dept. of Chemistry and Pharmaceutical Sciences, University of Ferrara, via L. Borsari 46, 44121 Ferrara, Italy, and Dept. of Drug Chemistry and Technology, "Sapienza" Università di Roma, P.le A. Moro 5, 00185 Roma, Italy

E-mail: cvz@unife.it; martina.catani@unife.it

Phone: +39 0532 455389. Fax: +39 0532 240709

Abstract

In this work a detailed study of mass transfer on Whelk-O1 and zwitterionic-teicoplanin chiral stationary phases (CSPs) has been performed. Columns were in house prepared by using latest generation fully- and superficially-porous particles (FPPs and SPPs). 2.5 μm diameter FPPs and 2.6 μm SPPs were used to prepare the Whelk-O1 CSPs. On the other hand, 1.9 μm FPPs and 2.0 μm SPPs were the base material for the zwitterionic-teicoplanin CSPs. By combining stop-flow and dynamic measurements, in a variety of experimental conditions (normal-phase and HILIC), this study has revealed that the adsorption of enantiomers on

*To whom correspondence should be addressed
†University of Ferrara
‡"Sapienza" Università di Roma

both CSPs is localized and that the adsorption-desorption kinetics depends on the loading of chiral selector, the larger the loading the slower the kinetics. This explains the unexpected, significant efficiency loss of columns packed with chiral SPPs, already at relatively low flow rates.

Introduction

In the last years, much effort has been dedicated to study mass transfer kinetics in reversed-phase (RP) liquid chromatography (LC).[1–13] These studies are broadly consistent in showing that superficially porous particles (SPPs) allow to achieve more efficient separations than fully porous ones (FPPs). The reasons why this happens depend, in part, on the presence of the impenetrabile inner core and, in part, on the rheological properties of SPPs. They can be explained with the aid of the van Deemter equation (here written in reduced coordinates):

$$h = a(\nu) + \frac{b}{\nu} + (c_s + c_{ads})\nu \tag{1}$$

where h is the reduced plate height, ν the reduced interstitial velocity, a the eddy dispersion, b the longitudinal diffusion, and c_s and c_{ads} the solid-liquid mass transfer and the adsorption-desorption kinetics terms, respectively. The presence of the impenetrable core reduces the physical space available for diffusion in SPPs, with clear advantages in terms of longitudinal diffusion, b, and liquid-solid mass transfer, c_s. In addition, for hydrophobic C18-based particles, it has been demonstrated that beds made of SPPs are characterized by diminished eddy dispersion over those packed with FPPs of similar characteristics.[5] Essentially, the roughness of SPPs allows for the formation of more radially homogeneous packed beds, owing to the reduction of particle slipping after releasing the high pressure employed during their packing. Finally, these studies have shown that – no matter particle morphology – the contribution to band broadening by the adsorption-desorption kinetics is always negligible in RP-LC (i.e., $c_{ads} = 0$ in Eq. 1), unless very large molecules are considered (such as, polypeptides or proteins with molecular weight larger than 50kDa).

On the contrary, only in a few studies mass transfer in chiral LC has been investigated from a fundamental viewpoint. This depends not only on the fact that highly efficient chiral particles (suitable for ultrafast separations) have been prepared only recently,[14–19] but also on the difficulty to interpret experimental data on strongly heterogeneous stationary phases, such as the chiral ones (CSPs).[20–22] Some studies have compared the performance of columns packed with superficially and fully porous chiral particles based

on their van Deemter curves. This approach has however some drawbacks. First of all, if the curves are not properly scaled to reduced coordinates, the comparison of the performance of columns packed with particles of different size is meaningless. In addition, parameters obtained by the nonlinear fitting of van Deemter curves do not have well-founded physical meaning.[5,23] Accordingly, they should not be employed for fundamental studies. However, the concept of the superiority of SPPs over FPPs for high efficient separations has taken over also in chiral chromatography.[19,24]

Another major issue in chiral chromatography is that the adsorption-desorption kinetics cannot be neglected.[5,25–27] Due to the complexity of chiral recognition mechanisms, indeed, chiral interactions can be very slow. The term c_{ads} in eq. 1 is however very difficult to estimate. Even the most advanced approaches to the study of mass transfer in LC show that c_{ads} cannot be evaluated independently. The so-called "subtraction method" – consisting in taking away from experimentally measured h the contributions of b and c_s estimated by stop-flow measurements[5] – leads indeed to the sum of c_{ads} and $a(\nu)$.

Some of the authors of this paper have recently reported on the comparison between the kinetic performance of Whelk-O1 and Teicoplanin CSPs. The efficiency of columns packed with SPPs was found to be comparable, or even worse than that of their fully porous counterparts.[14,15,18,28,29] Starting from this observation, in this work, a detailed study of mass transfer on Whelk-O1 and zwitterionic-teicoplanin CSPs has been performed. The CSPs were prepared on both SPPs (2.6 μm for the Whelk-O1 and 2.0 μm for the zwitterionic-teicoplanin one) and FFPs (2.5 and 1.9 μm, respectively) and operated in normal phase (NP) and hydrophilic interaction chromatography (HILIC).

It is commonly acknowledged that the Whelk-O1 selector is "fast" (meaning that it allows for fast adsorption-desorption kinetics), while teicoplanin is a "slow" one. This information essentially comes from spectroscopic (NMR) molecular studies, where chiral selectors are in solution (and not immobilized on the silica particles) and solvents are different from those commonly used in HPLC. To the best of our knowledge, on the other hand, there are not studies focused on the direct investigation of the kinetic properties of heterogeneous versions of these chiral selectors.

Experimental Section

Columns and materials

All solvents and reagents were purchased from Merck Sigma-Aldrich (St. Louis, MO, USA), so were *trans*-stilbene oxide (TSO) and Z-D,L-methionine (Z-D,L-Met). Titan monodispersed silica (1.9 μm, 120 Å, 282 m^2/g), Halo silica (2.0 μm, 90Å, 125 m^2/g, ρ=0.6) and teicoplanin chiral selector were from Merck Sigma-

Aldrich (St. Louis, MO, USA). Kromasil silica (2.5 μm particle size, 100 Å pore size, 323 m^2/g specific surface area) was from Akzo-Nobel (Bohus, Sweden). Accucore silica (2.6 μm, 80 Å, 130 m^2/g, ρ = 0.63) was from Thermo Fisher Scientific (Waltham, MA, USA). Whelk-O1 selector was generously donated by Regis Technologies Inc. (Morton Grove, IL, USA). 100 and 150 mm$\times$4.6 mm empty stainless steel columns were from IsoBar Systems by Idex (Erlangen, Germany). The former were employed for the preparation of teicoplanin columns. 150 mm columns were used for the preparation of Whelk-O1 columns. A 33 mm$\times$4.6 mm Micra column (Eprogen, Inc., USA) packed with 1.5 μm non-porous silica particles was purchased from DBA Italia s.r.l. (Italy) and employed for the estimation of bulk molecular diffusion coefficients (see later on). Fourteen polystyrene standards (from Supelco SigmaAldrich, Milan, Italy) with molecular weights 500, 2000, 2500, 5000, 9000, 17 500, 30 000, 50 000, 156 000, 330 000, 565 000, 1 030 000, 1 570 000, and 2 310 000 were employed for inverse size exclusion chromatography (ISEC). The mobile phases employed were: hexane/ethanol 90:10 %(v/v) for TSO on Whelk-O1 columns and ACN/H_2O 85:15 %(v/v) + 20 mM ammonium formiate for Z-D,L-Met on zwitterionic-teicoplanin columns.

Equipment

An UltiMate 3000 RS UHPLC chromatographic system from Thermo Fisher Dionex was used for the determination of van Deemter curves. This instrument consists of a dual gradient RS pump (flow rates up to 8.0 mL/min; pressure limit 800 bar under normal phase conditions), an in-line split loop well plate sampler, a thermostated RS column ventilated compartment and a diode array detector (UV Vanquish) with a low dispersion 2.5 μL flow cell. Detection wavelength was 214 nm (constant filter time: 0.002 s; data collection rate: 100 Hz; response time: 0.04 s). Two 350$\times$0.10 mm I.D. Viper capillaries were used to connect the injector to the column and the column to the detector. The extra-column peak variance (calculated through peak moments) was 4.0 μL^2 at a flow rate of 1.0 mL/min. ISEC experiments were carried out on an Agilent 1100 Series Capillary LC system equipped with a binary pump system, an autosampler, a column thermostat and a photodiode array detector. This equipment was also employed for peak parking experiments.

Column and particle porosity

Porosities of each column were evaluated through Inverse Size Exclusion Chromatography (ISEC).[30,31] 2 μL of polystirene standards dissolved in tetrahydrofuran were injected at a flow rate of 0.1 mL/min by using pure tetrahydrofuran as mobile phase. Retention volumes were corrected for the extra-column contribution before being plotted against the cubic root of the molecular weight (M_w).[32] The interstitial volume, V_e, was

calculated by extrapolating to M_w=0 the excluded branch of this plot and the interstitial porosity of the column was calculated as:

$$\epsilon_e = V_e / V_{col} \tag{2}$$

being V_{col} the geometrical volume of the column. The thermodynamic void volume, V_0, was calculated from the corrected elution volume of benzene in tetrahydrofuran and it was used to estimate the total porosity:

$$\epsilon_t = V_0 / V_{col} \tag{3}$$

Particle porous zone porosity was, finally, calculated according to the following equation:

$$\epsilon_p = \frac{\epsilon_t - \epsilon_e}{(1 - \epsilon_e)(1 - \rho^3)} \tag{4}$$

being ρ the core-to-particle diameter ratio ($\rho = 0$ for FPPs).

Estimation of diffusion coefficients

Peak parking method was used to estimate both effective, D_{eff}, and molecular, D_m, diffusion coefficients of TSO and Z-D,L-Met on the Whelk-O1 and zwitterionic-teicoplanin columns, respectively.[33–35] Measurements were performed at 35°C. For the calculation of the spatial peak variance σ_x^2, the following equation was used:

$$\sigma_x^2 = \frac{L^2}{N} \tag{5}$$

where L is the column length and N is the number of theoretical plates. All the data were corrected for the extra-column peak variance. Parking times were 0, 120, 600, 1800 and 2400 s. The flow rate applied for the estimation of the effective diffusion coefficients was 0.3 mL/min for Whelk-O1 columns and 0.2 mL/min for teicoplanin ones.

The molecular diffusion coefficient of TSO in hexane/ethanol 90:10 %(v/v) and of Z-D,L-Met in ACN/H_2O 85:15 %(v/v) + 20 mM ammonium formiate were measured by performing peak parking experiment in a column packed with non-porous particles (Micra column) at a flow rate of 0.1 mL/min. Temperature was

35°C. In this case:[5,35]

$$D_m = \frac{D_{eff}}{\gamma_e} \tag{6}$$

where γ_e is a geometrical parameter, called external obstruction factor, related to the tortuosity and constriction of inter-particle channels.[36] The value of γ_e was calculated by measuring D_{eff} (again by means of peak parking) for a molecule whose D_m is known from literature. To this purpose, thiourea in pure water at 25°C was used ($D_m = 1.33 \times 10^{-5}$ cm^2/s).[37] γ_e was found to be 0.68. Calculated D_m values for TSO and Z-D,L-Met in their respective mobile phases were 2.3×10^{-5} and 1.2×10^{-5} cm^2/sec.

van Deemter curve measurements

To study the dependence of the height equivalent to a theoretical plate on the mobile phase, flow rates were changed from 0.1 mL/min up to 4.0 mL/min, with constant steps of 0.1 mL/min. Injection volumes were 0.1-0.5 μL. Temperature was set at 35°C. Retention time and column efficiency (given as number of theoretical plates) of eluted peaks were automatically processed by the Chromeleon software (using peak width at half height, according to European Pharmacopeia) and corrected for the extra-column contribution.

Results and Discussion

To avoid burdening this section, fundamentals of mass transfer in porous particles can be found under Supplementary Information (SI). Hereafter, the results of these studies will be employed to estimate the different parameters of the van Deemter equation.

The characteristics of chiral particles studied in this work are listed in Table 1. Apart from information given by manufacturers (particle diameter, pore size and specific surface area), the table reports the bonding density of chiral selector (expressed both as μmol per gram of bare silica and μmol per square meter) and the calculated porosities (total, particle porous-zone and interstitial).

The synthesis and preparation of the CSPs, on both FPPs and SPPs, is very reproducible as described in detail in.[15,18,38,39] The specific bonding density (μmol/m^2) of SPPs was found to be noticeably larger than that of fully porous ones (+20% and +65%, respectively for Whelk-O1 and zwitterionic-teicoplanin particles). The loading of chiral selector has been traditionally correlated to the enantioselectivity of the phase. It is acknowledged that the larger the loading, the larger the enantioselectivity. However, this parameter may also affect the adsorption-desorption kinetics and it should therefore be considered in the kinetic

performance of different chiral particles.

For all columns, the interstitial porosity, ϵ_e, is very close to the theoretical value typical of randomly packed beds of spherical particles (0.4), in confirmation that beds were densely packed.[40] The pore zone porosity, ϵ_p, was smaller on SPPs than on FPPs, in agreement with specific bonding densities of chiral selectors reported in Table 1. Finally, the total porosity, ϵ_t, is smaller on columns made of SPPs than of FPPs, as a consequence of the unaccessible inner core present in the former.

To compare the performance of particles of different dimensions, reduced van Deemter curves have been used. They are shown in Figure 1. For the sake of comparison, each box of this figure reports the overlapped van Deemter curves of the first and second eluted enantiomer on each column (see figure caption for details). It is interesting to notice that at low reduced velocity, on each column, the two enantiomers have very similar h. The longitudinal diffusion b is the dominant mechanism of mass transfer in this region. It can be estimated through so-called peak parking experiment (stop-flow measurements, see Experimental session), which permit to evaluate the effective diffusion coefficient, D_{eff}. Once D_{eff} for each enantiomer is known ($D_{eff,i}$, with $i = 1, 2$ for the first and second eluted enantiomer, respectively), the corresponding b_i is calculated through the following equation (see eq. 5 of SI):

$$b_i = 2(1 + k_{1,i})\frac{D_{eff,i}}{D_m} \qquad i = 1, 2 \tag{7}$$

where $k_{1,i}$ is the zone retention factor – i.e., the retention factor referred to the interstitial volume[28,41,42] – of the i-th enantiomer. Table 2 reports the calculated b values for the two enantiomers. A first (expected) observation on these data is that b is smaller on SPPs than on FPPs (no matter the kind of selector), due to the presence of the solid core that reduces the space available for diffusion.[4,43,44] A second, more interesting one is that, within experimental errors, first and secondly eluted enantiomers are characterized by the same b. This happens on all the CSPs. This finding ($b_1 = b_2$) sheds light on the characteristics of surface diffusion, as it will be described in the following. Let us start by assuming a model of diffusion in porous media. For the sake of simplicity, in this work the so-called parallel (or Knox) model will be employed,[42] even if more sophisticated models of diffusion have been developed.[45] This first-choice model assumes that all mass fluxes inside and outside the particle are additive. Therefore, $D_{eff,i}$ can be expressed as a time-average of diffusion in the bulk mobile phase, D_m (obviously identical for the two enantiomers since no chiral additive was added to the mobile phase), and in the porous zone, $D_{p,i}$ ($i = 1, 2$), which can be different for the two enantiomers. Accordingly (see SI, eq. 11):

$$D_{eff,i} = \frac{\gamma_e D_m + \frac{1-\epsilon_e}{\epsilon_e}(1-\rho^3)D_{p,i}}{1 + k_{1,i}} \qquad i = 1, 2 \tag{8}$$

The next step is the application of the parallel model also to the porous zone, so that $D_{p,i}$ can, in turn, be written as the sum of two contributions, the diffusion through the stagnant mobile phase contained in the pores (where the molecular diffusion coefficient is D_m) and the surface diffusion, $D_{s,i}$:

$$D_{p,i} = \epsilon_p \gamma_p F(\lambda_m) D_m + (1 - \epsilon_p) K_{a,i} D_{s,i} \qquad i = 1, 2 \tag{9}$$

being γ_p the internal obstruction factor that accounts for the tortuosity and the complex structure of mesopores and F(λ_m) the hindrance diffusion factor describing the confinement of the sample within the narrow pores (of mesopore size λ_m). It is noteworthy to point out that $K_{a,i}$ is the binding constant of the i-th enantiomer on the chiral surface. Thus, differences between $K_{a,1}$ and $K_{a,2}$ are the origin of the enantioselectivity of the CSP.

The introduction of eqs. 9 and 8 in eq. 7 leads to a complex expression for b, given as eq. 13 of SI. By considering, however, the physical characteristic of the system under investigation – schematically represented in Figure 2 – it is evident how the only "chiral" zone (i.e., where enantiomers are subjected to selective interactions) is the surface of functionalized silica particles. On the other hand, the behavior of the two enantiomers in the other regions of the system (namely, interstitial and intraparticle stagnant mobile zone) is identical (and, in particular, their diffusivity will be the same). Therefore, if the condition $b_1 = b_2$ is applied, a very simple result is achieved, i.e. (see Eqs. 14-17 of SI):

$$K_{a,1} \times D_{s,1} = K_{a,2} \times D_{s,2} \tag{10}$$

and since enantiomers are resolved on these CSPs, it follows that:

$$K_{a,1} \neq K_{a,2} \tag{11}$$

from where, through eq. 10, one arrives to the conclusion that:

$$D_{s,1} = D_{s,2} = 0 \tag{12}$$

This result reveals that the adsorption of enantiomers on these CSPs is localized.

Table 2 shows that the solid liquid mass transfer resistance c_s (calculated by means of eq. 10 of SI) is smaller on SPPs than on FPPs, in agreement with the reduced intraparticle space available for diffusion on the former type of particles.[4,43,44] Since it has been just demonstrated that the adsorption on these CSPs is localized, it makes sense to find that c_s, for each couple of enantiomers, increases with retention. This is therefore the opposite of what happens in RPLC where the larger the retention the smaller c_s, being the

solid phase diffusion the most important mechanism of mass transfer through pores.[14,39]

In the second part of this study, we focus on the adsorption-desorption kinetics. By looking again at Fig. 1, it can be observed that van Deemter curves of first enantiomers consistently lay below those of the second ones and that the gap between the two curves is more pronounced on SPP columns than on FPP ones. This gap cannot be explained only in terms of c_s. For example, on the Teico SP 2.0 column (figure 1d), h of the second enantiomer at $\nu = 16$ is twice that of the first one. But only about 15% of this can be explained by c_s. On the other hand, this difference comes from the slow adsorption-desorption kinetics. As it was pointed out before, however, the term c_{ads} cannot be directly estimated through Eq. 1 and the substraction method. To overcome this issue, a semi-empirical approach has been adopted in this work. It is based on the comparison between first eluted enantiomers and achiral compounds of similar retention. They were nitrobenzene on the Whelk-O1 columns and adenosine on the teicoplanin-based ones (see details under SI). For these small molecules it is reasonable to assume that the adsorption-desorption kinetics is fast (i.e., $c_{ads} = 0$). Therefore, for nitrobenzene and adenosine, the approach based on the subtraction method permits to estimate $a(\nu)$. As an example, Fig. 3 shows that the behavior of $a(\nu)$ vs. ν for nitrobenzene (retention factor, $k = 1.3$) very well matches that of $(a(\nu) + c_{ads})$ vs. ν for the first eluted TSO enantiomer ($k = 1.2$) on the Whelk-O1 column made of 2.6 μm SPPs. Analogous plots for the other columns/compounds are reported under SI. In all cases, a very consistent matching between curves was observed. Thus, the conclusion of a fast adsorption-desorption kinetics can be drawn also for the first eluted enantiomers of TSO and Z-D,L-Met. In other words, through these plots, the dependence of the eddy dispersion on the reduced velocity for less retained enantiomers on the different columns can be estimated. The analysis can be pushed further, by assuming the eddy dispersion of the two enantiomers (on each column) to be the same. This seems reasonable since the trans-column eddy dispersion of enantiomers should not depend on retention, being the adsorption localized (the same happens, e.g., in HILIC[46]). As a conclusion of this study, in Fig. 4 the comparison between $a(\nu)$ vs. ν plots for fully- and superficially-porous columns is reported. It is evident from these plots that the eddy dispersion on SPP columns is comparable (for the zwitterionic-teicoplanin columns, Fig. 4b) or even higher (for the Whelk-O1 ones, Fig. 4a) than that of their totally porous counterparts.

Having estimated $a(\nu)$, c_{ads} can now be calculated by Eq. 1. The values listed in Table 2 show that c_{ads} is larger on SPPs than FPPs (on either Whelk-O1 or teicoplanin-based CSPs). This finding can be likely correlated to the higher specific loading of chiral selector of SPPs (see Table 1). Even if from a different perspective, this result agrees with the observation reported in[47] regarding the adsorption equilibria of TSO enantiomers on the same Whelk-O1 CSPs used in this work. By measuring the adsorption isotherms, Felletti et al. found that the binding constants of enantiomers were systematically higher on the SPPs than

on the FPPs.

Another interesting conclusion from data of Table 2 is that c_{ads}s are remarkably larger on the teicoplanin CSPs than on the Whelk-O1 ones. This confirms that teicoplanin is a "slow" chiral selector, compared to Whelk-O1. It is remarkable to point out that these measurements were carried out directly on the heterogeneous chiral selectors, under experimentally-relevant chromatographic conditions. Therefore, this information is particularly relevant to design particles to be operated at high flow rates for ultrafast high-performance enantioseparations.

Conclusions

The study of mass transfer phenomena in chiral chromatography is complicated by the intrinsic difficulty of directly estimating the adsorption-desorption kinetics. In this work, the impact of c_{ads} on kinetic performance of Whelk-O1 and teicoplanin-based CSPs made on both FPPs and SPPs has been quantified by means of a semi-empirical approach based on the comparison with achiral species for which the adsorption-desorption kinetics is negligible. This has revealed that the larger the surface density of chiral selector the slower the adsorption-desorption kinetics. Thus, since chiral SPPs were characterized by higher surface density of chiral selector than FPPs (both for Whelk-O1 and teicoplanin ones), counterintuitively, columns packed with FPPs exhibited better efficiency at high flow rates than columns made of SPPs.

The other relevant outcome of this study concerns the nature of surface diffusion. The application of the parallel model of diffusion to Whelk-O1 and zwitterionic teicoplanin CSPs, has allowed to point out that in NP and HILIC the surface diffusion of enantiomers is absent. Even though this could be somehow expected under these experimental conditions – see, e.g., references[48–50] for achiral separations – to the best of our knowledge this is the first time that it has been experimentally proved.

Figures and Tables

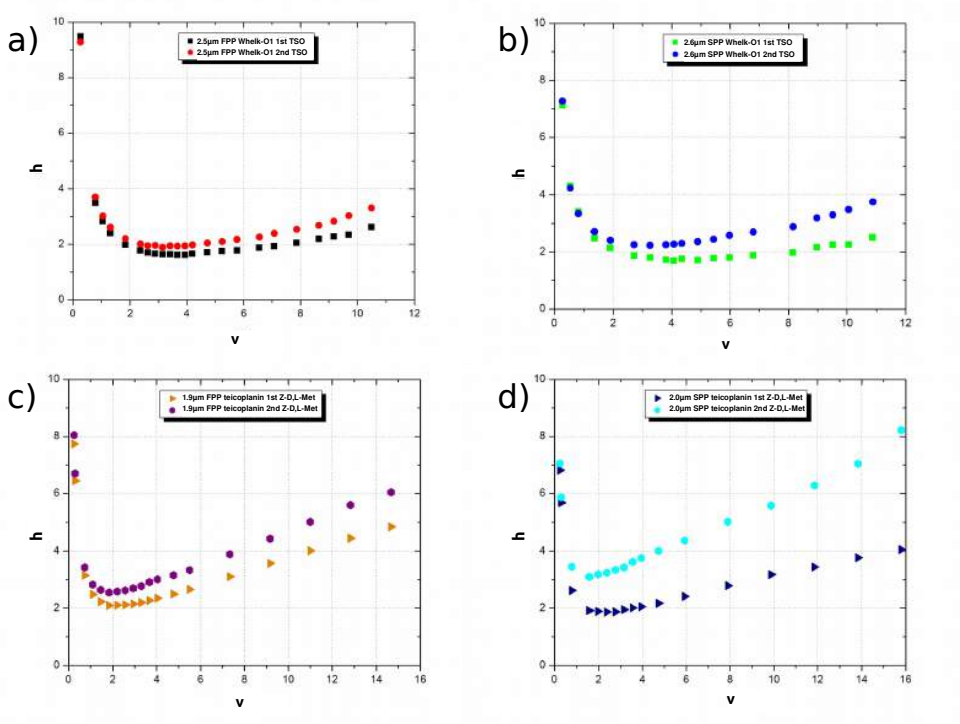

Figure 1: Reduced van Deemter curves of: (i) first (squares) and second (circles) eluted TSO enantiomers on the 2.5 μm FPP (box a) and the 2.6 μm SPP (box b) Whelk-O1 columns; and (ii) first (triangles) and second (hexagons) eluted Z-D,L-Met enantiomers on the 1.9 μm FPP (box c) and 2.0 μm SPP (box d) zwitterionic-teicoplanin columns.

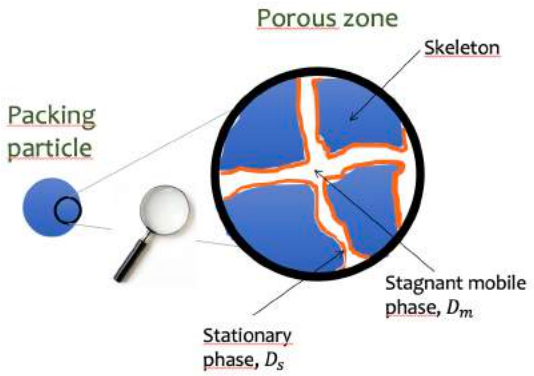

Figure 2: Schematic representation of the porous-zone physical model.

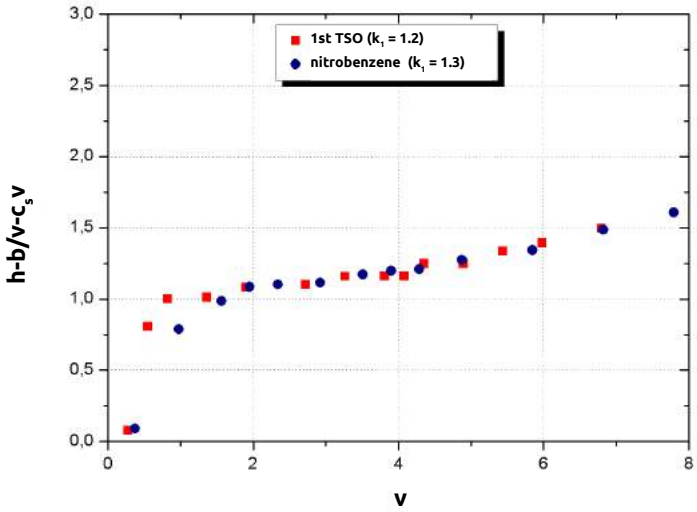

Figure 3: $a(\nu)$ vs. ν (nitrobenzene, circles) and $(a(\nu) + c_{ads})$ vs. ν (first eluted TSO enantiomer, squares) plots on the 2.6 μm SPP Whelk-O1 column.

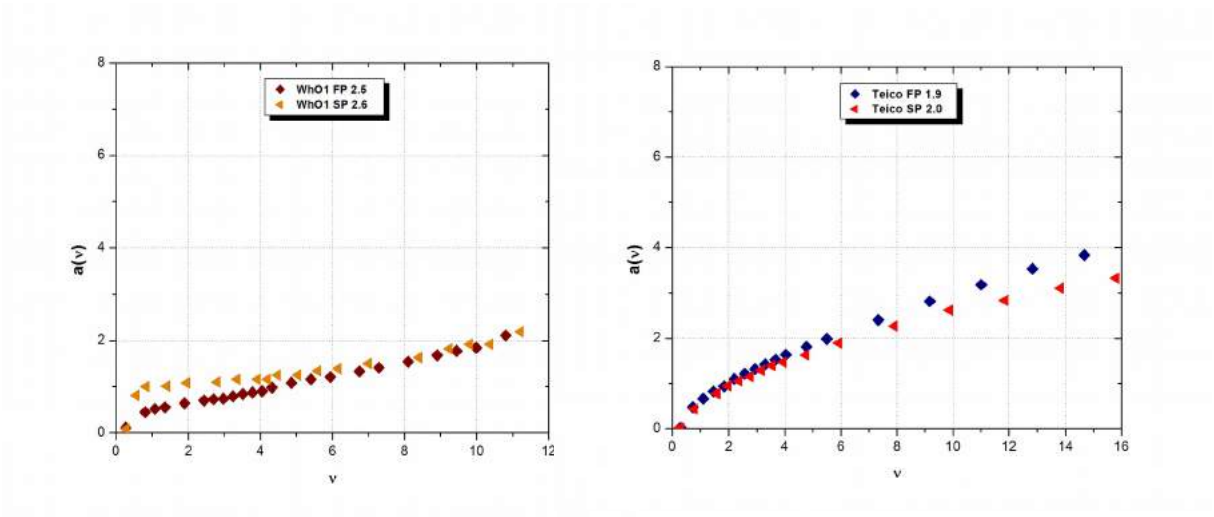

Figure 4: Dependence of $a(\nu)$ on ν for the four columns considered in this work. Left: eddy dispersion of TSO on the 2.6 μm SPP (triangles) and the 2.5 μm FPP (squares) Whelk-O1 columns. Right: eddy dispersion of Z-D,L-Met on the 1.9 μm FPP (squares) and the 2.0 μm SPP (triangles) zwitterionic-teicoplanin columns.

Table 1: Geometrical and physico-chemical characteristics of Whelk-O1 and Teicoplanin-based chiral particles and columns. Brand: commercial silica name; particle type: FPP = fully porous, SPP = superficially porous; d_p: particle diameter; A_s: specific surface area; ϵ_t: total porosity; ϵ_e: external porosity; ϵ_p: particle porous zone porosity.

Brand /Particle type	d_p μm	A_s m^2/g	Pore size Å	Bonding density μmol/g	μmol/m^2	ϵ_t	ϵ_e	ϵ_p
Kromasil /FPP	2.5	323	100	391	1.2	0.67	0.41	0.44
Accucore /SPP	2.6	130	80	190	1.5	0.52	0.41	0.25
Titan /FPP	1.9	282	120	76	0.3	0.66	0.42	0.41
Halo /SPP	2.0	125	90	56	0.5	0.54	0.41	0.27

Table 2: Zone retention factor (k_1), effective diffusion coefficient (D_{eff}), reduced longitudinal diffusion coefficient (b), reduced solid-liquid mass transfer resistance coefficient (c_s), particle diffusivity (D_p), reduced adsorption-desorption coefficient (c_{ads}) measured on the Whelk-O1 and Teicoplanin-based chiral particles.

Column	k_1		$D_{eff} \times 10^6$		b		c_s		$D_p \times 10^6$		c_{ads}
	1st	2nd	1st	2nd	1st	2nd	1st	2nd	1st	2nd	2nd
2.5μm FPP Whelk-O1	1.9	3.7	9.6	5.9	2.4	2.4	0.026	0.037	8.8	8.8	0.029
2.6μm SPP Whelk-O1	1.2	2.4	11.0	6.8	2.0	2.0	0.013	0.022	7.2	7.2	0.080
1.9μm FPP teicoplanin	3.1	4.7	2.9	2.2	2.0	2.0	0.060	0.064	3.0	3.0	0.115
2.0μm SPP teicoplanin	2.2	3.8	3.2	2.2	1.7	1.7	0.039	0.045	2.4	2.4	0.207

Acknowledgement

The authors thank the Italian University and Scientific Research Ministry (Grant PRIN 2017Y2PAB8_003) and the Laboratory Terra&Acqua Tech, member of Energy and Environment Cluster, Technopole of Ferrara of Emilia-Romagna High Technology Network. Dr. M. Carmosino and E. Bianchini from the University of Ferrara are acknowledged for technical support.

References

(1) Gritti, F.; Cavazzini, A.; Marchetti, N.; Guiochon, G. Comparison between the efficiencies of columns packed with fully and partially porous C_{18}-bonded silica materials. *J. Chromatogr. A* **2007**, *1157*, 289–303.

(2) Gritti, F.; Guiochon, G. A protocol for the measurement of all the parameters of the mass transfer kinetics in columns used in liquid chromatography. *J. Chromatogr. A* **2010**, *1217*, 5137–5151.

(3) Gritti, F.; Leonardis, I.; Shock, D.; Stevenson, P.; Shalliker, A.; Guiochon, G. Performance of columns packed with the new shell particles Kinetex-C_{18}. *J. Chromatogr. A* **2010**, *1217*, 1589–1603.

(4) Guiochon, G.; Gritti, F. Shell particles, trials, tribulations and triumphs. *J. Chromatogr. A* **2011**, *1218*, 1915–1938.

(5) Gritti, F.; Guiochon, G. Mass transfer kinetics, band broadening and column efficiency. *J. Chromatogr. A* **2012**, *1221*, 2–40.

(6) Liekens, A.; Denayer, J.; Desmet, G. Experimental investigation of the difference in B-term dominated band broadening between fully porous and porous-shell particles for liquid chromatography using the Effective Medium Theory. *J. Chromatogr. A* **2011**, *1218*, 4406–4416.

(7) Deridder, S.; Desmet, G. Effective medium theory expressions for the effective diffusion in chromatographic beds filled with porous, non-porous and porous-shell particles and cylinders. Part II: Numerical verification and quantitative effect of solid core on expected B-term band broadening. *J. Chromatogr. A* **2011**, *1218*, 46–56.

(8) Song, H.; Desmet, G.; Cabooter, D. Evaluation of the kinetic performance differences between Hydrophilic-Interaction Liquid Chromatography and Reversed-Phase Liquid Chromatography under conditions of identical packing structure. *Anal. Chem.* **2015**, *87*, 12331–12339.

(9) Andrés, A.; Broeckhoven, K.; Desmet, G. Methods for the experimental characterization and analysis of the efficiency and speed of chromatographic columns: a step-by-step tutorial. *Anal. Chim. Acta* **2015**, *894*, 20–34.

(10) Kiss, I.; Bacskay, I.; Kilár, F.; Felinger, A. Comparison of the mass transfer in totally porous and superficially porous stationary phases in liquid chromatography. *Anal. Bioanal. Chem.* **2010**, *397*, 1307–1314.

(11) Felinger, A. Diffusion time in core-shell packing materials. *J. Chromatogr. A* **2011**, *1218*, 1939–1941.

(12) Hlushkou, D.; Bruns, S.; Tallarek, U. High-performance computing of flow and transport in physically reconstructed silica monoliths. *J. Chromatogr. A* **2010**, *1217*, 3674–3682.

(13) Daneyko, A.; Hlushkou, D.; Baranau, V.; Khirevic, S.; Seidel-Morgenstern, A.; Tallarek, U. Computational investigation of longitudinal diffusion, eddy dispersion, and trans-particle mass transfer in

bulk, random packings of core-shell particles with varied shell thickness and shell diffusion coefficient. *J. Chromatogr. A* **2015**, *1407*, 139–156.

(14) Ismail, O. H.; Pasti, L.; Ciogli, A.; Villani, C.; Kocergin, J.; Anderson, S.; Gasparrini, F.; Cavazzini, A.; Catani, M. Pirkle-type chiral stationary phase on coreshell and fully porous particles: Are superficially porous particles always the better choice toward ultrafast high-performance enantioseparations? *J. Chromatogr. A* **2016**, *1466*, 96–104.

(15) Ismail, O. H.; Ciogli, A.; Villani, C.; Martino, M. D.; Pierini, M.; Cavazzini, A.; Bell, D. S.; Gasparrini, F. Ultra-fast high-efficiency enantioseparations by means of a teicoplanin-based chiral stationary phase made on sub-2 μm totally porous silica particles of narrow size distribution. *J. Chromatogr. A* **2016**, *1427*, 55–68.

(16) Patel, D. C.; Breitbach, Z. S.; Yu, J.; Nguyen, K. A.; Armstrong, D. W. Quinine bonded to superficially porous particles for high-efficiency and ultrafast liquid and supercritical fluid chromatography. *Anal. Chim. Acta* **2017**, *963*, 164–174.

(17) Kharaishvili, Q.; Jibuti, G.; Farkas, T.; Chankvetadze, B. Further proof to the utility of polysaccharide-based chiral selectors in combination with superficially porous silica particles as effective chiral stationary phases for separation of enantiomers in high-performance liquid chromatography. *J. Chromatogr. A* **2016**, *1467*, 163–168.

(18) Ismail, O. H.; Antonelli, M.; Ciogli, A.; Villani, C.; Cavazzini, A.; Catani, M.; Felletti, S.; Bell, D. S.; Gasparrini, F. Future perspectives in high efficient and ultrafast chiral liquid chromatography through zwitterionic teicoplanin-based 2μm superficially porous particles. *J. Chromatogr. A* **2017**, *1520*, 91–102.

(19) Patel, D. C.; Breitbach, Z. S.; Wahab, M. F.; Barhate, C. L.; Armstrong, D. W. Gone in seconds: praxis, performance and peculiarities of ultrafast chiral liquid chromatography with superficially porous particles. *Anal. Chem.* **2015**, *87*, 9137–9148.

(20) Gritti, F.; Guiochon, G. Possible resolution gain in enantioseparations afforded by core-shell particle technology. *J. Chromatogr. A* **2014**, *1348*, 87–96.

(21) Schmitt, K.; Woiwode, U.; Kohout, M.; Zhang, T.; Lindner, W.; Lämmerhofer, M. Comparison of small size fully porous particles and superficially porous particles of chiral anion-exchange type stationary phases in ultra-high performance liquid chromatography: effect of particle and pore size on chromatographic efficiency and kinetic performance. *J. Chromatogr. A* **2018**, *1569*, 149–159.

(22) Gritti, F.; Guiochon, G. Mass transfer mechanism in chiral reversed phase liquid chromatography. *J. Chromatogr. A* **2014**, *1332*, 35–45.

(23) Gritti, F.; Guiochon, G. General HETP equation for the study of mass-transfer mechanisms in RPLC. *Anal. Chem.* **2006**, *78*, 5392–5347.

(24) Spudeit, D. A.; Dolzan, M. D.; Breitbach, Z. S.; Barber, W. E.; Micke, G. A.; Armstrong, D. W. Superficially porous particles vs. fully porous particles for bonded high performance liquid chromatographic chiral stationary phases: Isopropyl cyclofructan 6. *J. Chromatogr. A* **2014**, *1363*, 89–95.

(25) Gritti, F.; Guiochon, G. Mass transfer mechanism in chiral reversed phase liquid chromatography. *J. Chromatogr. A* **2014**, *1332*, 35–45.

(26) Pasti, L.; Marchetti, N.; Guzzinati, R.; Catani, M.; Bosi, V.; Dondi, F.; Sepsey, A.; Felinger, A.; Cavazzini, A. Microscopic models of liquid chromatography: From ensemble-averaged information to resolution of fundamental viewpoint at single-molecule level. *TrAC* **2016**, *81*, 63–68.

(27) Catani, M.; Felletti, S.; Ismail, O. H.; Gasparrini, F.; Pasti, L.; Marchetti, N.; Luca, C. D.; Costa, V.; Cavazzini, A. New frontiers and cutting edge applications in ultra high performance liquid chromatography through latest generation superficially porous particles with particular emphasis to the field of chiral separations. *Anal. Bioanal. Chem* **2018**, *410*, 2457–2465.

(28) Catani, M.; Ismail, O. H.; Gasparrini, F.; Antonelli, M.; Pasti, L.; Marchetti, N.; Felletti, S.; Cavazzini, A. Recent advancements and future directions of superficially porous chiral stationary phases for ultrafast high-performance enantioseparations. *Analyst* **2017**, *142*, 555–566.

(29) Ismail, O. H.; Felletti, S.; Luca, C. D.; Pasti, L.; Marchetti, N.; Costa, V.; Gasparrini, F.; Cavazzini, A.; Catani, M. The way to ultrafast, high-throughput enantioseparations of bioactive compounds in liquid and supercritical fluid chromatography. *Molecules* **2018**, *23*, 2709.

(30) Halász, I.; Endele, R.; Asshauer, J. Ultimate limits in high-pressure liquid chromatography. *J. Chromatogr.* **1975**, *112*, 37–60.

(31) Halász, I.; Martin, K. Pore Size of Solids. *Angew. Chem. Int. Ed. Engl* **1978**, *17*, 901–908.

(32) Cavazzini, A.; Gritti, F.; Kaczmarski, K.; Marchetti, N.; Guiochon, G. Mass-transfer kinetics in a shell packing materials for chromatography. *Anal. Chem.* **2007**, *79*, 5972–5979.

(33) Gritti, F.; Guiochon, G. Theoretical and experimental impact of the bed aspect ratio on the axial dispersion coefficient of columns packed with 2.5μm particles. *J. Chromatogr. A* **2012**, *1262*, 107–121.

(34) Knox, J. H.; McLaren, L. New Gas Chromatographic Method for Measuring Gaseous Diffusion Coefficients and Obstructive Factors. *Anal. Chem.* **1964**, *36*, 1477–1482.

(35) Miyabe, K.; Matsumoto, Y.; Guiochon, G. Peak Parking-Moment Analysis. A Strategy for the Study of the Mass-Transfer Kinetics in the Stationary Phase. *Anal. Chem.* **2007**, *79*, 1970–1982.

(36) Giddings, J. C. Comparison of Theoretical Limit of Separating Speed in Gas and Liquid Chromatography. *Anal. Chem.* **1965**, *37*, 60–63.

(37) Ludlum, D.; Warner, R.; Smith, H. The Diffusion of thiourea in water at 25°C. *J. Phys. Chem* **1962**, *66*, 1540–1542.

(38) Ismail, O. H.; Catani, M.; Pasti, L.; Cavazzini, A.; Ciogli, A.; Villani, C.; Kotoni, D.; Gasparrini, F.; Bell, D. S. Experimental evidence of the kinetic performance achievable with columns packed with the new 1.9 μm fully porous particles Titan C_{18}. *J. Chromatogr. A* **2016**, *1454*, 86–92.

(39) Catani, M.; Ismail, O. H.; Cavazzini, A.; Ciogli, A.; Villani, C.; Pasti, L.; Cabooter, D.; Desmet, G.; Gasparrini, F.; Bell, D. S. Rationale behind the optimum efficiency of columns packed with the new 1.9 μm fully porous particles Titan C_{18}. *J. Chromatogr. A* **2016**, *1454*, 78–85.

(40) Desmet, G.; Deridder, S. Effective medium theory expressions for the effective diffusion in chromatographic beds filled with porous, non-porous and porous-shell particles and cylinders. Part I: Theory. *J. Chromatogr. A* **2011**, *1218*, 32–45.

(41) Desmet, G.; Broeckhoven, K.; Smet, J. D.; Deridder, S.; Baron, G. V.; Gzil, P. Errors involved in the existing B-term expressions for the longitudinal diffusion in fully porous chromatographic media. Part I: Computational data in ordered pillar arrays and effective medium theory. *J. Chromatogr. A* **2008**, *1188*, 171–188.

(42) Knox, J. H.; Scott, H. P. B and C terms in the van Deemter equation for liquid chromatography. *J. Chromatogr.* **1983**, *282*, 297–313.

(43) Cavazzini, A.; Gritti, F.; Kaczmarski, K.; Marchetti, N.; Guiochon, G. Mass-Transfer Kinetics in a Shell Packing Material for Chromatography. *Anal. Chem.* **2007**, *79*, 5972–5979.

(44) Deridder, S.; Catani, M.; Cavazzini, A.; Desmet, G. A theorethical study on the advantage of core-shell particles with radially-oriented mesopores. *J. Chromatogr. A* **2016**, *1456*, 137–144.

(45) Desmet, G.; Broeckhoven, K.; De Smet, J.; Deridder, S.; Baron, G. V.; Gzil, P. Errors involved in the existing B-term expressions for the longitudinal diffusion in fully porous chromatographic media. Part I: Computational data in ordered pillar arrays and effective medium theory. *J. Chromatogr. A* **2008**, *1188*, 171–188.

(46) Gritti, G.; Guiochon, G. Mass transfer mechanism in hydrophilic interaction chromatography. *J. Chromatogr. A* **2013**, *1302*, 55–64.

(47) Felletti, S.; De Luca, C.; Ismail, O. H.; Pasti, L.; Costa, V.; Gasparrini, F.; Cavazzini, A.; Catani, M. On the effect of chiral selector loading and mobile phase composition on adsorption properties of latest generation fully- and superficially-porous Whelk-O1 particles for high-efficient ultrafast enantioseparations. *J. Chromatogr. A* **2018**, *1579*, 41–48.

(48) Gritti, F.; Guiochon, G. Mass transfer kinetics, band broadening and column efficiency. *J. Chromatogr. A* **2012**, *1221*, 2–40.

(49) Miyabe, K.; Guiochon, G. Surface diffusion in reversed-phase liquid chromatography. *J. Chromatogr. A* **2010**, *1217*, 1713–1734.

(50) Jandera, P.; Hájek, T. Mobile phase effects on the retention on polar columns with special attention to the dual hydrophilic interactionreversedphase liquid chromatography mechanism, a review. *J. Sep. Sci.* **2018**, *41*, 145–152.

Paper IX

Pore size effect on zwitterionic teicoplanin based chiral stationary phases: kinetic and thermodynamic investigation.

Omar H. Ismail[1,], Martina Catani[1], Simona Felletti[1], Michael Ye[3], Alberto Cavazzini[1], Francesco Gasparrini[2,*]*

[1] Dipartimento di Scienze Chimiche e Farmaceutiche, Università di Ferrara, via L. Borsari 46, 44121 Ferrara, Italy;
[2] Dipartimento di Chimica e Tecnologie del Farmaco, "Sapienza" Università di Roma, P. le Aldo Moro 5, 00185 Roma, Italy
[3] Sigma-Aldrich/Supelco, 595 North Harrison Road, Bellefonte, PA, 16823, United States

Keywords: UHPC-Tzwitt, Superficially Porous Particles CSP, High porosity silica, Very-High Efficiency column.

* Corresponding authors
Email addresses: francesco.gasparrini@uniroma1.it (F. Gasparrini), omar.ismail@uniroma1.it (O.H. Ismail)

Abstract

In this work, a novel Chiral Stationary Phase (CSP) was developed by bonding the zwitterionic teicoplanin selector (TE_A2) onto a highly porous core-shell silica Halo 160Å 2.7 µm (UHPC-SPP-Halo160-Tzwitt 2.7) and it was compared to the already known zwitterionic teicoplanin SPP-Halo 90Å 2.0 and 2.7 µm. All these CSPs were packed into columns with a geometry of 100x4.6 mm L.xI.D. and characterized in terms of permeability, efficiency, retention power and enantioselectivity under Hydrophilic Liquid Interaction Chromatography (HILIC). Kinetic performances were mainly evaluated through the use of achiral and chiral van Deemter analyses giving excellent results: up to 315000 plates/m were achieved injecting naphthalene on the UHPC-SPP-Halo160-Tzwitt 2.7 with a very low reduced plate height of 1.17.
A large variety of chiral molecules (N-derivatized amino acids, pharmaceutical and agrochemical compounds) were tested on the three columns to investigate the application field and the practical benefits of using the SPP-Halo 160Å 2.7 µm-based column. Overall, as expected, lower retention factors were recorded on the UHPC-SPP-Halo160-Tzwitt 2.7 because of its small surface area, responsible of a lower amount of selector bonded on the silica matrix, but, at the same time, higher enantioselectivity values were observed in comparison to the other CSPs. This column exhibited resolutions comparable to those recorded by the 2.0 µm-based column on the most of separations but, taking into account the retention factors of both stationary phases, a considerable superiority of the high porosity CSP was proven on all analytes thanks to a great combination of high efficiencies and large enantioselectivity values.

1. Introduction

During the last fifteen years, since the commercialization of the first Ultra-High Performance Chromatography (UHPLC) system from Waters in 2004, the search of higher column efficiency, costs reduction and throughput enhancement has led to continuous improvements of the chromatographic instrumentation and particles technology. In fact, we have assisted to a consistent reduction of the silica particles size[1], from the 5-10 µm, typical of the HPLC, down to sub-2µm diameters producing efficiencies larger than 300000 plates/m. Furthermore, starting from 2006, a new silica technology, named Superficially Porous Particles (SPPs), Core-Shell or Fused-core®, has been developed[2-12]. This silica is made of particles with a solid core surrounded by a porous layer (generally representing the 20% of the total particle diameter). The main benefit of using superficially porous materials lies in the ability to achieve larger efficiency (with a reduced plate height (h_r) between 1.5-1.7[13]) in comparison with a column packed with a fully porous silica with the same particle diameter and, in addition, the separation process can be completed in shorter times.

Superficially porous silica, after the commercialization by Advanced Materials Technology, Inc, were employed only in the achiral field until Reischl *et al.*[14], to best of our knowledge, in 2011 with an anion exchanger chiral stationary phase, bonded the quinidine selector onto a superficially porous 2.7µm silica, separating different racemic derivatized amino acids. In 2012, Chankvetadze's group compared a 2.6µm SPP (from Phenomenex Inc.) polysaccharide-based CSP[15], to an analogue chiral FPP column, founding on the first column a higher enantioselectivity (with a comparable selector loading), a smaller drop of the column efficiency at high flow-rates and a higher enantioresolution[16-19]. In 2015, Armstrong and coworkers[20-23] evaluated the performance of some chiral selectors (cyclodextrin, cyclofructan-6 based and macrocyclic antibiotics) bonded on 2.7µm SPP silica. They found that this column outperforms, from the kinetic point of view, its FPP-CSPs (3-5 µm) counterpart. Meanwhile, some authors of this paper worked on a Pirkle-type CSP, bonding the Whelk-O1 chiral selector onto 1.8µm and 2.5µm FPP-Kromasil and on 2.6µm SPP-Accucore, stating the ability of the FPP-2.5µm to achieve better results than the SPP-2.6µm, both of them were overcome by the 1.8µm FPP[24-25]. Further, they also beat the sub-second separation, showing the first example of a baseline-enantioseparation in 0.9 second with a 10x3.0 mm L.xI.D. Fully Porous-based column. The same authors, in 2017, compared three columns packed with zwitterionic teicoplanin[26] CSPs SPP-Halo 2.0 and 2.7 and FPP-Titan 1.9 µm[27] demonstrating that this selector, differently from the Whelk-O1, showed better kinetic and thermodynamic performances on the sub-2µm superficially porous silica.

Recently, in 2018, Lammerhofer's group studied performance of different CSPs obtained by immobilizing tert-butylcarbamoylquinine selector (tBuCQN) on 1.7 µm Fully porous particles and on 2.7 µm superficially porous silica with different porosity[28]. They found that the 2.7 µm CSP outperform the FPP counterpart achieving higher efficiency and completing the analytical process in shorter times. In addition, they noticed that with both FPPs and SPPs an improvement of kinetic performance can be reached increasing the silica pore size.

In this study, we bonded the already known zwitterionic teicoplanin onto the SPP-Halo 160Å 2.7 µm silica aiming to evaluate the effect of the silica porosity and, consequently, the selector loading on this chiral stationary phase by comparing all data we have obtained to those of two columns packed with zwitterionic teicoplanin CSPs based on SPP-Halo 90Å 2.0 and 2.7 µm silica.

2. Theory

The efficiency of a column is usually evaluated through the well-known van Deemter equation (1), which correlates the plate height, H, to the linear velocity:

$$H = A + B/\mu + C \times \mu \quad (1)$$

where the A-term is the contribution of eddy dispersion, B-term is the longitudinal diffusion, C-term accounts for solid-liquid mass transfer resistance.
For the construction of van Deemter curves we used the flow-rate on the x-axis and the H (µm) on the y-axis.
The resolution (Rs), output values from Chromeleon 6.8 software, were calculated according to the European Pharmacopeia using peak width at half height ($W_{0.5}$).

3. Experimental

3.1 Materials and chemicals

All chemicals were purchased from Sigma-Aldrich (St. Louis, Mo, USA). HPLC gradient grade solvents were filtered before use on 0.2 µm Omnipore filters (Merck Millipore, Darmstadt, Germany). Chiral samples were available from previous studies or from Sigma-Aldrich (St. Louis, Mo, USA). Halo silica 2.0 µm and 2.7 µm 90Å (surface area 125 and 123 m^2/g, respectively), 2.7 µm 160Å (surface area 80 m^2/g) and teicoplanin selector were provided by Merck Sigma–Aldrich (St. Louis, MO, USA). Empty stainless steel columns, 100 mm x 4.6 mm L x I.D., were from IsoBar Systems by Idex (Wertheim-Mondfeld, Germany).

3.2 Instruments

The UPLC Acquity Waters (Milford, MA, USA) was employed for achiral tests aiming to properly evaluate the maxima efficiencies of low retained samples under HILIC conditions. This instrument includes a binary solvent manager with a maximum delivery flow rate of 2.0 mL/min, an auto-sampler with a 5 µL loop injection, a PDA detector including a 500 nL flow cell, 80 Hz acquisition rate, resolution 4.8 nm and no filter time constant was used. Data acquisition, data handling and instrument control were performed by Empower 3. The maximal backpressure for the UPLC system is 1000 bar at flow rates lower or equal to 1 mL/min, and value decreases linearly, in the range 1.0–2.0 mL/min, up to 600 bar at 2 mL/min. A standard UPLC Acquity Waters column heater, in still air conditions, with a maximum temperature of 65 °C was used. Inlet Viper capillary of 250 mm x 0.100 mm I.D. and outlet Viper capillary of 350 mm x 100 mm I.D. were used in order to minimize the extra-column contribution. In this configuration the instrument variance was measured using a zero dead-volume connector (instead of the column). The extra-column volume (obtained by injecting uracil) was 7.22 µL (variance, $\sigma^2_{v,\ extra}$= 1.02 μL^2 at 1.0 mL/min, eluent: acetonitrile/water 85/15 + 15mM ammonium formate, T: 35°C)[29].
The UHPLC chromatographic system used for all achiral tests in HILIC was an UltiMate 3000 RS system (Thermo Fisher Dionex Sunnyvale, California), equipped with a dual gradient RS pump, an in-line split loop Well Plate Sampler, a thermostatted RS Column Ventilated Compartment (temperature range 5-110 °C) and a diode array detector (Vanquish detector) with a low dispersion 2.0 µL flow cell, a filter time constant of 0.002 s, a data collection rate of 100 Hz and a response time of 0.04 s. The inlet and outlet viper tubes (2 x 350 mm × 0.100 mm I.D.) were employed. Data acquisition and processing

were performed with Chromeleon 6.8 software from Thermo Fisher. The extra-column peak variance (calculated through peak moments) was 3.94µL^2 at a flow-rate of 1.0 mL/min. Data acquisition, data handling and instrument control were performed by Chromeleon software.

3.3 Preparation of chiral stationary phases.

All columns were packed with CSPs synthesized according to the same Supelco proprietary bonding protocol immobilizing teicoplanin selector onto SPP-Halo 2.0µm and 2.7µm, leading to the zwitterionic chiral stationary phases (here *UHPC-SPP-Halo*90A-*Tzwitt 2.0, UHPC-SPP-Halo*90A-*Tzwitt 2.7 and UHPC-SPP-Halo*160A-*Tzwitt 2.7)*. All CSPs were slurry packed with a pneumatically driven Haskel pump (P_{max}~ 950 bar) into stainless steel columns.

Elemental analysis (CHN) of the different CSPs were used to extract values of selector loading and surface coverage. UHPC-SPP-Halo90A-Tzwitt 2.0: 5.75 %C, 0.74 %H and 0.63 %N, corresponding to 56 µmoles of selector per gram of silica and to 0.45 µmol/m^2 (based on N); UHPC-SPP-Halo90A-Tzwitt 2.7: 6.05 %C, 0.79 %H and 0.66 %N, corresponding to 59 µmoles of selector per gram of silica and to 0.47 µmol/m^2 (based on N); UHPC-SPP-Halo160A-Tzwitt 2.7: 5.67 %C, 0.68 %H and 0.71 %N, corresponding to 64 µmoles of selector per gram of silica and to 0.80 µmol/m^2 (based on N). As expected, the two SPP-Halo90A CSPs showed a comparable loading of selector but a lower surface density of teicoplanin in comparison with the Halo 2.7µm 160Å silica.

3.4 Methodology

All separations were performed under Hydrophilic Interaction Liquid Chromatography (HILIC) conditions by using a mobile phase made by ACN/H_2O 85:15 + 15 mM $HCOONH_4$ (^{MP}pH: 7.5). The injected volume was in the range of 0.5-1.0 µL. For data evaluation, the values of resolution (Rs) and the efficiency (N/m), output from Chromeleon software, were calculated according to the European Pharmacopeia using peak width at half height ($W_{0.5}$). Dead time (t_0) was estimated by injection of an unretained marker (naphthalene). All data were processed with Origin 6.0/8.0.

4. Results and Discussion

4.1 Physical characterization.

Aiming to fully characterize all columns (100 x 4.6 mm L.xI.D.), the first evaluation was made taking into account the pressure generated by all columns, the plot is showed in Fig.1, correlating the flow-rate with the column pressure. As can be easily observed from the figure, both SPP-2.7 columns exhibited a comparable pressure which resulted to be about the 40% lower than that recorded on the UHPC-SPP-Halo90-Tzwitt 2.0 because of its smaller particles diameter. The different pressure drop showed by the two columns packed with 2.7µm silica can be attributed to a different packing efficiency of the two columns

4.2 van Deemter analysis on achiral samples

All analyses were performed on a Dionex Ultimate 3000RS allowing to reach flow-rates higher than 2.0 mL/min, only van Deemter plots of naphthalene and uracil were made by using the Acquity Waters UPLC since these samples own a very low retention factor and a reduced extracolumn variance instrument ($\sigma^2_{v,\ extra}$= 1.02 µL^2 at a flow-rate of 1.0 mL/min) is required to reach the highest possible efficiency. We started from a minimum flow-rate of 0.2 mL/min up to 2.0 mL/min with a maximum operating pressure of 210 bar (on UHPC-SPP-Halo-Tzwitt 2.0 100x4.6 mm). The first

evaluation was made by using a mixture composed of naphthalene (void volume marker), thiourea, uracil and adenosine. In this work, all HETP (H) values were not corrected for the extra-column variance, H_{exp} was used for all van Deemter plots. All van Deemter curves were constructed with H_{exp} on the y-axes and flow-rate on the x-axis. In Fig. 2A van Deemter plots of naphtalene on the three columns are shown. As expected, thanks to its reduced particles diameter, an extraordinary efficiency was obtained by using the UHPC-SPP-Halo90A-Tzwitt 2.0 with more than 330000 theoretical plates per meter at a flow-rate of 2.0 mL/min corresponding to a plate height of 3.02 µm. Also the new UHPC-SPP-Halo160A-Tzwitt 2.7 provided an unexpected result generating a N/m: 316000 (H: 3.16 µm) at 2.0 mL/min. Lastly, the column packed with SPP-Halo 2.7 µm 90Å showed 272000 plates/m (H: 3.67 µm) at 1.5 mL/min. Looking at these plots deeply, we should pay specific attention to the reduced plate height (h_r (/)) (Fig. 2B) which allows to properly evaluate the kinetic performance of columns with different internal diameters or packed with silica with various particle diameters. Moreover, lower h_r values indicate a better quality of the packing procedure. In fact, an incredibly low h_r of 1.17 has been recorded on the UHPC-SPP-Halo160-Tzwitt 2.7, followed by the 1.36 and 1.51 of the columns packed with SPP-Halo90 2.7 and SPP-Halo90 2.0 respectively. On the one hand, it is evident that the packing procedure is more effective by using bigger particles (lower reduced plate height on both SPP-Halo 2.7µm)[30-31], on the other one, this process seems to be easier packing columns with teicoplanin-based CSP having a higher silica porosity (lower h_r on the SPP-Halo160 column than the SPP-Halo90 2.7 µm one). In the second step of the achiral kinetic evaluation, a compound more retained was studied (thiourea, *k'*: 0.5-0.6). Also in this case, the best column efficiency has been achieved with more than 310000 N/m (H: 3.21 µm, h_r: 1.60) by using the 2.0 µm-based column at a flow-rate of 1.5 mL/min and the UHPC-SPP-Halo90-Tzwitt 2.7 permitted to record almost 250000 plates/m (H= 4.03 µm, h_r: 1.49). As previously observed, the column packed with the 160Å CSP permitted to observe a very high efficiency, a N/m of 307000 was achieved at the same optimal flow rate of the 2.0 µm silica-based column, corresponding to a H: 3.25 µm and h_r: 1.17. In addition, it can be noticed from the van Deemter plot that the C-branch of the curve is extremely flat, comparably to the one of the UHPC-SPP-Halo90A-Tzwitt 2.0 giving the chance to perform analyses at flow-rates much higher than the optimal one with a consequent reduction of the separation time without significant efficiency loss. On the contrary, the SPP-Halo90 2.7 column showed a higher slope of the right branch of the van Deemter curve, typical of columns packed with silica particles of this diameter. This behaviour becomes even more evident taking into account compounds with higher retention factors. In Figure S1 van Deemter plots of adenosine (*k'*: 1.7-1.9 on the two 90Å silica-based columns and 1.01 on the 160Å one) are shown. About 270000 and 220000 plates/m were recorded on the SPP-Halo90 2.0 and 2.7 at 1.2 and 0.5 mL/min, respectively and an efficiency close to 250000 N/m was obtained on the SPP-Halo160 2.7 at 0.7 mL/min. The most important aspect relies in the ability to reach these efficiencies at higher flow-rates on the SPP-Halo90 2.0 and SPP-Halo160 2.7 in comparison to the UHPC-SPP-Halo90-Tzwitt 2.7 and, in addition, is evident the flatter form of the C-branch of these two columns permitting to analyse samples at high flow-rates maintaining large efficiencies.

4.3 Chromatograms analysis of achiral samples

The chromatographic traces of the separation of the mixture of the achiral probes naphthalene (void volume marker), thiourea, uracil and adenosine on the three columns, at their optimal flow-rate, are shown in Fig. 4A. Being the minimum of the van Deemter curve of UHPC-SPP-Halo90-Tzwitt 2.7 lower

than those of the other columns, obviously, a loss of speed of about 30% was observed. In addition, using the UHPC-SPP-Halo160-Tzwitt 2.7 we have to consider an important aspect: in fact, this CSP permit to obtain faster analyses also in comparison to the SPP-Halo90 2.0 because of its lower retention power maintaining a great separation of all analytes. As can be noticed from figure 4B, this column provides smaller *k'* than the two 90Å CSPs because of a lower selector loading on the silica matrix, but, at the same time, it maintains a comparable, or even higher, resolution. This aspect will be discussed more deeply in chapter 4.5.

4.4 van Deemter analysis on chiral compound

After the preliminary evaluation made by using the achiral mixture previously discussed, the kinetic profile of all columns was completed injecting the racemic chiral molecule (2-(4-chloro-phenoxy)-propionic acid) as probe for van Deemter analysis (Fig. 5A). The UHPC-SPP-Halo-Tzwitt 2.0 showed excellent results: almost 300000 plates/m, corresponding to H= 3.42µm (h_r: 1.71), were recorded for the first eluted enantiomer and almost 280000 on the second one at flow rates of 0.9 and 0.7 mL/min, respectively. Also the column packed with SPP-Halo160 2.7µm column showed great results: more than 240000 plates/m (H= 4.12 µm, h_r: 1.53) for the first eluted enantiomer at a flow rate of 0.5-0.6 mL/min were achieved. As expected, the column packed with the UHPC-SPP-Halo90-Tzwitt 2.7 was the less efficient exhibiting 211000 plates/m on the first peak (H: 4.74 µm, h_r: 1.76) at a flow rate of 0.5 mL/min. In addition, looking at the reduced plate height plot (Fig. 5B) the same trend recorded with the achiral evaluation was confirmed, in fact, the SPP-Halo160 2.7 µm column provided the lowest h_r (1.53) proving the excellent kinetic performance of this column also in the chiral field. Moreover, looking at the shape of the curves, the most important advantage of the UHPC-SPP-Halo-Tzwitt 2.0 resides in a very flat C-term of the van Deemter curve, also of chiral samples. This is an essential aspect to consider in the UHPLC field: a low C-term allows to perform the same analysis at a higher flow-rate without a consistent loss of efficiency (and resolution consequently). For example, moving from the optimal flow-rate to 3.0 mL/min the loss would be around 40% on the SPP-Halo 2.0 µm column, but more than 60% on the SPP-Halo 2.7 µm. Furthermore, SPP-Halo160 2.7 µm confirmed its ability to achieve its maximum performance at flow-rates higher than the 90Å analogue column.

Practical results are shown in Fig. 6 where chromatographic traces of the aryloxy acid separations on all columns are reported at their optimal flow-rates. As expected, the fastest separation was obtained by using the UHPC-SPP-Halo90-Tzwitt 2.0 permitting the separation of the two enantiomers in less than 4 minutes, about twice faster than the other two columns. On the other hand, the SPP-Halo160 2.7 µm-based column exhibited the highest resolution power thanks to its larger selectivity.

4.5 Separation of chiral molecules

4.5.1 Kinetic performance

After the evaluation of the physical and kinetic properties, all columns were tested for practical applications. A broad range of chiral analytes (including N-derivatized amino acids, agrochemical compounds and drugs or drug-like molecules) was tested under HILIC conditions. All kinetic data are summarized in Table 1S. A common trend can be observed: the most efficient column was the UHPC-SPP-Halo90-Tzwitt 2.0 µm but also the SPP-Halo160 2.7 µm was able to provide large N/m values in all cases (more than 250 000 and roughly 200 000, respectively, on many samples) whereas the SPP-Halo90 2.7µm produced significantly lower efficiencies. In fact, looking at the Table 1S, an average

loss of efficiency of the 35% for the first eluted enantiomer was observed on the UHPC-SPP-Halo90-Tzwitt 2.7 in comparison to the SPP-Halo90-Tzwitt 2µm. The chromatographic traces of four different chiral analytes on the three columns at the flow-rate of 1.0 mL/min are shown in Fig. 7. The best efficiencies were achieved injecting the pesticide haloxyfop (first two eluted enantiomers in Fig. 7A) with roughly 265 000 N/m for the first enantiomer on the SPP-Halo 2.0µm, and efficiency values that are 11% and 36% smaller on the SPP-Halo160 2.7 µm and SPP-Halo90 2.7µm, respectively.

4.5.2 Thermodynamic and resolution (Rs)

Thermodynamic parameters, retention (*k'*) and enantioselectivity (α) values in particular, for several chiral probes on the three CSPs are gathered in Fig. 8, S2 and Table S2. As expected, almost the same retention factors were obtained on the two SPP-Halo90 CSPs. On the other hand, the UHPC-SPP-Halo160-Tzwitt 2.7 exhibited a larger retention for about 80% of the chiral probes on the first eluted enantiomer. The second peak in many examples showed k'_2 values comparable to those of the SPP-Halo90 columns because of the higher enantioselectivity power of this column. Very similar α were observed on the two SPP-Halo90 CSPs ($\alpha_{average}$ = 1.53), which were 10% lower than those observed on the SPP-Halo160 2.7. This gap can be ascribed to the surface area of the silica used and, as consequence, to the amount of selector bonded on the silica matrix (Table 1): on the one hand, a smaller quantity of selector (substrate µmoles/g silica) is loaded on the two 90Å teicoplanin-based CSPs which could be responsible for the higher retention factors. On the other hand, a higher selector density was measured on the SPP-Halo160 2.7 in comparison to the other CSPs and, probably, it could be the cause of the higher enantioselectivity observed using columns packed with this CSP.
Taking into account the resolution, the UHPC-SPP-Halo90-Tzwitt 2.7 showed the lowest values for all samples (Fig. 9A and Table S2) and the SPP-Halo90-2.0 was pointed out to produce comparable resolutions to those recorded with the 160Å CSP. Since the resolution is a parameter made up of efficiency, enantioselectivity and retention, in Figure 9B the resolution power was expressed as the ratio $Rs/t_{r,2}$, by dividing the resolution for the retention time of the second eluted enantiomer. From this bar plot is evident how the SPP-Halo160 2.7 overcame the other two CSPs in any case because of a great combination of high enantioselectivity and large efficiencies on all analytes.

5. Conclusions

In this study, a new zwitterionic teicoplanin based CSP was synthetized by bonding the chiral selector on the high porosity Halo 160Å 2.7 µm superficially porous silica and compared to the SPP-Halo 90Å 2.0 and 2.7 µm analogue CSPs. All stationary phases were obtained through the same synthetic procedure and packed into 100x4.6 mm L.xI.D. columns which were evaluated from the physico chemical, kinetic and thermodynamic point of views. The UHPC-SPP-Halo160-Tzwitt 2.7 allowed to achieve more than 315000 theoretical plates/m on naphthalene at a flow-rate of 2.0 mL/min (H: 3.16 µm, h_r: 1.17) and a N/m of almost 250000 on a chiral aryloxy acid (H: 4.12 µm, h_r: 1.53) attesting the high efficiency of the packing procedure and the potential of this column. In addition, a reduction of the h_r moving from the SPP-Halo90 2.0 to the 2.7 and then SPP-Halo160 2.7 µm was observed, demonstrating that the packing procedure is easier in presence of higher particles diameter and wider pore silica. Several chiral molecules were tested on all columns and, as expected, the SPP-Halo90 2.0 provided the best efficiency values followed by the SPP-Halo160 2.7 µm and lastly the Halo 90Å 2.7 µm column. From the thermodynamic point of view, the SPP-Halo160 2.7 µm exhibited, obviously, lower retention factors on the first eluted enantiomer on every single analyte because of its lower

surface area responsible of a smaller amount (µmol substrate/g silica) of selector bonded, but, at the same time, this CSP showed higher enantioselectivity values thanks to a higher density (µmol substrate/m^2) of teicoplanin onto the silica surface in comparison to the other CSPs.

References

[1] U. Neue, The influence of particle size on column performance, Lecture presented at the 30th International Symposium & Exhibit on High Performance Liquid Phase Separations and Related Techniques, San Francisco, CA, June (2006) 17-22.

[2] J.J. DeStefano, T.J. Langlois, J.J. Kirkland, Characteristics of superficially-porous silica particles for fast HPLC: Some performance comparisons with sub-2-µm particles, J. Chromatogr. Sci. 46 (2008) 254–260

[3] G. Guiochon, F. Gritti, Shell particles, trials, tribulations and triumphs, J.Chromatogr. A 1218 (2011) 1915–1938.

[4] F. Gritti, T. Farkas, J. Heng, G. Guiochon, On the relationship between band broadening and the particle-size distribution of the packing material in liquid chromatography: theory and practice, J. Chromatogr. A 1218 (2011) 8209–8221.

[5] F. Gritti, G. Guiochon, Mass transfer kinetics, band broadening and column efficiency, J. Chromatogr. A 1221 (2012) 2–40.

[6] R. Hayes, A. Ahmed, T. Edge, H. Zhang, Core–shell particles: preparation, fundamentals and applications in high performance liquid chromatography, J.Chromatogr. A 1357 (2014) 36–52.

[7] M. Catani, O.H. Ismail, A. Cavazzini, A. Ciogli, C. Villani, L. Pasti, D. Cabooter, G.Desmet, F. Gasparrini, D.S. Bell, Rationale behind the optimum efficiency of columns packed with the new 1.9 µm fully porous particles Titan C18, J.Chromatogr. A 1454 (2016) 78–85.

[8] R.W. Brice, X. Zhang, L.A. Colón, Fused-core, sub-2 micron packings, and monolithic HPLC columns: a comparative evaluation, J. Sep. Sci. 32 (2009) 2723–2731.

[9] F. Gritti, I. Leonardis, D. Shock, P. Stevenson, A. Shalliker, G. Guiochon, Performance of columns packed with the new shell particles Kinetex-C18, J.Chromatogr. A 1217 (2010) 1589–1603.

[10] D.C. Patel, M.F. Wahab, D.W. Armstrong, Z.S. Breitbach, Advances in high-throughput and high-efficiency chiral liquid chromatographic separations, J.Chromatogr. A, 1467 (2016) 2-18

[11] M.F. Wahab, R.M. Wimalasinghe, Y. Wang, C.L. Barhate, D.C. Patel, D.W. Armstrong, Salient sub-second separations, Anal. Chem., 88 (2016) 8821-8826

[12] R.M. Wimalasinghe, C.A. Weatherly, Z.S. Breitbach, D.W. Armstrong, Hydroxypropyl beta cyclodextrin bonded superficially porous particle-based HILIC stationary phase, J. Liq. Chromatogr. Relat. Technol., 39 (2016) 459-464

[13] S. Fekete, E. Oláh, J. Fekete, Fast liquid chromatography: The domination of core-shell and very fine particles, J. Chromatogr. A. 1228 (2012) 57–71.

[14] R.J. Reischl, L. Hartmanova, M. Carrozzo, M. Huszar, P. Fruhauf, W. Lindner, Chemoselective and enantioselective analysis of proteinogenic amino acids utilizing N-derivatization and 1-D enantioselective anion-exchange chromatography in combination with tandem mass spectrometric detection, J. Chromatogr. A 1218 (2011) 8379–8387.

[15] B. Chankvetadze, Recent developments on polysaccharide-based chiral stationary phases for liquid-phase separation of enantiomers, J. Chromatogr. A. 1269 (2012) 26–51.

[16] S. Fanali, G. Ó Orazio, T. Farkas, B. Chankvetadze Comparative separation of enantiomers with totally porous and core-shell polysaccharide-based chiral stationary phases in nano liquid chromatography and capillary electrochromatography, J. Chromatogr. A, 1269 (2012), pp. 136-142

[17] S. Rocchi, S. Fanali, T. Farkas, B. Chankvetadze Effect of content of coating percentage of chiral selector and pore size of core-shell type silica support on the performance of amylose tris(3,5-

dimethylphenylcarbamate)-based chiral stationary phases in nano-liquid chromatography and capillary electrochromatography, J. Chromatogr. A, 1363 (2014), pp. 363-371.
[18] K. Lomsadze, G. Jibuti, T. Farkas, B. Chankvetadze, Comparative high-performance liquid chromatography enantioseparations on polysaccharide based chiral stationary phases prepared by coating totally porous and core-shell silica particles, J. Chromatogr. A 1234 (2012) 50–55.
[19] Q. Kharaishvili, G. Jibuti, T. Farkas, B. Chankvetadze, Further proof to the utility of polysaccharide-based chiral selectors in combination with superficially porous silica particles as effective chiral stationary phases for separation of enantiomers in high-performance liquid chromatography, J. Chromatogr. A. 1467 (2016) 163–168.
[20] D.A. Spudeit, M.D. Dolzan, Z.S. Breitbach, W.E. Barber, G.A. Micke, D.W. Armstrong, Superficially porous particles vs. fully porous particles for bonded high performance liquid chromatographic chiral stationary phases: Isopropyl cyclofructan 6, J. Chromatogr. A. 1363 (2014) 89–95.
[21] M.D. Dolzan, D.A. Spudeit, Z.S. Breitbach, W.E. Barber, G.A. Micke, D.W. Armstrong, Comparison of superficially porous and fully porous silica supports used for a cyclofructan 6 hydrophilic interaction liquid chromatographic stationary phase, J. Chromatogr. A. 1365 (2014) 124–
[22] C.L. Barhate, Z.S. Breitbach, E.C. Pinto, E.L. Regalado, C.J. Welch, D.W. Armstrong, Ultrafast separation of fluorinated and desfluorinated pharmaceuticals using highly efficient and selective chiral selectors bonded to superficially porous particles, J. Chromatogr. A. 1426 (2015) 241–247.
[23] D.C. Patel, Z.S. Breitbach, M.F. Wahab, C.L. Barhate, D.W. Armstrong, Gone in Seconds: Praxis, Performance, and Peculiarities of Ultrafast Chiral Liquid Chromatography with Superficially Porous Particles, Anal. Chem. 87 (2015) 9137–9148.
[24] O.H. Ismail, L. Pasti, A. Ciogli, C. Villani, J. Kocergin, S. Anderson, F. Gasparrini, A. Cavazzini, M. Catani, Pirkle-type chiral stationary phase on core–shell and fully porous particles: Are superficially porous particles always the better choice toward ultrafast high-performance enantioseparations?, J. Chromatogr. A. 1466 (2016) 96–104.
[25] M. Catani, O.H. Ismail, F. Gasparrini, M. Antonelli, L. Pasti, N. Marchetti, S. Felletti, A. Cavazzini, Recent advancements and future directions of superficially porous chiral stationary phases for ultrafast high-performance enantioseparations, Analyst. 142 (2017) 555–566.
[26] O.H. Ismail, A. Ciogli, C. Villani, M. De Martino, M. Pierini, A. Cavazzini, D.S. Bell, F. Gasparrini, Ultra-fast high-efficiency enantioseparations by means of a teicoplanin-based chiral stationary phase made on sub-2µm totally porous silica particles of narrow size distribution, J. Chromatogr. A. 1427 (2016) 55–68.
[27] O.H. Ismail, M. Antonelli, A. Ciogli, C. Villani, A. Cavazzini, M. Catani, S. Felletti, D.S. Bell, F. Gasparrini, Future perspectives in high efficient and ultrafast chiral liquid chromatography through zwitterionic teicoplanin-based 2-µm superficially porous particles, J. Chromatogr. A. 1520 (2017) 91–102.
[28] K. Schmitt, U. Woiwode, M. Kohout, T. Zhang, W. Lindner, M. Lämmerhofer, Comparison of small size fully porous particles and superficially porous particles of chiral anion-exchange type stationary phases in ultra-high performance liquid chromatography: effect of particle and pore size on chromatographic efficiency and kinetic performance, J. Chromatogr. A. 1569 (2018) 149–159.
[29] F. Gritti, G. Guiochon, Accurate measurements of peak variances: Importance of this accuracy in the determination of the true corrected plate heights of chromatographic columns, J. Chromatogr. A 1218 (2011) 4452–4461.
[30] J.J. DeStefano, B.E. Boyes, S.A. Schuster, W.L. Miles, J.J. Kirkland, Are sub-2µm particles best for separating small molecules? An alternative, J. Chromatogr. A. 1368 (2014) 163–172,
[31] Fekete, S. Ph.D. Thesis, Budapest University of Technology and Economics, Department of Inorganic and Analytical Chemistry. 2011.

Figure captions.

Figure 1. Backpressure ΔP_{col} vs. Flow-rate plots on UHPC-SPP-Halo90-Tzwitt 2.0 µm (Black square), UHPC-SPP-Halo90-Tzwitt 2.7 µm (Red circle) and UHPC- SPP-Halo160-Tzwitt 2.7 µm (Green triangle). Columns geometry: 100x4.6 mm L.xI.D.; Eluent: ACN/H_2O 85:15 + 15mM $HCOONH_4$, η: $0.41_5 x10^{-3}$ Pa x s, T: 35°C.

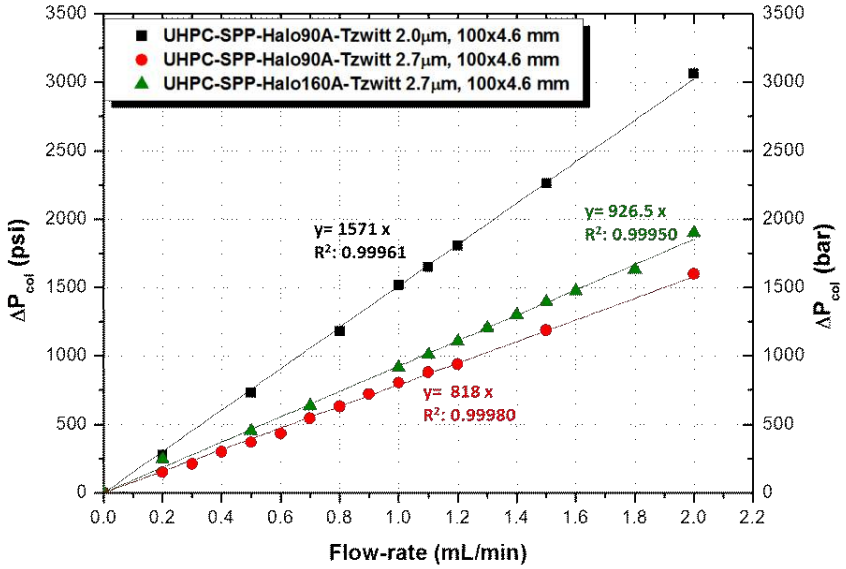

Figure 2. A) van Deemter plots (H vs Flow-rate) for naphthalene (void volume marker); B) Reduced van Deemter plots (h_r vs Flow-rate) for naphthalene on the UHPC-SPP-Halo90-Tzwitt 2.0 µm (Black square), UHPC-SPP-Halo90-Tzwitt 2.7 µm (Red circle) and UHPC- SPP-Halo160-Tzwitt 2.7 µm (Green triangle). Instrument: Acquity Waters UPLC; Eluent: ACN/H_2O 85:15 + 15mM $HCOONH_4$, T: 35°C.

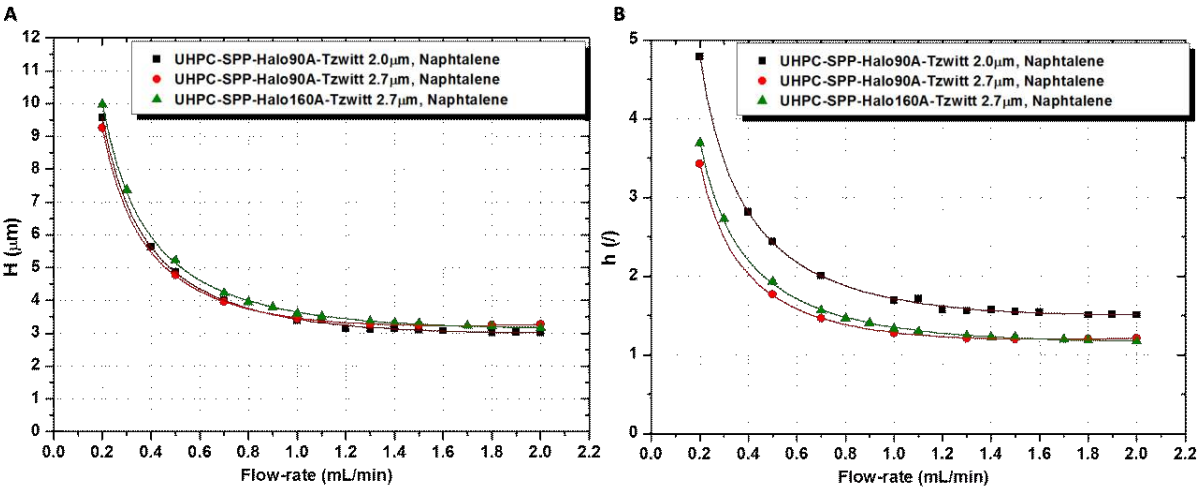

Figure 3. A) van Deemter plots (H vs Flow-rate) for thiourea (*k'*: 0.5-0.6); B) Reduced van Deemter plots (h_r vs Flow-rate) for thiourea on the UHPC-SPP-Halo90-Tzwitt 2.0 µm (Black square), UHPC-SPP-Halo90-Tzwitt 2.7 µm (Red circle) and UHPC- SPP-Halo160-Tzwitt 2.7 µm (Green triangle). Instrument: Acquity Waters UPLC; Eluent: ACN/H_2O 85:15 + 15mM $HCOONH_4$, T: 35°C

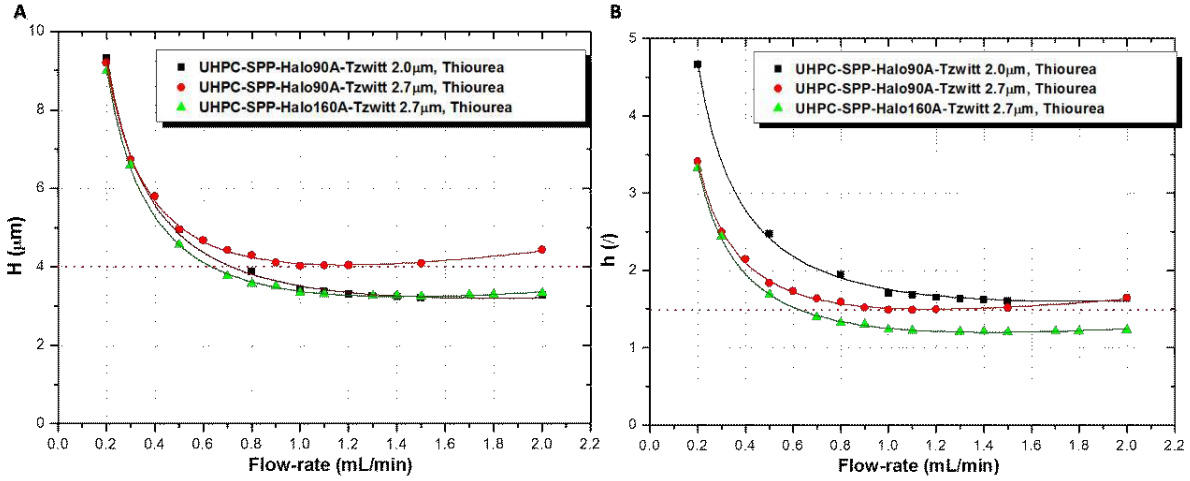

Figure 4. Separations of the achiral mixture (naphthalene, thiourea, uracil and adenosine) on the UHPC-SPP-Halo90-Tzwitt 2.0 µm (Black trace), UHPC-SPP-Halo90-Tzwitt 2.7 µm (Red trace) and UHPC- SPP-Halo160-Tzwitt 2.7 µm (Green trace) at their optimal flow-rates (A). Figure B) shows the same chromatograms as a function of the retention factor (*k'*). Columns geometry: 100x4.6 mm L.xI.D.; Instrument: Acquity Waters UPLC; Eluent: ACN/H_2O 85:15 + 15mM $HCOONH_4$, T: 35°C.

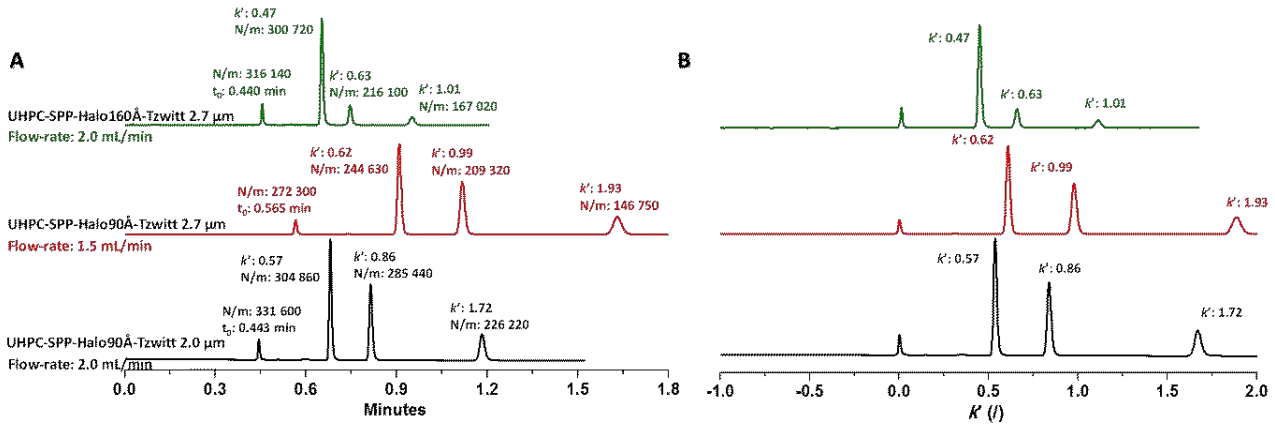

Figure 5. van Deemter plots of 1st (A) and 2nd (B) eluted enantiomers of the 2-(4-chloro-phenoxy)-propionic acid on the UHPC-SPP-Halo90-Tzwitt 2.0 µm (Black square), UHPC-SPP-Halo90-Tzwitt 2.7 µm (Red circle) and UHPC- SPP-Halo160-Tzwitt 2.7 µm (Green triangle). Instrument: Dionex Ultimate 3000RS; Eluent: ACN/H_2O 85:15 + 15mM $HCOONH_4$, T: 35°C.

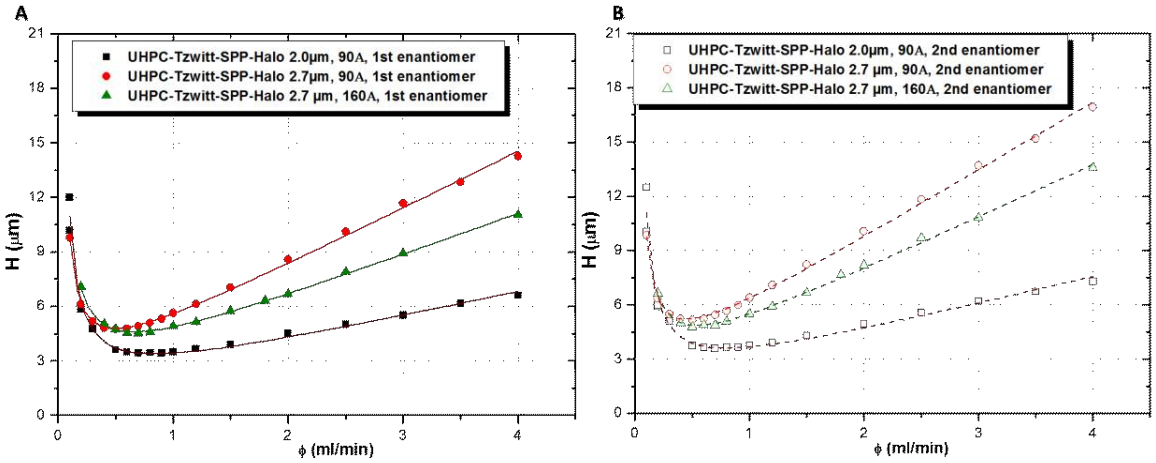

Figure 6. Chromatographic traces of the 2-(4-chloro-phenoxy)-propionic acid on the UHPC-SPP-Halo90-Tzwitt 2.0 µm (Black trace), UHPC-SPP-Halo90-Tzwitt 2.7 µm (Red trace) and UHPC- SPP-Halo160-Tzwitt 2.7 µm (Green trace) at their optimal flow-rates (A). Figure B) shows the same chromatograms as a function of the retention factor (*k'*). Columns geometry: 100x4.6 mm L.xI.D.; Instrument: Dionex Ultimate 3000RS; Eluent: ACN/H_2O 85:15 + 15mM $HCOONH_4$, T: 35°C.

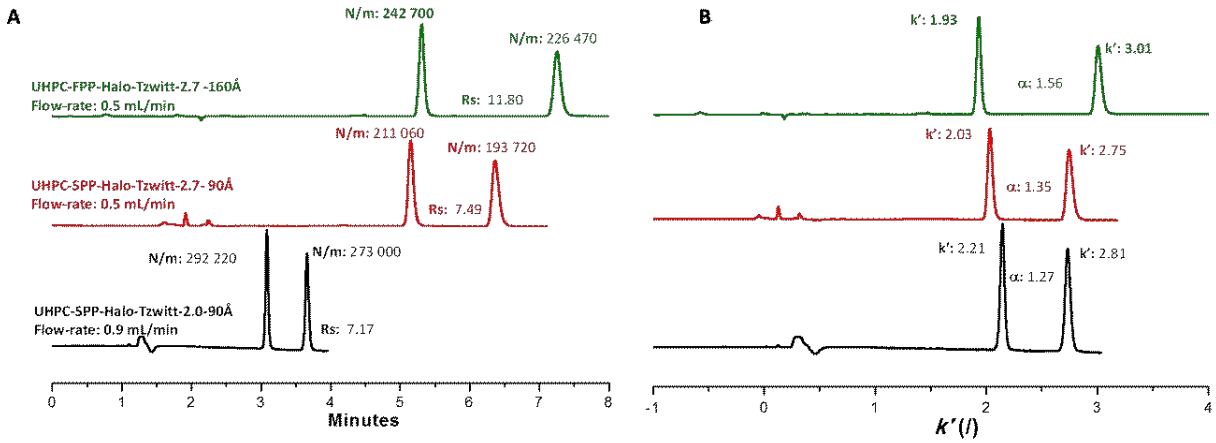

Figure 7. Separations of racemic analytes on the UHPC-SPP-Halo90-Tzwitt 2.0 µm (Black traces), UHPC-SPP-Halo90-Tzwitt 2.7 µm (Red traces) and UHPC- SPP-Halo160-Tzwitt 2.7 µm (Green traces) at flow-rate: 1.0 mL/min. (A) Haloxyfop + Ketorolac, (B) N-Fmoc-D,L-Phe, (C) N-Fmoc-D,L-Glu, (D) N-Z-D,L-Phe. Columns geometry: 100x4.6 mm L.xI.D.; Instrument: Dionex Ultimate 3000RS; Eluent: ACN/H_2O 85:15 + 15mM $HCOONH_4$, T: 35°C.

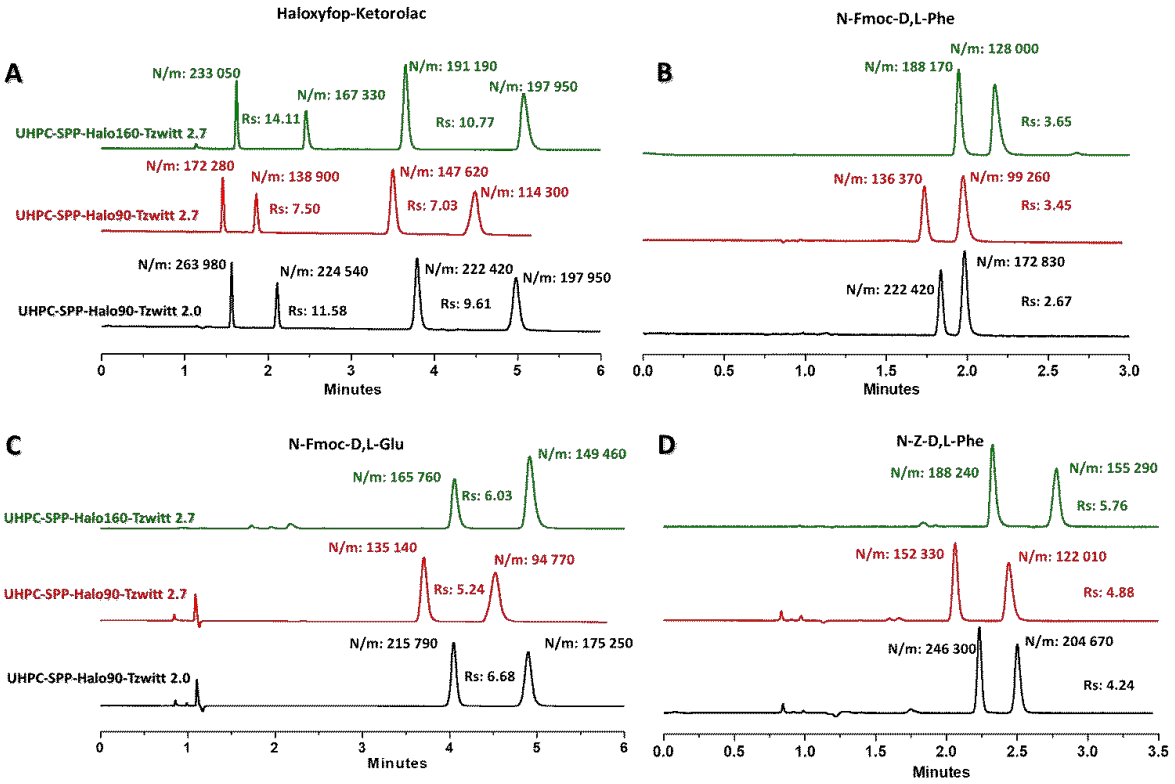

Figure 8. Bar plots of enantioselectivity values (α) recorded for different analytes on the UHPC-SPP-Halo90-Tzwitt 2.0 µm (Black), UHPC-SPP-Halo90-Tzwitt 2.7 µm (Red) and UHPC- SPP-Halo160-Tzwitt 2.7 µm (Green). Eluent: ACN/H_2O 85:15 + 15mM $HCOONH_4$, T: 35°C.

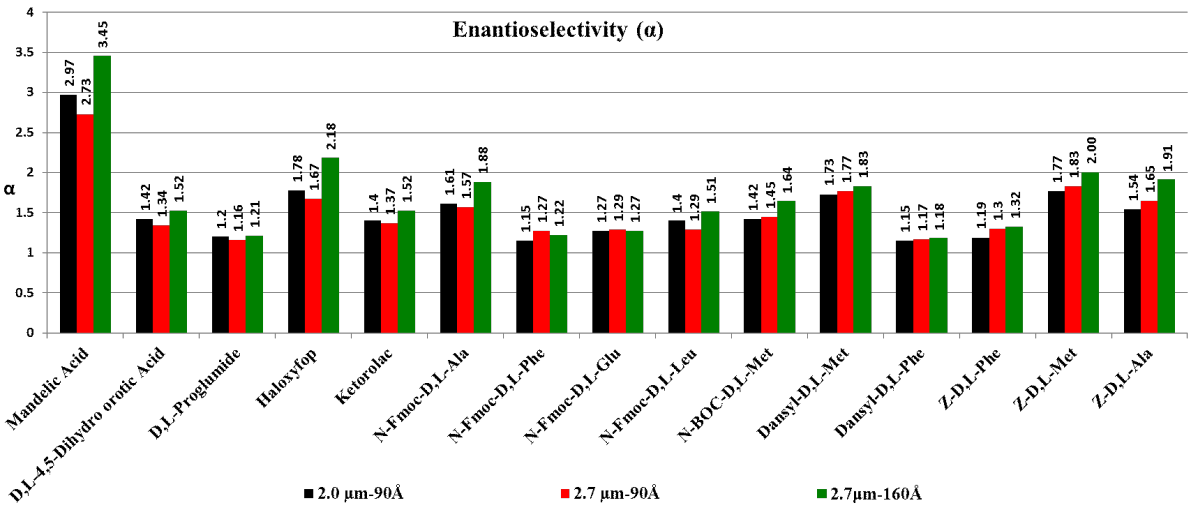

Figure 9. Bar plots of resolution (Rs) (A) and $Rs/t_{r,2}$ (B) obtained for different analytes on the UHPC-SPP-Halo90-Tzwitt 2.0 µm (Black), UHPC-SPP-Halo90-Tzwitt 2.7 µm (Red) and UHPC- SPP-Halo160-Tzwitt 2.7 µm (Green) at flow-rate: 1.0mL/min. Eluent: ACN/H_2O 85:15 + 15mM $HCOONH_4$, T: 35°C.

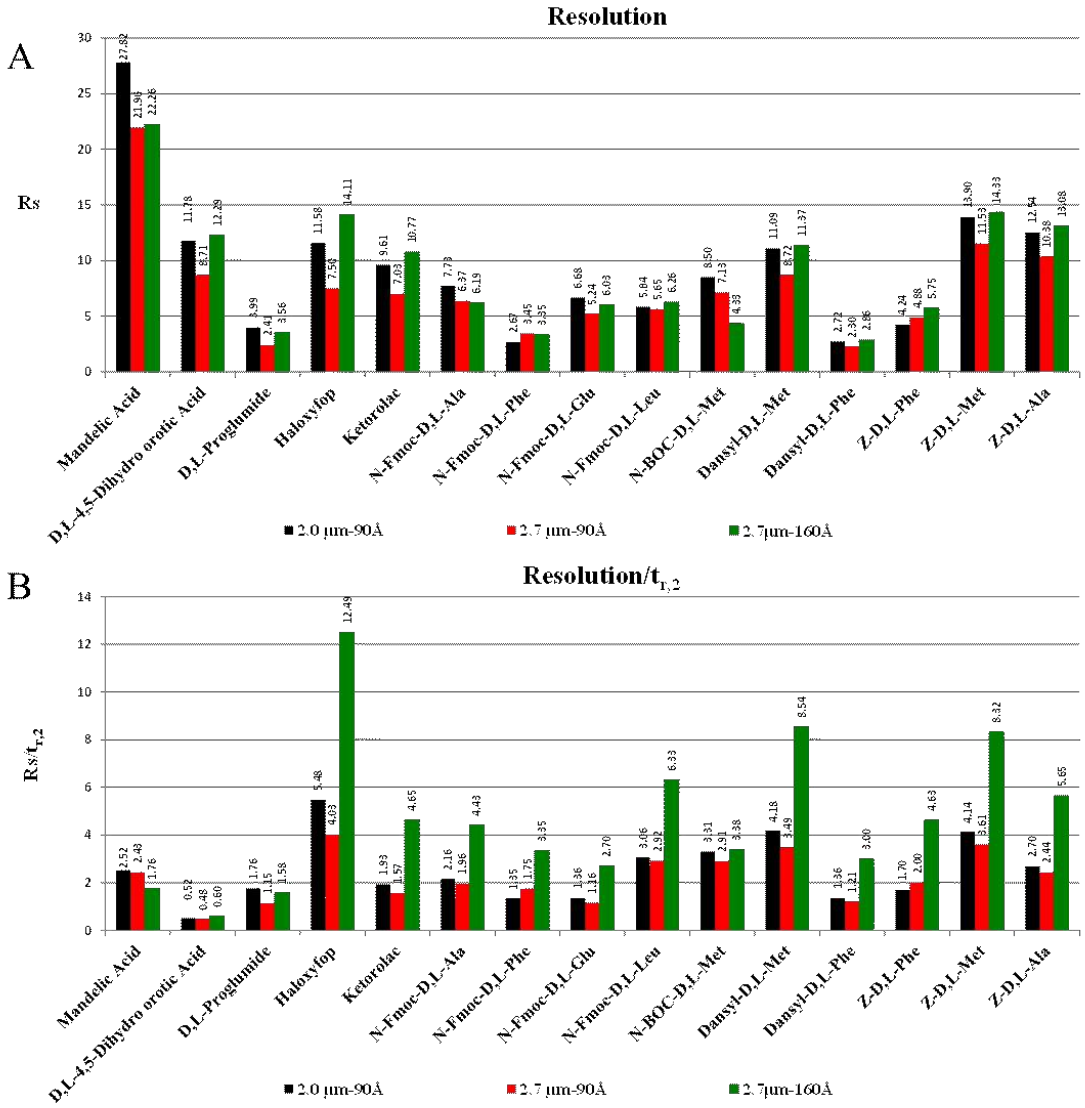

Table 1. Data obtained from elemental CHN analyses on the three zwitterionic teicoplanin CSPs

	Surface area [m^2/g]	%C	%H	%N	Substrate µmoles/g silica	Substrate µmoles/m^2
SPP-Halo90 2.0	125	5.75	0.74	0.63	55.72	0.45
SPP-Halo90 2.7	123	6.05	0.79	0.66	58.75	0.47
SPP-Halo160 2.7	80	5.67	0.68	0.71	63.73	0.80

Table 2. Experimental van Deemter analysis data under Hilic conditions on UHPC-SPP-Halo90-Tzwitt 2.0 µm, UHPC-SPP-Halo90-Tzwitt 2.7 µm and UHPC- SPP-Halo160-Tzwitt 2.7 µm. Columns geometry: 100x4.6 mm L.xI.D.; Eluent: ACN/H_2O 85:15 + 15mM $HCOONH_4$, T: 35°C.

Sample	k' (/)	H_{min} (µm)	h_{min} (/)	N/m	Flow-rate$_{opt}$ (mL/min)
Naphtalene	0.00	3.02	1.51	331 600	2.0
Thiourea	0.57	3.21	1.60_5	311 280	1.5
Uracil	0.86	3.22	1.61	310 660	1.2
Adenosine	1.72	3.71	1.85	269 750	1.2

UHPC-SPP-Halo90Å-Tzwitt 2.0 µm

Sample	k' (/)	H_{min} (µm)	h_{min} (/)	N/m	Flow-rate$_{opt}$ (mL/min)
Naphtalene	0.00	3.67	1.36	272 300	1.5
Thiourea	0.62	4.03	1.49	248 090	1.1
Uracil	0.99	4.19	1.55	238 920	0.8
Adenosine	1.93	4.50	1.67	222 040	0.5

UHPC-SPP-Halo90Å-Tzwitt 2.7 µm

Sample	k' (/)	H_{min} (µm)	h_{min} (/)	N/m	Flow-rate$_{opt}$ (mL/min)
Naphtalene	0.00	3.16	**1.17**	316 140	>2.0
Thiourea	0.47	3.25	1.20	307 360	1.5
Uracil	0.63	3.90	1.44	256 200	0.9
Adenosine	1.01	4.03	1.49	247 900	0.7

UHPC-SPP-Halo160Å-Tzwitt 2.7 µm

Paper X

http://www.americanpharmaceuticalreview.com/Featured-Articles/339730-Pirkle-Type-Chiral-Stationary-Phases-for-Ultra-High-Performance-Ultra-Fast-Enantioseparations/

New Whelk-O1 Pirkle-type chiral stationary phases for ultra-high performance ultra-fast enantioseparations

Martina Catani[(a) *]; Omar H. Ismail[(b) *]; Simona Felletti[(a)]; Francesco Gasparrini[(b)]; Luisa Pasti[(a)]; Valentina Costa[(a)]; Alberto Cavazzini[(a)]

a) Department of Chemistry and Pharmaceutical Sciences, University of Ferrara, via L. Borsari 46, 44121 Ferrara, Italy
b) Department of Drug Chemistry and Technology, "Sapienza" University of Rome, P.le A. Moro 5, 00185 Rome, Italy

[*]corresponding authors. E-mail addresses: martina.catani@unife.it; omar.ismail@uniroma1.it

Abstract

During the last decade, column manufacturers have put much effort into the design and preparation of materials (e.g., sub-2 micron fully porous and core-shell particles) suitable for highly efficient and fast separations in ultra high-performance liquid chromatography (UHPLC). It is a matter of fact that this advancement has so far only partially touched the field of chiral liquid chromatography. This delay has been essentially due to the lack of understanding of mass transfer processes in chiral chromatography, on the one hand, and to practical difficulties in the preparation of small chiral particles. Recently, Pirkle-type chiral stationary phases (CSPs) have been prepared by using both sub-2 micron fully porous and 2.6 micron core-shell silica particles as base materials. This report describes the employment of these CSPs to achieve not only very high performance but also ultrafast (less than one second) chiral separations in different chromatographic modes.

Introduction

In the last decade the field of chiral separations has been affected by a radical transformation. The attention of scientists and manufacturers has indeed moved from the research of novel CSPs with enhanced enantioselectivity to the preparation of new versions of already known CSPs prepared on kinetically highly efficient silica particles, such as the sub-2 micron fully porous particles (FPPs) and the 2.6 micron superficially porous ones (SPPs). Pressing requirements especially by pharmaceutical and medicinal industries – e.g., for the screening of large libraries of chiral molecules or, in general, for high-throughput analysis [1] – have indeed pushed towards the development of increasingly faster and efficient chiral separations, which could not be achieved on CSPs developed on typical 3-5 micron FPPs.

This new trend has had a tremendous impact on the analysis time. If indeed, until only ten years ago, several tens of minutes were the standard time required to perform chiral separations, [2] today the scenario has completely changed. [3] Many examples of chiral separations performed in few minutes, or even on sub-minute scale, have been reported thanks to the use of the above mentioned silica particles, be they FPPs [4, 5] or SPPs [6, 7,8, 9]. This report describes the employment of novel Pirkle-type Whelk-O1 CSPs in ultra-high performance chiral chromatography (UHPLC) for fast and ultra-fast (less than one second) enantioseparations.

New Whelk-O1 Pirkle-type CSPs for ultra-high performance, ultra-fast enantioseparations

Pirkle-type (even referred to generically as brush-type) CSPs were the first ones employed for the preparation of sub 2 micron chiral particles. [10] The choice of this selector for the transition from enantioselective high performance liquid chromatography (e-HPLC) to e-UHPLC finds its rationale in the ease to prepare sub-2 micron particles (absence of particle aggregation and clogging during their synthesis) [10] and on the supposed fast mass transfer kinetics proper of CSPs based on this class of selectors [9].

The first Pirkle type eUHPLC CSP was prepared in 2010 by Cancelliere et al. They functionalized 1.9 micron FPPs with DACH-DNB selector [5]. Kinetic performance of columns packed with this CSP was compared to that of columns packed with 4.3 and 2.6 micron DACH-DNB FPPs. The sub-2 micron column displayed both significant efficiency gain and reduced analysis times (see **Figure 1**) with respect of the other two particle formats by simultaneously maintaining comparable selectivity and improving the resolution (due to higher efficiency).

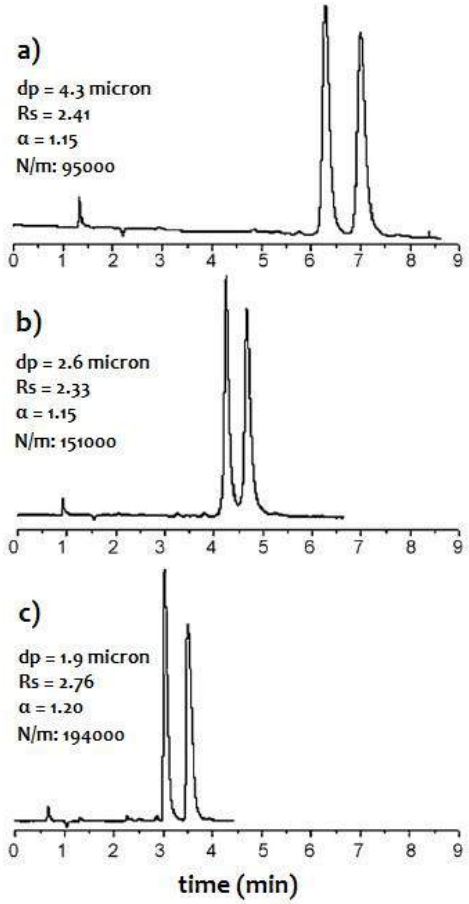

Figure 1: Chromatograms showing the separations of enantiomers of 2-methoxyphenyl methyl sulfoxide on columns packed with DACH-DNB FPPs at constant L/d_p (length/particle diameter) ratio: a) 150×4.1 mm, d_p = 4.3 micron, L/d_p = 35; b) 100×4.1 mm; d_p = 2.6 micron, L/d_p = 38; c) 75×4.1 mm; d_p = 1.9 micron, L/d_p = 39. Resolution (*Rs*), selectivity (α) and efficiency (number of theoretical plates per meter, *N/m*) are reported close to each chromatogram. Adapted from ref. 5 (D. Kotoni et al., *Anal. Chem.* 2012;84:6805-6813). Copyright (2012) American Chemical Society.

A few years later, the Whelk-O1 chiral selector (see **Figure 2**), probably the most popular and versatile one among the Pirkle-types, was employed to functionalize sub 2-micron FPPs [4, 8, 11, 12].

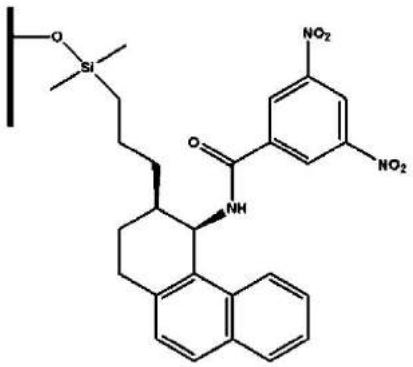

Figure 2: Schematic structure of (*R,R*)-Whelk-O1 CSP.

Whelk-O1 selector is well known for being able to discriminate a broad range of chiral compounds and for its stability at high pressure and temperature. Whelk-O1 CSPs can be used in normal phase (NP), polar organic mode (POM), reversed-phase (RP) and supercritical fluid chromatography (SFC) conditions. As shown as an example in **Figure 3**, this CSP allowed to achieve excellent chromatographic performance, with very large resolution and very symmetrical and thin peak shapes in ultrafast separations. [4]

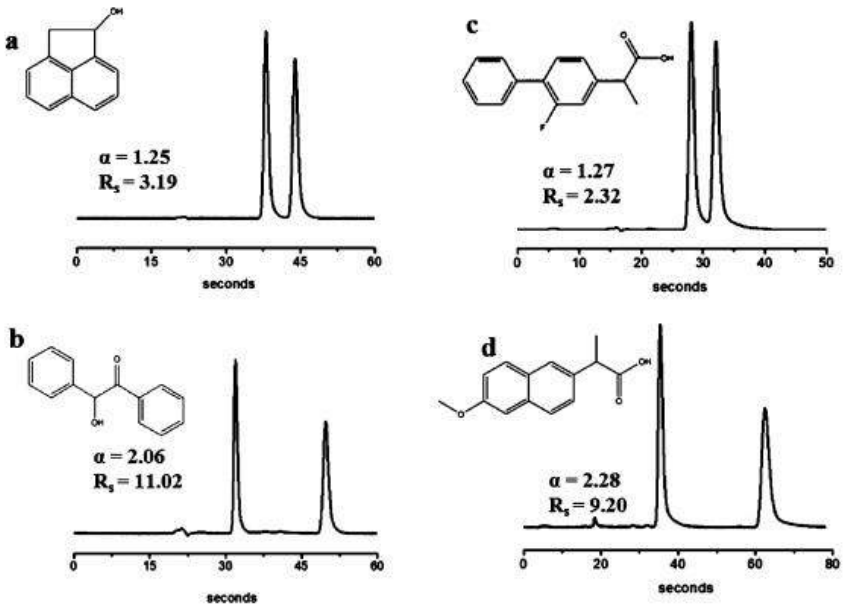

Figure 3: Examples of ultrafast enantioseparations performed on a 50 × 4.6 mm ID column packed with sub-2 micron Whelk-O1 particles. Acenaphtenol (a) and benzoin (b) separated in NP mode (mobile phase: hexane/ethanol 70:30 (% v/v), flow rate: 2 mL/min); flurbiprofen (c) and naproxen (d) separated in POM (mobile phase: acetonitrile + 0.2% acetic acid + 0.07% dietilamine (%v/v), flow rate: 2.5 mL/min). Selectivity (α) and resolution (R_s) are indicated close to each chromatogram. Reprinted with permission from ref. 4.

Short columns (5 cm) packed with sub 2-micron Whelk-O1 FPPs were successfully employed for the fast screening of a library of 129 racemic compounds (**Figure 4**) with significantly different physico-chemical properties (including organic acids, β-blockers, antidepressants, agrochemicals) in SFC. [2]

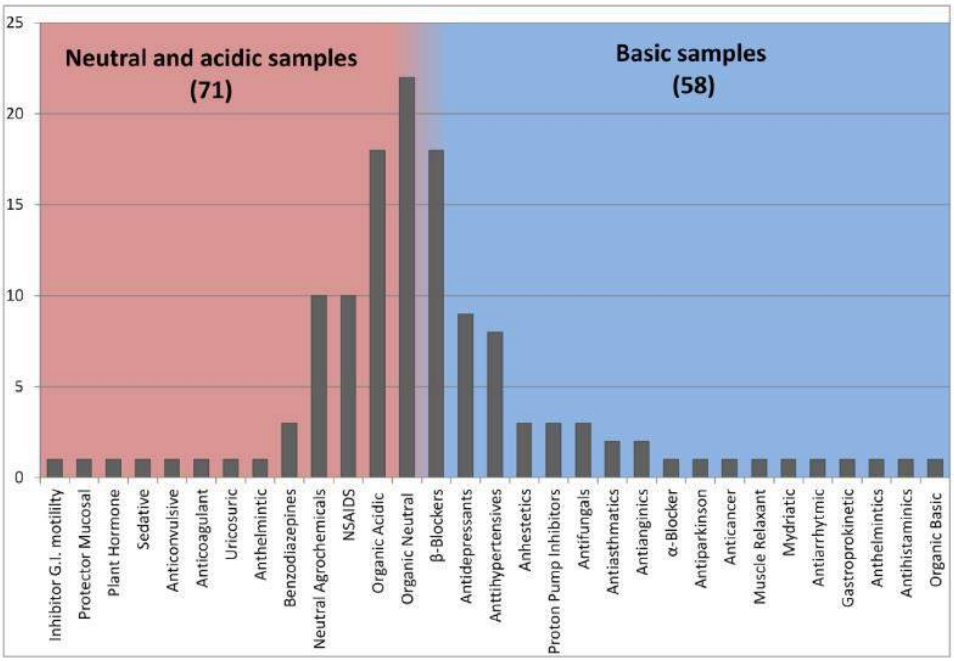

Figure 4: Classification of chiral compounds separated on a sub-2micron Whelk-O1 column in SFC. Reprinted with permission from Ref. 2.

The overall screening was carried out in less than 24 hours under fast gradient elution (9 minute total analysis time, including column reconditioning) by using a mixture of CO_2/methanol as mobile phase. The sub-2 micron fully porous Whelk-O1 CSP was found to be able to resolve even basic racemic mixtures, which are not traditionally easily separated on Whelk-O1 CSPs prepared on larger particles. Under NP conditions, these new columns exhibited kinetic performance comparable to those typical of achiral separations with efficiency in the order of 300,000 plates/meter (**figure 5**).
These efficiencies were even difficult to imagine only a few years ago in chiral chromatography. In 2016, Whelk-O1 chiral selector was employed also for the preparation of 2.6 micron SPPs. [8]

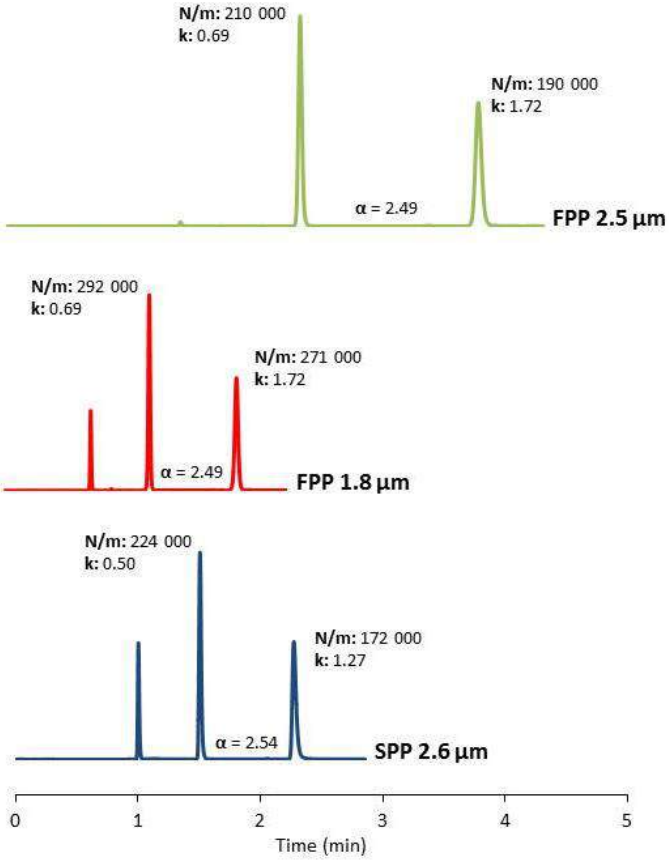

Figure 5: Chromatograms showing the separation of *trans*-stilbene oxide enantiomers on the three columns at the flow rate corresponding to the minimum of the van Deemter curve (from top to bottom, respectively, 1.2, 1.8 and 1.5 mL/min). CCl_4 was used as dead volume marker. For each peak retention factor (k) and efficiency as number of theoretical plates per meter (N/m) are reported.

With Whelk-O1 CSPs prepared on these highly performance particles, extraordinary results in terms of ultrafast enantioseparations were obtained thanks to the use of short columns (1 cm) and high flow rates. For instance, by employing 10 × 0.3 cm (length × I.D.) columns at a flow rate of 8 mL/min, the two enantiomers of *trans*-stilbene oxide were separated in less than one second on both the SPP and FPP columns (see **figure 6**).

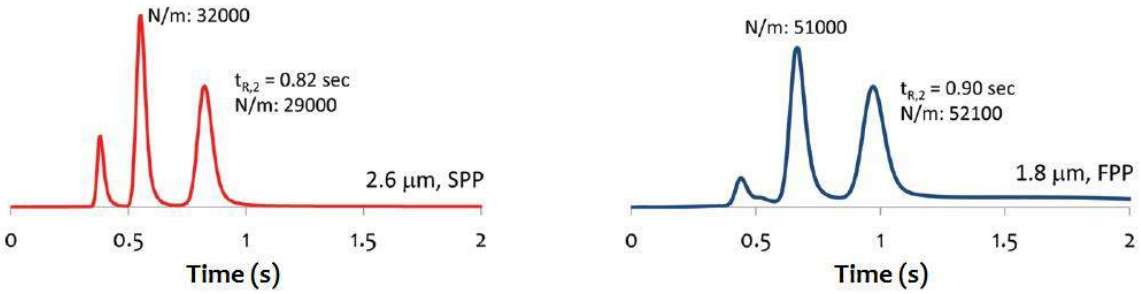

Figure 6: Ultrafast enantioseparation of *trans*-stilbene oxide enantiomers on 10 × 3.0 mm columns packed with Whelk-O1 SPP 2.6 µm (left) and Whelk-O1 FPP 1.8 µm (right). Adapted with permission from ref. 9 with permission from The Royal Society of Chemistry.

Conclusions

The transition from traditional e-HPLC to e-UHPLC has started and will continue in the future.
Whelk-O1 Pirkle-type chiral selectors definitely represent one of the successful examples of the enormous advantages that can be achieved, also in the field of chiral separations, by employing small silica particles with enhanced characteristics in terms of mass transfer. The issues in the preparation of small chiral particles seem to be overtaken. On the other hand, slurry packing of small particles (including core-shell ones) [13] has tremendously improved in the last years to the point that modern techniques of packing allow to obtain very efficient packed beds. Nowadays, CSPs able to perform as efficiently as typical reversed-phase stationary phases (with efficiency in the order of 300,000 theoretical plates per meter or more) have been already prepared and tested in laboratory, even if they are not yet commercially available. These phases can be operated in very different chromatographic modes and they are suitable for very high-pressure regimes. The future of chiral separations via liquid chromatography is strictly connected to the development of these new CSPs and will be characterized by very fast and efficient separations on columns of reduced length and diameter.

Bibliography

1. Mangelings D, Heyden YV. Screening approaches for chiral separations. In: E. Grushka NG, ed. *Advances in chromatography*. Vol 46. New York: CRC Press; 2007.

2. Sciascera L, Ismail OH, Ciogli A, et al. Expanding the potential of chiral chromatography for high-throughput screening of large compound libraries by means of sub-2 um Whelk-O1 stationary phase in supercritical fluid conditions. *J. Chromatogr. A*. 2015;1383:160-168.

3. Patel DC, Breitbach ZS, Wahab MF, Barhate CL, Armstrong DW. Gone in seconds: praxis, performance, and peculiarities of ultrafast chiral liquid chromatography with superficially porous particles. *Anal. Chem.* 2015;87:9137–9148.

4. Kotoni D, Ciogli A, Molinaro C, et al. Introducing enantioselective Ultrahigh-Pressure Liquid Chromatography (eUHPLC): Theoretical inspections and ultrafast separations on a new sub-2um Whelk-O1 stationary phase. *Anal. Chem.* 2012;84:6805-6813.

5. Cancelliere G, Ciogli A, D'Acquarica I, et al. Transition from enantioselective high performance to ultra-high performance liquid chromatography: A case study of a brush-type chiral stationary phase based on sub-5-micron to sub-2-micron silica particles. *J. Chromatogr. A*. 2010;1217:990-999.

6. Wahab MF, Wimalasinghe RM, Wang Y, Barhate CL, Patel DC, Armstrong DW. Salient sub-second separations. *Anal. Chem.* 2016;88:8821-8826.

7. Wimalasinghe RM, Weatherly CA, Breitbach ZS, Armstrong DW. Hydroxypropyl beta cyclodextrin bonded superficially porous particle-based HILIC stationary phases. *J. Liq. Chromatogr. Relat. Technol.* 2016;39:459-464.

8. Ismail OH, Pasti L, Ciogli A, et al. Pirkle-type chiral stationary phase on core-shell and fully porous particles: Are superficially porous particles always the better choice toward ultrafast high-performance enantioseparations? *J. Chromatogr. A*. 2016;1466:96-104.

9. Catani M, Ismail OH, Gasparrini F, et al. Recent advancements and future directions of superficially porous chiral stationary phases for ultrafast high-performance enantioseparations. *Analyst*. 2017;142:555-566.

10. Cavazzini A, Marchetti N, Guzzinati R, et al. Enantioseparation by ultra-high performance liquid chromatography. *TrAC, Trends Anal. Chem.* 2014;63:95-103.

11. Kotoni D, Ciogli A, D'Acquarica I, et al. Enantioselective ultra-high and high performance liquid chromatography: A comparative study of columns based on the Whelk-O1 selector. *J. Chromatogr. A*. 2012;1269:226-241.

12. Gasparrini F, Ciogli A, Pierini M, et al. The Evolution of Chiral Stationary Phases from HPLC to UHPLC. *LC/GC Eur.* 2014;27:128-137.

13. Patel DC, Breitbach ZS, Yu J, Nguyen KA, Armstrong DW. Quinine bonded to superficially porous particles for high-efficiency and ultrafast liquid and supercritical fluid chromatography. *Anal. Chim. Acta*. 2017;963:164-174.

Università degli Studi di Ferrara

Sezioni

Dottorati di ricerca

Il tuo indirizzo e-mail

fllsmn1@unife.it

Oggetto:

Dichiarazione di conformità della tesi di Dottorato

Io sottoscritto Dott. (Cognome e Nome)

Felletti Simona

Nato a:

Lugo

Provincia:

Ravenna

Il giorno:

02/06/1991

Avendo frequentato il Dottorato di Ricerca in:

Scienze Chimiche

Ciclo di Dottorato

32

Titolo della tesi:

Investigation of Mass Transfer Phenomena and Thermodynamic Properties of new Generation Porous Particles for High-Efficient Separations in Liquid Chromatography Through Experimental and Theoretical Approaches

Titolo della tesi (traduzione):

Studio dei fenomeni di trasferimento di massa e delle proprietà termodinamiche di particelle porose di nuova generazione per separazioni ad alta efficienza in cromatografia liquida attraverso approcci sperimentali e teorici

Tutore: Prof. (Cognome e Nome)

Cavazzini Alberto

Settore Scientifico Disciplinare (S.S.D.)

CHIM/01

Parole chiave della tesi (max 10):

Ultra-fast/ultra-high performance chromatography, enantioseparations, bioactive compounds, chiral stationary phases, adsorption isotherms, pharmaceuticals, inverse method, van Deemter

curves, mass transfer kinetics. Cromatografia ultra-veloce e ad alta efficienza, separazioni chirali, composti bioattivi, fasi stazionarie chirali, isoterme di adsorbimento, prodotti farmaceutici, metodo inverso, curve di van Deemter, cinetiche di trasferimento di massa.

Consapevole, dichiara

CONSAPEVOLE: (1) del fatto che in caso di dichiarazioni mendaci, oltre alle sanzioni previste dal codice penale e dalle Leggi speciali per l'ipotesi di falsità in atti ed uso di atti falsi, decade fin dall'inizio e senza necessità di alcuna formalità dai benefici conseguenti al provvedimento emanato sulla base di tali dichiarazioni; (2) dell'obbligo per l'Università di provvedere al deposito di legge delle tesi di dottorato al fine di assicurarne la conservazione e la consultabilità da parte di terzi; (3) della procedura adottata dall'Università di Ferrara ove si richiede che la tesi sia consegnata dal dottorando in 2 copie di cui una in formato cartaceo e una in formato pdf non modificabile su idonei supporti (CD-ROM, DVD) secondo le istruzioni pubblicate sul sito: http://www.unife.it/studenti/dottorato alla voce ESAME FINALE – disposizioni e modulistica; (4) del fatto che l'Università, sulla base dei dati forniti, archivierà e renderà consultabile in rete il testo completo della tesi di dottorato di cui alla presente dichiarazione attraverso l'Archivio istituzionale ad accesso aperto "EPRINTS.unife.it" oltre che attraverso i Cataloghi delle Biblioteche Nazionali Centrali di Roma e Firenze; DICHIARO SOTTO LA MIA RESPONSABILITA': (1) che la copia della tesi depositata presso l'Università di Ferrara in formato cartaceo è del tutto identica a quella presentata in formato elettronico (CD-ROM, DVD), a quelle da inviare ai Commissari di esame finale e alla copia che produrrò in seduta d'esame finale. Di conseguenza va esclusa qualsiasi responsabilità dell'Ateneo stesso per quanto riguarda eventuali errori, imprecisioni o omissioni nei contenuti della tesi; (2) di prendere atto che la tesi in formato cartaceo è l'unica alla quale farà riferimento l'Università per rilasciare, a mia richiesta, la dichiarazione di conformità di eventuali copie; (3) che il contenuto e l'organizzazione della tesi è opera originale da me realizzata e non compromette in alcun modo i diritti di terzi, ivi compresi quelli relativi alla sicurezza dei dati personali; che pertanto l'Università è in ogni caso esente da responsabilità di qualsivoglia natura civile, amministrativa o penale e sarà da me tenuta indenne da qualsiasi richiesta o rivendicazione da parte di terzi; (4) che la tesi di dottorato non è il risultato di attività rientranti nella normativa sulla proprietà industriale, non è stata prodotta nell'ambito di progetti finanziati da soggetti pubblici o privati con vincoli alla divulgazione dei risultati, non è oggetto di eventuali registrazioni di tipo brevettale o di tutela. PER ACCETTAZIONE DI QUANTO SOPRA RIPORTATO

Firma del dottorando

Ferrara, li 19/12/2019 (data) Firma del Dottorando Simona Felletti

Firma del Tutore Simona Felletti

Visto: Il Tutore Si approva Firma del Tutore Alberto Cavazzini

Alberto Cavazzini